/
Article / Book Information

( )	
Title(English)	Transport Properties of Resonant Fermi Gases
( )	
Author(English)	Keisuke Fujii
( )	: ( ), : , : 11878 , :2021 3 26 , : , : , , , ,
Citation(English)	Degree:Doctor (Science), Conferring organization: Tokyo Institute of Technology, Report number: 11878 , Conferred date:2021/3/26, Degree Type:Course doctor, Examiner:,,,,,
( )	
Type(English)	Doctoral Thesis

Tokyo Institute of Technology

Doctoral Thesis

Transport Properties
of Resonant Fermi Gases

Keisuke Fujii

Department of Physics, Tokyo Institute of Technology

February 13, 2021

Abstract

Owing to their high tunability, ultracold atoms provide versatile platforms for investigating interacting systems. Here, the quantum statistics of particles is controlled by the choice of atomic species and the space geometry by the operation of optical lattices. In addition, the strength of the interparticle interaction can be tuned from weak to strong through the Feshbach resonance. One of the ultracold atomic systems which take maximum advantage of this tunability is a two-component Fermi gas near the two-body resonance, which is referred to as a resonant Fermi gas. Because the interaction is characterized by only one parameter, the s-wave scattering length, the interaction effect appears only through the scattering length near the resonance. Thus, the resonant Fermi gas shows universal behaviors independent of the details of the interaction and forms an ideal example of a strongly correlated quantum many-body system. This universality and the high tunability connect the study of ultracold atoms to various other fields of physics.

In particular, a resonant Fermi gas in the unitarity limit, where the scattering length is tuned to infinity in three dimensions, shows remarkable universality because of the absence of length scales in the interaction. The emergence of the conformal invariance due to the absence of length scales is one representative example of the universality in the unitarity limit. The strong coupling, which is associated with conformality, motivates studies of the thermodynamic properties and the transport properties. For example, the system achieves an almost "perfect fluid" in the unitarity limit, where the bulk viscosity vanishes and the shear viscosity has a remarkably small ratio to the entropy density. Although the strong coupling leads to intriguing transport properties, it makes the calculations of transport coefficients difficult.

This thesis investigates the transport properties of two-component Fermi gases near the two-body resonance in two and three dimensions. We particularly focus on their transport coefficients, such as the bulk viscosity, the shear viscosity, and the thermal conductivity, for an arbitrary scattering length. In order to carry out reliable analysis in the strongly correlated regime, such as near the unitarity limit, we need non-perturbative methods. One of the non-perturbative methods is to use the conformal symmetry that emerges in the unitarity limit. The application of this symmetry-based approach to hydrodynamics revealed the vanishing bulk viscosity in the unitarity limit. Another non-perturbative approach is an expansion in terms of the fugacity, called the quantum virial expansion. In the high-temperature and low-density regime, this expansion is valid because the fugacity is small.

First of all, we focus on the bulk viscosity, which characterizes the dissipation caused by an expansion of the fluid volume. The vanishing bulk viscosity in the unitarity limit is intuitively understood because the entropy does not change before and after an isotropic expansion of the

fluid due to no interaction scales. In order to investigate the bulk viscosity for a finite scattering length, we extend the intuitive understanding of the vanishing bulk viscosity at unitarity to the case where the scattering length is finite. To do this, we construct hydrodynamics with a finite and spacetime-dependent scattering length. We show that the spacetime-dependent scattering length uniquely enters into a viscous term so as to represent the expansion and contraction of the fluid in both normal and superfluid phases. Consequently, we find that the entropy production due to the modulation of the scattering length is proportional to the bulk viscosity. Based on this finding, we propose a novel experimental probe for the bulk viscosity via the entropy production rate when the scattering length is temporally varied in a uniform system.

Next, we evaluate the transport coefficients via the Kubo formulas in the quantum virial expansion. Among the transport coefficients, we first discuss the bulk viscosity. As shown by our hydrodynamic equations, we can find the bulk viscosity in the dissipation produced by the varying scattering length. We confirm that the bulk viscosity can be found in the response to the scattering length from the linear response theory without relying on the hydrodynamics. We also express the Kubo formula for the bulk viscosity with a response function of the contact, which is the thermodynamically conjugate quantity to the scattering length. We then review the evaluation of the bulk viscosity up to the second order in fugacity. The bulk viscosity calculated from the quantum virial expansion does not fully agree with the one calculated from the kinetic theory. We point out that this discrepancy is due to a breakdown of the quasiparticle approximation underlying the kinetic theory at the first order in fugacity.

Finally, we compute the remaining two transport coefficients, i.e., the shear viscosity and the thermal conductivity, in the quantum virial expansion. In the calculations of these two transport coefficients, there is a singularity that reduces the order of the fugacity. We give an exact microscopic computation for the shear viscosity and the thermal conductivity in the high-temperature limit by taking into account the singularity. We derive a self-consistent equation for the vertex function which is needed to obtain the transport coefficients in the high-temperature limit. In particular, we show that the self-consistent equation is identical to the linearized Boltzmann equation. In addition to the microscopic theory using the quantum virial expansion, the kinetic theory has been used as another approach for transport in the high-temperature limit. Our results provide a direct relation between the two approaches and provide an interpretation of the kinetic theory in the high-temperature limit from the microscopic theory.

List of Publications

Publications relevant to this thesis

1. <u>Keisuke Fujii</u> and Yusuke Nishida,
   "Bulk viscosity of resonating fermions revisited: Kubo formula, sum rule, and the dimer and high-temperature limits,"
   Phys. Rev. A **102**, 023310 (2020). [arXiv:2004.12154]

2. <u>Keisuke Fujii</u> and Yusuke Nishida,
   "Hydrodynamics with spacetime-dependent scattering length,"
   Phys. Rev. A **98**, 063634 (2018). [arXiv:1807.07983]

Publications irrelevant to this thesis

1. Takuya Furusawa, <u>Keisuke Fujii</u> and Yusuke Nishida,
   "Hall viscosity in the A-phase of superfluid ^{3}He,"
   [arXiv:2008.08276]

2. Kazutaka Takahashi, Yuki Hino, <u>Keisuke Fujii</u>, and Hisao Hayakawa,
   "Full counting statistics and fluctuation-dissipation relation for periodically driven systems,"
   J. Stat. Phys. (2020) [arXiv:2003.11935]

3. Kazutaka Takahashi, <u>Keisuke Fujii</u>, Yuki Hino, and Hisao Hayakawa,
   "Nonadiabatic Control of Geometric Pumping,"
   Phys. Rev. Lett. **124**, 150602 (2020). [arXiv:1909.02202]

4. <u>Keisuke Fujii</u> and Yusuke Nishida,
   "Low-energy effective field theory of superfluid ^{3}He-B and its gyromagnetic and Hall responses,"
   Ann. Phys. **395**, 170-182 (2018) [arXiv:1610.06330]

Contents

Chapter 1

Introduction

1.1 Dilute gases near the Feshbach resonance in ultracold atoms

Ultracold atoms are created by laser cooling and evaporative cooling of an atomic cluster trapped in a vacuum by magnetic and optical methods [1–3]. By selecting the atomic species that constitute the cluster, we can create both fermionic and bosonic many-body systems. For instance, popular atomic species for bosonic systems are ^{87}Rb and ^{23}Na, and for fermionic systems ^{40}K and ^{6}Li. After evaporative cooling, ultracold atomic gases typically reach a number density n of about 10^{12} cm^{-3} at the center of the trap, with temperatures T of about 50 nK, resulting in ultracold dilute gases.[1] For typical experimental conditions, the quantum degeneracy temperature $T_{\text{deg}} \equiv \hbar^2 n^{2/3}/(2mk_{\text{B}})$, where m is the mass of the atoms, is near or below one microkelvin. Thus, the gases achieve quantum degeneracy and provide ideal platforms for study of quantum many-body systems.

More importantly, in ultracold atoms, the s-wave scattering length a, which is defined from the two-body scattering amplitude, can be tuned by applying an external magnetic field through the Feshbach resonance. The Feshbach resonance occurs when the kinetic energy of an incoming particle coincides with the binding energy in a closed channel [4]. For ultracold atoms, we trap atoms with the hyperfine structure and adjust the energy difference between open and closed channels, causing the Feshbach resonance between the hyperfine states. Because the energy difference between the hyperfine states can be controlled using an external magnetic field, we can induce the Feshbach resonances with the magnetic field. In the vicinity of the resonance, the scattering length a is given by

$$a = a_{\text{bg}} \left(1 - \frac{\Delta_B}{B - B_0} \right), \tag{1.1.1}$$

where the background scattering length a_{bg} represents the off-resonant value, Δ_B is the resonance width, and B_0 is the resonance position [5]. Fig. 1.1 shows the Feshbach resonances for a Bose–Einstein condensation of optically trapped ^{23}Na atoms [6]. Fig. 1.1 demonstrates the tunability of the scattering length, according to Eq. (1.1.1).

The tunability of the scattering length enables a situation where only the scattering length is relevant to the length scales of the interparticle interaction. For a short-range interaction

---

[1]One can see the diluteness of ultracold atoms by comparing the number densities of other systems. For instance, the number density of an ideal gas at 273.15 K (0°C) and 1 atm is 2.7×10^{19} cm^{-3}. In the same condition, the number densities of metals are typically about 10^{22} cm^{-3}.
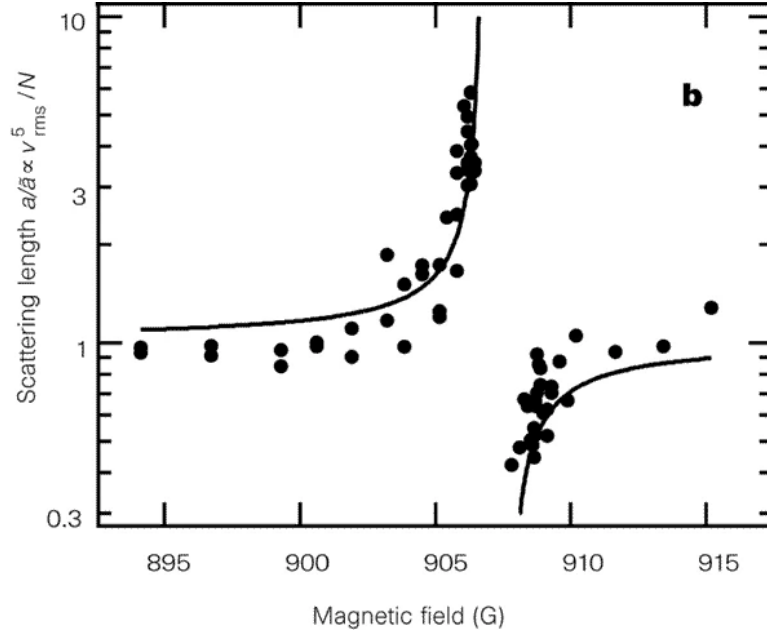
Figure 1.1:   Observation of the magnetically tuned scattering length for a Bose-Einstein condensation of optically trapped ^{23}Na atoms using the Feshbach resonance [6]. The horizontal axis represents the magnetic field, and the resonance occurs at about 907 G. The vertical axis represents the scattering length normalized to the background scattering length $a_{\rm bg} = \tilde{a}$, measured by the expansion after release from the trap. The solid line represents the scattering length given by Eq. (1.1.1).

at low energies,[2] the length scales due to the interaction are given by the scattering length a and the radius $r_{\rm R}$ of the interaction potential. In addition to the length scales due to the interaction, the gases have two length scales: the average interparticle distance $n^{-1/3}$ and the thermal de Broglie wavelength $\lambda_T \equiv \hbar\sqrt{2\pi/(mk_{\rm B}T)}$. Since the ultracold atomic gases are cold and dilute, the average interparticle distance and the thermal de Broglie wavelength are sufficiently larger than the radius $r_{\rm R}$. Moreover, the absolute value of the scattering length can be tuned to be sufficiently larger than $r_{\rm R}$. Therefore, in the vicinity of the resonance, the gases meet the condition of

$$r_{\rm R} \quad \ll \quad n^{-1/3},\ \lambda_T,\ |a|. \tag{1.1.2}$$

In this thesis, we refer to a two-component Fermi gas that satisfies this condition as a resonant Fermi gas. This condition allows $r_{\rm R}$ to be regarded as zero, which is referred to as the zero-range limit. In the zero-range limit, the interaction is characterized only by the scattering length. Because the interaction effects appear only through the scattering length, physical quantities show a universal behavior independent of the details of the interaction potential. Furthermore, the interaction strength can be tuned according to the scattering length, which is a remarkable feature of ultracold atoms [7]. This universality and the tunability of the

---

[2]A "short-range" interaction here does not need to decay exponentially, as long as its potential radius is small. For example, a typical interaction potential has a long-range tail of van der Waals potential r^{-6}, but with a radius of about 1 nm.

interaction strength connect the study of ultracold atoms to various fields of physics, such as high T_c-superconductors, nuclear matter, neutron stars, and quark-gluon plasmas [8,9].

For example, the tunability enabled the observation of the BCS-BEC crossover [10–15]. The BCS-BEC crossover is the phenomenon in resonant Fermi gases which vary without a phase transition from the fermionic superfluid described by the Bardeen–Cooper–Schrieffer theory to the bosonic superfluid of a Bose–Einstein condensate of tightly bound molecules, along with an increase in the attractive interaction strength between the particles. This increase in the attractive interaction can be realized by increasing the inverse of the scattering length, resulting in a free Fermi gas for $(k_\mathrm{F}a)^{-1} \to -\infty$ and a free Bose gas for $(k_\mathrm{F}a)^{-1} \to +\infty$, where k_F is the Fermi wavevector. Here, the radius r_R is assumed to be small $k_\mathrm{F}r_\mathrm{R} \to 0$. Fermionic superfluids with a large scattering length have been suggested to be linked to nuclear matter [16,17] and high-T_c superconductors [18].

1.2 Thermodynamic properties of resonant Fermi gases

For a mass-balanced two-component, i.e., spin-1/2, Fermi gas with a large scattering length, which we refer to as a resonant Fermi gas, the free energy F is entirely determined only by the temperature T, the volume V, the number of particles N, and the scattering length a, due to the universality. With the help of the dimensional analysis, one can write down the free energy as

$$F(T,V,N;a) = \varepsilon_\mathrm{F} N f_F(k_\mathrm{B}T/\varepsilon_\mathrm{F}, \hbar a/\sqrt{2m\varepsilon_\mathrm{F}}), \qquad (1.2.1)$$

where $\varepsilon_\mathrm{F} \equiv \left(2\pi^2 N/V\right)^{2/3} \hbar^2/(2m)$ is the Fermi energy, and f_F is a function of two dimensionless ratios. This function f_F is significant in the regime with a large scattering length because it is responsible for the universality. In particular, at the resonance point, where the scattering length diverges, the function f_F turns into a single-variable function $\tilde{f}_F(k_\mathrm{B}T/\varepsilon_\mathrm{F})$ defined by

$$\tilde{f}_F(k_\mathrm{B}T/\varepsilon_\mathrm{F}) \equiv \lim_{|a|\to\infty} f_F(k_\mathrm{B}T/\varepsilon_\mathrm{F}, \hbar a/\sqrt{2m\varepsilon_\mathrm{F}}). \qquad (1.2.2)$$

The thermodynamic properties are governed by the single-variable function $\tilde{f}_F$, just like the free Fermi gas, although the system is strongly interacting. The thermodynamics at the resonance point is referred to as the universal thermodynamics [19–21], and the function $\tilde{f}_F$ was measured in ultracold atoms experiments [22–24].

The limit with an infinite scattering length is called the unitarity limit because it saturates the s-wave scattering cross-section to the maximum value allowed by the unitarity condition of the scattering matrix. A resonant Fermi gas in the unitarity limit, which we refer to as the unitary Fermi gas, is the most pronounced system for the universality owing to the absence of length scales in the interaction. The universal thermodynamics is an example of the universal properties of the unitary Fermi gas. The absence of length scales also makes the unitary Fermi gas a conformal invariant system, which is another example of the universal properties [25–27]. The conformal invariance provides insights into some properties of the unitary Fermi gas in terms of symmetry, as we see later.

Another universal property of the resonant Fermi gases is universal relations that connect their short-range correlations to thermodynamic properties [28–34]. Because the universal relations hold for any number of particles, temperature, and scattering length, they offer

valuable information even in the strongly correlated regime. For example, the wavevector
spectrum has a power-law tail at large $|\boldsymbol{k}|$ as

$$\lim_{|\boldsymbol{k}|\to\infty} |\boldsymbol{k}|^4 n_\sigma(\boldsymbol{k}) = C \qquad (\sigma =\uparrow,\downarrow), \tag{1.2.3}$$

where the spectrum $n_\sigma(\boldsymbol{k})$ is normalized so that the total number of fermions with spin σ is
given by

$$N_\sigma = \int \frac{\mathrm{d}\boldsymbol{k}}{(2\pi)^3} n_\sigma(\boldsymbol{k}). \tag{1.2.4}$$

The origin of the power-law tail lies in the short-range singularity due to the zero-range limit.
Here, C is the coefficient of the tail of the spectrum $n_\sigma(\boldsymbol{k})$ and is called the contact. The
contact characterizes the short-range correlation because it appears due to the short-range
singularity. On the other hand, the contact is also related to thermodynamic quantities. A
representative example is the adiabatic relation:

$$\left(\frac{\partial F}{\partial a^{-1}}\right)_{T,V,N} = -\frac{\hbar^2}{4\pi m} C. \tag{1.2.5}$$

Eqs. (1.2.3) and (1.2.5) connect the short-range correlations and the thermodynamic quanti-
ties through the contact. The contact plays a central role in the universal relations. While
the contact appears in various thermodynamic quantities originating from Eq. (1.2.5), it also
appears in power-law tails of various physical quantities such as the dynamical structure fac-
tor [35–38] and the viscosity spectral function [36,39], as well as in the wavenumber spectrum.

1.3 Transport properties of resonant Fermi gas

The universality of the resonant Fermi gases appears not only in thermodynamics but also
in transport phenomena. The transport properties can be experimentally investigated from
observations, such as the expansion dynamics after release from the trap [40,41]. The atten-
uation and dissipation in these processes are governed by the shear viscosity η and the bulk
viscosity ζ [42,43]. It has been confirmed that the shear viscosity is remarkably small [44–48],
and the bulk viscosity is zero in the unitarity limit [46]. Because of the small viscosities, the
resonant Fermi gases are said to be an almost "perfect fluid."

The vanishing bulk viscosity in the unitarity limit can be understood in terms of the
conformal invariance [49]. The bulk viscosity appears as a coefficient of the entropy production
associated with the expansion and contraction of the fluid. In scale-invariant systems, because
of the absence of intrinsic length scales, the entropy of the system does not increase during an
isotropic expansion, where the fluid velocity $\boldsymbol{v}(t,\boldsymbol{x})$ at point $\boldsymbol{x}$ being $\boldsymbol{v}(t,\boldsymbol{x}) = c\boldsymbol{x}$ with some
constant c. This non-production of the entropy means that the bulk viscosity is zero. The
vanishing bulk viscosity can be seen in the non-damping mode for expansion and contraction.
In particular, the unitary Fermi gas in a harmonic trap has an oscillating mode that expands
and contracts with twice the trap potential frequency, which is called the breathing mode [27,
50, 51]. Conversely, the presence of the bulk viscosity is a signal of the breaking of scale
invariance. For example, the model of the two-dimensional Fermi gases in the zero-range
limit classically has a scale invariance, but the scale invariance is broken by quantum effects,

which result in the appearance of the scattering length. This breaking can be detected via the bulk viscosity and was measured from the damping of the breathing mode [52–55].

For the shear viscosity, a conjecture about the ratio of the shear viscosity η to the entropy density s is of interest [56]. This conjecture is that the ratio η/s should be bounded from below as

$$\frac{\eta}{s} \geq \frac{\hbar}{4\pi k_{\mathrm{B}}}. \tag{1.3.1}$$

This conjecture was originally derived from gravity duals based on string theory and proposed for relativistic quantum field theories at finite temperature and zero chemical potential. However, since Eq. (1.3.1) does not involve the speed of light, it was speculated that Eq. (1.3.1) might be valid even in nonrelativistic systems. This conjecture has motivated the search for the "perfect fluid" which realizes, or at least comes close to, the lower-bound. In particular, because a $\mathcal{N} = 4$ supersymmetric Yang-Mills theory in the limit of infinite 't Hooft coupling realizes the lower bound of the ratio [57], strongly correlated systems such as the unitary Fermi gas is expected to realize the "perfect fluid." In fact, the minimum values of the ratio η/s was estimated for some fluids: $\eta/s \sim 25$ for H_2O, $\eta/s \sim 8.8$ for ^{4}He, $\eta/s \sim 6.3$ for ^{6}Li at unitarity, and $\eta/s \sim 5.0$ for quark-gluon plasma, with $\hbar/(4\pi k_{\mathrm{B}})$ as the unit [58, 59]. The unitary Fermi gas is said to achieve a ratio close to the lower bound. Although there are some counter-proposals that suggest different lower bounds on the ratio [60–64], it is interesting that the ratio has a non-zero lower bound, and it is an important problem to derive the lower bound from the principles of quantum statistical physics. The resonant Fermi gas provides a research platform for this problem.

1.4 Purposes and outline of this thesis

In this thesis, we investigate transport phenomena of the resonant Fermi gases in two and three dimensions to understand the universal nature of transport in strongly correlated quantum many-body systems. We particularly focus on the transport coefficients such as the bulk viscosity, the shear viscosity, and the thermal conductivity. We perform two studies to discuss the transport coefficients for an arbitrary scattering length: construction of hydrodynamics with a spacetime-dependent scattering length [Chapter 3] and evaluation of the transport coefficients in the quantum virial expansion [Chapthers 4 and 5].

We begin with a review of the universality of the resonant Fermi gas in Chapter 2. Then, as preparation for calculating the transport coefficients, we review the Kubo formulas for the transport coefficients [65–68]. Finally, we review the kinetic theory approach to the transport coefficients in the high-temperature limit [69–75].

In Chapter 3, we focus on the bulk viscosity. As already explained, the bulk viscosity vanishes in the unitarity limit [49]. This vanishing bulk viscosity at unitarity is intuitively understood because the entropy is not produced during an isotropic expansion of the fluid due to no reference scales in interactions. In order to investigate the bulk viscosity for a finite scattering length, we extend this intuitive understanding of the isotropic expansion at unitarity to the case where the scattering length is finite. A finite scattering length, which is the only reference scale in the interaction, characterizes the isotropic expansion process. Namely, the expansion process is understood as an increase in the fluid volume relative to the reference volume element a^3. This understanding of the expansion as the

comparison of the volumes suggests that an isotropic expansion of the fluid volume at a fixed scattering length can be regarded as equivalent to a contraction of the scattering length at a fixed fluid density. We consider a resonant Fermi gas whose scattering length is modulated over spacetime to construct hydrodynamic equations that involve this equivalence. One can realize the spacetime-dependent scattering length by applying a modulated magnetic field over spacetime because the scattering length is tuned via an external magnetic field [76–78]. We show that the spacetime-dependent scattering length enters the hydrodynamic equations uniquely so as to represent the expansion and contraction of the fluid in both normal and superfluid phases. As a consequence of our hydrodynamics, we propose a novel experimental probe for the bulk viscosity via the entropy density production due to a temporal change in the scattering length. Also, we find that a leading dissipative correction to the contact density due to the spacetime-dependent scattering length is proportional to the bulk viscosity.

We calculate the bulk viscosity in Chapter 4 and the shear viscosity and the thermal conductivity in Chapter 5 using a systematic expansion method whose expansion parameter is the fugacity $z \equiv e^{\mu/(k_\mathrm{B}T)}$. Here, T is the temperature, and μ the chemical potential. In the high-temperature and low-density regime $n\lambda_T^d \ll 1$, the fugacity z is small. Thus, physical quantities can be expanded systematically in terms of the fugacity. This expansion, which is called the quantum virial expansion, has been widely used to calculate thermodynamic quantities because it is valid even in strongly coupled regimes such as near the unitarity limit [79–88]. The transport coefficients were recently computed via the Kubo formulas in the quantum virial expansion [39, 89–93]. As reviewed in Chapter 2, the transport coefficients in the high-temperature limit were calculated using the kinetic theory [69–75]. For the bulk viscosity, the microscopic results using the quantum virial expansion are not consistent with the kinetic ones. In contrast, for the shear viscosity and the thermal conductivity, the microscopic results with an approximate resummation in the quantum virial expansion are consistent with the kinetic results in the relaxation-time approximation.

In Chapter 4, we calculate the bulk viscosity in the quantum virial expansion. As shown in Chapter 3, the bulk viscosity can be found in the response of the contact when the scattering length is varied. We express the Kubo formula for the bulk viscosity with the contact-contact response function and confirm that the bulk viscosity is found in the response of the contact to the varying scattering length from the linear response theory. We then review the computaition of the contact-contact response function up to the second order of the fugacity and the evaluation of the bulk viscosity. We discuss the computation for the bulk viscosity using the kinetic theory in the high-temperature limit and show that the kinetic theory is not capable of computing the bulk viscosity up to the second order of the fugacity.

In the calculations of the shear viscosity and the thermal conductivity, there is a singularity that reduces the order of the fugacity by one. In Chapter 5, we give an exact microscopic computation for the shear viscosity and the thermal conductivity in the leading order of the fugacity by taking into account the singularity. We derive the self-consistent equation for the vertex function which is needed to obtain the transport coefficients in the high-temperature limit (or equivalently, in the leading order). Furthermore, we show that the self-consistent equation is equivalent to the linearized Boltzmann equation, which means that the microscopic calculations agree with the kinetic calculations without any approximation for the transport coefficients in the high-temperature limit.

Finally, in Chapter 6, we conclude this thesis and discuss some remarks on prospects.

In what follows, we set $\hbar = k_{\rm B} = 1$ and employ the shorthand notations $\partial_t \equiv \partial/\partial t$, $\partial_i \equiv \partial/\partial x^i$ and $\phi \overset{\leftrightarrow}{\partial}_\mu \psi \equiv [\phi(\partial_\mu \psi) - (\partial_\mu \phi)\psi]/2$ with $\mu = t$ or i. Unless otherwise specified, we assume implicit sums over repeated indices for the subscript of the spatial coordinates as well as for $[v_i]^2 \equiv v_i v_i$. Also, an integration over a d-dimensional wavevector or momentum is denoted by $\int_{\boldsymbol{k}} \equiv \int \mathrm{d}\boldsymbol{k}/(2\pi)^d$ for the sake of brevity.

Chapter 2

Review for transport of resonant Fermi gases

In this section, we review three topics in relevance to the transport of the resonant Fermi gases. We first review the universality of the resonant Fermi gases in Sec. 2.1. We next review the Kubo formulas for transport coefficients in Sec. 2.2. Sec. 2.3 is devoted to a review of the kinetic theory approach for the resonant Fermi gases at high temperatures.

2.1 Universality of resonant Fermi gases

For the resonant Fermi gases, we consider a two-component fermionic many-body system, consisting of spin ↑- and ↓-particles with the same mass m in two and three dimensions.

2.1.1 Two-body scattering

Let us discuss the scattering problem between two particles with different spins in three dimensions. We discuss the scattering problem in two dimensions later. By focusing on the relative motion, the problem can be reduced to that of a single particle scattered by a spherical potential $V(|\boldsymbol{x}|)$. The single-particle problem is described by the three-dimensional Schrödinger equation given by

$$\left[-\frac{1}{2m_r}\nabla^2 + V(|\boldsymbol{x}|) \right] \Psi(\boldsymbol{x}) = E\Psi(\boldsymbol{x}), \tag{2.1.1}$$

where $m_r \equiv m/2$ denotes the reduced mass and E the scattering energy. To obtain scattering states, we suppose that the energy E is positive and denote it as $E = k^2/(2m_r)$ with momentum $k > 0$ of the incoming particle. Let the radius of the potential be $r_{\rm R}$, and let the potential decrease sufficiently in $|\boldsymbol{x}| \gg r_{\rm R}$. A boundary condition at infinity imposes that the wave function is a superposition of the plane wave e^{ikz} of the incoming particle and the outward scattering wave $e^{ik|\boldsymbol{x}|}/|\boldsymbol{x}|$:

$$\Psi(\boldsymbol{x}) \xrightarrow{|\boldsymbol{x}| \to \infty} e^{ikz} + f_k(\Omega)\frac{e^{ik|\boldsymbol{x}|}}{|\boldsymbol{x}|}, \tag{2.1.2}$$

where $f_k(\Omega)$ is the scattering amplitude and Ω the spherical angles of an outgoing direction. For the spherical potential, the angular momentum ℓ is a good quantum number, so that the

scattering amplitude $f_k(\Omega)$ can be decomposed into independent partial-wave components as

$$f_k(\Omega) = \sum_{\ell=0}^{\infty} (2\ell + 1) f_\ell(k) P_\ell(\cos\theta), \tag{2.1.3}$$

where $P_\ell(\cos\theta)$ denotes the Legendre polynomials and θ is the angle between the incoming direction (z-axis) and an outgoing direction. The scattering amplitude for the ℓ-th partial wave can be represented as

$$f_\ell(k) = \frac{1}{k \cot \delta_\ell(k) - ik}, \tag{2.1.4}$$

where $\delta_\ell(k)$ is the ℓ-th wave phase shift [94].

If the potential $V(|\boldsymbol{x}|)$ decreases exponentially, the phase shift is expand for small k as

$$\delta_\ell(k) \sim k^{2\ell+1}. \tag{2.1.5}$$

In reality, the interaction potential between particles is estimated as r^{-n} at large distance, as in the van der Waals potential r^{-6}. In this case, the phase shift for small k is given by [94, 95]

$$\delta_\ell(k) \sim \begin{cases} k^{2\ell+1} & \ell < (n-3)/2, \\ k^4 & \ell \geq (n-3)/2. \end{cases} \tag{2.1.6}$$

Considering the case of the van der Waals potential $n = 6$, a low-energy expansion of the phase shift is given by

$$k \cot \delta_\ell(k) = \begin{cases} -a^{-1} + \dfrac{r_{\rm eff}}{2} k^2 + O(k^3) & \ell = 0, \\ O(k^{-2}) & \ell = 1, \\ O(k^{-3}) & \ell \geq 2, \end{cases} \tag{2.1.7}$$

where a is the s-wave scattering length and $r_{\rm eff}$ the effective range. Therefore, at low energies, the zeroth scattering amplitude $f_{\ell=0}(k)$ is dominant and the scattering amplitude is expressed as

$$f_k(\Omega) = f_{\ell=0}(k) = -\frac{1}{a^{-1} - \dfrac{r_{\rm eff}}{2} k^2 + ik}. \tag{2.1.8}$$

For further low-energy approximation, we assume that the absolute value of the effective range is at most about the radius of the potential: $|r_{\rm eff}| \lesssim r_{\rm R}$. This assumption is satisfied experimentally by using atoms whose resonance width Δ_B of Eq. (1.1.1) is large, and such a resonance with a large resonance width is called the broad Feshbach resonance [7]. Under this assumption, as discussed in Chapter 1, we can ignore the effective range along with the potential radius when the absolute value of the scattering length is sufficiently larger than the potential radius. Thus, in the zero-range limit $r_{\rm R} \to 0$, the effective-range term becomes irrelevant and the scattering amplitude is simply obtained by

$$f_k(\Omega) = -\frac{1}{a^{-1} + ik}. \tag{2.1.9}$$

Since poles of the scattering amplitude on the positive imaginary axis of k correspond to bound states, there is a bound state with the following binding energy $E_{\rm bind}$ for $a > 0$:

$$E_{\rm bind} = \frac{k_{\rm pole}^2}{2m_r} = -\frac{1}{ma^2} \qquad ([f_{k_{\rm pole}}(\Omega)]^{-1} = 0). \tag{2.1.10}$$

At this point, we can see the universality that the behaviors of the system do not depend on the details of the interaction potential $V(|\boldsymbol{x}|)$. The scattering amplitude (2.1.9) is expressed only by the scattering length a, which means that the system shows the same behavior at low energies even for different interaction potentials as long as the scattering length is the same.

We briefly discuss two-body scattering in two dimensions. In two dimensions, the boundary condition at infinity is given by

$$\Psi(\boldsymbol{x}) \xrightarrow{|\boldsymbol{x}|\to\infty} e^{ikx} - \sqrt{\frac{i}{8\pi k}} f_k(\theta) \frac{e^{ik|\boldsymbol{x}|}}{\sqrt{|\boldsymbol{x}|}}. \tag{2.1.11}$$

For the spherical potential, the scattering amplitude is decomposed into independent partial-wave components as [8, 96]

$$f_k(\theta) = \sum_{\ell=0}^{\infty} (2 - \delta_{\ell,0}) f_\ell(k) \cos(\ell\theta). \tag{2.1.12}$$

The scattering amplitude for the ℓ-th partial wave is expressed by the phase shift $\delta_\ell(k)$ as

$$f_\ell(k) = \frac{-4}{\cot\delta_\ell(k) - i} = -4e^{i\delta_\ell(k)} \sin\delta_\ell(k). \tag{2.1.13}$$

As in the three-dimensional case, the zeroth partial wave component $f_{\ell=0}(k)$ is dominant at low energies, and the low-energy expansion of the scattering amplitude is obtained by

$$f_k(\theta) = f_{\ell=0}(k) = \frac{-4\pi}{2\ln(ka) - i\pi}, \tag{2.1.14}$$

where a is the scattering length in two dimensions. In two dimensions, the scattering length a is always positive and the attractive potential with any strength induces a zero-energy bound state. Also, the scattering amplitude has a pole corresponding to the bound state of the binding energy $E_{\text{bind}} = -1/(ma^2)$, as in the case of three dimensions.

2.1.2   Contact interaction

By virtue of the universality, we can take a simple interaction potential among the potentials with the scattering length a. According to the zero-range limit, we employ a delta function potential as the interaction potential, which is called a contact interaction. Then, in the second-quantized formalism, the Hamiltonian of the two-component fermions in d spatial dimensions is given by

$$\hat{H} = \sum_{\sigma=\uparrow,\downarrow} \int d\boldsymbol{x}\, \hat{\psi}_\sigma^\dagger(\boldsymbol{x}) \frac{-\nabla^2}{2m} \hat{\psi}_\sigma(\boldsymbol{x}) + \frac{g}{2} \sum_{\sigma,\rho} \int d\boldsymbol{x}\, \hat{\psi}_\sigma^\dagger(\boldsymbol{x}) \hat{\psi}_\rho^\dagger(\boldsymbol{x}) \hat{\psi}_\rho(\boldsymbol{x}) \hat{\psi}_\sigma(\boldsymbol{x}), \tag{2.1.15}$$

where g is the bare coupling constant between two fermions. Here, the annihilation and creation operators satisfy the canonical anti-commutation relations

$$\begin{aligned} \{\hat{\psi}_\sigma(\boldsymbol{x}),\, \hat{\psi}_\rho^\dagger(\boldsymbol{y})\} &= \delta_{\sigma\rho}\delta^d(\boldsymbol{x} - \boldsymbol{y}), \\ \{\hat{\psi}_\sigma(\boldsymbol{x}),\, \hat{\psi}_\rho(\boldsymbol{y})\} &= \{\hat{\psi}_\sigma^\dagger(\boldsymbol{x}),\, \hat{\psi}_\rho^\dagger(\boldsymbol{y})\} = 0. \end{aligned} \tag{2.1.16}$$

Let us consider the two-body scattering T-matrix to discuss two-body scattering in this model. The T-matrix $\mathcal{T}_2(p_0, \boldsymbol{p})$ obeys the following Lippmann-Schwinger equation:

$$
-i\mathcal{T}_2(p_0, \boldsymbol{p}) = -ig + \frac{1}{L^d} \int \frac{\mathrm{d}k_0}{2\pi} \sum_{\boldsymbol{k}} (-ig)
$$
$$
\times \frac{i}{\frac{p_0}{2} - k_0 - \epsilon_{\boldsymbol{p}/2-\boldsymbol{k}} + i0^+} \frac{i}{\frac{p_0}{2} + k_0 - \epsilon_{\boldsymbol{p}/2+\boldsymbol{k}} + i0^+} \left(-i\mathcal{T}_2(p_0, \boldsymbol{p}) \right),
\tag{2.1.17}
$$

where $\epsilon_{\boldsymbol{p}} \equiv \boldsymbol{p}^2/(2m)$ is the kinetic energy and 0^+ denotes an infinitesimal positive real number. Here, L^d is the volume of the system and we take the infinite-volume limit $L^{-d} \sum_{\boldsymbol{k}} \to \int_{\boldsymbol{k}}$ as needed. From the Lippmann-Schwinger equation, the T-matrix can be written as

$$
\mathcal{T}_2(p_0, \boldsymbol{p}) = \frac{1}{g^{-1} - \Pi_{\mathrm{polar}}(p_0, \boldsymbol{p})},
\tag{2.1.18}
$$

where $\Pi_{\mathrm{polar}}(p_0, \boldsymbol{p})$ is the polarization function given by

$$
\Pi_{\mathrm{polar}}(p_0, \boldsymbol{p}) = -i\frac{1}{L^d} \int \frac{\mathrm{d}k_0}{2\pi} \sum_{\boldsymbol{k}} \frac{i}{\frac{p_0}{2} - k_0 - \epsilon_{\boldsymbol{p}/2-\boldsymbol{k}} + i0^+} \frac{i}{\frac{p_0}{2} + k_0 - \epsilon_{\boldsymbol{p}/2+\boldsymbol{k}} + i0^+}
$$
$$
= \frac{1}{L^d} \sum_{\boldsymbol{k}} \frac{1}{p_0 - \epsilon_{\boldsymbol{p}}/2 - 2\epsilon_{\boldsymbol{k}} + i0^+}.
\tag{2.1.19}
$$

This polarization function has a ultraviolet divergence for $d = 2, 3$. To avoid this divergence, we employ a dimensional regularization. The polarization function in the infinite-volume limit is computed as

$$
\Pi_{\mathrm{polar}}(p_0, \boldsymbol{p}) = \int_{\boldsymbol{k}} \frac{1}{p_0 - \epsilon_{\boldsymbol{p}}/2 - \frac{k^2}{m} + i0^+} = -m \frac{\Gamma(1 - d/2)}{(4\pi)^{d/2}} (-m(p_0 - \epsilon_{\boldsymbol{p}}/2) - i0^+)^{d/2-1},
\tag{2.1.20}
$$

where we use the following identities for the gamma function:

$$
\frac{\Gamma(x)\Gamma(y)}{\Gamma(x+y)} = \int_0^1 \mathrm{d}s \, s^{y-1}(1-s)^{x-1} = (-1)^y \int_0^\infty \mathrm{d}s \, \frac{s^{y-1}}{(1-s)^{x+y}}.
\tag{2.1.21}
$$

In Eq. (2.1.20), the divergence of the polarization function is expressed by that of the gamma function. The analytic contionuation for the gamma function eliminates the divergence for $d = 3$ because of $\Gamma(-1/2) = -2\sqrt{\pi}$. Also, the divergence for $d = 2$ can be avoided by setting $d = 2 - \delta$ and expanding the gamma function for an infinitesimally small quantity δ. Therefore, the T-matrix in the infinite-volume limit is found to be

$$
\mathcal{T}_2(p_0, \boldsymbol{p}) = \mathcal{T}_a(p_0 - \epsilon_{\boldsymbol{p}}/2 + i0^+),
\tag{2.1.22}
$$

where we define the T-matrix in the center-of-mass frame as

$$
\mathcal{T}_a(\varepsilon + i0^+) = \frac{1}{g^{-1} - \frac{m}{(d-2)\Omega_{d-1}}(-m\varepsilon - i0^+)^{d/2-1}}
\tag{2.1.23}
$$

with

$$
\Omega_{d-1} \equiv \frac{(4\pi)^{d/2}}{2\Gamma(2 - d/2)} = \begin{cases} 2\pi & d = 2, \\ 4\pi & d = 3. \end{cases}
\tag{2.1.24}
$$

The on-shell T-matrix in the center-of-mass frame is related to the scattering amplitude, $-(4\pi/m)f_k(\Omega) = \mathcal{T}_a(\boldsymbol{p}^2/m + i0^+)$ for $d = 3$ and $(1/m)f_k(\theta) = \mathcal{T}_a(\boldsymbol{p}^2/m + i0^+)$ for $d = 2$. From these relations, we define the scattering length a in d spatial dimensions so that the pole existing for $a > 0$ corresponds to the binding energy $E_{\text{bind}} = -1/(ma^2)$, and thus we find

$$\frac{1}{g} = \frac{ma^{2-d}}{(d-2)\Omega_{d-1}}, \tag{2.1.25}$$

and

$$\mathcal{T}_a(\varepsilon + i0^+) = \frac{\Omega_{d-1}}{m}\frac{d-2}{a^{2-d} - (-m\varepsilon - i0^+)^{d/2-1}}$$

$$= \begin{cases} \dfrac{1}{m}\dfrac{-4\pi}{\ln(-ma^2\varepsilon - i0^+)} & d = 2, \\[3mm] \dfrac{4\pi}{m}\dfrac{1}{a^{-1} - \sqrt{-m\varepsilon - i0^+}} & d = 3. \end{cases} \tag{2.1.26}$$

Eq. (2.1.25) connects the bare coupling constant g to the scattering length a in the dimensional regularization.

2.2   Kubo formulas for transport coefficients

In this section, we review the Kubo formulas for transport coefficients, especially viscosity coefficients. Transport coefficients are defined in hydrodynamics as coefficients for dissipation. The Kubo formulas are obtained by matching linear responses computed in a microscopic theory with those computed in hydrodynamics. Our discussion here follows mainly that in Ref. [68].

2.2.1   Microscopics

Let us first consider a microscopic system that is weakly perturbed by an external field. For viscosity coefficients, the external field is taken to be a vector potential corresponding to a fluid velocity. The perturbed Hamiltonian is given by

$$\hat{H}^A(t) = \sum_\sigma \int d\boldsymbol{x}\, \frac{[\vec{D}\psi_\sigma(\boldsymbol{x})]^\dagger \cdot [\vec{D}\psi_\sigma(\boldsymbol{x})]}{2m} + \hat{V}, \tag{2.2.1}$$

where $\vec{D} \equiv \nabla - i\boldsymbol{A}(t, \boldsymbol{x})$ is the covariant derivative. Here, the unperturbed Hamiltonian $\hat{H}$ is intended to be a general Hamiltonian, including the one with the contact interaction of Eq. (2.1.15). The current density operator is defined by

$$\hat{\mathcal{J}}_i^A(t, \boldsymbol{x}) \equiv -m\frac{\delta \hat{H}^A(t)}{\delta A_i(t, \boldsymbol{x})} = \hat{\mathcal{J}}_i(\boldsymbol{x}) - \hat{\mathcal{M}}(\boldsymbol{x})\frac{A_i(t, \boldsymbol{x})}{m}, \tag{2.2.2}$$

where $\hat{\mathcal{M}}(\boldsymbol{x})$ and $\hat{\mathcal{J}}_i(\boldsymbol{x})$ is the unperturbed mass density operator and mass current density operator given by

$$\hat{\mathcal{M}}(\boldsymbol{x}) = m\sum_\sigma \hat{\psi}_\sigma^\dagger(\boldsymbol{x})\hat{\psi}_\sigma(\boldsymbol{x}), \qquad \hat{\mathcal{J}}_i(\boldsymbol{x}) = -i\sum_\sigma \hat{\psi}_\sigma^\dagger(\boldsymbol{x})\overleftrightarrow{\partial_i}\hat{\psi}_\sigma(\boldsymbol{x}). \tag{2.2.3}$$

Suppose that at the initial time $t = -\infty$, the external field is zero, i.e., $A_i(-\infty, \boldsymbol{x}) = 0$, and the density matrix operator is prepared in thermal equilibrium,

$$\hat{\rho}(-\infty) = \hat{\rho}_{\text{eq}} = \frac{1}{Z} e^{-\beta(\hat{H} - \mu\hat{N})}, \tag{2.2.4}$$

with the partition function $Z \equiv \text{Tr}[e^{-\beta(\hat{H} - \mu\hat{N})}]$. Then, according to the linear response theory, the expectation value of the mass current density is given by

$$\begin{aligned}
\mathcal{J}_i(t, \boldsymbol{x}) &\equiv \text{Tr}[\hat{\mathcal{J}}_i^A(t, \boldsymbol{x})\hat{\rho}(t)] \\
&= \langle \hat{\mathcal{J}}_i^A(t, \boldsymbol{x}) \rangle + i \int_{-\infty}^t \mathrm{d}t' \int \mathrm{d}\boldsymbol{x}' \, \langle [\hat{\mathcal{J}}_i(t, \boldsymbol{x}), \hat{\mathcal{J}}_j(t', \boldsymbol{x}')] \rangle \frac{A_j(t', \boldsymbol{x}')}{m} + O(A^2),
\end{aligned} \tag{2.2.5}$$

where $\hat{\mathcal{O}}(t, \boldsymbol{x}) \equiv e^{i\hat{H}t}\hat{\mathcal{O}}(\boldsymbol{x})e^{-i\hat{H}t}$ is an operator in the Heisenberg picture and $\langle \hat{\mathcal{O}} \rangle \equiv \text{Tr}[\hat{\mathcal{O}}\hat{\rho}_{\text{eq}}]$ is an expectation value at the thermal equilibrium. By setting $\langle \hat{\mathcal{M}}(t, \boldsymbol{x}) \rangle = \mathcal{M}$ and $\langle \hat{\mathcal{J}}_i(t, \boldsymbol{x}) \rangle = 0$, the Fourier components of the expectation value is obtained by

$$\begin{aligned}
\mathcal{J}_i(w, \boldsymbol{k}) &\equiv \int_{-\infty}^{\infty} \mathrm{d}t \int \mathrm{d}\boldsymbol{x} \, e^{iwt - i\boldsymbol{k}\cdot\boldsymbol{x}} \mathcal{J}_i(t, \boldsymbol{x}) \\
&= -\left[\mathcal{M}\delta_{ij} - \mathcal{R}_{\mathcal{J}_i\mathcal{J}_j}(w, \boldsymbol{k}) \right] \frac{A_j(w, \boldsymbol{k})}{m} + O(A^2),
\end{aligned} \tag{2.2.6}$$

where the response function $\mathcal{R}_{\mathcal{AB}}(w, \boldsymbol{k})$ is defined by

$$\mathcal{R}_{\mathcal{AB}}(w, \boldsymbol{k}) \equiv i \int_0^{\infty} \mathrm{d}t \int \mathrm{d}\boldsymbol{x} \, e^{iwt - i\boldsymbol{k}\cdot\boldsymbol{x}} \langle [\hat{\mathcal{A}}(t, \boldsymbol{x}), \hat{\mathcal{B}}(0, \boldsymbol{0})] \rangle. \tag{2.2.7}$$

Here, w represents a complex frequency with $\text{Im}[w] > 0$. Although w is eventually replaced by $\omega + i0^+$ for a real frequency ω, it is technically helpful to work in the upper-half plane of the complex frequency w in the process of the computation and to deal with the infinitesimal imaginary part $i0^+$ at the very end.

2.2.2 Hydrodynamics

Next, we consider the same system in terms of hydrodynamics. Hydrodynamics is a low-energy effective theory describing long-time and long-distance dynamics for correlated systems and is valid on scales larger than scales that characterize the thermalization process, such as a relaxation time and a mean free path. On this scale, the system is considered to be in local thermal equilibrium, where thermal equilibrium is realized at each point in spacetime, and local thermodynamic quantities describe the system. Hydrodynamic equations describing the motion of the local thermodynamic quantities are given in the form of continuity equations for mass, momentum, and energy [97],

$$\partial_t \mathcal{M}(t, \boldsymbol{x}) + \partial_i \mathcal{J}_i(t, \boldsymbol{x}) = 0, \tag{2.2.8}$$

$$\partial_t \mathcal{J}_i(t, \boldsymbol{x}) + \partial_j \Pi_{ij}(t, \boldsymbol{x}) = \frac{1}{m}\left[\mathcal{M}(t, \boldsymbol{x})E_i(t, \boldsymbol{x}) + \mathcal{J}_j(t, \boldsymbol{x})F_{ij}(t, \boldsymbol{x}) \right], \tag{2.2.9}$$

$$\partial_t \mathcal{H}(t, \boldsymbol{x}) + \partial_i \mathcal{Q}_i(t, \boldsymbol{x}) = \frac{1}{m}\mathcal{J}_i(t, \boldsymbol{x}) \cdot E_i(t, \boldsymbol{x}), \tag{2.2.10}$$

where $\Pi_{ij}(t, \boldsymbol{x})$ denotes the stress tensor, $\mathcal{H}(t, \boldsymbol{x})$ the energy density, $\mathcal{Q}_i(t, \boldsymbol{x})$ the energy current density. The right-hand sides of these equations represent the external forces due to

the external vector field as the electric field $E_i(t, \boldsymbol{x}) = -\partial_t A_i(t, \boldsymbol{x})$ and the magnetic field $F_{ij}(t, \boldsymbol{x}) = \partial_i A_j(t, \boldsymbol{x}) - \partial_j A_i(t, \boldsymbol{x})$. In order for the hydrodynamic equations to form a set of closed equations, the conserved charge densities and their current densities are to be expressed in terms of the local thermodynamic quantities and the fluid velocity $v_i(t, \boldsymbol{x})$. Such equations for the densities and the current densities are called constitutive relations. The constitutive relations for normal fluids read

$$\mathcal{J}_i(t, \boldsymbol{x}) = \mathcal{M}(t, \boldsymbol{x}) v_i(t, \boldsymbol{x}), \tag{2.2.11}$$

$$\mathcal{H}(t, \boldsymbol{x}) = \mathcal{E}(t, \boldsymbol{x}) + \frac{\mathcal{M}(t, \boldsymbol{x})}{2} [v_i(t, \boldsymbol{x})]^2, \tag{2.2.12}$$

$$\Pi_{ij}(t, \boldsymbol{x}) = \mathcal{P}(t, \boldsymbol{x}) \delta_{ij} + \mathcal{M}(t, \boldsymbol{x}) v_i(t, \boldsymbol{x}) v_j(t, \boldsymbol{x}) - \sigma_{ij}(t, \boldsymbol{x}), \tag{2.2.13}$$

$$\mathcal{Q}_i(t, \boldsymbol{x}) = \Big[\mathcal{H}(t, \boldsymbol{x}) + \mathcal{P}(t, \boldsymbol{x}) \Big] v_i(t, \boldsymbol{x}) - \sigma_{ij}(t, \boldsymbol{x}) v_j(t, \boldsymbol{x}) + q_i(t, \boldsymbol{x}), \tag{2.2.14}$$

where $\mathcal{E}(t, \boldsymbol{x})$ is the internal energy density and $\mathcal{P}(t, \boldsymbol{x})$ the pressure. The viscous tensor σ_{ij} and the heat flux $q_i(t, \boldsymbol{x})$ are given by

$$\sigma_{ij}(t, \boldsymbol{x}) = \eta \left[\partial_i v_j(t, \boldsymbol{x}) + \partial_j v_i(t, \boldsymbol{x}) - \frac{2}{d} \delta_{ij} \nabla \cdot \boldsymbol{v}(t, \boldsymbol{x}) \right] + \zeta \delta_{ij} \nabla \cdot \boldsymbol{v}(t, \boldsymbol{x}) \tag{2.2.15}$$

and

$$q_i(t, \boldsymbol{x}) = -\kappa \partial_i T(t, \boldsymbol{x}), \tag{2.2.16}$$

where $T(t, \boldsymbol{x})$ is the temperature. Also, η, ζ and κ are transport coefficients, called the shear viscosity, the bulk viscosity and the thermal conductivity, respectively. We choose the mass density $\mathcal{M}(t, \boldsymbol{x})$ and the internal energy density $\mathcal{E}(t, \boldsymbol{x})$ as the independent variables in thermodynamics. Then, the pressure $\mathcal{P}(t, \boldsymbol{x}) = \mathcal{P}(\mathcal{M}(t, \boldsymbol{x}), \mathcal{E}(t, \boldsymbol{x}))$ and the temperature $T(t, \boldsymbol{x}) = T(\mathcal{M}(t, \boldsymbol{x}), \mathcal{E}(t, \boldsymbol{x}))$ are locally determined from the thermodynamic relations. Thus, Eqs. (2.2.8)–(2.2.16) form a set of closed equations with $\mathcal{M}(t, \boldsymbol{x})$, $\mathcal{E}(t, \boldsymbol{x})$ and $v_i(t, \boldsymbol{x})$ as independent variables.

To find the mass current density, we solve the hydrodynamic equations for a weak external field $A_i(t, \boldsymbol{x})$ by linearizing them. Depending on the weak external field, the thermodynamic variables slightly deviate from their global equilibrium values $\mathcal{M}$ and $\mathcal{E}$, and the fluid velocity is small, all of which are $O(A)$:

$$\delta \mathcal{M}(t, \boldsymbol{x}) \equiv \mathcal{M}(t, \boldsymbol{x}) - \mathcal{M}, \quad \delta \mathcal{E}(t, \boldsymbol{x}) \equiv \mathcal{E}(t, \boldsymbol{x}) - \mathcal{E}, \quad v_i(t, \boldsymbol{x}) \quad \sim \quad O(A). \tag{2.2.17}$$

Then, the hydrodynamic equations are linearized and their spacetime Fourier transformations are given by

$$-iw \delta \mathcal{M}(w, \boldsymbol{k}) + \mathcal{M} i k_i v_i(w, \boldsymbol{k}) = 0, \tag{2.2.18}$$

$$-iw \mathcal{M} v_i(w, \boldsymbol{k}) + i k_i \left[\left(\frac{\partial \mathcal{P}}{\partial \mathcal{M}} \right)_{\mathcal{E}} \delta \mathcal{M}(w, \boldsymbol{k}) + \left(\frac{\partial \mathcal{P}}{\partial \mathcal{E}} \right)_{\mathcal{M}} \delta \mathcal{E}(w, \boldsymbol{k}) \right]$$
$$+ \eta \boldsymbol{k}^2 v_i(w, \boldsymbol{k}) + \left(\zeta + \frac{d-2}{d} \eta \right) k_i k_j v_j(w, \boldsymbol{k}) = iw \mathcal{M} \frac{A_i(w, \boldsymbol{k})}{m}, \tag{2.2.19}$$

$$-iw \delta \mathcal{E}(w, \boldsymbol{k}) + i k_i \Big(\mathcal{E} + \mathcal{P} \Big) v_i(w, \boldsymbol{k})$$
$$+ \kappa \boldsymbol{k}^2 \left[\left(\frac{\partial T}{\partial \mathcal{M}} \right)_{\mathcal{E}} \delta \mathcal{M}(w, \boldsymbol{k}) + \left(\frac{\partial T}{\partial \mathcal{E}} \right)_{\mathcal{M}} \delta \mathcal{E}(w, \boldsymbol{k}) \right] = 0. \tag{2.2.20}$$

By eliminating $\delta\mathcal{M}(w, \boldsymbol{k})$ and $\delta\mathcal{E}(w, \boldsymbol{k})$, the mass current density up to $O(k^2)$ is found to be

$$\mathcal{J}_i(w, \boldsymbol{k}) = -\left[\mathcal{M}\delta_{ij} - \mathcal{M}c_s^2\frac{k_ik_j}{(iw)^2} + \eta\frac{\boldsymbol{k}^2}{iw}\delta_{ij} + \left(\zeta + \frac{d-2}{d}\eta\right)\frac{k_ik_j}{iw} + O(k^3)\right]\frac{A_j(w, \boldsymbol{k})}{m} + O(A^2),$$

(2.2.21)

where the adiabatic speed of sound c_s is defined by

$$c_s^2 \equiv \left(\frac{\partial\mathcal{P}}{\partial\mathcal{M}}\right)_{\mathcal{S}/\mathcal{M}} = \frac{\mathcal{E} + \mathcal{P}}{\mathcal{M}}\left(\frac{\partial\mathcal{P}}{\partial\mathcal{E}}\right)_{\mathcal{M}} + \left(\frac{\partial\mathcal{P}}{\partial\mathcal{M}}\right)_{\mathcal{E}}.$$

(2.2.22)

Here, the themodynamic quantities obey

$$\mathcal{E} + \mathcal{P} = T\mathcal{S} + \mu\mathcal{M}, \qquad \mathrm{d}\mathcal{E} = T\mathrm{d}\mathcal{S} + \mu\mathrm{d}\mathcal{M},$$

(2.2.23)

where $\mathcal{S}$ is the entropy density and μ the mass chemical potential.

2.2.3 Kubo formulas for viscosity coefficients

By matching the current responses between the microscopic and hydrodynamic descriptions in Eqs. (2.2.6) and (2.2.21) at low frequencies and wavevectors, we find

$$-\mathcal{R}_{\mathcal{J}_i\mathcal{J}_j}(w, \boldsymbol{k}) = -\mathcal{M}c_s^2\frac{k_ik_j}{(iw)^2} + \eta\frac{\boldsymbol{k}^2}{iw}\delta_{ij} + \left(\zeta + \frac{d-2}{d}\eta\right)\frac{k_ik_j}{iw} + O(k^3).$$

(2.2.24)

The purpose of this section is to derive the viscosity coefficients by taking the appropriate limit for this equation.

Kubo's canonical correlation function

It is useful to represent the response function, not in terms of the conserved charge density, but in terms of its current density, i.e., the stress tensor, because response functions for conserved charge densities can have long-range correlations [67, 98]. Using $iwe^{iwt} = \partial_t e^{iwt}$, the temporal integral by parts leads to

$$iw\mathcal{R}_{\mathcal{J}_i\mathcal{J}_j}(w, \boldsymbol{k}) = -i\int_0^\infty \mathrm{d}t\int \mathrm{d}\boldsymbol{x}\, e^{iwt-i\boldsymbol{k}\cdot\boldsymbol{x}}\langle[\partial_t\hat{\mathcal{J}}_i(t, \boldsymbol{x}),\, \hat{\mathcal{J}}_j(0, \boldsymbol{0})]\rangle$$
$$- i\int \mathrm{d}\boldsymbol{x}\, e^{-i\boldsymbol{k}\cdot\boldsymbol{x}}\langle[\hat{\mathcal{J}}_i(0, \boldsymbol{x}),\, \hat{\mathcal{J}}_j(0, \boldsymbol{0})]\rangle.$$

(2.2.25)

The second term vanishes because the equal-time commutator is computed as [99]

$$[\hat{\mathcal{J}}_i(\boldsymbol{x}),\, \hat{\mathcal{J}}_j(\boldsymbol{y})] = -i\left(\hat{\mathcal{J}}_j(\boldsymbol{x})\partial_i + \hat{\mathcal{J}}_i(\boldsymbol{y})\partial_j\right)\delta^d(\boldsymbol{x} - \boldsymbol{y}).$$

(2.2.26)

Then, using the momentum continuity equation for the unperturbed mass current density operator,

$$\partial_t\hat{\mathcal{J}}_i(t, \boldsymbol{x}) + \partial_j\hat{\Pi}_{ij}(t, \boldsymbol{x}) = 0,$$

(2.2.27)

with the stress tensor operator $\hat{\Pi}_{ij}(t, \boldsymbol{x})$, the response function is further written as

$$iw\mathcal{R}_{\mathcal{J}_i\mathcal{J}_j}(w, \boldsymbol{k}) = i\int_0^\infty \mathrm{d}t\int \mathrm{d}\boldsymbol{x}\, e^{iwt-i\boldsymbol{k}\cdot\boldsymbol{x}}\langle[\partial_k\hat{\Pi}_{ik}(t, \boldsymbol{x}),\, \hat{\mathcal{J}}_j(0, \boldsymbol{0})]\rangle$$

(2.2.28)

$$= -k_k\int_0^\infty \mathrm{d}t\int \mathrm{d}\boldsymbol{x}\, e^{iwt-i\boldsymbol{k}\cdot\boldsymbol{x}}\langle[\hat{\Pi}_{ik}(t, \boldsymbol{x}),\, \hat{\mathcal{J}}_j(0, \boldsymbol{0})]\rangle.$$

(2.2.29)

Furthermore, because of the spacetime translational invariance, the expectation value of the commutator turns into

$$\langle[\hat{\Pi}_{ik}(t,\boldsymbol{x}),\ \hat{\mathcal{J}}_j(0,\boldsymbol{0})]\rangle = \langle[\hat{\Pi}_{ik}(0,\boldsymbol{0}),\ \hat{\mathcal{J}}_j(-t,-\boldsymbol{x})]\rangle \tag{2.2.30}$$

$$= \langle\hat{\Pi}_{ik}(0,\boldsymbol{0})\hat{\mathcal{J}}_j(-t,-\boldsymbol{x}) - \hat{\Pi}_{ik}(0,\boldsymbol{0})e^{-\beta\hat{H}}\hat{\mathcal{J}}_j(-t,-\boldsymbol{x})e^{\beta\hat{H}}\rangle \tag{2.2.31}$$

$$= -\int_0^\beta \mathrm{d}\tau\, \partial_\tau\langle\hat{\Pi}_{ik}(0,\boldsymbol{0})e^{-\tau\hat{H}}\hat{\mathcal{J}}_j(-t,-\boldsymbol{x})e^{\tau\hat{H}}\rangle \tag{2.2.32}$$

$$= i\int_0^\beta \mathrm{d}\tau\,\langle\hat{\Pi}_{ik}(0,\boldsymbol{0})\partial_t\hat{\mathcal{J}}_j(-t+i\tau,-\boldsymbol{x})\rangle, \tag{2.2.33}$$

where the number operator $\hat{N}$ commutes with the other operators, i.e., $e^{\beta\mu\hat{N}}\hat{\mathcal{O}}e^{-\beta\mu\hat{N}} = \hat{\mathcal{O}}$. By using the momentum continuity equation (2.2.27) again, we arrive at

$$iw\mathcal{R}_{\mathcal{J}_i\mathcal{J}_j}(w,\boldsymbol{k}) = -k_k k_l \int_0^\infty \mathrm{d}t \int \mathrm{d}\boldsymbol{x}\, e^{iwt-i\boldsymbol{k}\cdot\boldsymbol{x}} \int_0^\beta \mathrm{d}\tau\,\langle\delta\hat{\Pi}_{ik}(0,\boldsymbol{0})\delta\hat{\Pi}_{jl}(-t+i\tau,-\boldsymbol{x})\rangle, \tag{2.2.34}$$

where $\delta\hat{\Pi}_{ij}(t,\boldsymbol{x}) \equiv \hat{\Pi}_{ij}(t,\boldsymbol{x}) - \langle\hat{\Pi}_{ij}(t,\boldsymbol{x})\rangle$ is introduced to incorporate the boundary contribution at spatial infinity with the clustering property,

$$\lim_{|\boldsymbol{x}|\to\infty}\langle\hat{\Pi}_{ik}(0,\boldsymbol{0})\hat{\Pi}_{jl}(-t+i\tau,-\boldsymbol{x})\rangle = \lim_{|\boldsymbol{x}|\to\infty}\langle\hat{\Pi}_{ik}(0,\boldsymbol{0})\rangle\langle\hat{\Pi}_{jl}(-t+i\tau,-\boldsymbol{x})\rangle. \tag{2.2.35}$$

Using Kubo's canonical correlation function [65] defined by

$$\mathcal{K}_{\mathcal{AB}}(w,\boldsymbol{k}) \equiv \int_0^\infty \mathrm{d}t \int \mathrm{d}\boldsymbol{x}\, e^{iwt-i\boldsymbol{k}\cdot\boldsymbol{x}} \int_0^\beta \frac{\mathrm{d}\tau}{\beta}\,\langle\delta\hat{\mathcal{A}}(t-i\tau,\boldsymbol{x})\delta\hat{\mathcal{B}}(0,\boldsymbol{0})\rangle, \tag{2.2.36}$$

the right-hand side of Eq. (2.2.34) can be written simply as

$$iw\mathcal{R}_{\mathcal{J}_i\mathcal{J}_j}(w,\boldsymbol{k}) = -\beta k_k k_l \mathcal{K}_{\Pi_{ik}\Pi_{jl}}(w,\boldsymbol{k}), \tag{2.2.37}$$

and thus Eq. (2.2.24) is rewritten as

$$\lim_{w\to i0^+}\left[\beta\mathcal{K}_{\Pi_{ik}\Pi_{jl}}(w,\boldsymbol{0})\frac{k_k k_l}{\boldsymbol{k}^2} + \frac{\mathcal{M}c_s^2}{iw}\frac{k_i k_j}{\boldsymbol{k}^2}\right] = \eta\delta_{ij} + \left(\zeta + \frac{d-2}{d}\eta\right)\frac{k_i k_j}{\boldsymbol{k}^2}. \tag{2.2.38}$$

Kubo formulas

Let us extract the viscosity coefficients from Eq. (2.2.38). Here, the fourth-rank tensor $\mathcal{K}_{\Pi_{ik}\Pi_{jl}}(w,\boldsymbol{0})$ is invariant under the exchange of $i \leftrightarrow k$ and $j \leftrightarrow l$ by the definition of the stress tensor and is also invaritnt under the exchange of $(ik) \leftrightarrow (jl)$ according to the Onsager reciprocity. Because of the symmetry of the subscripts and the rotational symmetry, $\mathcal{K}_{\Pi_{ik}\Pi_{jl}}(w,\boldsymbol{0})$ is represented by a linear combination of $\delta_{ij}\delta_{kl} + \delta_{il}\delta_{jk}$ and $\delta_{ik}\delta_{jl}$. By determining their coefficients to be consistent with Eq. (2.2.38), we find

$$\lim_{w\to i0^+}\left[\beta\mathcal{K}_{\Pi_{ik}\Pi_{jl}}(w,\boldsymbol{0}) + \frac{\mathcal{M}c_s^2}{iw}\delta_{ij}\delta_{kl}\right] = \eta(\delta_{ij}\delta_{kl} + \delta_{il}\delta_{jk}) + \left(\zeta - \frac{2}{d}\eta\right)\delta_{ik}\delta_{jl}, \tag{2.2.39}$$

where the shear and bulk viscosities are given by

$$\eta = \lim_{w\to i0^+}\beta\mathcal{K}_{\Pi_{xy}\Pi_{xy}}(w,\boldsymbol{0}), \tag{2.2.40}$$

$$\zeta = \lim_{w\to i0^+}\left[\beta\mathcal{K}_{\Pi\Pi}(w,\boldsymbol{0}) + \frac{\mathcal{M}c_s^2}{iw}\right], \tag{2.2.41}$$

with the trace of the stress tensor $\hat{\Pi}(t, \boldsymbol{x}) \equiv \hat{\Pi}_{ii}(t, \boldsymbol{x})/d$.

By replacing the complex frequency w with $\omega + i0^+$, one can see that the second term of the bulk viscosity has a peak originating from the gapless sound propagation,

$$\frac{\mathcal{M}c_s^2}{iw} \to \frac{\mathcal{M}c_s^2}{i(\omega + i0^+)} = \mathcal{M}c_s^2 \left(-i\mathrm{P}\frac{1}{\omega} - \pi\delta(\omega) \right), \tag{2.2.42}$$

where the symbol P stands for the principal value of the integral. The singularity that this peak brings in the limit of $\omega \to 0$ is canceled by the same singularity produced by the first term. Actually, the two terms can be combined as

$$\beta\mathcal{K}_{\Pi\Pi}(w, \mathbf{0}) + \frac{\mathcal{M}c_s^2}{iw} = \beta\mathcal{K}_{\tilde{\Pi}\tilde{\Pi}}(w, \mathbf{0}), \tag{2.2.43}$$

where we introduce a modified stress tensor operator $\hat{\tilde{\Pi}}(t, \boldsymbol{x})$ as

$$\hat{\tilde{\Pi}}(t, \boldsymbol{x}) \equiv \hat{\Pi}(t, \boldsymbol{x}) - \left[\left(\frac{\partial\mathcal{P}}{\partial\mathcal{M}} \right)_{\mathcal{E}} \hat{\mathcal{M}}(t, \boldsymbol{x}) + \left(\frac{\partial\mathcal{P}}{\partial\mathcal{E}} \right)_{\mathcal{M}} \hat{\mathcal{H}}(t, \boldsymbol{x}) \right]. \tag{2.2.44}$$

Here, $\hat{\mathcal{M}}(t, \boldsymbol{x})$ and $\hat{\mathcal{H}}(t, \boldsymbol{x})$ are the mass and energy density operators, respectively. In the operator $\hat{\tilde{\Pi}}(t, \boldsymbol{x})$, the pressure fluctuations that cause sound waves are eliminated from the trace of the stress tensor operator. Eq. (2.2.43) is derived from the following properties of the canonical correlation function,

$$\mathcal{K}_{\mathcal{N}\mathcal{O}}(w, \mathbf{0}) = -\frac{1}{iw} \left(\frac{\partial\langle\mathcal{O}(\mathbf{0})\rangle}{\partial(\beta\mu)} \right)_\beta, \qquad \mathcal{K}_{\mathcal{H}\mathcal{O}}(w, \mathbf{0}) = \frac{1}{iw} \left(\frac{\partial\langle\mathcal{O}(\mathbf{0})\rangle}{\partial\beta} \right)_{\beta\mu}, \tag{2.2.45}$$

and the thermodynamic relations for $\langle\hat{\mathcal{M}}(\boldsymbol{x})\rangle = \mathcal{M}$, $\langle\hat{\mathcal{H}}(\boldsymbol{x})\rangle = \mathcal{E}$, and $\langle\hat{\Pi}(\boldsymbol{x})\rangle = \mathcal{P}$. Therefore, the bulk viscosity is given by

$$\zeta = \lim_{w \to i0^+} \beta\mathcal{K}_{\tilde{\Pi}\tilde{\Pi}}(w, \mathbf{0}). \tag{2.2.46}$$

Eqs. (2.2.40) and (2.2.46) are the Kubo formulas for the viscosity coefficients in Refs. [66,68].

From Kubo's correlation function to response function

Finally, we rewrite Kubo's correlation function into the response function. By using $iwe^{iwt} = \partial_t e^{iwt}$ in Kubo's correlation function, the temporal integration by parts leads to

$$\begin{aligned} \beta\mathcal{K}_{\mathcal{A}\mathcal{B}}(w, \boldsymbol{k}) &= \frac{1}{iw} \int_0^\infty \mathrm{d}t \int \mathrm{d}\boldsymbol{x} \, \partial_t e^{iwt} e^{-i\boldsymbol{k}\cdot\boldsymbol{x}} \int_0^\beta \mathrm{d}\tau \, \langle\delta\hat{\mathcal{A}}(t - i\tau, \boldsymbol{x})\delta\hat{\mathcal{B}}(0, \mathbf{0})\rangle \\ &= -\frac{1}{iw} \int_0^\infty \mathrm{d}t \int \mathrm{d}\boldsymbol{x} \, e^{iwt - i\boldsymbol{k}\cdot\boldsymbol{x}} \int_0^\beta \mathrm{d}\tau \, \langle\partial_t\delta\hat{\mathcal{A}}(t - i\tau, \boldsymbol{x})\delta\hat{\mathcal{B}}(0, \mathbf{0})\rangle \\ &\quad - \frac{1}{iw} \int \mathrm{d}\boldsymbol{x} \, e^{-i\boldsymbol{k}\cdot\boldsymbol{x}} \int_0^\beta \mathrm{d}\tau \, \langle\delta\hat{\mathcal{A}}(-i\tau, \boldsymbol{x})\delta\hat{\mathcal{B}}(0, \mathbf{0})\rangle. \end{aligned} \tag{2.2.47}$$

Then, the integral over τ can be rewritten as

$$\begin{aligned} \int_0^\beta \mathrm{d}\tau \, \langle\partial_t\delta\hat{\mathcal{A}}(t - i\tau, \boldsymbol{x})\delta\hat{\mathcal{B}}(0, \mathbf{0})\rangle &= i \int_0^\beta \mathrm{d}\tau \, \langle\partial_\tau\delta\hat{\mathcal{A}}(t - i\tau, \boldsymbol{x})\delta\hat{\mathcal{B}}(0, \mathbf{0})\rangle \\ &= i\langle[e^{\beta\hat{H}}\delta\hat{\mathcal{A}}(t, \boldsymbol{x})e^{-\beta\hat{H}} - \delta\hat{\mathcal{A}}(t, \boldsymbol{x})]\delta\hat{\mathcal{B}}(0, \mathbf{0})\rangle \\ &= -i\langle[\delta\hat{\mathcal{A}}(t, \boldsymbol{x}), \, \delta\hat{\mathcal{B}}(0, \mathbf{0})]\rangle \\ &= -i\langle[\hat{\mathcal{A}}(t, \boldsymbol{x}), \, \hat{\mathcal{B}}(0, \mathbf{0})]\rangle, \end{aligned} \tag{2.2.48}$$

so that we obtain

$$\beta\mathcal{K}_{\mathcal{AB}}(w,\boldsymbol{k}) = \frac{\mathcal{R}_{\mathcal{AB}}(w,\boldsymbol{k}) - \int_0^\beta \mathrm{d}\tau \int \mathrm{d}\boldsymbol{x}\, e^{-i\boldsymbol{k}\cdot\boldsymbol{x}} \langle \delta\hat{\mathcal{A}}(-i\tau,\boldsymbol{x})\delta\hat{\mathcal{B}}(0,\boldsymbol{0})\rangle}{iw}. \tag{2.2.49}$$

According to the Kubo formulas for the viscosity coefficients of Eqs. (2.2.40) and (2.2.46), we introduce the complex shear viscosity as

$$\eta(w) = \frac{\mathcal{R}_{\Pi_{xy}\Pi_{xy}}(\omega + i0^+,\boldsymbol{0}) - \int_0^\beta \mathrm{d}\tau \int \mathrm{d}\boldsymbol{x}\, \langle \delta\hat{\Pi}_{xy}(-i\tau,\boldsymbol{x})\delta\hat{\Pi}_{xy}(0,\boldsymbol{0})\rangle}{iw}, \tag{2.2.50}$$

and the complex bulk viscosity as

$$\zeta(w) = \frac{\mathcal{R}_{\Pi\Pi}(\omega + i0^+,\boldsymbol{0}) - \int_0^\beta \mathrm{d}\tau \int \mathrm{d}\boldsymbol{x}\, \langle \delta\hat{\tilde{\Pi}}(-i\tau,\boldsymbol{x})\delta\hat{\tilde{\Pi}}(0,\boldsymbol{0})\rangle}{iw}. \tag{2.2.51}$$

The viscosity coefficients are given by the real part of the complex viscosities for $w \to \omega + i0^+$ in the static limit $\omega \to 0$:

$$\eta = \lim_{\omega\to 0} \mathrm{Re}[\eta(\omega + i0^+)], \tag{2.2.52}$$

$$\zeta = \lim_{\omega\to 0} \mathrm{Re}[\zeta(\omega + i0^+)]. \tag{2.2.53}$$

2.2.4   Kubo formula for thermal conductivity

It is necessary for computing the thermal conductivity to apply a temperature gradient to the system, which produces the heat flux. In the discussion of the viscosity coefficients, we have introduced the vector potential as an external field corresponding to the fluid velocity. An external field corresponding to the temperature is introduced as a gravitational potential because the temperature is coupled with a Hamiltonian in the Boltzmann distribution [68]. By applying the gravitational potential as an external field, the energy current density can be calculated by both microscopics and hydrodynamics, just as in the case of the viscosities. By comparing the energy current response, the Kubo formula for the thermal conductivity is given by

$$T\kappa = \lim_{w\to i0^+} \beta\mathcal{K}_{\mathcal{J}_x^q \mathcal{J}_x^q}(w,\boldsymbol{0}), \tag{2.2.54}$$

where $\hat{\mathcal{J}}_i^q(t,\boldsymbol{x})$ denotes the heat current density operator defined by

$$\hat{\mathcal{J}}_i^q(t,,\boldsymbol{x}) = \hat{\mathcal{Q}}_i(t,\boldsymbol{x}) - \frac{\mathcal{E}+\mathcal{P}}{\mathcal{M}}\hat{\mathcal{J}}_i(t,\boldsymbol{x}). \tag{2.2.55}$$

The heat current density is defined by subtracting the current density multiplied by the enthalpy from the energy current density. In the same way as the viscosity coefficients, the complex thermal conductivity is introduced as

$$T\kappa(w) = \frac{\mathcal{R}_{\mathcal{J}_x^q \mathcal{J}_x^q}(w,\boldsymbol{0}) - \int_0^\beta \mathrm{d}\tau \int \mathrm{d}\boldsymbol{x}\, \langle \delta\hat{\mathcal{J}}_x^q(-i\tau,\boldsymbol{x})\delta\hat{\mathcal{J}}_x^q(0,\boldsymbol{0})\rangle}{iw}, \tag{2.2.56}$$

and the thermal conductivity is given by

$$\kappa = \lim_{\omega\to 0} \mathrm{Re}[\kappa(\omega + i0^+)]. \tag{2.2.57}$$

2.3 Kinetic theory at high temperatures

This section is devoted to a review of kinetic theory approach to transport for the resonant Fermi gases at high temperatures [69–73].

2.3.1 Boltzmann equation

The kinetic theory describes collective motions of particles forming a gas with a one-body distribution function in the phase space. We first consider a simple gas composed of identical particles. Let us define a one-body distribution function $f(t, \boldsymbol{x}, \boldsymbol{p})$ so that $f(t, \boldsymbol{x}, \boldsymbol{p})\Delta\boldsymbol{x}\Delta\boldsymbol{p}$ is the number of particles in a microvolume element $\Delta\boldsymbol{x}\Delta\boldsymbol{p}$ of the $(2d)$-dimensional phase space spanned by the coordinates and momentums. The variation of the number of particles in the volume element is caused by collisions between particles:

$$\frac{\mathrm{d}}{\mathrm{d}t}f(t, \boldsymbol{x}, \boldsymbol{p}) = \left(\frac{\partial}{\partial t}f(t, \boldsymbol{x}, \boldsymbol{p})\right)_{\mathrm{coll}}. \tag{2.3.1}$$

The left-hand side reads

$$\frac{\mathrm{d}}{\mathrm{d}t}f(t, \boldsymbol{x}, \boldsymbol{p}) = \frac{\partial}{\partial t}f(t, \boldsymbol{x}, \boldsymbol{p}) + \dot{x}_i\frac{\partial}{\partial r_i}f(t, \boldsymbol{x}, \boldsymbol{p}) + \dot{p}_i\frac{\partial}{\partial p_i}f(t, \boldsymbol{x}, \boldsymbol{p}), \tag{2.3.2}$$

where the time derivatives $\dot{r}_i$ and $\dot{p}_i$ are determined by the canonical equations of motion:

$$\dot{x}_i = \frac{\partial E(t, \boldsymbol{x}, \boldsymbol{p})}{\partial p_i}, \qquad \dot{p}_i = -\frac{\partial E(t, \boldsymbol{x}, \boldsymbol{p})}{\partial x_i}, \tag{2.3.3}$$

with the single-particle energy $E(t, \boldsymbol{x}, \boldsymbol{p})$. For nonrelativistic gases, we suppose that the energy $E(t, \boldsymbol{x}, \boldsymbol{p})$ is given by

$$E(t, \boldsymbol{x}, \boldsymbol{p}) = \frac{\boldsymbol{p}^2}{2m} + U(t, \boldsymbol{x}), \tag{2.3.4}$$

and thus the left-hand side is written as

$$\frac{\mathrm{d}}{\mathrm{d}t}f(t, \boldsymbol{x}, \boldsymbol{p}) = \frac{\partial}{\partial t}f(t, \boldsymbol{x}, \boldsymbol{p}) + \frac{p_i}{m}\frac{\partial}{\partial r_i}f(t, \boldsymbol{x}, \boldsymbol{p}) + F_i(t, \boldsymbol{x})\frac{\partial}{\partial p_i}f(t, \boldsymbol{x}, \boldsymbol{p}), \tag{2.3.5}$$

where $U(t, \boldsymbol{x})$ is a potential energy and $F_i(t, \boldsymbol{x}) \equiv -\partial_i U(t, \boldsymbol{x})$ is its external force.

The left-hand side of Eq. (2.3.1), called the streaming term, is simply written using the one-body distribution function, as in Eq. (2.3.5), because it is determined by the motion of a single particle only. On the other hand, the right-hand side, called the collision term, cannot be strictly described without two- or more-body distribution functions because collision processes involve multiple particles. The collision term is approximately given by the following form using the one-body distribution function only:

$$\left(\frac{\partial f_{\boldsymbol{p}}}{\partial t}\right)_{\mathrm{coll}} = \int_{\boldsymbol{p}_2, \boldsymbol{k}_1, \boldsymbol{k}_2} \mathcal{W}(\boldsymbol{k}_1, \boldsymbol{k}_2 | \boldsymbol{p}, \boldsymbol{p}_2)\Big[f_{\boldsymbol{k}_1}f_{\boldsymbol{k}_2}(1 + cf_{\boldsymbol{p}})(1 + cf_{\boldsymbol{p}_2}) - (1 + cf_{\boldsymbol{k}_1})(1 + cf_{\boldsymbol{k}_2})f_{\boldsymbol{p}}f_{\boldsymbol{p}_2}\Big], \tag{2.3.6}$$

where $\mathcal{W}(\boldsymbol{k}_1, \boldsymbol{k}_2 | \boldsymbol{p}, \boldsymbol{p}_2)$ is the transition rate and $f_{\boldsymbol{p}}$ is the shorthand notation of $f(t, \boldsymbol{x}, \boldsymbol{p})$. The transision rate represents the probability that two particles with momenta $\boldsymbol{p}$ and $\boldsymbol{p}_2$ collide and then have momenta $\boldsymbol{k}_1$ and $\boldsymbol{k}_2$, respectively. Here, c represents statistics of particles:

$c = 0$ for classical particles, $c = 1$ for bosons, and $c = -1$ for fermions. The time-evolution equation for $f(t, \boldsymbol{x}, \boldsymbol{p})$ given by Eqs. (2.3.5) and (2.3.6) is called the Boltzmann equation.

Let us move on to our subject, the resonant Fermi gas. For the resonant Fermi gas, we need to consider the spin degrees of freedom $\sigma =\uparrow, \downarrow$. We introduce a distribution function for each spin degree of freedom $f_\sigma(t, \boldsymbol{x}, \boldsymbol{p})$. The Boltzmann equation for $f_\sigma(t, \boldsymbol{x}, \boldsymbol{p})$ is given by

$$\frac{\partial}{\partial t} f_\sigma(t, \boldsymbol{x}, \boldsymbol{p}) + \frac{p_i}{m} \frac{\partial}{\partial r_i} f_\sigma(t, \boldsymbol{x}, \boldsymbol{p}) + F_i(t, \boldsymbol{x}) \frac{\partial}{\partial p_i} f_\sigma(t, \boldsymbol{x}, \boldsymbol{p}) = \left(\frac{\partial}{\partial t} f_\sigma(t, \boldsymbol{x}, \boldsymbol{p}) \right)_{\text{coll};\sigma}. \quad (2.3.7)$$

The streaming term remains in the same form because it is determined by the motion of a single particle, but the collision term is modified to describe collisions between particles with different spins:

$$\left(\frac{\partial}{\partial t} f_\sigma(t, \boldsymbol{x}, \boldsymbol{p}) \right)_{\text{coll};\sigma} = \int_{\boldsymbol{p}_2, \boldsymbol{k}_1, \boldsymbol{k}_2} \mathcal{W}(\boldsymbol{k}_1, \boldsymbol{k}_2 | \boldsymbol{p}, \boldsymbol{p}_2)$$
$$\times \left[f_{\sigma;\boldsymbol{k}_1} f_{\bar{\sigma};\boldsymbol{k}_2} (1 - f_{\sigma;\boldsymbol{p}})(1 - f_{\bar{\sigma};\boldsymbol{p}_2}) - (1 - f_{\sigma;\boldsymbol{k}_1})(1 - f_{\bar{\sigma};\boldsymbol{k}_2}) f_{\sigma;\boldsymbol{p}} f_{\bar{\sigma};\boldsymbol{p}_2} \right], \quad (2.3.8)$$

where $\bar{\sigma}$ denotes the opposite spin to σ. Because the Boltzmann equations for $f_{\uparrow;\boldsymbol{p}}$ and $f_{\downarrow;\boldsymbol{p}}$ switch to each other under spin reversal, the distribution functions of both components are always equal when both $f_{\uparrow;\boldsymbol{p}}$ and $f_{\downarrow;\boldsymbol{p}}$ are equal in an initial state. We consider only such states, and define $f(t, \boldsymbol{x}, \boldsymbol{p})$ as $f(t, \boldsymbol{x}, \boldsymbol{p}) = f_\uparrow(t, \boldsymbol{x}, \boldsymbol{p}) = f_\downarrow(t, \boldsymbol{x}, \boldsymbol{p})$. Then, the distribution function $f(t, \boldsymbol{x}, \boldsymbol{p})$ obeys the same equation as in the case of the simple gas, i.e., Eqs. (2.3.5) and (2.3.6) with $c = -1$.

Furthermore, we focus on the high-temperature limit, where the thermal de Broglie wavelength is sufficiently smaller than the average interparticle distance. In the high-temperature limit, the collision term can be taken to be that for classical particles ($c = 0$). Also, the two-body scattering is dominant in the limit, so that the transition rate is given by

$$\mathcal{W}(\boldsymbol{k}_1, \boldsymbol{k}_2 | \boldsymbol{p}, \boldsymbol{p}_2) = |\mathcal{T}_a(\tfrac{(\boldsymbol{k}_1 - \boldsymbol{k}_2)^2}{4m} + i0^+)|^2 (2\pi)^{d+1} \delta^d(\boldsymbol{k}_1 + \boldsymbol{k}_2 - \boldsymbol{p} - \boldsymbol{p}_2) \delta(\epsilon_{\boldsymbol{k}_1} + \epsilon_{\boldsymbol{k}_2} - \epsilon_{\boldsymbol{p}} - \epsilon_{\boldsymbol{p}_2}), \quad (2.3.9)$$

where $\epsilon_{\boldsymbol{p}} = \boldsymbol{p}^2/(2m)$ is the kinetic energy and the two-body scattering T-matrix $\mathcal{T}_a(\varepsilon + i0^+)$ is given by Eq. (2.1.26):

$$|\mathcal{T}_a(\tfrac{(\boldsymbol{k}_1 - \boldsymbol{k}_2)^2}{4m} + i0^+)|^2 = \begin{cases} \dfrac{16\pi^2}{m^2} \dfrac{1}{\ln^2(a^2 \frac{(\boldsymbol{k}_1 - \boldsymbol{k}_2)^2}{4}) + \pi^2} & d = 2, \\[3mm] \dfrac{16\pi^2}{m^2} \dfrac{1}{a^{-2} + \frac{(\boldsymbol{k}_1 - \boldsymbol{k}_2)^2}{4}} & d = 3. \end{cases} \quad (2.3.10)$$

Eventually, the resonant Fermi gas in the high-temperature limit is kinematically described by the Boltzmann equation for classical particles of Eqs. (2.3.5) and (2.3.6) with $c = 0$, employing the transition rate of Eqs. (2.3.9) and (2.3.10).

2.3.2   Properties of the Boltzmann equation

In preparation for the calculations of the transport coefficients, we review the properties of the Boltzmann equation for the resonant Fermi gas [100].

Collision invariants and continuity equations

Let us consider the following integral:

$$\Phi_f(t, \boldsymbol{x}) \equiv \int_{\boldsymbol{p}} \left(\frac{\partial f_{\boldsymbol{p}}}{\partial t}\right)_{\text{coll}} \varphi(\boldsymbol{p}), \tag{2.3.11}$$

where $\varphi(\boldsymbol{p})$ is an arbitrary function of momentum $\boldsymbol{p}$. From the symmetries of the transision rate

$$\mathcal{W}(\boldsymbol{k}_1, \boldsymbol{k}_2 | \boldsymbol{p}, \boldsymbol{p}_2) = \mathcal{W}(\boldsymbol{k}_1, \boldsymbol{k}_2 | \boldsymbol{p}_2, \boldsymbol{p}) = \mathcal{W}(\boldsymbol{k}_2, \boldsymbol{k}_1 | \boldsymbol{p}, \boldsymbol{p}_2) = \mathcal{W}(\boldsymbol{p}, \boldsymbol{p}_2 | \boldsymbol{k}_1, \boldsymbol{k}_2), \tag{2.3.12}$$

the integral $\Phi_f(t, \boldsymbol{x})$ turns into

$$\Phi_f(t, \boldsymbol{x}) = \frac{1}{4} \int_{\boldsymbol{p}, \boldsymbol{p}_2, \boldsymbol{k}_1, \boldsymbol{k}_2} \mathcal{W}(\boldsymbol{k}_1, \boldsymbol{k}_2 | \boldsymbol{p}, \boldsymbol{p}_2) \left[f_{\boldsymbol{k}_1} f_{\boldsymbol{k}_2} - f_{\boldsymbol{p}} f_{\boldsymbol{p}_2} \right] \left(\varphi(\boldsymbol{p}) + \varphi(\boldsymbol{p}_2) - \varphi(\boldsymbol{k}_1) - \varphi(\boldsymbol{k}_2) \right). \tag{2.3.13}$$

When $\varphi(\boldsymbol{p})$ satisfies

$$\varphi(\boldsymbol{p}) + \varphi(\boldsymbol{p}_2) = \varphi(\boldsymbol{k}_1) + \varphi(\boldsymbol{k}_2) \tag{2.3.14}$$

for any sets of possible momenta in the collision, the integral $\Phi_f(t, \boldsymbol{x})$ becomes zero for any distribution function. Eq. (2.3.14) means that the sum of the physical quantity $\varphi(\boldsymbol{p})$ of the two colliding particles is invariant before and after the collision. Therefore, when the physical quantity $\varphi(\boldsymbol{p})$ is a conserved quantity in the collision process, $\Phi_f(t, \boldsymbol{x})$ is zero. We assume that conserved quantities in the collision process are only the number of particles, momentum and energy. The number of particles, momentum and energy correspond to the following functions:

$$\varphi(\boldsymbol{p}) = \{1, \, p_i, \, \epsilon_{\boldsymbol{p}}\}. \tag{2.3.15}$$

These quantities are called the collision invariants.

By multiplying the Boltzmann equation with the collision invariants and integrating over $\boldsymbol{p}$, we can obtain continuity equations

$$\partial_t n(t, \boldsymbol{x}) + \partial_i j_i(t, \boldsymbol{x}) = 0, \tag{2.3.16}$$

$$m \partial_t j_i(t, \boldsymbol{x}) + \partial_j \Pi_{ij}(t, \boldsymbol{x}) = n(t, \boldsymbol{x}) F_i(t, \boldsymbol{x}), \tag{2.3.17}$$

$$\partial_t \mathcal{H}(t, \boldsymbol{x}) + \partial_i Q_i(t, \boldsymbol{x}) = F_i(t, \boldsymbol{x}) j_i(t, \boldsymbol{x}), \tag{2.3.18}$$

for the number of particles, momentum, and energy. Here, the physical quantities read

$$n(t, \boldsymbol{x}) = 2 \int_{\boldsymbol{p}} f(t, \boldsymbol{x}, \boldsymbol{p}), \tag{2.3.19}$$

$$j_i(t, \boldsymbol{x}) = 2 \int_{\boldsymbol{p}} \frac{p_i}{m} f(t, \boldsymbol{x}, \boldsymbol{p}), \tag{2.3.20}$$

$$\mathcal{H}(t, \boldsymbol{x}) = 2 \int_{\boldsymbol{p}} \epsilon_{\boldsymbol{p}} f(t, \boldsymbol{x}, \boldsymbol{p}), \tag{2.3.21}$$

$$\Pi_{ij}(t, \boldsymbol{x}) = 2 \int_{\boldsymbol{p}} \frac{p_i p_j}{m} f(t, \boldsymbol{x}, \boldsymbol{p}), \tag{2.3.22}$$

$$Q_i(t, \boldsymbol{x}) = 2 \int_{\boldsymbol{p}} \frac{p_i}{m} \epsilon_{\boldsymbol{p}} f(t, \boldsymbol{x}, \boldsymbol{p}), \tag{2.3.23}$$

for the number density, number current density, energy density, stress tensor, and energy current density. Here, the prefactor 2 is the number of spin degrees of freedom.

H-Theorem and equilibrium distribution

Let us show the H-theorem, one of the most important properties of the Boltzmann equation. We introduce Boltzmann's $\mathscr{H}(t, \boldsymbol{x})$ and its current density defined by

$$\mathscr{H}(t, \boldsymbol{x}) \equiv \int_{\boldsymbol{p}} f(t, \boldsymbol{x}, \boldsymbol{p}) \ln f(t, \boldsymbol{x}, \boldsymbol{p}), \tag{2.3.24}$$

$$\mathscr{H}_i(t, \boldsymbol{x}) \equiv \int_{\boldsymbol{p}} \frac{p_i}{m} f(t, \boldsymbol{x}, \boldsymbol{p}) \ln f(t, \boldsymbol{x}, \boldsymbol{p}). \tag{2.3.25}$$

These quantities satisfy

$$\partial_t \mathscr{H}(t, \boldsymbol{x}) + \partial_i \mathscr{H}_i(t, \boldsymbol{x}) = \int_{\boldsymbol{p}} \left(\frac{\partial f_{\boldsymbol{p}}}{\partial t}\right)_{\text{coll}} \ln f(t, \boldsymbol{x}, \boldsymbol{p}) \tag{2.3.26}$$

$$= -\frac{1}{4} \int_{\boldsymbol{p}, \boldsymbol{p}_2, \boldsymbol{k}_!, \boldsymbol{k}_2} \mathcal{W}(\boldsymbol{k}_1, \boldsymbol{k}_2 | \boldsymbol{p}, \boldsymbol{p}_2) \Big[f_{\boldsymbol{k}_1} f_{\boldsymbol{k}_2} - f_{\boldsymbol{p}} f_{\boldsymbol{p}_2} \Big]$$

$$\times \Big(\ln[f_{\boldsymbol{k}_1} f_{\boldsymbol{k}_2}] - \ln[f_{\boldsymbol{p}} f_{\boldsymbol{p}_2}] \Big). \tag{2.3.27}$$

Here, the following inequality holds:

$$(x - y)(\ln x - \ln y) \geq 0 \qquad \text{for any} \quad x, y > 0, \tag{2.3.28}$$

where the equality sign applies if, and only if, $x = y$. Therefore, we obtain

$$\partial_t \mathscr{H}(t, \boldsymbol{x}) + \partial_i \mathscr{H}_i(t, \boldsymbol{x}) \leq 0, \tag{2.3.29}$$

where the equality sign applies if, and only if, $f(t, \boldsymbol{x}, \boldsymbol{p})$ satisfies

$$f_{\boldsymbol{k}_1} f_{\boldsymbol{k}_2} = f_{\boldsymbol{p}} f_{\boldsymbol{p}_2}, \tag{2.3.30}$$

for any sets of possible momenta in the collision. The inequality (2.3.29) is called the H-theorem and is considered to be the molecular counterpart of the law of increasing entropy.

When the equality condition (2.3.30) holds, the collision term is obviously zero. In addition, when the collision term is zero, the equality condition (2.3.30) is true because the equality sign of Eq. (2.3.29) holds from Eq. (2.3.26). Therefore, the vanishing collision term and the equality condition (2.3.30) are equivalent:

$$\left(\frac{\partial f_{\boldsymbol{p}}}{\partial t}\right)_{\text{coll}} = 0 \qquad \Leftrightarrow \qquad f_{\boldsymbol{k}_1} f_{\boldsymbol{k}_2} = f_{\boldsymbol{p}} f_{\boldsymbol{p}_2}. \tag{2.3.31}$$

Here, we define the local thermal equilibrium distribution $f^{\text{eq}}(t, \boldsymbol{x}, \boldsymbol{p})$ so that the collision term is zero. Then, from the condition (2.3.30), the equilibrium distribution $f^{\text{eq}}(t, \boldsymbol{x}, \boldsymbol{p})$ satisfies

$$\ln f^{\text{eq}}_{\boldsymbol{k}_1} + \ln f^{\text{eq}}_{\boldsymbol{k}_2} = \ln f^{\text{eq}}_{\boldsymbol{p}} + \ln f^{\text{eq}}_{\boldsymbol{p}_2} \tag{2.3.32}$$

for any sets of possible momenta in the collision. This equation is the same as the condition for the collision invariants of Eq. (2.3.14). Because the collision invariants are only the number of particles, momentum and energy, $\ln f^{\text{eq}}_{\boldsymbol{p}}$ is represented as a linear combination of the collision invariants. Therefore, the equilibrium distribution is given by the Maxwell–Boltzmann distribution as

$$f^{\text{eq}}(t, \boldsymbol{x}, \boldsymbol{p}) = \exp\left[\beta(t, \boldsymbol{x}) \left(\frac{(\boldsymbol{p} - m\boldsymbol{v}(t, \boldsymbol{x}))^2}{2m} - \mu(t, \boldsymbol{x})\right)\right], \tag{2.3.33}$$

where $\beta(t, \boldsymbol{x})$, $v_i(t, \boldsymbol{x})$, and $\mu(t, \boldsymbol{x})$ correspond to the local inverse temperature, the local velocity and the local chemical potential, respectively.

2.3.3 From the Boltzmann equation to hydrodynamics

We derive hydrodynamics from the Boltzmann equation and find the formulas for the transport coefficients [101]. For simplicity, let potential $U(t, \boldsymbol{x})$ be zero in the following. Let us expand the distribution function around the local thermal equilibrium,

$$f(t, \boldsymbol{x}, \boldsymbol{p}) = f^{\mathrm{eq}}(t, \boldsymbol{x}, \boldsymbol{p}) + \delta f(t, \boldsymbol{x}, \boldsymbol{p}). \tag{2.3.34}$$

The parameters of $f^{\mathrm{eq}}(t, \boldsymbol{x}, \boldsymbol{p})$, i.e., $\beta(t, \boldsymbol{x})$, $v_i(t, \boldsymbol{x})$, and $\mu(t, \boldsymbol{x})$, are determined by the matching conditions,

$$0 = \int_{\boldsymbol{p}} \delta f_{\boldsymbol{p}} = \int_{\boldsymbol{p}} p_i \delta f_{\boldsymbol{p}} = \int_{\boldsymbol{p}} \epsilon_{\boldsymbol{p}} \delta f_{\boldsymbol{p}}. \tag{2.3.35}$$

These conditions impose the coincidence between the conserved quantities calculated using $f(t, \boldsymbol{x}, \boldsymbol{p})$ and those calculated using $f^{\mathrm{eq}}(t, \boldsymbol{x}, \boldsymbol{p})$.

Constitutive relations

The continuity equations are given by Eqs. (2.3.16), (2.3.17), and (2.3.18). Substituting the expansion (2.3.34) into Eqs. (2.3.19)–(2.3.23), the constitutive relations read

$$n(t, \boldsymbol{x}) = 2 \int_{\boldsymbol{p}} f^{\mathrm{eq}}(t, \boldsymbol{x}, \boldsymbol{p}) = 2 e^{\beta(t,\boldsymbol{x})\mu(t,\boldsymbol{x})} \left(\frac{m}{2\pi\beta(t, \boldsymbol{x})} \right)^{d/2}, \tag{2.3.36}$$

$$j_i(t, \boldsymbol{x}) = 2 \int_{\boldsymbol{p}} \frac{p_i}{m} f^{\mathrm{eq}}(t, \boldsymbol{x}, \boldsymbol{p}) = n(t, \boldsymbol{x}) v_i(t, \boldsymbol{x}), \tag{2.3.37}$$

$$\mathcal{H}(t, \boldsymbol{x}) = 2 \int_{\boldsymbol{p}} \epsilon_{\boldsymbol{p}} f^{\mathrm{eq}}(t, \boldsymbol{x}, \boldsymbol{p}) = \mathcal{E}(t, \boldsymbol{x}) + \frac{m[v_i(t, \boldsymbol{x})]^2}{2} n(t, \boldsymbol{x}), \tag{2.3.38}$$

$$\Pi_{ij}(t, \boldsymbol{x}) = 2 \int_{\boldsymbol{p}} \frac{p_i p_j}{m} \Big(f^{\mathrm{eq}}(t, \boldsymbol{x}, \boldsymbol{p}) + \delta f(t, \boldsymbol{x}, \boldsymbol{p}) \Big) \tag{2.3.39}$$

$$= \mathcal{P}(t, \boldsymbol{x}) + mn(t, \boldsymbol{x}) v_i(t, \boldsymbol{x}) v_j(t, \boldsymbol{x}) - \sigma_{ij}(t, \boldsymbol{x}), \tag{2.3.40}$$

$$\mathcal{Q}_i(t, \boldsymbol{x}) = 2 \int_{\boldsymbol{p}} \frac{p_i}{m} \epsilon_{\boldsymbol{p}} \Big(f^{\mathrm{eq}}(t, \boldsymbol{x}, \boldsymbol{p}) + \delta f(t, \boldsymbol{x}, \boldsymbol{p}) \Big) \tag{2.3.41}$$

$$= \Big(\mathcal{H}(t, \boldsymbol{x}) + \mathcal{P}(t, \boldsymbol{x}) \Big) v_i(t, \boldsymbol{x}) - \sigma_{ij}(t, \boldsymbol{x}) v_j(t, \boldsymbol{x}) + q_i(t, \boldsymbol{x}), \tag{2.3.42}$$

with the use of the matching conditions (2.3.35). Here, $\mathcal{E}(t, \boldsymbol{x})$ and $\mathcal{P}(t, \boldsymbol{x})$ are the internal energy density and the pressure, respectively:

$$\mathcal{E}(t, \boldsymbol{x}) = \frac{d}{2} \mathcal{P}(t, \boldsymbol{x}) = 2 \int_{\boldsymbol{p}} \epsilon_{\boldsymbol{p}} e^{-\beta(t,\boldsymbol{x})[\epsilon_{\boldsymbol{p}} - \mu(t,\boldsymbol{x})]} = \frac{d e^{\beta(t,\boldsymbol{x})\mu(t,\boldsymbol{x})}}{\beta(t, \boldsymbol{x})} \left(\frac{m}{2\pi\beta(t, \boldsymbol{x})} \right)^{d/2}. \tag{2.3.43}$$

While $f^{\mathrm{eq}}(t, \boldsymbol{x}, \boldsymbol{p})$ determines the local thermodynamic quantities, the deviation $\delta f(t, \boldsymbol{x}, \boldsymbol{p})$ determines the dissipative terms provided by the viscous tensor $\sigma_{ij}(t, \boldsymbol{x})$ and the heat flux $q_i(t, \boldsymbol{x})$,

$$\sigma_{ij}(t, \boldsymbol{x}) = -2 \int_{\boldsymbol{p}} \frac{[p_i - mv_i(t, \boldsymbol{x})][p_j - mv_j(t, \boldsymbol{x})]}{m} \delta f(t, \boldsymbol{x}, \boldsymbol{p}), \tag{2.3.44}$$

$$q_i(t, \boldsymbol{x}) = 2 \int_{\boldsymbol{p}} \frac{p_i - mv_i(t, \boldsymbol{x})}{m} \frac{[\boldsymbol{p} - m\boldsymbol{v}(t, \boldsymbol{x})]^2}{2m} \delta f(t, \boldsymbol{x}, \boldsymbol{p}). \tag{2.3.45}$$

Therefore, our problem is to determine the deviation $\delta f(t, \boldsymbol{x}, \boldsymbol{p})$ up to the first order of the derivatives of the velocity and the temperature from the Boltzmann equation, and to compute the dissipative terms.

Linearized Boltzmann equation

We derive an equation for finding $\delta f(t, \boldsymbol{x}, \boldsymbol{p})$ from the Boltzmann equation. With the help of the thermodynamic relation,

$$\mathrm{d}(\beta \mathcal{P}) = -\mathcal{E}\mathrm{d}\beta + n\mathrm{d}(\beta \mu), \tag{2.3.46}$$

and the zeroth-order hydrodynamic equations, we have

$$\left(\partial_t + v_j(t, \boldsymbol{x})\partial_j\right)\beta(t, \boldsymbol{x}) = \beta(t, \boldsymbol{x})\left(\frac{\partial \mathcal{P}}{\partial \mathcal{E}}\right)_n [\nabla \cdot \boldsymbol{v}(t, \boldsymbol{x})], \tag{2.3.47}$$

$$\left(\partial_t + v_j(t, \boldsymbol{x})\partial_j\right)[\beta(t, \boldsymbol{x})\mu(t, \boldsymbol{x})] = -\beta(t, \boldsymbol{x})\left(\frac{\partial \mathcal{P}}{\partial n}\right)_\mathcal{E} [\nabla \cdot \boldsymbol{v}(t, \boldsymbol{x})], \tag{2.3.48}$$

$$\left(\partial_t + v_j(t, \boldsymbol{x})\partial_j\right)v_i(t, \boldsymbol{x}) = -\frac{\partial_i \mathcal{P}(t, \boldsymbol{x})}{mn(t, \boldsymbol{x})}. \tag{2.3.49}$$

Then, the streaming term turns into

$$\frac{\partial}{\partial t}f_{\boldsymbol{p}}^{\mathrm{eq}} + \frac{p_i}{m}\frac{\partial}{\partial x^i}f_{\boldsymbol{p}}^{\mathrm{eq}} = \beta(t, \boldsymbol{x})f_{\boldsymbol{p}}^{\mathrm{eq}}\left[\pi_{ij}(\boldsymbol{p})\frac{V_{ij}(t, \boldsymbol{x})}{2} + \pi(\boldsymbol{p})[\nabla \cdot \boldsymbol{v}(t, \boldsymbol{x})] - j_i^q(\boldsymbol{p})\partial_i \ln \beta(t, \boldsymbol{x})\right], \tag{2.3.50}$$

with the shear strain rate tensor $V_{ij}(t, \boldsymbol{x})$,

$$V_{ij}(t, \boldsymbol{x}) \equiv \partial_i v_j(t, \boldsymbol{x}) + \partial_j v_i(t, \boldsymbol{x}) - \frac{2}{d}\delta_{ij}[\nabla \cdot \boldsymbol{v}(t, \boldsymbol{x})], \tag{2.3.51}$$

and

$$\pi_{ij}(\boldsymbol{p}) = \frac{p_i p_j}{m} - \frac{\boldsymbol{p}^2}{dm}\delta_{ij}, \tag{2.3.52}$$

$$\pi(\boldsymbol{p}) = \frac{\boldsymbol{p}^2}{dm} - \epsilon_{\boldsymbol{p}}\left(\frac{\partial \mathcal{P}}{\partial \mathcal{E}}\right)_n - \left(\frac{\partial \mathcal{P}}{\partial n}\right)_\mathcal{E}, \tag{2.3.53}$$

$$j_i^q(\boldsymbol{p}) = \left(\epsilon_{\boldsymbol{p}} - \frac{\mathcal{E} + \mathcal{P}}{n}\right)\frac{p_i}{m}. \tag{2.3.54}$$

Here, we take the local rest frame that is $v_i(t, \boldsymbol{x}) = 0$ and yet $\partial_i v_j(t, \boldsymbol{x}) \neq 0$. In the high-temperature limit, from Eq. (2.3.43), we have

$$\left(\frac{\partial \mathcal{P}}{\partial \mathcal{E}}\right)_n = \frac{2}{d}, \qquad \left(\frac{\partial \mathcal{P}}{\partial n}\right)_\mathcal{E} = 0, \tag{2.3.55}$$

and thus $\pi(\boldsymbol{p})$ is equal to zero.

On the other hand, by substituing the expansion (2.3.34), the collision term is linearized as

$$\left(\frac{\partial f_{\boldsymbol{p}}}{\partial t}\right)_{\mathrm{coll}} = -\beta(t, \boldsymbol{x})f_{\boldsymbol{p}}^{\mathrm{eq}}\int_{\boldsymbol{p}_2, \boldsymbol{k}_1, \boldsymbol{k}_2} f_{\boldsymbol{p}_2}^{\mathrm{eq}}\mathcal{W}(\boldsymbol{k}_1, \boldsymbol{k}_2|\boldsymbol{p}, \boldsymbol{p}_2)\left[\phi_{\boldsymbol{p}} + \phi_{\boldsymbol{p}_2} - \phi_{\boldsymbol{k}_1} - \phi_{\boldsymbol{k}_2}\right]$$
$$= -\beta(t, \boldsymbol{x})f_{\boldsymbol{p}}^{\mathrm{eq}}e^{\beta(t, \boldsymbol{x})\mu(t, \boldsymbol{x})}\mathcal{L}_{\mathrm{kin}}[\phi_{\boldsymbol{p}}], \tag{2.3.56}$$

where we take $\delta f_{\boldsymbol{p}} = \beta(t, \boldsymbol{x}) f_{\boldsymbol{p}}^{\mathrm{eq}} \phi_{\boldsymbol{p}}$ and introduce the linearized collision operator $\mathcal{L}_{\mathrm{kin}}$. By combining Eqs. (2.3.50) and (2.3.56), we obtain the linearized Boltzmann equation

$$\pi_{ij}(\boldsymbol{p}) \frac{V_{ij}(t, \boldsymbol{x})}{2} - j_i^q(\boldsymbol{p}) \partial_i \ln \beta(t, \boldsymbol{x}) = -e^{\beta(t, \boldsymbol{x}) \mu(t, \boldsymbol{x})} \mathcal{L}_{\mathrm{kin}}[\phi_{\boldsymbol{p}}]. \tag{2.3.57}$$

According to the form of the left-hand side, we choose $\phi_{\boldsymbol{p}}$ as

$$\phi_{\boldsymbol{p}} = -e^{-\beta(t, \boldsymbol{x}) \mu(t, \boldsymbol{x})} \left[\varphi_{ij}(\boldsymbol{p}) \frac{V_{ij}(t, \boldsymbol{x})}{2} - \varphi_i(\boldsymbol{p}) \partial_i \ln \beta(t, \boldsymbol{x}) \right]. \tag{2.3.58}$$

Then, the linearized Boltzmann equation is separated into equations for the shear strain rate tensor,

$$
\begin{aligned}
\pi_{ij}(\boldsymbol{p}) &= \mathcal{L}_{\mathrm{kin}}[\varphi_{ij}(\boldsymbol{p})] \\
&= \int_{\boldsymbol{p}_2, \boldsymbol{k}_1, \boldsymbol{k}_2} e^{-\beta \epsilon_{\boldsymbol{p}_2}} \mathcal{W}(\boldsymbol{k}_1, \boldsymbol{k}_2 | \boldsymbol{p}, \boldsymbol{p}_2) \Big[\varphi_{ij}(\boldsymbol{p}) + \varphi_{ij}(\boldsymbol{p}_2) - \varphi_{ij}(\boldsymbol{k}_1) - \varphi_{ij}(\boldsymbol{k}_2) \Big],
\end{aligned}
\tag{2.3.59}
$$

and for the temperature gradient,

$$
\begin{aligned}
j_i^q(\boldsymbol{p}) &= \mathcal{L}_{\mathrm{kin}}[\varphi_i(\boldsymbol{p})] \\
&= \int_{\boldsymbol{p}_2, \boldsymbol{k}_1, \boldsymbol{k}_2} e^{-\beta \epsilon_{\boldsymbol{p}_2}} \mathcal{W}(\boldsymbol{k}_1, \boldsymbol{k}_2 | \boldsymbol{p}, \boldsymbol{p}_2) \Big[\varphi_i(\boldsymbol{p}) + \varphi_i(\boldsymbol{p}_2) - \varphi_i(\boldsymbol{k}_1) - \varphi_i(\boldsymbol{k}_2) \Big].
\end{aligned}
\tag{2.3.60}
$$

We can determine the deviation $\delta f_{\boldsymbol{p}}$ by solving Eqs. (2.3.59) and (2.3.60) together with the matching conditions (2.3.35).

Transport coefficients

With the use of $\delta f_{\boldsymbol{p}} = \beta(t, \boldsymbol{x}) f_{\boldsymbol{p}}^{\mathrm{eq}} \phi_{\boldsymbol{p}}$, the strain tensor and the heat current density are written as

$$\sigma_{ij}(t, \boldsymbol{x}) = -2\beta(t, \boldsymbol{x}) \int_{\boldsymbol{p}} \pi_{ij}(\boldsymbol{p}) f_{\boldsymbol{p}}^{\mathrm{eq}} \phi_{\boldsymbol{p}}, \tag{2.3.61}$$

$$q_i(t, \boldsymbol{x}) = 2\beta(t, \boldsymbol{x}) \int_{\boldsymbol{p}} j_i^q(\boldsymbol{p}) f_{\boldsymbol{p}}^{\mathrm{eq}} \phi_{\boldsymbol{p}}, \tag{2.3.62}$$

in the local rest frame. These dissipative terms in hydrodynamics are given by

$$\sigma_{ij}(t, \boldsymbol{x}) = \eta V_{ij}(t, \boldsymbol{x}) + \zeta \delta_{ij} [\nabla \cdot \boldsymbol{v}(t, \boldsymbol{x})], \qquad q_i(t, \boldsymbol{x}) = -\kappa \partial_i T(t, \boldsymbol{x}). \tag{2.3.63}$$

By substituting Eq. (2.3.58) into Eqs. (2.3.61) and (2.3.62) and comparing them to Eq. (2.3.63), we find the shear viscosity and the thermal conductivity,

$$\eta = 2\beta \int_{\boldsymbol{p}} e^{-\beta \epsilon_{\boldsymbol{p}}} \pi_{xy}(\boldsymbol{p}) \varphi_{xy}(\boldsymbol{p}), \tag{2.3.64}$$

$$T\kappa = 2\beta \int_{\boldsymbol{p}} e^{-\beta \epsilon_{\boldsymbol{p}}} j_x^q(\boldsymbol{p}) \varphi_x(\boldsymbol{p}), \tag{2.3.65}$$

where the spacetime dependence of the thermodynamic quantities are dropped. In the high-temperature limit, the bulk viscosity ζ vanishes because $\phi_{\boldsymbol{p}}$ does not have a term proportional to the bulk strain rate $[\nabla \cdot \boldsymbol{v}(t, \boldsymbol{x})]$ due to $\pi(\boldsymbol{p}) = 0$.

2.3.4   Linearized collision operator

We focus on the shear viscosity and discuss the linearized Boltzmann equation of Eq. (2.3.59). The following argument can apply to the thermal conductivity as well. The shear viscosity is obtained from Eq. (2.3.64) using the solution $\varphi_{xy}(\boldsymbol{p})$ of Eq. (2.3.59).

Inner product

Associated with Eq. (2.3.64), we introduce an inner product as

$$\langle \varphi_1,\, \varphi_2 \rangle \equiv \int_{\boldsymbol{p}} e^{-\beta \epsilon_{\boldsymbol{p}}} \varphi_1(\boldsymbol{p}) \varphi_2(\boldsymbol{p}), \tag{2.3.66}$$

where $\varphi_1(\boldsymbol{p})$ and $\varphi_2(\boldsymbol{p})$ are arbitrary real functions of $\boldsymbol{p}$. From the definition, this inner product satisfies

$$\text{linearity} \ : \ \langle \varphi,\, a\varphi_1 + b\varphi_2 \rangle = a\langle \varphi,\, \varphi_1 \rangle + b\langle \varphi,\, \varphi_2 \rangle, \tag{2.3.67}$$

$$\text{conjugate symmetry} \ : \ \langle \varphi_1,\, \varphi_2 \rangle = \langle \varphi_2,\, \varphi_1 \rangle, \tag{2.3.68}$$

$$\text{positivity} \ : \ \langle \varphi,\, \varphi \rangle \geq 0, \tag{2.3.69}$$

$$\text{non-degenerate} \ : \ \langle \varphi,\, \varphi \rangle = 0 \quad \Rightarrow \quad \varphi = 0, \tag{2.3.70}$$

where φ, φ_1, and φ_2 are any real functions of $\boldsymbol{p}$ and a and b are any real numbers. With the use of this inner product, Eq. (2.3.64) is written as

$$\eta = 2\beta \langle \pi_{xy},\, \varphi_{xy} \rangle = 2\beta \langle \mathcal{L}_{\text{kin}}[\varphi_{xy}],\, \varphi_{xy} \rangle. \tag{2.3.71}$$

Here, the linearized collision operator $\mathcal{L}_{\text{kin}}$ is self-adjoint for this inner product,

$$\langle \varphi_1, \mathcal{L}_{\text{kin}}[\varphi_2] \rangle = \frac{1}{4} \int_{\boldsymbol{p},\boldsymbol{p}_2,\boldsymbol{k}_1,\boldsymbol{k}_2} e^{-\beta(\epsilon_{\boldsymbol{p}}+\epsilon_{\boldsymbol{p}_2})} \mathcal{W}(\boldsymbol{k}_1,\boldsymbol{k}_2|\boldsymbol{p},\boldsymbol{p}_2) \Big[\varphi_1(\boldsymbol{p}) + \varphi_1(\boldsymbol{p}_2) - \varphi_1(\boldsymbol{k}_1) - \varphi_1(\boldsymbol{k}_2) \Big]$$
$$\times \Big[\varphi_2(\boldsymbol{p}) + \varphi_2(\boldsymbol{p}_2) - \varphi_2(\boldsymbol{k}_1) - \varphi_2(\boldsymbol{k}_2) \Big]$$
$$= \langle \mathcal{L}_{\text{kin}}[\varphi_1],\, \varphi_2 \rangle. \tag{2.3.72}$$

In particular, the positivity of the transition rate leads to

$$\langle \varphi, \mathcal{L}_{\text{kin}}[\varphi] \rangle = \frac{1}{4} \int_{\boldsymbol{p},\boldsymbol{p}_2,\boldsymbol{k}_1,\boldsymbol{k}_2} e^{-\beta(\epsilon_{\boldsymbol{p}}+\epsilon_{\boldsymbol{p}_2})} \mathcal{W}(\boldsymbol{k}_1,\boldsymbol{k}_2|\boldsymbol{p},\boldsymbol{p}_2) \Big[\varphi(\boldsymbol{p}) + \varphi(\boldsymbol{p}_2) - \varphi(\boldsymbol{k}_1) - \varphi(\boldsymbol{k}_2) \Big]^2 \geq 0, \tag{2.3.73}$$

which means that the linearized collision operator $\mathcal{L}_{\text{kin}}$ is non-negative. The equality sign holds if and only if $\varphi(\boldsymbol{p})$ is the collision invariants. Therefore, the linearized collision operator $\mathcal{L}_{\text{kin}}$ has zero eigenvalue for the collision invariants and positive eigenvalues for the other eigenfunctions. Because the matching conditions (2.3.35) make the solution $\varphi_{xy}(\boldsymbol{p})$ orthogonal to the collision invariants, it can be expressed as

$$\varphi_{xy}(\boldsymbol{p}) = \mathcal{L}_{\text{kin}}^{-1}[\pi_{xy}(\boldsymbol{p})], \tag{2.3.74}$$

where $\mathcal{L}_{\text{kin}}^{-1}$ denotes the inverse of the linearized collision operator in the orthogonal complement space for the collision invariants.

Relaxation-time approximation

Because the linearized Boltzmann equation is difficult to solve analytically, it is usually solved by expanding $\varphi_{xy}(\boldsymbol{p})$ by polynomials. Here, let $\varphi_{xy}^{\text{trial}}(\boldsymbol{p})$ be the approximate solution to the linearized Boltzmann equation. The Schwarz inequality leads to

$$\langle \varphi_{xy}^{\text{trial}}, \mathcal{L}_{\text{kin}}[\varphi_{xy}^{\text{trial}}] \rangle \langle \varphi_{xy}, \mathcal{L}_{\text{kin}}[\varphi_{xy}] \rangle \geq \langle \varphi_{xy}^{\text{trial}}, \mathcal{L}_{\text{kin}}[\varphi_{xy}] \rangle^2. \tag{2.3.75}$$

Using this inequality for Eq. (2.3.71), it is possible to evaluate the lower bound of the shear viscosity as

$$\eta \geq 2\beta \frac{\langle \varphi_{xy}^{\text{trial}}, \mathcal{L}_{\text{kin}}[\varphi_{xy}] \rangle^2}{\langle \varphi_{xy}^{\text{trial}}, \mathcal{L}_{\text{kin}}[\varphi_{xy}^{\text{trial}}] \rangle} = 2\beta \frac{\langle \varphi_{xy}^{\text{trial}}, \pi_{xy} \rangle^2}{\langle \varphi_{xy}^{\text{trial}}, \mathcal{L}_{\text{kin}}[\varphi_{xy}^{\text{trial}}] \rangle} = \eta_{\text{LB}}. \tag{2.3.76}$$

The equal sign is true if and only if the trial function $\varphi_{xy}^{\text{trial}}(\boldsymbol{p})$ is proportional to the solution $\varphi_{xy}(\boldsymbol{p})$.

Here, as the simplest approximation, we take $\varphi_{xy}^{\text{trial}}(\boldsymbol{p})$ as

$$\varphi_{xy}^{\text{trial}}(\boldsymbol{p}) = e^{\beta\mu} \tau_\eta \pi_{xy}(\boldsymbol{p}). \tag{2.3.77}$$

This trial function is a solution when the collision term is approximated to

$$\left(\frac{\partial f_{\boldsymbol{p}}}{\partial t} \right)_{\text{coll;relax}} = -\frac{f_{\boldsymbol{p}} - f_{\boldsymbol{p}}^{\text{eq}}}{\tau_\eta}. \tag{2.3.78}$$

Employing this collision term is called the relaxation-time approximation, where τ_η is referred to as the relaxation time for the shear viscosity. The relaxation time τ_η is defined so that the shear viscosity in the relaxation-time approximation η_{relax} coincides with the lower bound of the shear viscosity η_{LB}. The shear viscosity in the relaxation-time approximation is calculated as

$$\eta_{\text{relax}} = 2\beta \langle \pi_{xy}, e^{\beta\mu} \tau_\eta \pi_{xy} \rangle = 2\beta e^{\beta\mu} \tau_\eta \langle \pi_{xy}, \pi_{xy} \rangle, \tag{2.3.79}$$

whereas the lower bound η_{LB} is given as

$$\eta_{\text{LB}} = 2\beta \frac{\langle \pi_{xy}, \pi_{xy} \rangle}{\langle \pi_{xy}, \mathcal{L}_{\text{kin}}[\pi_{xy}] \rangle} \langle \pi_{xy}, \pi_{xy} \rangle. \tag{2.3.80}$$

The relaxation time τ_η is found to be

$$\tau_\eta = \frac{\langle \pi_{xy}, \pi_{xy} \rangle}{\langle \pi_{xy}, e^{\beta\mu} \mathcal{L}_{\text{kin}}[\pi_{xy}] \rangle}, \tag{2.3.81}$$

and thus the relaxation time is given by the inverse of the expectation value of the linearized collision operator with $\pi_{xy}(\boldsymbol{p})$ corresponding to the shear strain.

2.4 Summary

This chapter devoted to a review of topics related to our study of the resonant Fermi gases. In Sec. 2.1, we reviewed the universality of the resonant Fermi gases from the perspective of the two-body scattering. We also introduced the contact interaction model in the second-quantized formalism to describe the resonant Fermi gas [Eq. (2.1.15)] and derived the two-body scattering T-matrix [Eq. (2.1.26)]. The T-matrix due to the two-body scattering in

vacuum plays an important role in the high-temperature limit. In Sec. 2.2, we gave the Kubo formulas for the transport coefficients [Eqs. (2.2.52), (2.2.53), and (2.2.57)]. We will compute the transport coefficients in Chapters 4 and 5 via these Kubo formulas. We also introduced hydrodynamics, which defines the transport coefficients. The formulation of hydrodynamics, consisting of the continuity equations and the constitutive relations, will be the basis for extensions of the hydrodynamic equations in Chapter 3. In Sec. 2.3, we gave the kinetic description of the resonant Fermi gas and derived the computation method for the transport coefficients using the kinetic theory. The linearized Boltzmann equations of Eqs. (2.3.59) and (2.3.60) will be derived from the microscopic theory using the quantum virial expansion in Chapter 5.

The vanishing bulk viscosity in the unitarity limit can be found via the Kubo formula (2.2.46). In the free and unitarity limit, where the system is conformal invariant, $\hat{\Pi}(t, \boldsymbol{x}) = 2\hat{\mathcal{H}}(t, \boldsymbol{x})/d$ holds [see Eq. (A.1.30) in Appendix A]. Accordingly, the equation of state obeys $\mathcal{P} = 2\mathcal{E}/d$, so that the modified stress tensor $\hat{\tilde{\Pi}}(t, \boldsymbol{x})$ of Eq. (2.2.44) turns into zero. Therefore, the bulk viscosity is found to be zero in the free and unitarity limit.

Chapter 3

Hydrodynamics with spacetime-dependent scattering length

In this chapter, we focus on the bulk viscosity among the transport coefficients. It was shown that the bulk viscosity vanishes in the unitarity limit because of no interaction scales [49]. The vanishing bulk viscosity at unitarity is intuitively understood because the entropy does not change before and after an isotropic expansion due to no interaction scales. We extend this intuitive understanding to the case where the scattering length is finite in order to investigate the bulk viscosity for a finite scattering length. When the scattering length is finite, an isotropic expansion of the fluid volume at a fixed scattering length can be regarded as equivalent to a contraction of the scattering length at a fixed fluid density because there are no reference scales other than the scattering length in contact interactions. We consider the resonant Fermi gas whose scattering length is modulated over spacetime to construct hydrodynamic equations that involve this equivalence. In Sec. 3.1, we introduce a Hamiltonian with the spacetime-dependent scattering length and derive operator identities including continuity equations. Hydrodynamic equations must be consistent with the equations obtained from the expectation values of the operator identities. We construct constitutive relations for normal fluids in Sec. 3.2 and for superfluids in Sec. 3.3. In Sec. 3.4, we summarize our findings and propose possible applications to ultracold atoms.

3.1 Quantum field theory

3.1.1 Spacetime-dependent scattering length for hydrodynamics

In ultracold atoms, the scattering length can be tuned by applying an external magnetic field via the Feshbach resonance. By modulating the applied magnetic field spatially and temporally, one can make the scattering length dependent on space and time. To investigate the role of the spacetime-dependent scattering length in the low-energy dynamics, we employ hydrodynamics. Hydrodynamics is a low-energy effective theory for dynamics on scales sufficiently larger than the scales that characterize the thermalization of the system, such as a relaxation time and a mean free path. For the hydrodynamics, we suppose that the spacetime modu-

lation of the scattering length is sufficiently smooth. We consider a resonant Fermi gas with the spacetime-dependent scattering length in d dimensions whose Hamiltonian is provided by

$$\hat{H}(t) = \int d\boldsymbol{x} \left[\sum_{\sigma=\uparrow,\downarrow} \left(\frac{[D_i\hat{\psi}_\sigma(t,\boldsymbol{x})]^\dagger[D_i\hat{\psi}_\sigma(t,\boldsymbol{x})]}{2m} - A_t(t,\boldsymbol{x})\hat{\psi}_\sigma^\dagger(t,\boldsymbol{x})\hat{\psi}_\sigma(t,\boldsymbol{x}) \right) \right.$$
$$\left. + \frac{g(t,\boldsymbol{x})}{2} \sum_{\sigma,\rho} \hat{\psi}_\sigma^\dagger(t,\boldsymbol{x})\hat{\psi}_\rho^\dagger(t,\boldsymbol{x})\hat{\psi}_\rho(t,\boldsymbol{x})\hat{\psi}_\sigma(t,\boldsymbol{x}) \right], \tag{3.1.1}$$

where the coupling constant $g(t,\boldsymbol{x})$ is connected to the scattering length in the dimensional regularization via Eq. (2.1.25):

$$\frac{1}{g(t,\boldsymbol{x})} = \frac{ma(t,\boldsymbol{x})^{2-d}}{(d-2)\Omega_{d-1}}. \tag{3.1.2}$$

Here, we employ the Heisenberg picture, and $D_\mu \equiv \partial_\mu - iA_\mu(t,\boldsymbol{x})$ is the covariant derivative and an external gauge field $A_\mu(t,\boldsymbol{x})$ is introduced for generality. The temporal component $A_t(t,\boldsymbol{x})$ represents the trapping potential, whereas the vector potential $A_i(t,\boldsymbol{x})$ appears in noninertial frames.

3.1.2   Continuity equations

The annihilation and creation operators obey the equal-time anti-commutation relations

$$\{\hat{\psi}_\sigma(t,\boldsymbol{x}),\ \hat{\psi}_\tau^\dagger(t,\boldsymbol{y})\} = \delta_{\sigma\tau}\delta^d(\boldsymbol{x}-\boldsymbol{y}),$$
$$\{\hat{\psi}_\sigma(t,\boldsymbol{x}),\ \hat{\psi}_\tau(t,\boldsymbol{y})\} = \{\hat{\psi}_\sigma^\dagger(t,\boldsymbol{x}),\ \hat{\psi}_\tau^\dagger(t,\boldsymbol{y})\} = 0. \tag{3.1.3}$$

The time-evolution equation for $\hat{\psi}_\sigma(t,\boldsymbol{x})$ is obtained by the Heisenberg equation of motion:

$$i\partial_t\hat{\psi}_\sigma(t,\boldsymbol{x}) = [\hat{\psi}_\sigma(t,\boldsymbol{x}),\ \hat{H}(t)]$$
$$= \left[-\frac{D_iD_i}{2m} - A_t(t,\boldsymbol{x}) + g(t,\boldsymbol{x})\sum_\tau \hat{\psi}_\tau^\dagger(t,\boldsymbol{x})\psi_\tau(t,\boldsymbol{x}) \right]\hat{\psi}_\sigma(t,\boldsymbol{x}). \tag{3.1.4}$$

This equation is invariant under the gauge transformation of

$$\psi_\sigma(t,\boldsymbol{x}) \to e^{i\chi(t,\boldsymbol{x})}\hat{\psi}_\sigma(t,\boldsymbol{x}), \qquad A_\mu(t,\boldsymbol{x}) \to A_\mu(t,\boldsymbol{x}) + \partial_\mu\chi(t,\boldsymbol{x}). \tag{3.1.5}$$

We can write the continuity equations for the mass, momentum, and energy. The mass, momentum, and energy density operators are defined by

$$\hat{\mathcal{M}}(t,\boldsymbol{x}) = m\sum_\sigma \hat{\psi}_\sigma^\dagger(t,\boldsymbol{x})\hat{\psi}_\sigma(t,\boldsymbol{x}), \tag{3.1.6}$$

$$\hat{\mathcal{J}}_i(t,\boldsymbol{x}) = -i\sum_\sigma \hat{\psi}_\sigma^\dagger(t,\boldsymbol{x})\overleftrightarrow{D_i}\hat{\psi}_\sigma(t,\boldsymbol{x}), \tag{3.1.7}$$

$$\hat{\mathcal{H}}(t,\boldsymbol{x}) = \sum_\sigma \frac{[D_i\hat{\psi}_\sigma(t,\boldsymbol{x})]^\dagger[D_i\hat{\psi}_\sigma(t,\boldsymbol{x})]}{2m} + \frac{g(t,\boldsymbol{x})}{2}\sum_{\sigma,\rho} \hat{\psi}_\sigma^\dagger(t,\boldsymbol{x})\hat{\psi}_\rho^\dagger(t,\boldsymbol{x})\hat{\psi}_\rho(t,\boldsymbol{x})\hat{\psi}_\sigma(t,\boldsymbol{x}).$$
$$\tag{3.1.8}$$

The continuity equations can be straightforwardly derived from the Heisenberg equation (3.1.4) and are given by

$$\partial_t \hat{\mathcal{M}}(t, \boldsymbol{x}) + \partial_i \hat{\mathcal{J}}_i(t, \boldsymbol{x}) = 0, \tag{3.1.9}$$

$$\partial_t \hat{\mathcal{J}}_i(t, \boldsymbol{x}) + \partial_j \hat{\Pi}_{ij}(t, \boldsymbol{x}) = F_{it}(t, \boldsymbol{x}) \frac{\hat{\mathcal{M}}(t, \boldsymbol{x})}{m} + F_{ij}(t, \boldsymbol{x}) \frac{\hat{\mathcal{J}}_j(t, \boldsymbol{x})}{m} - \frac{\partial_i a(t, \boldsymbol{x})}{\Omega_{d-1} a(t, \boldsymbol{x})^{d-1}} \frac{\hat{\mathcal{C}}(t, \boldsymbol{x})}{m}, \tag{3.1.10}$$

$$\partial_t \hat{\mathcal{H}}(t, \boldsymbol{x}) + \partial_i \hat{\mathcal{Q}}_i(t, \boldsymbol{x}) = F_{it}(t, \boldsymbol{x}) \frac{\hat{\mathcal{J}}_i(t, \boldsymbol{x})}{m} + \frac{\partial_t a(t, \boldsymbol{x})}{\Omega_{d-1} a(t, \boldsymbol{x})^{d-1}} \frac{\hat{\mathcal{C}}(t, \boldsymbol{x})}{m}, \tag{3.1.11}$$

where $F_{\mu\nu}(t, \boldsymbol{x}) \equiv \partial_\mu A_\nu(t, \boldsymbol{x}) - \partial_\nu A_\mu(t, \boldsymbol{x})$ denotes the field strength tensor and the right-hand sides of the momentum and energy continuity equations represent the external forces and powers supplied by $A_\mu(t, \boldsymbol{x})$ and $a(t, \boldsymbol{x})$. The stress tensor $\hat{\Pi}_{ij}(t, \boldsymbol{x})$, the energy current density $\hat{\mathcal{Q}}_i(t, \boldsymbol{x})$, and the contact density $\hat{\mathcal{C}}(t, \boldsymbol{x})$ are defined by

$$\hat{\Pi}_{ij}(t, \boldsymbol{x}) = \sum_\sigma \frac{[D_i \hat{\psi}_\sigma(t, \boldsymbol{x})]^\dagger [D_j \hat{\psi}_\sigma(t, \boldsymbol{x})] + [D_j \hat{\psi}_\sigma(t, \boldsymbol{x})]^\dagger [D_i \hat{\psi}_\sigma(t, \boldsymbol{x})]}{2m}$$
$$+ \delta_{ij} \left[\frac{g(t, \boldsymbol{x})}{2} \sum_{\sigma,\tau} \hat{\psi}_\sigma^\dagger(t, \boldsymbol{x}) \hat{\psi}_\rho^\dagger(t, \boldsymbol{x}) \hat{\psi}_\rho(t, \boldsymbol{x}) \hat{\psi}_\sigma(t, \boldsymbol{x}) - \frac{\partial_i \partial_i}{4m} \left(\sum_\sigma \hat{\psi}_\sigma^\dagger(t, \boldsymbol{x}) \hat{\psi}_\sigma(t, \boldsymbol{x}) \right) \right], \tag{3.1.12}$$

$$\hat{\mathcal{Q}}_i(t, \boldsymbol{x}) = \sum_\sigma \frac{[D_i \hat{\psi}_\sigma(t, \boldsymbol{x})]^\dagger [D_j D_j \hat{\psi}_\sigma(t, \boldsymbol{x})] - [D_j D_j \hat{\psi}_\sigma(t, \boldsymbol{x})]^\dagger [D_i \hat{\psi}_\sigma(t, \boldsymbol{x})]}{4im^2}$$
$$+ \frac{g(t, \boldsymbol{x})}{im} \sum_{\sigma,\tau} \hat{\psi}_\sigma^\dagger(t, \boldsymbol{x}) \left(\hat{\psi}_\rho^\dagger(t, \boldsymbol{x}) \overleftrightarrow{D_i} \hat{\psi}_\rho(t, \boldsymbol{x}) \right) \hat{\psi}_\sigma(t, \boldsymbol{x}), \tag{3.1.13}$$

$$\hat{\mathcal{C}}(t, \boldsymbol{x}) = \frac{m^2 g(t, \boldsymbol{x})^2}{2} \sum_{\sigma,\tau} \hat{\psi}_\sigma^\dagger(t, \boldsymbol{x}) \hat{\psi}_\rho^\dagger(t, \boldsymbol{x}) \hat{\psi}_\rho(t, \boldsymbol{x}) \hat{\psi}_\sigma(t, \boldsymbol{x}). \tag{3.1.14}$$

The contact obtained by integrating the contact density $\hat{\mathcal{C}}(t, \boldsymbol{x})$ over the whole space is the important quantity in the universal relations of the resonant Fermi gases [29].

In addition to the continuity equations, the trace of the stress tensor satisfies

$$\hat{\Pi}_{ii}(t, \boldsymbol{x}) = 2\hat{\mathcal{H}}(t, \boldsymbol{x}) + \frac{\hat{\mathcal{C}}(t, \boldsymbol{x})}{m\Omega_{d-1} a(t, \boldsymbol{x})^{d-2}} - \frac{d}{4m^2} \partial_i \partial_i \hat{\mathcal{M}}(t, \boldsymbol{x}). \tag{3.1.15}$$

In the unitarity limit, the divergence of the scattering length results in Eq. (3.1.15) without the second term on the right-hand side, which represents the nonrelativistic counterpart of the traceless condition for conformality (see Appendix A). The second term represents conformal symmetry breaking due to the scattering length. Here, we note that the stress tensor operator (3.1.12) is not unique. One can add any term $\hat{\Delta}_{ij}(t, \boldsymbol{x})$ satisfying $\partial_j \hat{\Delta}_{ij}(t, \boldsymbol{x}) = 0$ to the stress tensor operator without changing the form of the continuity equation for the momentum. For example, by modifying the stress tensor to

$$\hat{\Pi}_{ij}(t, \boldsymbol{x}) \rightarrow \hat{\Pi}_{ij}(t, \boldsymbol{x}) - \frac{d}{d-1} \left(\delta_{ij} \partial_k \partial_k - \partial_i \partial_j \right) \frac{\hat{\mathcal{M}}(t, \boldsymbol{x})}{4m^2}, \tag{3.1.16}$$

the last term is eliminated. This ambiguity, however, has no effect within the hydrodynamics up to first order in derivatives and is irrelevant to our discussion below.

3.2 Hydrodynamics for normal fluids

3.2.1 Constitutive relations

To move on to hydrodynamics, we define the expectation values for the operators as

$$\mathcal{O}(t, \boldsymbol{x}) \equiv \mathrm{Tr}\left[\hat{\rho}\hat{\mathcal{O}}(t, \boldsymbol{x})\right], \tag{3.2.1}$$

where the density matrix operator $\hat{\rho}$ is arbitrary but independent of time because we work in the Heisenberg picture. Then, Eqs. (3.1.9), (3.1.10), and (3.1.11) lead to

$$\partial_t \mathcal{M}(t, \boldsymbol{x}) + \partial_i \mathcal{J}_i(t, \boldsymbol{x}) = 0, \tag{3.2.2}$$

$$\partial_t \mathcal{J}_i(t, \boldsymbol{x}) + \partial_j \Pi_{ij}(t, \boldsymbol{x}) = F_{it}(t, \boldsymbol{x})\frac{\mathcal{M}(t, \boldsymbol{x})}{m} + F_{ij}(t, \boldsymbol{x})\frac{\mathcal{J}_j(t, \boldsymbol{x})}{m} - \frac{\partial_i a(t, \boldsymbol{x})}{\Omega_{d-1}a(t, \boldsymbol{x})^{d-1}}\frac{\mathcal{C}(t, \boldsymbol{x})}{m}, \tag{3.2.3}$$

$$\partial_t \mathcal{H}(t, \boldsymbol{x}) + \partial_i \mathcal{Q}_i(t, \boldsymbol{x}) = F_{it}(t, \boldsymbol{x})\frac{\mathcal{J}_i(t, \boldsymbol{x})}{m} + \frac{\partial_t a(t, \boldsymbol{x})}{\Omega_{d-1}a(t, \boldsymbol{x})^{d-1}}\frac{\mathcal{C}(t, \boldsymbol{x})}{m}. \tag{3.2.4}$$

These are the continuity equations in the hydrodynamics. Also, the operator identity (3.1.15) leads to

$$\Pi_{ii}(t, \boldsymbol{x}) = 2\mathcal{H}(t, \boldsymbol{x}) + \frac{\mathcal{C}(t, \boldsymbol{x})}{m\Omega_{d-1}a(t, \boldsymbol{x})^{d-2}} + O(\partial^2). \tag{3.2.5}$$

Hydrodynamics requires constitutive relations that express the physical quantities in terms of fluid variables in order for the continuity equations to form a set of closed equations. Here, the fluid variables are the local thermodynamic quantities and the fluid velocity $v_i(t, \boldsymbol{x})$. The constitutive relations for normal fluids read

$$\mathcal{J}_i(t, \boldsymbol{x}) = \mathcal{M}(t, \boldsymbol{x})v_i(t, \boldsymbol{x}), \tag{3.2.6}$$

$$\mathcal{H}(t, \boldsymbol{x}) = \mathcal{E}(t, \boldsymbol{x}) + \frac{\mathcal{M}(t, \boldsymbol{x})}{2}v_i(t, \boldsymbol{x})^2, \tag{3.2.7}$$

$$\Pi_{ij}(t, \boldsymbol{x}) = \mathcal{P}(t, \boldsymbol{x})\delta_{ij} + \mathcal{M}(t, \boldsymbol{x})v_i(t, \boldsymbol{x})v_j(t, \boldsymbol{x}) - \sigma_{ij}^{(a)}(t, \boldsymbol{x}), \tag{3.2.8}$$

$$\mathcal{Q}_i(t, \boldsymbol{x}) = \left[\mathcal{H}(t, \boldsymbol{x}) + \mathcal{P}(t, \boldsymbol{x})\right]v_i(t, \boldsymbol{x}) - \sigma_{ij}^{(a)}(t, \boldsymbol{x})v_j(t, \boldsymbol{x}) + q_i^{(a)}(t, \boldsymbol{x}), \tag{3.2.9}$$

for the momentum density, the energy density, the stress tensor, and the energy current density, respectively. Here, $\mathcal{E}(t, \boldsymbol{x})$ is the internal energy density and $\mathcal{P}(t, \boldsymbol{x})$ is the pressure, while $\sigma_{ij}^{(a)}(t, \boldsymbol{x})$ and $q_i^{(a)}(t, \boldsymbol{x})$ are the dissipative corrections to the stress tensor and the energy current density, respectively. If the scattering length is uniform over space and time, these constitutive relations have to return to Eqs. (2.2.11)–(2.2.14). Therefore, only the derivatives of the scattering length can be added to Eqs. (2.2.11)–(2.2.14), and the dissipative terms $\sigma_{ij}^{(a)}(t, \boldsymbol{x})$ and $q_i^{(a)}(t, \boldsymbol{x})$ can contain the derivatives of the sattering length in addition to the usual ones.[1]

The constitutibe relation for the contact density $\mathcal{C}(t, \boldsymbol{x})$ is obtained by substituting the constitutive relations for the energy density and the stress tensor of Eqs. (3.2.7) and (3.2.8)

---

[1]Note that the conserved charge densities do not have dissipative corrections, including the derivatives of the scattering length. This is because the conserved charge densities match the local thermodynamic quantities in the fluid rest frame $v_i(t, \boldsymbol{x}) = 0$. That is, $\mathcal{J}_i(t, \boldsymbol{x}) = 0$ and $\mathcal{H}(t, \boldsymbol{x}) = \mathcal{E}(t, \boldsymbol{x})$ hold in the fluid rest frame.

into Eq. (3.2.5):

$$\frac{\mathcal{C}(t, \boldsymbol{x})}{m\Omega_{d-1}a(t, \boldsymbol{x})^{d-2}} = d\mathcal{P}(t, \boldsymbol{x}) - 2\mathcal{E}(t, \boldsymbol{x}) - \sigma_{ii}^{(a)}(t, \boldsymbol{x}) + O(\partial^2). \tag{3.2.10}$$

Here, we introduce the contact density in local thermal equilibrium as

$$\frac{\mathcal{C}_{\text{eq}}(t, \boldsymbol{x})}{m\Omega_{d-1}a(t, \boldsymbol{x})^{d-2}} \equiv d\mathcal{P}(t, \boldsymbol{x}) - 2\mathcal{E}(t, \boldsymbol{x}), \tag{3.2.11}$$

which is understood as the local extension of one of the universal relations known as the pressure relation [28, 29]. With the use of $\mathcal{C}_{\text{eq}}(t, \boldsymbol{x})$, the constitutive relation for the contact density is written as

$$\mathcal{C}(t, \boldsymbol{x}) = \mathcal{C}_{\text{eq}}(t, \boldsymbol{x}) - m\Omega_{d-1}a(t, \boldsymbol{x})^{d-2}\sigma_{ii}^{(a)}(t, \boldsymbol{x}) + O(\partial^2). \tag{3.2.12}$$

3.2.2 Entropy production

To determine the dissipative corrections of $\sigma_{ij}^{(a)}(t, \boldsymbol{x})$ and $q_i^{(a)}(t, \boldsymbol{x})$, let us discuss entropy production. The entropy density $\mathcal{S}(t, \boldsymbol{x})$ is introduced as

$$\mathcal{E}(t, \boldsymbol{x}) + \mathcal{P}(t, \boldsymbol{x}) = T(t, \boldsymbol{x})\mathcal{S}(t, \boldsymbol{x}) + \mu(t, \boldsymbol{x})\mathcal{M}(t, \boldsymbol{x}), \tag{3.2.13}$$

where $T(t, \boldsymbol{x})$ and $\mu(t, \boldsymbol{x})$ are the local temperature and the local mass chemical potential, respectively. We choose $\mathcal{M}(t, \boldsymbol{x})$ and $\mathcal{E}(t, \boldsymbol{x})$ as the independent variables of thermodynamics and regard the entropy density as a function of $\mathcal{M}(t, \boldsymbol{x})$, $\mathcal{E}(t, \boldsymbol{x})$, and $a(t, \boldsymbol{x})$. With the help of the dimensional analysis, the entropy density is written as

$$\mathcal{S}(t, \boldsymbol{x}) = a(t, \boldsymbol{x})^{-d}f_S(a(t, \boldsymbol{x})^d\mathcal{M}(t, \boldsymbol{x})/m, \, ma(t, \boldsymbol{x})^{d+2}\mathcal{E}(t, \boldsymbol{x})), \tag{3.2.14}$$

where $f_S(\theta_1, \theta_2)$ is a function of two dimensionless ratios. Using this expression, we obtain the derivative of $\mathcal{S}(t, \boldsymbol{x})$ with respect to $a(t, \boldsymbol{x})$ as

$$\begin{aligned}
a(t, \boldsymbol{x})\frac{\partial \mathcal{S}(t, \boldsymbol{x})}{\partial a(t, \boldsymbol{x})} &= -d\mathcal{S}(t, \boldsymbol{x}) + d\mathcal{M}(t, \boldsymbol{x})\frac{\partial \mathcal{S}(t, \boldsymbol{x})}{\partial \mathcal{M}(t, \boldsymbol{x})} + (d+2)\mathcal{E}(t, \boldsymbol{x})\frac{\partial \mathcal{S}(t, \boldsymbol{x})}{\partial \mathcal{E}(t, \boldsymbol{x})} \\
&= -d\mathcal{S}(t, \boldsymbol{x}) + d\mathcal{M}(t, \boldsymbol{x})\left(-\frac{\mu(t, \boldsymbol{x})}{T(t, \boldsymbol{x})}\right) + (d+2)\mathcal{E}(t, \boldsymbol{x})\left(\frac{1}{T(t, \boldsymbol{x})}\right) \\
&= -\frac{d\mathcal{P}(t, \boldsymbol{x}) - 2\mathcal{E}(t, \boldsymbol{x})}{T(t, \boldsymbol{x})}.
\end{aligned} \tag{3.2.15}$$

Together with Eq. (3.2.11), we obtain

$$T(t, \boldsymbol{x})\frac{\partial \mathcal{S}(t, \boldsymbol{x})}{\partial a(t, \boldsymbol{x})} = -\frac{\mathcal{C}_{\text{eq}}(t, \boldsymbol{x})}{m\Omega_{d-1}a(t, \boldsymbol{x})^{d-1}}, \tag{3.2.16}$$

which is the local extension of one of the universal relations known as the adiabatic relation [28, 29]. The total differential of $\mathcal{S}(t, \boldsymbol{x})$ is given by

$$T(t, \boldsymbol{x})\mathrm{d}\mathcal{S}(t, \boldsymbol{x}) = \mathrm{d}\mathcal{E}(t, \boldsymbol{x}) - \mu(t, \boldsymbol{x})\mathrm{d}\mathcal{M}(t, \boldsymbol{x}) - \frac{\mathcal{C}_{\text{eq}}(t, \boldsymbol{x})}{m\Omega_{d-1}a(t, \boldsymbol{x})^{d-1}}\mathrm{d}a(t, \boldsymbol{x}). \tag{3.2.17}$$

Since the derivatives of the entropy density are related to the derivatives of the other conserved charge densities by Eq. (3.2.17), the continuity equations for the other conserved

charge quantities lead to the continuity equation for the entropy, called the entropy production equation,

$$\partial_t \mathcal{S}(t, \boldsymbol{x}) + \partial_i \left[\mathcal{S}(t, \boldsymbol{x}) v_i(t, \boldsymbol{x}) + \frac{q_i^{(a)}(t, \boldsymbol{x})}{T(t, \boldsymbol{x})} \right] = \frac{\Phi(t, \boldsymbol{x})}{T(t, \boldsymbol{x})}. \tag{3.2.18}$$

Here, the dissipation function $\Phi(t, \boldsymbol{x})$ is given by

$$\begin{aligned}
\Phi(t, \boldsymbol{x}) = &-q_i^{(a)}(t, \boldsymbol{x}) \frac{\partial_i T(t, \boldsymbol{x})}{T(t, \boldsymbol{x})} + \sigma_{ij}^{(a)}(t, \boldsymbol{x}) \partial_i v_j(t, \boldsymbol{x}) \\
&- \sigma_{ii}^{(a)}(t, \boldsymbol{x}) \Big[\partial_t \ln a(t, \boldsymbol{x}) + v_k(t, \boldsymbol{x}) \partial_k \ln a(t, \boldsymbol{x}) \Big] + O(\partial^3).
\end{aligned} \tag{3.2.19}$$

We then impose the second law of thermodynamics in local thermal equilibrium, i.e., the entropy production rate is non-negative for arbitrary field configurations of $T(t, \boldsymbol{x})$, $v_i(t, \boldsymbol{x})$, and $a(t, \boldsymbol{x})$. Then, the dissipative corrections up to first order in derivatives are found to be

$$q_i^{(a)}(t, \boldsymbol{x}) = -\kappa(t, \boldsymbol{x}) \partial_i T(t, \boldsymbol{x}) + O(\partial^2), \tag{3.2.20}$$

$$\sigma_{\langle ij \rangle}^{(a)}(t, \boldsymbol{x}) = \eta(t, \boldsymbol{x}) V_{ij}(t, \boldsymbol{x}) + O(\partial^2), \tag{3.2.21}$$

$$\sigma_{ii}^{(a)}(t, \boldsymbol{x}) = d\zeta(t, \boldsymbol{x}) V^{(a)}(t, \boldsymbol{x}) + O(\partial^2), \tag{3.2.22}$$

and

$$\kappa(t, \boldsymbol{x}) \geq 0, \qquad \eta(t, \boldsymbol{x}) \geq 0, \qquad \zeta(t, \boldsymbol{x}) \geq 0, \tag{3.2.23}$$

where the traceless part of the viscous term is introduced as

$$\sigma_{\langle ij \rangle}^{(a)}(t, \boldsymbol{x}) = \sigma_{ij}^{(a)} - \delta_{ij} \frac{\sigma_{kk}(t, \boldsymbol{x})}{d}. \tag{3.2.24}$$

Here, $V_{ij}(t, \boldsymbol{x})$ is the usual shear strain rate tensor defined by Eq. (2.3.51), but

$$V^{(a)}(t, \boldsymbol{x}) \equiv \partial_k v_k(t, \boldsymbol{x}) - d \Big[\partial_t \ln a(t, \boldsymbol{x}) + v_k(t, \boldsymbol{x}) \partial_k \ln a(t, \boldsymbol{x}) \Big] \tag{3.2.25}$$

is the bulk strain rate tensor modified by the spacetime-dependent scattering length. The transport coefficients, $\kappa(t, \boldsymbol{x})$, $\eta(t, \boldsymbol{x})$, and $\zeta(t, \boldsymbol{x})$, depend on space and time because they are locally specified by $\mathcal{M}(t, \boldsymbol{x})$, $\mathcal{E}(t, \boldsymbol{x})$ and $a(t, \boldsymbol{x})$, Substituting these dissipation corrections into Eq. (3.2.19), the dissipation function results in

$$\Phi(t, \boldsymbol{x}) = \kappa(t, \boldsymbol{x}) \frac{[\partial_i T(t, \boldsymbol{x})]^2}{T(t, \boldsymbol{x})} + \frac{\eta(t, \boldsymbol{x})}{2} [V_{ij}(t, \boldsymbol{x})]^2 + \zeta(t, \boldsymbol{x}) [V^{(a)}(t, \boldsymbol{x})]^2 + O(\partial^3). \tag{3.2.26}$$

Thus, the second law of thermodynamics is satisfied.

We can see that the dissipation function has a term involving the spacetime-dependent scattering length as

$$\Phi(t, \boldsymbol{x}) \sim \frac{\zeta(t, \boldsymbol{x})}{a(t, \boldsymbol{x})^2} [\partial_t a(t, \boldsymbol{x})]^2 \sim \zeta(t, \boldsymbol{x}) a(t, \boldsymbol{x})^2 \left(\partial_t \frac{1}{a(t, \boldsymbol{x})} \right)^2. \tag{3.2.27}$$

In order for such terms to be non-divergent, the bulk viscosity must vanish at the least as

$$\zeta(t, \boldsymbol{x}) \sim a(t, \boldsymbol{x})^2 \qquad \text{for} \quad a(t, \boldsymbol{x}) \to 0 \tag{3.2.28}$$

and

$$\zeta(t, \boldsymbol{x}) \sim \frac{1}{a(t, \boldsymbol{x})^2} \qquad \text{for} \quad \frac{1}{a(t, \boldsymbol{x})} \to 0, \tag{3.2.29}$$

assuming that the hydrodynamics is applicable in both limits. In particular, the latter behavior is consistent with the vanishing bulk viscosity of the unitary Fermi gas in a normal phase [46, 49, 74, 89–91].

3.3 Hydrodynamics for superfluids

3.3.1 Superfluid velocity

We can construct the hydrodynamic equations for superfluids in a similar way. The hydrodynamics for superfluids is given by Landau's two-fluid model [97]. In the two-fluid model, there is a superfluid component, whose velocity is microscopically defined by

$$u_i(t, \boldsymbol{x}) \equiv \frac{\partial_i \theta(t, \boldsymbol{x}) - A_i(t, \boldsymbol{x})}{m}, \tag{3.3.1}$$

in addition to the normal fluid component. Here, $\theta(t, \boldsymbol{x})$ is the condensate phase normalized so as to transform as $\theta(t, \boldsymbol{x}) \to \theta(t, \boldsymbol{x}) + \chi(t, \boldsymbol{x})$ under the U(1) gauge transformation (3.1.5). The time derivative of $u_i(t, \boldsymbol{x})$ can be written formally as

$$\partial_t u_i(t, \boldsymbol{x}) + \partial_i \left(\frac{[u_j(t, \boldsymbol{x})]^2}{2} + \nu(t, \boldsymbol{x}) \right) = \frac{F_{it}(t, \boldsymbol{x})}{m}, \tag{3.3.2}$$

where $\nu(t, \boldsymbol{x})$ is defined by

$$\nu(t, \boldsymbol{x}) \equiv -\frac{\partial_t \theta(t, \boldsymbol{x}) - A_t(t, \boldsymbol{x})}{m} - \frac{[u_i(t, \boldsymbol{x})]^2}{2}. \tag{3.3.3}$$

This quantity $\nu(t, \boldsymbol{x})$ is a scalar under the Galilean transformation and corresponds to the mass chemical potential if the system is uniform over space and time [26]. In the hydrodynamics, Eq. (3.3.2) is regarded as the time-evolution equation for $u_i(t, \boldsymbol{x})$, and $\nu(t, \boldsymbol{x})$ is given by the constitutive relation,

$$\nu(t, \boldsymbol{x}) = \mu(t, \boldsymbol{x}) + \mu'^{(a)}(t, \boldsymbol{x}), \tag{3.3.4}$$

where $\mu(t, \boldsymbol{x})$ is the local chemical potential and $\mu'^{(a)}(t, \boldsymbol{x})$ is its dissipative correction.

3.3.2 Constitutive relations

The two-fluid model has $\mathcal{M}(t, \boldsymbol{x})$, $\mathcal{E}(t, \boldsymbol{x})$, $v_i(t, \boldsymbol{x})$, and $u_i(t, \boldsymbol{x})$ as independent variables. The time evolution for these eight variables is described by the continuity equations of Eqs. (3.2.2), (3.2.3), and (3.2.4), and the time-evolution equation of Eq. (3.3.2). Here, the continuity equations remain the same because they follow from the operator identities. The constitutive relations is modified due to the presence of the superfluid velocity, and read

$$\mathcal{M}(t, \boldsymbol{x}) = \mathcal{M}_n(t, \boldsymbol{x}) + \mathcal{M}_s(t, \boldsymbol{x}), \tag{3.3.5}$$

$$\mathcal{J}_i(t, \boldsymbol{x}) = \mathcal{M}_n(t, \boldsymbol{x}) v_i(t, \boldsymbol{x}) + \mathcal{M}_s(t, \boldsymbol{x}) u_i(t, \boldsymbol{x}), \tag{3.3.6}$$

$$\mathcal{H}(t, \boldsymbol{x}) = \mathcal{E}(t, \boldsymbol{x}) + \mathcal{J}_i(t, \boldsymbol{x}) u_i(t, \boldsymbol{x}) - \frac{\mathcal{M}(t, \boldsymbol{x})}{2} [u_i(t, \boldsymbol{x})]^2, \tag{3.3.7}$$

$$\Pi_{ij}(t, \boldsymbol{x}) = \mathcal{P}(t, \boldsymbol{x}) \delta_{ij} + \mathcal{M}_n(t, \boldsymbol{x}) v_i(t, \boldsymbol{x}) v_j(t, \boldsymbol{x}) + \mathcal{M}_s(t, \boldsymbol{x}) u_i(t, \boldsymbol{x}) u_j(t, \boldsymbol{x}) - \sigma_{ij}^{(a)}(t, \boldsymbol{x}), \tag{3.3.8}$$

$$\mathcal{Q}_i(t, \boldsymbol{x}) = \left[\mathcal{H}(t, \boldsymbol{x}) + \mathcal{P}(t, \boldsymbol{x}) \right] v_i(t, \boldsymbol{x}) - \left[\mu(t, \boldsymbol{x}) + \frac{1}{2} [u_j(t, \boldsymbol{x})]^2 \right] \mathcal{M}_s(t, \boldsymbol{x}) w_i(t, \boldsymbol{x})$$
$$- \sigma_{ij}^{(a)}(t, \boldsymbol{x}) v_j(t, \boldsymbol{x}) - \mu'^{(a)}(t, \boldsymbol{x}) \mathcal{M}_s(t, \boldsymbol{x}) w_i(t, \boldsymbol{x}) + q_i^{(a)}(t, \boldsymbol{x}), \tag{3.3.9}$$

for the mass density, the momentum density, the energy density, the stress tensor, and the energy current density, respectively. Here, $\mathcal{M}_n(t, \boldsymbol{x})$ and $\mathcal{M}_s(t, \boldsymbol{x})$ are the normal fluid and superfluid components of the total mass density, and $w_i(t, \boldsymbol{x})$ is the relative velocity between the two components:

$$w_i(t, \boldsymbol{x}) \equiv v_i(t, \boldsymbol{x}) - u_i(t, \boldsymbol{x}). \tag{3.3.10}$$

Because one cannot take an inertial frame in which the velocities of both components are zero simultaneously in general, the thermodynamics of a superfluid phase is considered in a rest frame of $u_i(t, \boldsymbol{x}) = 0$. In such a frame, the relative velocity appears in the thermodynamic relations:

$$\left(\frac{\partial \mathcal{S}(t, \boldsymbol{x})}{\partial \mathcal{M}(t, \boldsymbol{x})} \right)_{\mathcal{E}, \mathcal{M}_n w_i, a} = -\frac{\mu(t, \boldsymbol{x})}{T(t, \boldsymbol{x})}, \tag{3.3.11}$$

$$\left(\frac{\partial \mathcal{S}(t, \boldsymbol{x})}{\partial \mathcal{E}(t, \boldsymbol{x})} \right)_{\mathcal{M}, \mathcal{M}_n w_i, a} = \frac{1}{T(t, \boldsymbol{x})}, \tag{3.3.12}$$

$$\left(\frac{\partial \mathcal{S}(t, \boldsymbol{x})}{\partial [\mathcal{M}_n(t, \boldsymbol{x}) w_i(t, \boldsymbol{x})]} \right)_{\mathcal{M}, \mathcal{E}, a} = -\frac{w_i(t, \boldsymbol{x})}{T(t, \boldsymbol{x})}, \tag{3.3.13}$$

where the entropy density $\mathcal{S}(t, \boldsymbol{x})$ is provided by

$$\mathcal{P}(t, \boldsymbol{x}) + \mathcal{E}(t, \boldsymbol{x}) - \mathcal{M}_n(t, \boldsymbol{x})[w_i(t, \boldsymbol{x})]^2 = T(t, \boldsymbol{x})\mathcal{S}(t, \boldsymbol{x}) + \mu(t, \boldsymbol{x})\mathcal{M}(t, \boldsymbol{x}). \tag{3.3.14}$$

The constitutive relation for the contact density $\mathcal{C}(t, \boldsymbol{x})$ is obtained by substituting the constitutive relations for the energy density and the stress tensor of Eqs. (3.3.7) and (3.3.8) into Eq. (3.2.5):

$$\frac{\mathcal{C}(t, \boldsymbol{x})}{m\Omega_{d-1}a(t, \boldsymbol{x})^{d-2}} = d\mathcal{P}(t, \boldsymbol{x}) - 2\mathcal{E}(t, \boldsymbol{x}) + \mathcal{M}_n(t, \boldsymbol{x})[w_i(t, \boldsymbol{x})]^2 - \sigma_{ii}^{(a)}(t, \boldsymbol{x}) + O(\partial^2). \tag{3.3.15}$$

We introduce the contact density in local thermal equilibrium as

$$\frac{\mathcal{C}_{\text{eq}}(t, \boldsymbol{x})}{m\Omega_{d-1}a(t, \boldsymbol{x})^{d-2}} \equiv d\mathcal{P}(t, \boldsymbol{x}) - 2\mathcal{E}(t, \boldsymbol{x}) + \mathcal{M}_n(t, \boldsymbol{x})[w_i(t, \boldsymbol{x})]^2, \tag{3.3.16}$$

which is the pressure relation for the two-fluid model. With the use of $\mathcal{C}_{\text{eq}}(t, \boldsymbol{x})$, the constitutive relation for the contact density is written as

$$\mathcal{C}(t, \boldsymbol{x}) = \mathcal{C}_{\text{eq}}(t, \boldsymbol{x}) - m\Omega_{d-1}a(t, \boldsymbol{x})^{d-2}\sigma_{ii}^{(a)}(t, \boldsymbol{x}) + O(\partial^2). \tag{3.3.17}$$

3.3.3   Entropy production

We regard the entropy density as a function of $\mathcal{M}(t, \boldsymbol{x})$, $\mathcal{E}(t, \boldsymbol{x})$, $\mathcal{M}_n(t, \boldsymbol{x})w_i(t, \boldsymbol{x})$, and $a(t, \boldsymbol{x})$. With the help of the dimensional analysis, the entropy density is written as

$$\mathcal{S}(t, \boldsymbol{x}) = a(t, \boldsymbol{x})^{-d}f_S(a(t, \boldsymbol{x})^d\mathcal{M}(t, \boldsymbol{x})/m,\, ma(t, \boldsymbol{x})^{d+2}\mathcal{E}(t, \boldsymbol{x}),\, a(t, \boldsymbol{x})^{d+1}\mathcal{M}_n(t, \boldsymbol{x})w_i(t, \boldsymbol{x})), \tag{3.3.18}$$

where $f_S(\theta_1, \theta_2, \theta_3)$ is a function of three dimensionless ratios. Using this expression, we obtain the derivative of $\mathcal{S}(t, \boldsymbol{x})$ with respect to $a(t, \boldsymbol{x})$ as

$$
\begin{aligned}
a(t, \boldsymbol{x}) \frac{\partial \mathcal{S}(t, \boldsymbol{x})}{\partial a(t, \boldsymbol{x})} &= -d\mathcal{S}(t, \boldsymbol{x}) + d\mathcal{M}(t, \boldsymbol{x}) \frac{\partial \mathcal{S}(t, \boldsymbol{x})}{\partial \mathcal{M}(t, \boldsymbol{x})} + (d+2)\mathcal{E}(t, \boldsymbol{x}) \frac{\partial \mathcal{S}(t, \boldsymbol{x})}{\partial \mathcal{E}(t, \boldsymbol{x})} \\
&\quad + (d+1)\mathcal{M}_n(t, \boldsymbol{x}) w_i(t, \boldsymbol{x}) \frac{\partial \mathcal{S}(t, \boldsymbol{x})}{\partial [\mathcal{M}_n(t, \boldsymbol{x}) w_i(t, \boldsymbol{x})]} \\
&= -\frac{d\mathcal{P}(t, \boldsymbol{x}) - 2\mathcal{E}(t, \boldsymbol{x}) + \mathcal{M}_n(t, \boldsymbol{x})[w_i(t, \boldsymbol{x})]^2}{T(t, \boldsymbol{x})}.
\end{aligned}
\tag{3.3.19}
$$

Together with Eq. (3.3.16), we obtain

$$
T(t, \boldsymbol{x}) \frac{\partial \mathcal{S}(t, \boldsymbol{x})}{\partial a(t, \boldsymbol{x})} = -\frac{\mathcal{C}_{\text{eq}}(t, \boldsymbol{x})}{m\Omega_{d-1} a(t, \boldsymbol{x})^{d-1}},
\tag{3.3.20}
$$

which is the adiabatic relation for the two-fluid model. For the two-fluid model, the total differential of $\mathcal{S}(t, \boldsymbol{x})$ is given by

$$
\begin{aligned}
T(t, \boldsymbol{x}) \mathrm{d}\mathcal{S}(t, \boldsymbol{x}) &= \mathrm{d}\mathcal{E}(t, \boldsymbol{x}) - \mu(t, \boldsymbol{x}) \mathrm{d}\mathcal{M}(t, \boldsymbol{x}) \\
&\quad - w_i(t, \boldsymbol{x}) \mathrm{d}[\mathcal{M}_n(t, \boldsymbol{x}) w_i(t, \boldsymbol{x})] - \frac{\mathcal{C}_{\text{eq}}(t, \boldsymbol{x})}{m\Omega_{d-1} a(t, \boldsymbol{x})^{d-1}} \mathrm{d}a(t, \boldsymbol{x}).
\end{aligned}
\tag{3.3.21}
$$

We can calculate the continuity equation for the entropy by using the continuity equations and the constitutive relations, and obtain the following entropy production equation:

$$
\partial_t \mathcal{S}(t, \boldsymbol{x}) + \partial_i \left[\mathcal{S}(t, \boldsymbol{x}) v_i(t, \boldsymbol{x}) + \frac{q_i^{(a)}(t, \boldsymbol{x})}{T(t, \boldsymbol{x})} \right] = \frac{\Phi(t, \boldsymbol{x})}{T(t, \boldsymbol{x})},
\tag{3.3.22}
$$

where the dissipation function $\Phi(t, \boldsymbol{x})$ is given by

$$
\begin{aligned}
\Phi(t, \boldsymbol{x}) &= -q_i^{(a)}(t, \boldsymbol{x}) \frac{\partial_i T(t, \boldsymbol{x})}{T(t, \boldsymbol{x})} + \sigma_{ij}^{(a)}(t, \boldsymbol{x}) \partial_i v_j(t, \boldsymbol{x}) \\
&\quad - \sigma_{ii}^{(a)}(t, \boldsymbol{x}) \Big[\partial_t \ln a(t, \boldsymbol{x}) + v_k(t, \boldsymbol{x}) \partial_k \ln a(t, \boldsymbol{x}) \Big] \\
&\quad + \mu'^{(a)}(t, \boldsymbol{x}) \partial_i \Big[\mathcal{M}_s(t, \boldsymbol{x}) w_i(t, \boldsymbol{x}) \Big] + O(\partial^3).
\end{aligned}
\tag{3.3.23}
$$

We impose the second law of thermodynamics in local thermal equilibrium, i.e., the entropy production rate is non-negative for arbitrary field configurations of $T(t, \boldsymbol{x})$, $v_i(t, \boldsymbol{x})$, $\mathcal{M}_s(t, \boldsymbol{x}) w_i(t, \boldsymbol{x})$, and $a(t, \boldsymbol{x})$. Then, the dissipative corrections up to first order in derivatives are found to be

$$
q_i^{(a)}(t, \boldsymbol{x}) = -\kappa(t, \boldsymbol{x}) \partial_i T(t, \boldsymbol{x}) + O(\partial^2),
\tag{3.3.24}
$$

$$
\sigma_{\langle ij \rangle}^{(a)}(t, \boldsymbol{x}) = \eta(t, \boldsymbol{x}) V_{ij}(t, \boldsymbol{x}) + O(\partial^2),
\tag{3.3.25}
$$

$$
\sigma_{ii}^{(a)}(t, \boldsymbol{x}) = d\zeta_1(t, \boldsymbol{x}) \partial_i[\mathcal{M}_s(t, \boldsymbol{x}) w_i(t, \boldsymbol{x})] + d\zeta_2(t, \boldsymbol{x}) V^{(a)}(t, \boldsymbol{x}) + O(\partial^2),
\tag{3.3.26}
$$

$$
\mu'^{(a)}(t, \boldsymbol{x}) = \zeta_3(t, \boldsymbol{x}) \partial_i \Big[\mathcal{M}_s(t, \boldsymbol{x}) w_i(t, \boldsymbol{x}) \Big] + \zeta_4(t, \boldsymbol{x}) V^{(a)}(t, \boldsymbol{x}) + O(\partial^2),
\tag{3.3.27}
$$

and

$$
\kappa(t, \boldsymbol{x}) \geq 0, \quad \eta(t, \boldsymbol{x}) \geq 0, \quad \zeta_2(t, \boldsymbol{x}) \geq 0, \quad \zeta_3(t, \boldsymbol{x}) \geq 0, \quad \zeta_2(t, \boldsymbol{x})\zeta_3(t, \boldsymbol{x}) \geq \zeta_1(t, \boldsymbol{x})^2.
\tag{3.3.28}
$$

where $V_{ij}(t, \boldsymbol{x})$ and $V^{(a)}(t, \boldsymbol{x})$ are the shear and bulk strain rate tensors defined by Eqs. (2.3.51) and (3.2.25), respectively. Because of the Onsager reciprocity, we have $\zeta_1(t, \boldsymbol{x}) = \zeta_4(t, \boldsymbol{x})$. The transport coefficients, $\kappa(t, \boldsymbol{x})$, $\eta(t, \boldsymbol{x})$, $\zeta_1(t, \boldsymbol{x})$, $\zeta_2(t, \boldsymbol{x})$, and $\zeta_3(t, \boldsymbol{x})$, depend on space and time because they are locally specified by $\mathcal{M}(t, \boldsymbol{x})$, $\mathcal{E}(t, \boldsymbol{x})$, $\mathcal{M}_n(t, \boldsymbol{x})w_i(t, \boldsymbol{x})$, and $a(t, \boldsymbol{x})$. Substituting these dissipation corrections into Eq. (3.3.23), the dissipation function results in

$$\Phi(t, \boldsymbol{x}) = \kappa(t, \boldsymbol{x})\frac{[\partial_i T(t, \boldsymbol{x})]^2}{T(t, \boldsymbol{x})} + \frac{\eta(t, \boldsymbol{x})}{2}[V_{ij}(t, \boldsymbol{x})]^2 + 2\zeta_1(t, \boldsymbol{x})V^{(a)}(t, \boldsymbol{x})\partial_i[\mathcal{M}_s(t, \boldsymbol{x})w_i(t, \boldsymbol{x})]$$

$$+ \zeta_2(t, \boldsymbol{x})[V^{(a)}(t, \boldsymbol{x})]^2 + \zeta_3(t, \boldsymbol{x})\Big(\partial_i[\mathcal{M}_s(t, \boldsymbol{x})w_i(t, \boldsymbol{x})]\Big)^2 + O(\partial^3). \qquad (3.3.29)$$

Thus, the second law of thermodynamics is satisfied.

We can see that the dissipation function has terms involving the spacetime-dependent scattering length as

$$\Phi(t, \boldsymbol{x}) \sim \frac{\zeta_1(t, \boldsymbol{x})}{a(t, \boldsymbol{x})}[\partial_t a(t, \boldsymbol{x})] + \frac{\zeta_2(t, \boldsymbol{x})}{a(t, \boldsymbol{x})^2}[\partial_t a(t, \boldsymbol{x})]^2$$

$$\sim \zeta_1(t, \boldsymbol{x})a(t, \boldsymbol{x})\left(\partial_t\frac{1}{a(t, \boldsymbol{x})}\right) + \zeta_2(t, \boldsymbol{x})a(t, \boldsymbol{x})^2\left(\partial_t\frac{1}{a(t, \boldsymbol{x})}\right)^2. \qquad (3.3.30)$$

In order for such terms to be non-divergent, the bulk viscosity must disappear at the least as

$$\zeta_1(t, \boldsymbol{x}) \sim a(t, \boldsymbol{x}), \qquad \zeta_2(t, \boldsymbol{x}) \sim a(t, \boldsymbol{x})^2 \qquad \text{for} \quad a(t, \boldsymbol{x}) \to 0 \qquad (3.3.31)$$

and

$$\zeta_1(t, \boldsymbol{x}) \sim \frac{1}{a(t, \boldsymbol{x})}, \qquad \zeta_2(t, \boldsymbol{x}) \sim \frac{1}{a(t, \boldsymbol{x})^2} \qquad \text{for} \quad \frac{1}{a(t, \boldsymbol{x})} \to 0, \qquad (3.3.32)$$

assuming that the hydrodynamics is applicable in both limits. In particular, the latter behaviors are consistent with the vanishing bulk viscosities of the unitary Fermi gas in a superfluid phase [49, 102, 103].

3.4   Summary

Hydrodynamics is a low-energy effective theory describing long-time and long-distance physics of correlated systems out of thermal equilibrium. The hydrodynamic equations are provided by the continuity equations and the constitutive relations, which form a set of closed equations. In this chapter, we constructed the hydrodynamic equations including the spacetime-dependent scattering length as an external field. We showed that it not only appears explicitly as an external source of the momentum and energy continuity equations [Eqs. (3.2.3) and (3.2.4)], but also enters the constitutive relations through the modified bulk strain rate tensor [Eq. (3.2.25)] in both normal and superfluid phases. The expression of the modified bulk strain rate tensor can be understood intuitively from the equivalence between $\partial_k v_k(t, \boldsymbol{x})$ and $-d\partial_t \ln a(t, \boldsymbol{x}) = -[\partial_t a(t, \boldsymbol{x})^d]/a(t, \boldsymbol{x})^d$. Because the interaction has no scale other than the scattering length, the expansion (contraction) rate of the fluid volume represented by $\partial_k v_k(t, \boldsymbol{x})$ is equivalent to the contraction (expansion) rate of the volume element $a(t, \boldsymbol{x})^d$ represented by $-[\partial_t a(t, \boldsymbol{x})^d]/a(t, \boldsymbol{x})^d$. Furthermore, to ensure the Galilean invariance, the time derivative term $\partial_t \ln a(t, \boldsymbol{x})$ has to be accompanied by $v_k(t, \boldsymbol{x})\partial_k \ln a(t, \boldsymbol{x})$ so as to form the material derivative $\partial_t + v_k(t, \boldsymbol{x})\partial_k$. As a result, the spacetime-dependent scattering length

is added to the original bulk strain rate tensor $\partial_k v_k(t, \boldsymbol{x})$ in the form of Eq. (3.2.25). Because the isotropic expansion of the fluid volume is associated with a scale transformation, we can also derive the modified bulk strain tensor in terms of the Galilean and conformal symmetries, as detailed in Appendix B.

Finally, we summarize the physical implications to be extracted from our findings. As already shown in Eqs. (3.2.29) and (3.3.32), the vanishing bulk viscosities in the unitarity limit can be reproduced in both normal and superfluid phases [46, 49, 74, 89–91, 102, 103]. In addition, let us consider for brevity the case where the scattering length depends only on time and varies slowly in a uniform system at rest. From the constitutive relations and the dissipative corrections, i.e., Eqs. (3.2.12) and (3.2.22) for the normal phase and Eqs. (3.3.17) and (3.3.26) for the superfluid phase, the contact density is obtained as

$$\mathcal{C}(t) = \mathcal{C}_{\mathrm{eq}}(t) + d^2 m \Omega_{d-1} \zeta(t) a(t)^{d-3} \dot{a}(t) + O(\dot{a}^2), \tag{3.4.1}$$

where $\zeta(t)$ for the normal phase should be replaced with $\zeta_2(t)$ for the superfluid phase. Here, the time variation of the scattering length does not cause the fluid velocity in a uniform system. The continuity equation for the energy further leads to

$$\dot{\mathcal{H}}(t) = \frac{\mathcal{C}_{\mathrm{eq}}(t)}{m \Omega_{d-1} a(t)^{d-1}} \dot{a}(t) + d^2 \frac{\zeta(t)}{a(t)^2} \dot{a}(t)^2 + O(\dot{a}^3). \tag{3.4.2}$$

Similarly, Eqs. (3.2.26) and (3.3.29) prove that the entropy density is produced as

$$T(t)\dot{\mathcal{S}}(t) = d^2 \frac{\zeta(t)}{a(t)^2} \dot{a}(t)^2 + O(\dot{a}^3). \tag{3.4.3}$$

The energy and entropy densities have the contributions proportional to the bulk viscosity due to the time-dependent scattering length. We will confirm Eqs. (3.4.1)–(3.4.3) microscopically by employing the linear response theory in Chapter 4. These results of Eqs. (3.4.1)–(3.4.3) may be useful as a novel probe to measure the bulk viscosity in ultracold atom experiments.[2] For example, when the scattering length is periodically modulated as

$$a(t)^{-1} = \delta b \sin(\omega t), \tag{3.4.4}$$

the entropy production can be expressed as

$$T(t)\dot{\mathcal{S}}(t) = \zeta'(t) \left(d\omega \delta b \right)^2 \cos^2(\omega t) + O(\omega^3, \delta b^3), \tag{3.4.5}$$

where, according to Eqs. (3.2.29) and (3.3.32), we define $\zeta'(t)$ as the coefficient of the tail of the bulk viscosity in the unitarity limit,

$$\zeta'(t) \equiv \zeta(t) a(t)^2. \tag{3.4.6}$$

In the unitarity limit, the bulk viscosity itself vanishes, but $\zeta'(t)$ is supposed to be finite and the modulated scattering length may be useful to measure it.

---

[2] A uniform system can be realized experimentally, for example, by using an optical box trap [104].

Chapter 4

Bulk viscosity in the quantum virial expansion

In this chapter, we compute the bulk viscosity of the resonant Fermi gas. To perform a reliable computation in the strongly correlated regime, such as the unitarity limit, we employ the quantum virial expansion as a non-perturbative method. In Sec. 4.1, we review the quantum virial expansion and specifically calculate the thermodynamic quantities of the resonant Fermi gas. In Sec. 4.2, we first derive the Kubo formula for the bulk viscosity expressed by the contact-contact response function and confirm that the bulk viscosity appears in the response of the contact to a variation of the scattering length from the viewpoint of the linear response theory. We next review the bulk viscosity calculation via the Kubo formula in the quantum virial expansion [89–91]. Then, we compare the obtained bulk viscosity with that derived in the kinetic theory and discuss the origin of the discrepancy between them. This chapter is concluded by a summary in Sec. 4.3.

4.1 Quantum virial expansion

At high temperatures, where $n\lambda_T^d \ll 1$ holds for the particle number density n and the thermal de Broglie wavelength $\lambda_T \equiv \sqrt{2\pi/(mT)}$, correlations between particles are effectively weak. As already discussed, the resonant Fermi gas has three length scales: the average interparticle distance $n^{-1/d}$, the thermal de Broglie wavelength λ_T, and the scattering length a. All of them are sufficiently larger than the other length scales of the interaction potential, which are typically represented by the radius of the interaction r_R. In the quantum virial expansion for the resonant Fermi gas, we consider a regime in which the gas meets the condition of

$$r_R \ll \lambda_T \ll n^{-1/d}, \qquad r_R \ll a, \tag{4.1.1}$$

which is referred to as the high-temperature regime.

4.1.1 Formulation

Physical quantities in thermal equilibrium are calculated from the expectation values in the grand canonical ensemble:

$$\langle \hat{\mathcal{O}} \rangle \equiv \frac{1}{Z} \text{Tr}\left[e^{-\beta(\hat{H} - \mu\hat{N})} \hat{\mathcal{O}} \right], \tag{4.1.2}$$

where Z is the grand canonical partition function provided by

$$Z = \mathrm{Tr}\left[e^{-\beta(\hat{H}-\mu\hat{N})}\right], \tag{4.1.3}$$

with the inverse temperature $\beta = T^{-1}$ and the chemical potential μ. The trace can be decomposed into each particle number sector as

$$\mathrm{Tr}\left[e^{-\beta(\hat{H}-\mu\hat{N})}\hat{\mathcal{O}}\right] = \sum_{N=0}^{\infty} \mathrm{Tr}_N\left[e^{-\beta(\hat{H}-\mu\hat{N})}\hat{\mathcal{O}}\right] = \sum_{N=0}^{\infty} z^N \mathrm{Tr}_N\left[e^{-\beta\hat{H}}\hat{\mathcal{O}}\right], \tag{4.1.4}$$

where Tr_N denotes the trace restricted to the N-body sector and $z \equiv e^{\beta\mu}$ is the fugacity. At high temperatures with a fixed number of particles, the chemical potential μ diverges to $-\infty$, so that the fugacity becomes small $z \ll 1$ and it plays the role of an expansion parameter. Then, the expectation value can be expanded in terms of z as

$$\langle\hat{\mathcal{O}}\rangle = z\langle\hat{\mathcal{O}}\rangle^{(1)} + z^2\langle\hat{\mathcal{O}}\rangle^{(2)} + O(z^3), \tag{4.1.5}$$

with

$$\langle\hat{\mathcal{O}}\rangle^{(1)} = \mathrm{Tr}_1\left[e^{-\beta\hat{H}}\hat{\mathcal{O}}\right], \tag{4.1.6}$$

$$\langle\hat{\mathcal{O}}\rangle^{(2)} = \mathrm{Tr}_2\left[e^{-\beta\hat{H}}\hat{\mathcal{O}}\right] - \mathrm{Tr}_1\left[e^{-\beta\hat{H}}\hat{\mathcal{O}}\right]\mathrm{Tr}_1\left[e^{-\beta\hat{H}}\right], \tag{4.1.7}$$

where the zero particle sector is obviously $\mathrm{Tr}_0[e^{-\beta\hat{H}}] = 1$ and the physical quantity $\hat{\mathcal{O}}$ is supposed to be zero in vacuum: $\mathrm{Tr}_0[e^{-\beta\hat{H}}\hat{\mathcal{O}}] = 0$. This expansion is called the quantum virial expansion [105], which is valid in the high-temperature regime. The low-order coefficients for the fugacity can be computed from few-body problems.

4.1.2 Matsubara formalism

To discuss specific calculations in the quantum virial expansion, we introduce the Matsubara formalism. We consider a resonant Fermi gas in d spatial dimensions whose Hamiltonian is given by

$$\hat{H} = \sum_{\sigma=\uparrow,\downarrow} \int \mathrm{d}\boldsymbol{x}\, \hat{\psi}_\sigma^\dagger(\boldsymbol{x})\frac{-\nabla^2}{2m}\hat{\psi}_\sigma(\boldsymbol{x}) + \sum_{\sigma,\rho} \int \mathrm{d}\boldsymbol{x}\, \frac{g}{2}\hat{\psi}_\sigma^\dagger(\boldsymbol{x})\hat{\psi}_\rho^\dagger(\boldsymbol{x})\hat{\psi}_\rho(\boldsymbol{x})\hat{\psi}_\sigma(\boldsymbol{x}). \tag{4.1.8}$$

Here, we employ the Schrödinger picture, and the annihilation and creation operators obey the canonical anti-commutation relations,

$$\begin{aligned}
\{\hat{\psi}_\sigma(\boldsymbol{x}),\, \hat{\psi}_\rho^\dagger(\boldsymbol{y})\} &= \delta_{\sigma\rho}\delta^d(\boldsymbol{x}-\boldsymbol{y}), \\
\{\hat{\psi}_\sigma(\boldsymbol{x}),\, \hat{\psi}_\rho(\boldsymbol{y})\} &= \{\hat{\psi}_\sigma^\dagger(\boldsymbol{x}),\, \hat{\psi}_\rho^\dagger(\boldsymbol{y})\} = 0.
\end{aligned} \tag{4.1.9}$$

In the dimensional regularization, the bare coupling constant g is related to the scattering length a as in Eq. (2.1.25):

$$\frac{1}{g} = \frac{ma^{2-d}}{(d-2)\Omega_{d-1}}, \tag{4.1.10}$$

with $\Omega_{d-1} \equiv (4\pi)^{d/2}/2\Gamma(2-d/2) = 2\pi, 4\pi$ for $d = 2, 3$.

For the Matsubara formalism, we introduce the imaginary-time representation of an operator $\hat{\mathcal{O}}$ as

$$\hat{\mathcal{O}}(\tau) \equiv e^{\tau(\hat{H}-\mu\hat{N})}\hat{\mathcal{O}}e^{-\tau(\hat{H}-\mu\hat{N})}, \qquad (0 \leq \tau \leq \beta). \tag{4.1.11}$$

Using the annihilation and creation operators in the imaginary-time representation, we define the single-particle Green function as

$$\mathcal{G}_{\sigma\sigma'}(\tau, \boldsymbol{x}; \tau', \boldsymbol{x}') \equiv -\langle \mathcal{T}_\tau \hat{\psi}_\sigma(\tau, \boldsymbol{x})\hat{\psi}^\dagger_{\sigma'}(\tau', \boldsymbol{x}') \rangle, \tag{4.1.12}$$

where $\mathcal{T}_\tau$ denotes the time-ordering operator for the imaginary time:

$$\mathcal{T}_\tau \hat{\psi}_\sigma(\tau, \boldsymbol{x})\hat{\psi}^\dagger_{\sigma'}(\tau', \boldsymbol{x}') \equiv \Theta(\tau - \tau')\hat{\psi}_\sigma(\tau, \boldsymbol{x})\hat{\psi}^\dagger_{\sigma'}(\tau', \boldsymbol{x}') - \Theta(\tau' - \tau)\hat{\psi}^\dagger_{\sigma'}(\tau', \boldsymbol{x}')\hat{\psi}_\sigma(\tau, \boldsymbol{x}), \tag{4.1.13}$$

with the step function $\Theta(\tau)$. We note that $\hat{\psi}^\dagger_\sigma(\tau, \boldsymbol{x}) \equiv e^{\tau(\hat{H}-\mu\hat{N})}\hat{\psi}^\dagger_\sigma(\boldsymbol{x})e^{-\tau(\hat{H}-\mu\hat{N})}$ is not the hermitian conjugate operator of $\hat{\psi}_\sigma(\tau, \boldsymbol{x})$. From translational and spin-rotational symmetries, the Green function can be expressed as

$$\mathcal{G}_{\sigma\sigma'}(\tau, \boldsymbol{x}; \tau', \boldsymbol{x}') = \delta_{\sigma\sigma'}\mathcal{G}(\tau - \tau', \boldsymbol{x} - \boldsymbol{x}'). \tag{4.1.14}$$

We further introduce the spatiotemporal Fourier transformations of the annihilation and creation operators as

$$\begin{aligned}
\hat{\psi}_\sigma(\omega_m^F, \boldsymbol{k}) &= \frac{1}{\sqrt{\beta}L^{d/2}} \int_0^\beta \mathrm{d}\tau \int \mathrm{d}\boldsymbol{x}\, e^{i\omega_m^F\tau - i\boldsymbol{k}\cdot\boldsymbol{x}}\hat{\psi}_\sigma(\tau, \boldsymbol{x}), \\
\hat{\psi}^\dagger_\sigma(\omega_m^F, \boldsymbol{k}) &= \frac{1}{\sqrt{\beta}L^{d/2}} \int_0^\beta \mathrm{d}\tau \int \mathrm{d}\boldsymbol{x}\, e^{-i\omega_m^F\tau + i\boldsymbol{k}\cdot\boldsymbol{x}}\hat{\psi}^\dagger_\sigma(\tau, \boldsymbol{x}),
\end{aligned} \tag{4.1.15}$$

where $\omega_m^F = 2\pi(m + 1/2)/\beta$ is the fermionic Matsubara frequency. Then, the spatiotemporal Fourier transformation of the single-particle Green function is introduced as

$$\mathcal{G}(i\omega_m^F, \boldsymbol{k}) = \int_0^\beta \mathrm{d}\tau \int \mathrm{d}\boldsymbol{x}\, e^{i\omega_m^F\tau - i\boldsymbol{k}\cdot\boldsymbol{x}}\mathcal{G}(\tau, \boldsymbol{x}). \tag{4.1.16}$$

In particular, the single-particle Green function for free fermions, referred to as the free propagator, takes the simple form of

$$G(i\omega_m^F, \boldsymbol{k}) = \frac{1}{i\omega_m^F - \epsilon_{\boldsymbol{k}} + \mu}, \tag{4.1.17}$$

with the single-particle energy $\epsilon_{\boldsymbol{k}} = \boldsymbol{k}^2/(2m)$. The free propagator $G(i\omega_m^F, \boldsymbol{k})$ in Matsubara frequency and momentum space plays the role of a building block in the quantum virial expansion, as well as in general diagrammatic techniques.

We also introduce the pair propagator $D(i\omega_l^B, \boldsymbol{k})$ [106], represented diagrammatically in Fig. 4.1, as

$$-D(i\omega_l^B, \boldsymbol{k}) = -g + \frac{1}{\beta L^d}\sum_m\sum_{\boldsymbol{p}}(-g)G_\uparrow(i\omega_m^F, \boldsymbol{p})G_\downarrow(i\omega_n^B - i\omega_m^F, \boldsymbol{k} - \boldsymbol{p})(-g) + \cdots, \tag{4.1.18}$$

where $\omega_l^B = 2\pi l/\beta$ is the bosonic Matsubara frequency. We can write the pair propagator $D(i\omega_l^B, \boldsymbol{k})$ as

$$D(i\omega_l^B, \boldsymbol{k}) = \frac{1}{g^{-1} + \tilde{\Pi}_{\mathrm{polar}}(i\omega_l^B, \boldsymbol{k})}, \tag{4.1.19}$$
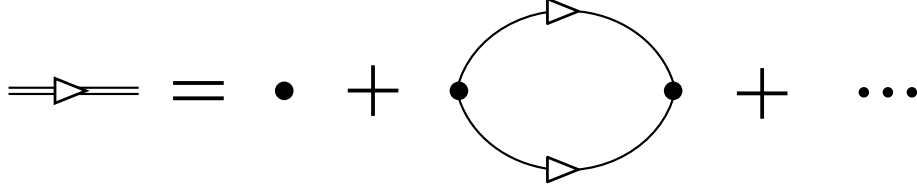
Figure 4.1: Diagrammatic representation of the pair propagator. The pair propagator, described by the double line, consists of the single line and the dot, representing the free propagator of Eq. (4.1.17) and the bare coupling constant $(-g)$, respectively.

where $\tilde{\Pi}_{\text{polar}}(i\omega_l^B, \boldsymbol{k})$ is the polarization function in the medium,

$$\tilde{\Pi}_{\text{polar}}(i\omega_l^B, \boldsymbol{k}) \equiv \frac{1}{\beta L^d} \sum_m \sum_{\boldsymbol{p}} \frac{1}{i\omega_m^F - \epsilon_{\boldsymbol{p}} + \mu} \frac{1}{i\omega_l^B - i\omega_m^F - \epsilon_{\boldsymbol{k}-\boldsymbol{p}} + \mu}. \tag{4.1.20}$$

The summation over the Matsubara frequency results in

$$\tilde{\Pi}_{\text{polar}}(i\omega_l^B, \boldsymbol{k}) = -\frac{1}{L^d} \sum_{\boldsymbol{p}} \frac{1 - f_F(\epsilon_{\boldsymbol{k}+\boldsymbol{p}/2} - \mu) - f_F(\epsilon_{\boldsymbol{k}-\boldsymbol{p}/2} - \mu)}{i\omega_n - \epsilon_{\boldsymbol{p}}/2 - 2\epsilon_{\boldsymbol{k}} + 2\mu}, \tag{4.1.21}$$

where $f_F(\varepsilon)$ is the Fermi-Dirac distribution function:

$$f_F(\varepsilon) = \frac{1}{e^{\beta\varepsilon} + 1}. \tag{4.1.22}$$

Therefore, we obtain

$$[D(i\omega_l^B, \boldsymbol{k})]^{-1} = \frac{1}{g} - \frac{1}{L^d} \sum_{\boldsymbol{p}} \frac{1 - f_F(\epsilon_{\boldsymbol{k}/2+\boldsymbol{p}} - \mu) - f_F(\epsilon_{\boldsymbol{k}/2-\boldsymbol{p}} - \mu)}{i\omega_l^B - \epsilon_{\boldsymbol{k}}/2 - 2\epsilon_{\boldsymbol{p}} + 2\mu}. \tag{4.1.23}$$

Here, the Fermi-Dirac distribution function $f_F(\varepsilon - \mu)$ is at least the first order of z:

$$f_F(\varepsilon - \mu) = \frac{1}{z^{-1}e^{\beta\varepsilon} + 1} = ze^{-\beta\epsilon} + O(z^2). \tag{4.1.24}$$

Therefore, the pair propagator $D(i\omega_l^B, \boldsymbol{k})$ is expanded in terms of z as

$$D(i\omega_l^B, \boldsymbol{k}) = \mathcal{T}_a(i\omega_l^B - \epsilon_{\boldsymbol{k}}/2 + 2\mu) + O(z), \tag{4.1.25}$$

where $\mathcal{T}_a(i\omega_l^B - \epsilon_{\boldsymbol{k}}/2 + 2\mu)$ is the two-body scattering T-matrix in the center-of-mass frame defined by

$$\mathcal{T}_a(w) \equiv \left[\frac{1}{g} - \frac{1}{L^d} \sum_{\boldsymbol{p}} \frac{1}{w - 2\epsilon_{\boldsymbol{p}}}\right]^{-1}. \tag{4.1.26}$$

This definition is consistent with the two-body scattering T-matrix in Chapter 2 [Eqs. (2.1.18), (2.1.19), and (2.1.22)]. With the use of Eq. (4.1.10), the T-matrix in the infinite-volume limit $L^{-d} \sum_{\boldsymbol{p}} \to \int_{\boldsymbol{p}}$ is represented as

$$\mathcal{T}_a(w) = \frac{\Omega_{d-1}}{m} \frac{d-2}{a^{2-d} - (-mw)^{d/2-1}}. \tag{4.1.27}$$

Since the pair propagator has the zeroth-order term for the fugacity due to the two-body scattering in vacuum, it plays the role of a building block in the quantum virial expansion in addition to the free propagator $G(i\omega_m^F, \boldsymbol{k})$. Namely, we can evaluate the leading order of physical quantities for the fugacity by the diagrammatic approach with the free propagtor $G(i\omega_m^F, \boldsymbol{k})$ and the T-matrix $\mathcal{T}_a(i\omega_l^B - \epsilon_{\boldsymbol{k}}/2 + 2\mu)$.

In the Matsubara frequency representation, the fugacity appears through the expansion of the distribution function resulting from the Matsubara frequency summation. Thus, it is difficult to find the fugacity dependence in the Matsubara frequency representation before summing over the Matsubara frequency. On the other hand, the free propagator in the imaginary-time representation has an explicit fugacity dependence,

$$G(\tau, \boldsymbol{k}) = -e^{-\tau(\epsilon_{\boldsymbol{k}}-\mu)}[\Theta(\tau) - f_F(\epsilon_{\boldsymbol{k}} - \mu)] = \sum_{N=0}^{\infty} z^N G^{(N)}(\tau, \boldsymbol{k}), \qquad (4.1.28)$$

with

$$G^{(N)}(\tau, \boldsymbol{k}) = \begin{cases} -e^{\tau\mu}e^{-\tau\epsilon_{\boldsymbol{k}}}\Theta(\tau) & N = 0, \\ -e^{\tau\mu}e^{-\tau\epsilon_{\boldsymbol{k}}}\left(e^{-\beta\epsilon_{\boldsymbol{k}}}\right)^N & N \geq 1. \end{cases} \qquad (4.1.29)$$

With the use of $G^{(N)}(\tau, \boldsymbol{k})$, we can express the coefficients of each order for the fugacity in the quantum virial expansion. In fact, the diagrammatic computational method for the quantum virial expansion is established in the imaginary-time representation, not in the Matsubara frequency representation [86,87]. In particular, the zeroth-order term $G^{(0)}(\tau, \boldsymbol{k})$ runs only in the forward direction for the imaginary time because it involves $\Theta(\tau)$. Thus, we can estimate the order of each diagram for the fugacity from the number of propagators going backward in the imaginary time when an imaginary time is assigned to each vertex. Nevertheless, we mainly employ the Matsubara frequency representation. We rely on the technique in the imaginary-time representation only when we estimate the order of diagrams for the fugacity. The Matsubara frequency representation is more convenient than the imaginary-time representation for the resummation discussed in Chapter 5.

4.1.3   Thermodynamic quantities

As a concrete example, we review the thermodynamic quantities of the resonant Fermi gas in the quantum virial expansion. The thermodynamic potential Ω in the grand canocnial ensemble is defined by

$$\Omega = -\frac{1}{\beta} \ln Z. \qquad (4.1.30)$$

The partition function is expanded in terms of the fugacity as

$$Z = 1 + z \operatorname{Tr}_1\left[e^{-\beta\hat{H}}\right] + z^2 \operatorname{Tr}_2\left[e^{-\beta\hat{H}}\right] + O(z^3), \qquad (4.1.31)$$

and then the thermodynamic potential is expanded as

$$\beta\frac{\Omega}{L^d} = -\frac{2}{\lambda_T^d}\left[b_1 z + b_2 z^2 + O(z^3)\right], \qquad (4.1.32)$$

where L^d is the volume of the system and the prefactor 2 is the number of the spin degrees of freedom. The coefficients b_n are referred to as the n-th order virial expansion coefficients [88],

and they determine the quantum virial expansion of the thermodynamic quantities. Here, b_1 is fixed by the one-body problem, so that it is obtained as $b_1 = 1$ from the results for the free Fermi gas [see Eq. (4.1.50)].

Here, the thermodynamic relations of the resonant Fermi gas are given by

$$\mathcal{E} + \mathcal{P} = T\mathcal{S} + \mu n, \tag{4.1.33}$$

$$\mathrm{d}\mathcal{E} = T\mathrm{d}\mathcal{S} + \mu \mathrm{d}n + \frac{\mathcal{C}_{\mathrm{eq}}}{m\Omega_{d-1}a^{d-1}}\mathrm{d}a, \tag{4.1.34}$$

where $\mathcal{E}$ is the internal energy density, $\mathcal{P}$ the pressure, $\mathcal{S}$ the entropy density, and $\mathcal{C}_{\mathrm{eq}}$ the contact density. Here, the last term on the right-hand side of Eq. (4.1.34) represents the adiabatic relation, which is one of the universal relations of the resonant Fermi gas [28]. From these relations, we obtain

$$\mathrm{d}(\beta\mathcal{P}) = -\mathcal{E}\mathrm{d}\beta + n\,\mathrm{d}\ln z - \frac{\beta\mathcal{C}_{\mathrm{eq}}}{m\Omega_{d-1}a^{d-1}}\mathrm{d}a. \tag{4.1.35}$$

In the infinite-volume limit, with the use of this thermodynamic relation and $\Omega = -\mathcal{P}L^d$, the thermodynamic quantities are found as

$$\beta\mathcal{P} = \frac{2}{\lambda_T^d}\left[z + b_2 z^2 + O(z^3)\right], \tag{4.1.36}$$

$$\mathcal{E} = -\left(\frac{\partial(\beta\mathcal{P})}{\partial\beta}\right)_{z,a} = \frac{d}{2}\mathcal{P} - \frac{2}{\lambda_T^d}\frac{\partial b_2}{\partial\beta}z^2 + O(z^3), \tag{4.1.37}$$

$$n = z\left(\frac{\partial(\beta\mathcal{P})}{\partial z}\right)_{\beta,a} = \frac{2}{\lambda_T^d}\left[z + 2b_2 z^2 + O(z^3)\right], \tag{4.1.38}$$

$$\frac{\mathcal{C}_{\mathrm{eq}}}{m\Omega_{d-1}a^{d-1}} = -\frac{1}{\beta}\left(\frac{\partial(\beta\mathcal{P})}{\partial a}\right)_{\beta,z} = -\frac{2}{\beta\lambda_T^d}\frac{\partial b_2}{\partial a}z^2 + O(z^3). \tag{4.1.39}$$

To find the virial expansion coefficients, we calculate the particle number density n by using

$$n = \sum_{\sigma=\uparrow,\downarrow}\langle\hat{\psi}_\sigma^\dagger(0,\boldsymbol{x})\hat{\psi}_\sigma(0,\boldsymbol{x})\rangle = 2\mathcal{G}(\tau = -0^+, \boldsymbol{x} = \boldsymbol{0}) = \lim_{\tau\to-0^+}\frac{2}{\beta L^d}\sum_m\sum_{\boldsymbol{k}}e^{-i\omega_m^F\tau}\mathcal{G}(i\omega_m^F, \boldsymbol{k}). \tag{4.1.40}$$

Thus, we only need to find the Green function $\mathcal{G}(i\omega_m^F, \boldsymbol{k})$. We introduce the self-energy $\Sigma(i\omega_m^F, \boldsymbol{k})$ such that the Green function has the form of

$$\mathcal{G}(i\omega_m^F, \boldsymbol{k}) = \frac{1}{i\omega_m^F - \epsilon_{\boldsymbol{k}} + \mu - \Sigma(i\omega_m^F, \boldsymbol{k})}. \tag{4.1.41}$$

The leading order of the self-energy can be evaluated from the diagram in Fig. 4.2 and is given by

$$\Sigma_{\mathrm{LO}}(i\omega_m^F, \boldsymbol{k}) = \frac{1}{\beta L^d}\sum_n\sum_{\boldsymbol{p}}D(i\omega_m^F + i\omega_n^F, \boldsymbol{k} + \boldsymbol{p})G(i\omega_n^F, \boldsymbol{p}). \tag{4.1.42}$$
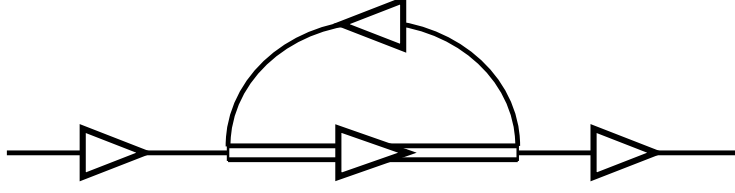
Figure 4.2:   Diagrammatic representation of the leading-order fermion self-energy. See the caption of Fig. 4.1 for the meaning of the symbols. In this diagram, one can assign an imaginary time to each vertex such that only the leftward free propagator goes backward in the imaginary time. The fact that at least one propagator goes backward in the imaginary time means that this diagram has a first-order contribution of the fugacity. Only this diagram provides the self-energy at $O(z)$.

With the use of Eq. (4.1.25), the self-energy is calculated as

$$\Sigma_{\mathrm{LO}}(i\omega_m^F, \boldsymbol{k}) = \frac{1}{\beta L^d} \sum_n \sum_{\boldsymbol{p}} \frac{\mathcal{T}_a(i\omega_m^F + i\omega_n^F - \epsilon_{\boldsymbol{k}+\boldsymbol{p}}/2 + 2\mu)}{i\omega_n^F - \epsilon_{\boldsymbol{p}} + \mu} + O(z)$$

$$= -\frac{1}{L^d} \sum_{\boldsymbol{p}} \oint_\gamma \frac{dw}{2\pi i} f_F(w) \frac{\mathcal{T}_a(i\omega_m^F + w - \epsilon_{\boldsymbol{k}+\boldsymbol{p}}/2 + 2\mu)}{w - \epsilon_{\boldsymbol{p}} + \mu} + O(z) \qquad (4.1.43)$$

$$= \frac{1}{L^d} \sum_{\boldsymbol{p}} f_F(\epsilon_{\boldsymbol{p}} - \mu) \mathcal{T}_a(i\omega_m^F + \epsilon_{\boldsymbol{p}} - \epsilon_{\boldsymbol{k}+\boldsymbol{p}}/2 + \mu) + O(z^2),$$

where γ consists of counterclockwise closed contours around the singularities of $f_F(w)$ in the complex plane of w. Only the pole of the free propagator $w = \epsilon_{\boldsymbol{k}} - \mu$ leads to the first-order contribution for the fugacity. Thus, by using Eq. (4.1.24), we obtain the self-energy up to first order for the fugacity as

$$\Sigma_{\mathrm{LO}}(i\omega_m^F, \boldsymbol{k}) = \frac{z}{L^d} \sum_{\boldsymbol{p}} e^{-\beta\epsilon_{\boldsymbol{p}}} \mathcal{T}_a(i\omega_m^F + \epsilon_{\boldsymbol{p}} - \epsilon_{\boldsymbol{k}+\boldsymbol{p}}/2 + \mu) + O(z^2). \qquad (4.1.44)$$

From the self-energy $\Sigma_{\mathrm{LO}}(i\omega_m^F, \boldsymbol{k})$, the particle number density n is given by

$$n = \frac{2}{\beta} \sum_m \int_{\boldsymbol{k}} e^{i\omega_m^F 0^+} \left[G(i\omega_m^F, \boldsymbol{k}) + G(i\omega_m^F, \boldsymbol{k})\Sigma_{\mathrm{LO}}(i\omega_m^F, \boldsymbol{k})G(i\omega_m^F, \boldsymbol{k}) + O(z^2) \right]$$

$$= \frac{2}{\beta} \sum_m \int_{\boldsymbol{k}} \left[\frac{e^{i\omega_m^F 0^+}}{i\omega_m^F - \epsilon_{\boldsymbol{k}} + \mu} + e^{i\omega_m^F 0^+} \frac{\Sigma_{\mathrm{LO}}(i\omega_m^F, \boldsymbol{k})}{[i\omega_m^F - \epsilon_{\boldsymbol{k}} + \mu]^2} + O(z^2) \right] \qquad (4.1.45)$$

$$= 2\int_{\boldsymbol{k}} f_F(\epsilon_{\boldsymbol{k}} - \mu) - 2\int_{\boldsymbol{k}} \oint_\gamma \frac{dw}{2\pi i} f_F(w) \frac{\Sigma_{\mathrm{LO}}(w, \boldsymbol{k})}{[w - \epsilon_{\boldsymbol{k}} + \mu]^2} + O(z^3),$$

where we take the infinite-volume limit $L^{-d}\sum_{\boldsymbol{k}} \to \int_{\boldsymbol{k}}$ and rewrite the Matsubara frequency summation as the contour integral on γ. Here, γ can be deformed according to the singularities of the integrand, as depicted in Fig. 4.3:

$$\gamma \rightarrow \gamma_+ + \gamma_-,$$
$$\gamma_+ : w = \varepsilon + i0^+, \qquad \varepsilon = -\infty \to +\infty, \qquad (4.1.46)$$
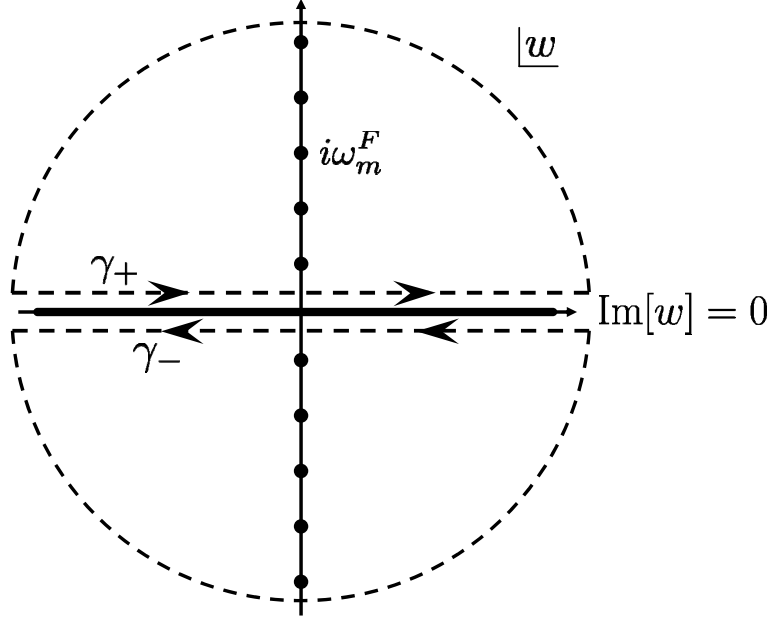$$\gamma_- : w = \varepsilon - i0^+, \qquad \varepsilon = +\infty \to -\infty.$$

Figure 4.3: Deformation of the integral contour γ. Because the singularities of the integrated function except for $f_F(w)$ in Eq. (4.1.45) are located on the real axis, the integral contour is deformed to straight lines γ_+ and γ_- that are parallel to and slightly shifted from the real axis. Here, the contribution on the circle with infinite radius is negligible.

Then, the contour integral is expressed as

$$\oint_\gamma \frac{\mathrm{d}w}{2\pi i} f_F(w) \frac{\Sigma_{\mathrm{LO}}(w, \boldsymbol{k})}{[w - \epsilon_{\boldsymbol{k}} + \mu]^2} = -\int_{-\infty}^{+\infty} \frac{\mathrm{d}\varepsilon}{\pi} f_F(\varepsilon) \operatorname{Im}\left[\frac{\Sigma_{\mathrm{LO}}(\varepsilon - i0^+, \boldsymbol{k})}{[\varepsilon - \epsilon_{\boldsymbol{k}} + \mu - i0^+]^2}\right] \tag{4.1.47}$$

$$= -z^2 \int_{-\infty}^{+\infty} \frac{\mathrm{d}\varepsilon}{\pi} e^{-\beta\varepsilon} e^{-\beta\epsilon_{\boldsymbol{k}+\boldsymbol{p}}/2} \operatorname{Im}\left[\frac{\mathcal{T}_a(\varepsilon - i0^+)}{[\varepsilon - \epsilon_{\boldsymbol{k}-\boldsymbol{p}}/2 - i0^+]^2}\right] + O(z^3). \tag{4.1.48}$$

Therefore, the particle number density n is obtained as

$$n = 2z \int_{\boldsymbol{k}} e^{-\beta\epsilon_{\boldsymbol{k}}} - 2z^2 \int_{\boldsymbol{k}} e^{-2\beta\epsilon_{\boldsymbol{k}}}$$
$$+ 2z^2 \int_{\boldsymbol{k},\boldsymbol{p}} \int_{-\infty}^{+\infty} \frac{\mathrm{d}\varepsilon}{\pi} e^{-\beta\varepsilon} e^{-\beta\epsilon_{\boldsymbol{k}+\boldsymbol{p}}/2} \operatorname{Im}\left[\frac{\mathcal{T}_a(\varepsilon - i0^+)}{[\varepsilon - \epsilon_{\boldsymbol{k}-\boldsymbol{p}}/2 - i0^+]^2}\right] + O(z^3). \tag{4.1.49}$$

By comparing this with Eq. (4.1.38), we find the virial expansion coefficients as

$$b_1 = \lambda_T^d \int_{\boldsymbol{k}} e^{-\beta\epsilon_{\boldsymbol{k}}} = 1, \tag{4.1.50}$$

$$b_2 = -\frac{\lambda_T^d}{2} \int_{\boldsymbol{k}} e^{-2\beta\epsilon_{\boldsymbol{k}}} + \frac{\lambda_T^d}{2} \int_{\boldsymbol{k},\boldsymbol{p}} \int_{-\infty}^{+\infty} \frac{\mathrm{d}\varepsilon}{\pi} e^{-\beta\varepsilon} e^{-\beta\epsilon_{\boldsymbol{k}+\boldsymbol{p}}/2} \operatorname{Im}\left[\frac{\mathcal{T}_a(\varepsilon - i0^+)}{[\varepsilon - \epsilon_{\boldsymbol{k}-\boldsymbol{p}}/2 - i0^+]^2}\right]$$

$$= -\frac{1}{2 \cdot 2^{d/2}} + \frac{2^{d/2}}{4\Omega_{d-1}} \int_{-\infty}^{+\infty} \frac{\mathrm{d}\varepsilon}{\pi} e^{-\beta\varepsilon} \operatorname{Im}\left[\frac{m^2 \mathcal{T}_a(\varepsilon - i0^+)}{[-m\varepsilon + i0^+]^{2-d/2}}\right]. \tag{4.1.51}$$

The second term of the second virial expansion coefficient is known as the Beth-Uhlenbeck term [107]. In particular, when $d = 3$ and $|a| = \infty$, one can find $b_2 = 3/(4\sqrt{2})$, which is consistent with experimental results for the unitary Fermi gas [22–24].

From the virial expansion coefficients, the thermodynamic quantities can be calculated according to Eqs. (4.1.36)–(4.1.39). For later use, we calculate the contact density. From Eq. (4.1.39) and

$$\frac{\partial}{\partial a}\mathcal{T}_a(\varepsilon + i0^+) = -\frac{2(-m\varepsilon - i0^+)^{2-d/2}}{ma^{d-1}}\frac{\partial}{\partial \varepsilon}\mathcal{T}_a(\varepsilon + i0^+), \qquad (4.1.52)$$

the contact density is given by

$$\mathcal{C}_{\mathrm{eq}} = z^2\frac{2^{d/2}}{\lambda_T^d}\int_{-\infty}^{+\infty}\frac{\mathrm{d}\varepsilon}{\pi}e^{-\beta\varepsilon}\,\mathrm{Im}\big[m^2\mathcal{T}_a(\varepsilon - i0^+)\big] + O(z^3). \qquad (4.1.53)$$

Here, the imaginary part of $\mathcal{T}_a(\varepsilon - i0^+)$ is provided by

$$\mathrm{Im}[\mathcal{T}_a(\varepsilon - i0^+)] = \Theta(a)\frac{2\Omega_{d-1}}{m^2 a^{4-d}}\pi\delta(\varepsilon + \tfrac{1}{ma^2}) + \Theta(\varepsilon)ma^{d-2}\rho_a(\varepsilon), \qquad (4.1.54)$$

with

$$\rho_a(\varepsilon) \equiv \begin{cases} \dfrac{2\pi}{[\ln(ma^2\varepsilon)]^2 + \pi^2} & d = 2, \\[3mm] \dfrac{\mathrm{sgn}(a)\sqrt{ma^2\varepsilon}}{a^{-2} + m\varepsilon} & d = 3, \end{cases} \qquad (4.1.55)$$

which consists of a bound-state peak at the binding energy $E_{\mathrm{bind}} = -1/(ma^2)$ and a continuum of scattering states for positive energies. Therefore, the contact density for $d = 3$ has the analytic expression of [21]

$$\mathcal{C}_{\mathrm{eq}} = z^2\frac{16\pi}{\lambda_T^4}\left[1 + \frac{\sqrt{\pi}}{\tilde{a}}e^{\tilde{a}^{-1}}\left(1 + \mathrm{erf}\left(\tilde{a}^{-1}\right)\right)\right] + O(z^3), \qquad (4.1.56)$$

where the dimensionless scattering length is introduced as $\tilde{a} \equiv \sqrt{2\pi}a/\lambda_T = \sqrt{m/\beta}a$.

4.2   Bulk viscosity

We reviewed the quantum virial expansion with a warming-up calculation of the thermodynamic quantities. We now turn to the bulk viscosity via the Kubo formula and evaluate it in the quantum virial expansion.

4.2.1   Contact-contact response function

The complex bulk viscosity is given by Eq. (2.2.51):

$$\zeta(w) = \frac{\mathcal{R}_{\Pi\Pi}(w, \mathbf{0}) - \int_0^\beta \mathrm{d}\tau \int \mathrm{d}\boldsymbol{x}\,\langle\delta\hat{\bar{\Pi}}(-i\tau, \boldsymbol{x})\delta\hat{\bar{\Pi}}(0, \mathbf{0})\rangle}{iw}. \qquad (4.2.1)$$

The bulk viscosity coefficient is provided by the real part of the complex bulk viscosity in the static limit [Eq. (2.2.53)],

$$\zeta = \lim_{\omega\to 0}\mathrm{Re}[\zeta(\omega + i0^+)]. \qquad (4.2.2)$$

The response function $\mathcal{R}_{\mathcal{AB}}(w, \boldsymbol{k})$ is defined by Eq. (2.2.7):

$$\mathcal{R}_{\mathcal{AB}}(w, \boldsymbol{k}) = i \int_0^\infty \mathrm{d}t \int \mathrm{d}\boldsymbol{x} \, e^{iwt - i\boldsymbol{k}\cdot\boldsymbol{x}} \langle [\hat{A}(t, \boldsymbol{x}), \, \hat{B}(0, \boldsymbol{0})] \rangle. \tag{4.2.3}$$

Here, $\hat{\Pi}(t, \boldsymbol{x}) = \hat{\Pi}_{ii}(t, \boldsymbol{x})/d$ is the trace of the stress tensor operator divided by d and the modified stress tensor operator $\hat{\tilde{\Pi}}(t, \boldsymbol{x})$ is defined by Eq. (2.2.44).

In the resonant Fermi gas, the trace of the stress tensor operator obeys

$$\hat{\Pi}(t) \equiv \int \mathrm{d}\boldsymbol{x} \, \frac{\hat{\Pi}_{ii}(t, \boldsymbol{x})}{d} = \frac{2}{d}\hat{H}(t) + \frac{\hat{C}(t)}{dm\Omega_{d-1}a^{d-2}}, \tag{4.2.4}$$

which follows from Eq. (3.1.15). Here, the contact operator $\hat{C}(t)$ is defined by the integral over the whole space of the contact density operator $\hat{\mathcal{C}}(t, \boldsymbol{x})$:

$$\hat{C}(t) \equiv \int \mathrm{d}\boldsymbol{x} \, \hat{\mathcal{C}}(t, \boldsymbol{x}) = \int \mathrm{d}\boldsymbol{x} \, \frac{(mg)^2}{2} \sum_{\sigma, \rho} \hat{\psi}_\sigma^\dagger(t, \boldsymbol{x}) \hat{\psi}_\rho^\dagger(t, \boldsymbol{x}) \hat{\psi}_\rho(t, \boldsymbol{x}) \hat{\psi}_\sigma(t, \boldsymbol{x}). \tag{4.2.5}$$

The substitution of Eq. (4.2.4) into the response function leads to

$$\begin{aligned}
\mathcal{R}_{\Pi\Pi}(w, \boldsymbol{0}) &= \frac{i}{L^d} \int_0^\infty \mathrm{d}t \, e^{iwt} \langle [\hat{\Pi}(t), \, \hat{\Pi}(0)] \rangle \\
&= \frac{1}{(dm\Omega_{d-1}a^{d-2})^2} \frac{i}{L^d} \int_0^\infty \mathrm{d}t \, e^{iwt} \langle [\hat{C}(t), \, \hat{C}(0)] \rangle \\
&= \frac{1}{(dm\Omega_{d-1}a^{d-2})^2} \mathcal{R}_{CC}(w, \boldsymbol{0}),
\end{aligned} \tag{4.2.6}$$

where the commutator of the Hamiltonian with any operator in the grand canonical ensemble can be dropped. Furthermore, the second term of the right-hand side of Eq. (4.2.1) is written as

$$\begin{aligned}
\int_0^\beta \mathrm{d}\tau \int \mathrm{d}\boldsymbol{x} \, \langle \delta\hat{\tilde{\Pi}}(-i\tau, \boldsymbol{x}) \delta\hat{\tilde{\Pi}}(0, \boldsymbol{0}) \rangle &= \int_{-\infty}^\infty \frac{d\omega}{\pi} \beta \mathcal{K}_{\tilde{\Pi}\tilde{\Pi}}(\omega + i0^+, \boldsymbol{0}), \\
&= \int_{-\infty}^\infty \frac{d\omega}{\pi} \zeta(\omega + i0^+),
\end{aligned} \tag{4.2.7}$$

where $\mathcal{K}_{\mathcal{AB}}(w, \boldsymbol{k})$ is Kubo's correlation function defined by Eq. (2.2.36) and the frequency integration sets the two operators at equal time. The frequency integration of the complex bulk viscosity provides the sum rule, which was derived in Refs. [36, 108]:

$$\int_{-\infty}^\infty \frac{d\omega}{\pi} \zeta(\omega + i0^+) = -\frac{1}{d^2 m\Omega_{d-1}a^{d-3}} \left(\frac{\partial \mathcal{C}_{\text{eq}}}{\partial a} \right)_{n, \mathcal{S}}. \tag{4.2.8}$$

Therefore, the complex bulk viscosity is obtained as

$$\zeta(w) = \frac{1}{iw} \frac{\mathcal{R}_{CC}(w, \boldsymbol{0})}{(dm\Omega_{d-1}a^{d-2})^2} + \frac{1}{iw} \frac{1}{d^2 m\Omega_{d-1}a^{d-3}} \left(\frac{\partial \mathcal{C}_{\text{eq}}}{\partial a} \right)_{n, \mathcal{S}}. \tag{4.2.9}$$

The contact-contact response function is more favorable for the calculation of the complex bulk viscosity than the stress-stress response function. Since the response function is expressed by the expectation value in the grand canonical ensemble, it can be evaluated in the quantum virial expansion.

4.2.2   Linear response to the contact

According to the linear response theory, the contact-contact response function appears in the response of the contact to a variation of the scattering length, which is a conjugate variable to the contact as in Eq. (4.1.34). In fact, we derived the response of the contact in the hydrodynamic framework [Eq. (3.4.1)] and found the bulk viscosity appears. Let us confirm that Eq. (3.4.1) can be reproduced by combining the linear response to the contact with the Kubo formula for the bulk viscosity of Eq. (4.2.9). We consider the system which is perturbed by a slightly modulated scattering length from its constant value as

$$a(t) = a_0 + \delta a(t). \tag{4.2.10}$$

We consider a certain frequency mode by setting $\delta a(t) = e^{-iwt}\delta a$ with $\text{Im}(w) > 0$. Along with the variation of the scattering length, the Hamiltonian in the Schrödinger picture varies as[1]

$$\hat{H}_a(t) = \hat{H} + \frac{\hat{C}}{m\Omega_{d-1}a_0^{d-1}}\delta a(t). \tag{4.2.11}$$

The density matrix operator also varies as

$$\hat{\rho}_a(t) = \hat{\rho}_{\text{eq}} + \delta\hat{\rho}(t), \tag{4.2.12}$$

where $\hat{\rho}_{\text{eq}} \equiv e^{-\beta(\hat{H}-\mu\hat{N})}/Z$ is the equilibrium density matrix and

$$\delta\hat{\rho}(t) = -\frac{i}{m\Omega_{d-1}a_0^{d-1}}\int_{-\infty}^{t}\mathrm{d}t'\,e^{-i\hat{H}(t-t')}[\hat{C},\,\hat{\rho}_{\text{eq}}]e^{i\hat{H}(t-t')}\delta a(t'), \tag{4.2.13}$$

up to first order for the perturbation. The expectation value of the contact operator is then given by

$$C_a(t) \equiv \text{Tr}[\hat{C}_a(t)\hat{\rho}_a(t)] = \text{Tr}[\hat{C}\hat{\rho}_{\text{eq}}] + \text{Tr}[\hat{C}\delta\hat{\rho}(t)] + O(\delta a^2). \tag{4.2.14}$$

The second term is written as

$$\begin{aligned}
\text{Tr}[\hat{C}\delta\hat{\rho}(t)] &= -\frac{i}{m\Omega_{d-1}a_0^{d-1}}\int_{-\infty}^{t}\mathrm{d}t'\,\langle[\hat{C}(t),\,\hat{C}(t')]\rangle\delta a(t') \\
&= -\frac{i}{m\Omega_{d-1}a_0^{d-1}}\int_{0}^{\infty}\mathrm{d}t'\,\langle[\hat{C}(t'),\,\hat{C}(0)]\rangle e^{iwt'}\delta a(t),
\end{aligned} \tag{4.2.15}$$

where $\hat{C}(t) \equiv e^{i\hat{H}t}\hat{C}e^{-i\hat{H}t}$ is the unperturbed contact operator in the interaction picture. From Eq. (4.2.9), we find the bulk viscosity as

$$-\frac{i}{m\Omega_{d-1}a_0^{d-1}}\int_{0}^{\infty}\mathrm{d}t'\,e^{iwt'}\langle[\hat{C}(t'),\,\hat{C}(0)]\rangle = -iwd^2m\Omega_{d-1}a_0^{d-3}L^d\zeta(w) + \left(\frac{\partial\mathcal{C}_{\text{eq}}}{\partial a}\right)_{n,\mathcal{S}}, \tag{4.2.16}$$

so that the second term of Eq. (4.2.14) is expressed as

$$\text{Tr}[\hat{C}\delta\hat{\rho}(t)] = \delta a(t)\left(\frac{\partial\mathcal{C}_{\text{eq}}}{\partial a}\right)_{n,\mathcal{S}} + \delta\dot{a}(t)d^2m\Omega_{d-1}a_0^{d-3}L^d\zeta + O(\delta\ddot{a}). \tag{4.2.17}$$

---

[1]Here, the contact does not vary: $\partial\hat{\mathcal{C}}(\boldsymbol{x})/\partial a = 0$. To see this, we need to employ the cutoff regularization rather than the dimensional regularization of Eq. (4.1.10). In the cutoff regularization, the coupling constant g is related to the scattering length a as $(mg)^{-1} = ((d-2)\Omega_{d-1})^{-1}[a^{2-d} - \Lambda^{d-2}/(\Gamma(d/2)\Gamma(2-d/2))]$. In the limit of $\Lambda \to \infty$, the coupling constant goes to zero, i.e., $g \to 0$, while the contact density operator remains finite. Thus, we get $\partial\hat{\mathcal{C}}(\boldsymbol{x})/\partial a = 2(mg)\hat{\mathcal{C}}(\boldsymbol{x})/(\Omega_{d-1}a^{d-1}) \to 0$.

Therefore, the linear response of the contact is obtained as

$$C_a(t) = C_{eq}[a(t)] + d^2 m \Omega_{d-1} a_0^{d-3} L^d \zeta \dot{a}(t) + O(\delta a^2, \delta \ddot{a}), \qquad (4.2.18)$$

with $C_{eq}[a(t)] \equiv \mathrm{Tr}[\hat{C} \hat{\rho}_{eq}] + (\partial C/\partial a)_{n,\mathcal{S}} \delta a(t) + O(\delta a^2)$. Furthermore, the expectation value of the energy continuity equation (3.1.11) integrated over the whole space leads to

$$\begin{aligned} \dot{H}(t) &= \frac{C_a(t)}{m \Omega_{d-1} a(t)^{d-1}} \dot{a}(t) \\ &= \frac{C_{eq}[a(t)]}{m \Omega_{d-1} a(t)^{d-1}} \dot{a}(t) + L^d d^2 \frac{\zeta}{a(t)^2} \dot{a}(t)^2 + O(\delta a^3, \delta \ddot{a}). \end{aligned} \qquad (4.2.19)$$

Then, the thermodynamic relation (4.1.34) provides the entropy production at the rate of

$$T \dot{S}(t) = \dot{H}(t) - \frac{C_{eq}[a(t)]}{m \Omega_{d-1} a(t)^{d-1}} \dot{a}(t) = L^d d^2 \frac{\zeta}{a(t)^2} \dot{a}(t)^2 + O(\delta a^3, \delta \ddot{a}). \qquad (4.2.20)$$

Therefore, dividing Eqs. (4.2.18), (4.2.19), and (4.2.20) by the volume, we arrive at Eqs. (3.4.1), (3.4.2), and (3.4.3), respectively, from a microscopic perspective without relying on the hydrodynamics.

4.2.3 Evaluation

We calculate the bulk viscosity from Eq. (4.2.9) in the quantum virial expansion. We first evaluate the contact-contact response function. The response function is obtained from the analytic continuation for the imaginary-time correlator,

$$\mathcal{R}_{\mathcal{A}\mathcal{B}}(w, \mathbf{0}) = \chi_{\mathcal{A}\mathcal{B}}(w, \mathbf{0}). \qquad (4.2.21)$$

Here, the imaginary-time correlator is defined by

$$\chi_{\mathcal{A}\mathcal{B}}(i\omega^B, \boldsymbol{k}) \equiv \int_0^\beta \mathrm{d}\tau \int \mathrm{d}\boldsymbol{x} \, e^{i\omega^B \tau - i\boldsymbol{k}\cdot\boldsymbol{x}} \langle \mathcal{T}_\tau \hat{\mathcal{A}}(\tau, \boldsymbol{x}) \hat{\mathcal{B}}(0, \mathbf{0}) \rangle, \qquad (4.2.22)$$

where $\hat{\mathcal{A}}(\tau, \boldsymbol{x})$ and $\hat{\mathcal{B}}(\tau, \boldsymbol{x})$ are operators in the imaginary-time representation. The leading order of the contact-contact correlator is depicted diagrammatically in Fig. 4.4, and the correlator is given by

$$\begin{aligned} \chi_{CC}(i\omega^B, \boldsymbol{k}) &= \frac{m^4}{\beta L^d} \sum_l \sum_{\boldsymbol{p}} D(i\omega^B + i\omega_l^B, \boldsymbol{k} + \boldsymbol{p}) D(i\omega_l^B, \boldsymbol{p}) \\ &= \frac{m^4}{\beta L^d} \sum_l \sum_{\boldsymbol{p}} \mathcal{T}_a(i\omega^B + i\omega_l^B - \epsilon_{\boldsymbol{k}+\boldsymbol{p}}/2 + 2\mu) \mathcal{T}_a(i\omega_l^B - \epsilon_{\boldsymbol{p}}/2 + 2\mu), \end{aligned} \qquad (4.2.23)$$

where only the leading-order contribution is considered and higher-order contributions are dropped. With the use of

$$\mathcal{T}_a(w) = \int_{-\infty}^\infty \frac{\mathrm{d}\varepsilon}{\pi} \frac{\mathrm{Im}[\mathcal{T}_a(\varepsilon - i0^+)]}{w - \varepsilon}, \qquad (4.2.24)$$
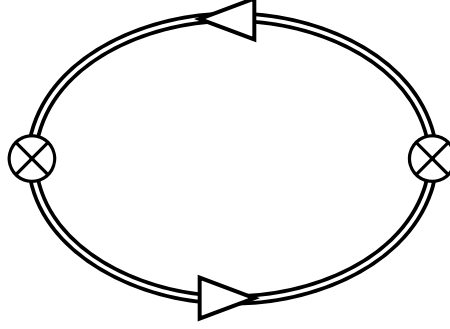
Figure 4.4:   Diagrammatic representation of the contact-contact correlator.   The double line represents the pair propagator, and the crossed dot shows the contact density operator insertion. The diagram has a second-order contribution for the fugacity, which is the leading order in the high-temperature limit.

we can perform the summation over the Matsubara frequency and obtain

$$\chi_{CC}(i\omega^B, \boldsymbol{k}) = \frac{m^4}{L^d} \sum_{\boldsymbol{p}} \int_{-\infty}^{\infty} \frac{\mathrm{d}\varepsilon}{\pi} \int_{-\infty}^{\infty} \frac{\mathrm{d}\varepsilon'}{\pi} \Big(f_B(\varepsilon + \epsilon_{\boldsymbol{k}+\boldsymbol{p}}/2 - 2\mu) - f_B(\varepsilon' + \epsilon_{\boldsymbol{p}}/2 - 2\mu) \Big)$$
$$\times \frac{\mathrm{Im}[\mathcal{T}_a(\varepsilon - i0^+)]\,\mathrm{Im}[\mathcal{T}_a(\varepsilon' - i0^+)]}{i\omega^B - \varepsilon + \varepsilon' - \epsilon_{\boldsymbol{k}+\boldsymbol{p}}/2 + \epsilon_{\boldsymbol{p}}/2}, \tag{4.2.25}$$

where $f_B(\varepsilon)$ is the Bose-Einstein distribution function:

$$f_B(\varepsilon) = \frac{1}{e^{\beta\varepsilon} - 1}. \tag{4.2.26}$$

Because of $f_B(\varepsilon - 2\mu) = z^2 e^{-\beta\varepsilon} + O(z^4)$, the correlator at zero momentum in the infinite-volume limit is reduced to

$$\chi_{CC}(i\omega^B, \boldsymbol{0}) = \frac{2^{d/2} z^2}{\lambda_T^d} \int_{-\infty}^{\infty} \frac{\mathrm{d}\varepsilon}{\pi} \int_{-\infty}^{\infty} \frac{\mathrm{d}\varepsilon'}{\pi} \frac{e^{-\beta\varepsilon} - e^{-\beta\varepsilon'}}{i\omega^B - \varepsilon + \varepsilon'} \mathrm{Im}[m^2 \mathcal{T}_a(\varepsilon - i0^+)]\,\mathrm{Im}[m^2 \mathcal{T}_a(\varepsilon' - i0^+)], \tag{4.2.27}$$

and the contact-contact response function is given by

$$\frac{\mathcal{R}_{CC}(w, \boldsymbol{0})}{(dm\Omega_{d-1}a^{d-2})^2} = \frac{1}{(dm\Omega_{d-1}a^{d-2})^2} \frac{2^{d/2} z^2}{\lambda_T^d} \int_{-\infty}^{\infty} \frac{\mathrm{d}\varepsilon}{\pi} \int_{-\infty}^{\infty} \frac{\mathrm{d}\varepsilon'}{\pi} \frac{e^{-\beta\varepsilon} - e^{-\beta\varepsilon'}}{w - \varepsilon + \varepsilon'} \tag{4.2.28}$$
$$\times \mathrm{Im}[m^2 \mathcal{T}_a(\varepsilon - i0^+)]\,\mathrm{Im}[m^2 \mathcal{T}_a(\varepsilon' - i0^+)].$$

We next evaluate the partial derivative of the contact density with respect to a. Since the contact density is given by Eq. (4.1.53), its partial derivative is written as

$$\left(\frac{\partial \mathcal{C}_{\mathrm{eq}}}{\partial a} \right)_{\beta, z} = z^2 \frac{2^{d/2}}{\lambda_T^d} \int_{-\infty}^{+\infty} \frac{\mathrm{d}\varepsilon}{\pi} e^{-\beta\varepsilon} \mathrm{Im}\left[m^2 \frac{\partial}{\partial a} \mathcal{T}_a(\varepsilon - i0^+) \right] + O(z^3). \tag{4.2.29}$$

Because the partial derivative with respect to a at fixed n and $\mathcal{S}$ is equivalent to that at fixed β and z in the leading order for the fugacity, we get

$$\frac{1}{d^2 m\Omega_{d-1}a^{d-3}} \left(\frac{\partial \mathcal{C}_{\mathrm{eq}}}{\partial a} \right)_{n, \mathcal{S}} = \frac{1}{(dm\Omega_{d-1}a^{d-2})^2} z^2 \frac{2^{d/2}}{\lambda_T^d} \int_{-\infty}^{+\infty} \frac{\mathrm{d}\varepsilon}{\pi} \int_{-\infty}^{+\infty} \frac{\mathrm{d}\varepsilon'}{\pi} \frac{e^{-\beta\varepsilon} - e^{-\beta\varepsilon'}}{\varepsilon - \varepsilon'}$$
$$\times \mathrm{Im}[m^2 \mathcal{T}_a(\varepsilon - i0^+)]\,\mathrm{Im}[m^2 \mathcal{T}_a(\varepsilon' - i0^+)] + O(z^3), \tag{4.2.30}$$

where the following identity is used:

$$2\,\text{Im}[m\mathcal{T}_a(\varepsilon - i0^+)]\,\text{Re}[m\mathcal{T}_a(\varepsilon - i0^+)] = \Omega_{d-1}a^{d-1}\frac{\partial}{\partial a}\,\text{Im}[m\mathcal{T}_a(\varepsilon - i0^+)]. \tag{4.2.31}$$

Therefore, we obtain the complex bulk viscosity of Eq. (4.2.9) as

$$\zeta(w) = \frac{2^{d/2}z^2}{(d\Omega_{d-1}a^{d-2})^2\lambda_T^d}\int_{-\infty}^{\infty}\frac{d\varepsilon}{\pi}\int_{-\infty}^{\infty}\frac{d\varepsilon'}{\pi}\frac{e^{-\beta\varepsilon}-e^{-\beta\varepsilon'}}{\varepsilon-\varepsilon'}\frac{\text{Im}[m\mathcal{T}_a(\varepsilon - i0^+)]\,\text{Im}[m\mathcal{T}_a(\varepsilon' - i0^+)]}{i(w-\epsilon+\epsilon')}. \tag{4.2.32}$$

We find that the real part of $\zeta(\omega + i0^+)$ reproduces the bulk viscosity spectral function in Refs. [89–91]:

$$\text{Re}[\zeta(\omega+i0^+)] = \frac{2^{d/2}z^2}{(d\Omega_{d-1}a^{d-2})^2\lambda_T^d}\frac{1-e^{-\beta\omega}}{\omega}\int_{-\infty}^{\infty}\frac{d\varepsilon}{\pi}e^{-\beta\varepsilon}\,\text{Im}[m\mathcal{T}_a(\varepsilon+\omega-i0^+)]\,\text{Im}[m\mathcal{T}_a(\varepsilon-i0^+)]. \tag{4.2.33}$$

With the use of Eq. (4.1.54), the bulk viscosity spectral function is expressed as

$$\text{Re}[\zeta(\omega + i0^+)] = \frac{2^{d/2}z^2}{d^2\lambda_T^d}\frac{1-e^{-\beta|\omega|}}{|\omega|}e^{\frac{\beta}{ma^2}}\frac{2}{ma^2}\Theta(a)\left[\frac{2}{ma^2}\pi\delta(\omega)+\rho_a(|\omega|-\tfrac{1}{ma^2})\Theta(|\omega|-\tfrac{1}{ma^2})\right]$$
$$+\frac{2^{d/2}z^2}{d^2\lambda_T^d}\frac{1-e^{-\beta|\omega|}}{|\omega|}\int_0^{\infty}\frac{d\varepsilon}{\pi}e^{-\beta\varepsilon}\rho_a(\varepsilon)\rho_a(\varepsilon+|\omega|)+O(z^3). \tag{4.2.34}$$

We can see that Eq. (4.2.34) has a term proportional to $\Theta(a)\delta(\omega)$ coming from the product of the bound-state peaks in Eq. (4.2.33). This peak contribution $\Theta(a)\delta(\omega)$ is considered to be broadened by incorporating higher-order contributions for the fugacity [89, 90].

By taking the static limit $\omega \to 0$ for Eq. (4.2.34) for $a < 0$, we obtain the bulk viscosity coefficient up to second order for the fugacity as

$$\zeta_{d=2} = \frac{z^2}{2\lambda_T^2}\int_0^{\infty}\frac{dx}{\pi}e^{-x}\left[\frac{2\pi}{[\ln(x\tilde{a}^2)]^2+\pi^2}\right]^2+O(z^3), \tag{4.2.35}$$

$$\zeta_{d=3} = \frac{2\sqrt{2}z^2}{9\pi\lambda_T^3}\frac{-1+(1+\tilde{a}^{-2})\exp(\tilde{a}^{-2})\Gamma(0,\tilde{a}^{-2})}{\tilde{a}^2}+O(z^3), \tag{4.2.36}$$

where $\tilde{a} = \sqrt{2\pi}a/\lambda_T$ is the dimensionless scattering length and $\Gamma(s,x)$ is the upper incomplete gamma function:

$$\Gamma(s,x) = \int_x^{\infty}dt\,t^{s-1}e^{-t}. \tag{4.2.37}$$

Here, because the upper incomplete gamma function is expanded as

$$\Gamma(0,z) = -\gamma - \ln(z) - \sum_{k=1}^{\infty}\frac{1}{k!}\frac{(-z)^k}{k}, \tag{4.2.38}$$

with the Euler's constant γ, the bulk viscosity coefficient $\zeta_{d=3}$ exhibits the non-analyticity in the unitarity limit $|a| \to \infty$:

$$\zeta_{d=3} = \frac{2\sqrt{2}z^2}{9\pi\lambda_T^3}\frac{\ln(\tilde{a}^2e^{-1-\gamma})}{\tilde{a}^2}+O(z^2\tilde{a}^{-4},z^3). \tag{4.2.39}$$

In contrast, in the free-particle limit $|a| \rightarrow 0$, the bulk viscosity coefficient $\zeta_{d=3}$ has the asymptotic form of

$$\zeta_{d=3} = \frac{2\sqrt{2}z^2}{9\pi\lambda_T^3}\tilde{a}^2 + O(z^2\tilde{a}^4, z^3), \tag{4.2.40}$$

which is analytic. In two dimensions, the bulk viscosity coefficient $\zeta_{d=2}$ has the asymptotic form of

$$\zeta_{d=2} = \frac{z^2}{\lambda_T^2}\frac{2\pi}{[\ln(\tilde{a}^2 e^{-\gamma})]^4} + O(z^2[\ln(\tilde{a}^2)]^{-6}, z^3). \tag{4.2.41}$$

The non-analysis of Eq. (4.2.39) is considered to be regularized by higher-order contributions, and $a^2\zeta_{d=3}$ converges to a finite value in the unitarity limit [90].

4.2.4   Kinetic theory approach

The bulk viscosity coefficient in the limit of $a \rightarrow \infty$ was calculated in the kinetic theory, and it is given by

$$\lim_{a\to\infty} \zeta_{d=3;\mathrm{kin}} = \frac{z^2}{12\sqrt{2}\lambda_T^3\tilde{a}^2} \tag{4.2.42}$$

for three dimensions [74] and

$$\lim_{a\to\infty} \zeta_{d=2;\mathrm{kin}} = \frac{z^2}{2\lambda_T^2\pi[\ln(\tilde{a}^2)]^4} \tag{4.2.43}$$

for two dimensions [75]. These results disagree with Eqs. (4.2.39) and (4.2.35). In three dimensions, Eqs. (4.2.39) and (4.2.42) have different forms as a function of the scattering length. In two dimensions, Eqs. (4.2.41) and (4.2.43) are different by a constant factor.

   To understand the discrepancy, we review the kinetic theory approach for the bulk viscosity coefficient [74, 75]. The bulk viscosity in the high-temperature limit was computed by employing the Landau kinetic equation for quasiparticles,

$$\frac{\partial}{\partial t}f_{\boldsymbol{p}} + \frac{\partial E_{\boldsymbol{p}}}{\partial \boldsymbol{p}} \cdot \frac{\partial}{\partial \boldsymbol{x}}f_{\boldsymbol{p}} - \frac{\partial E_{\boldsymbol{p}}}{\partial \boldsymbol{x}} \cdot \frac{\partial}{\partial \boldsymbol{p}}f_{\boldsymbol{p}} = \left(\frac{\partial f_{\boldsymbol{p}}}{\partial t}\right)_{\mathrm{coll}}, \tag{4.2.44}$$

where the collision term is given by

$$\left(\frac{\partial f_{\boldsymbol{p}}}{\partial t}\right)_{\mathrm{coll}} = \int_{\boldsymbol{p}_2,\boldsymbol{k}_1,\boldsymbol{k}_2} \mathcal{W}(\boldsymbol{k}_1,\boldsymbol{k}_2|\boldsymbol{p},\boldsymbol{p}_2)\left[f_{\boldsymbol{k}_1}f_{\boldsymbol{k}_2}(1-f_{\boldsymbol{p}})(1-f_{\boldsymbol{p}_2}) - (1-f_{\boldsymbol{k}_1})(1-f_{\boldsymbol{k}_2})f_{\boldsymbol{p}}f_{\boldsymbol{p}_2}\right], \tag{4.2.45}$$

with the transition rate of

$$\mathcal{W}(\boldsymbol{k}_1,\boldsymbol{k}_2|\boldsymbol{p},\boldsymbol{p}_2) = |\mathcal{T}_a(\tfrac{(\boldsymbol{k}_1-\boldsymbol{k}_2)^2}{4m}+i0^+)|^2(2\pi)^{d+1}\delta^d(\boldsymbol{k}_1+\boldsymbol{k}_2-\boldsymbol{p}-\boldsymbol{p}_2)\delta(E_{\boldsymbol{k}_1}+E_{\boldsymbol{k}_2}-E_{\boldsymbol{p}}-E_{\boldsymbol{p}_2}). \tag{4.2.46}$$

Here, $f_{\boldsymbol{p}} = f(t,\boldsymbol{x},\boldsymbol{p})$ is a nonequilibrium distribution function of fermions for each spin component and the quasiparticle energy $E_{\boldsymbol{p}} = E_{\boldsymbol{p}}[f]$ is given as a functional of the nonequilibrium distribution function. In the high-temperature limit, the quasiparticle energy is obtained from the real part of the self-energy of Eq. (4.1.43) where the Fermi-Dirac distribution function $f_F(\epsilon_{\boldsymbol{p}} - \mu)$ is replaced by the nonequilibrium distribution function $f_{\boldsymbol{p}}$:

$$\begin{aligned} E_{\boldsymbol{p}}[f] &= \epsilon_{\boldsymbol{p}} + \mathrm{Re}\left[\Sigma_{\mathrm{LO}}(\epsilon_{\boldsymbol{p}} - \mu - i0^+, \boldsymbol{p})\right]\big|_{f_F(\epsilon_{\boldsymbol{p}}-\mu)\to f_{\boldsymbol{p}}} \\ &= \epsilon_{\boldsymbol{p}} + \int_{\boldsymbol{p}'} \mathrm{Re}\left[\mathcal{T}_a(\tfrac{(\boldsymbol{p}-\boldsymbol{p}')^2}{4m} - i0^+)\right]f_{\boldsymbol{p}'}. \end{aligned} \tag{4.2.47}$$

As discussed in Chapter 2, if the quasiparticle energy is set to $E_{\boldsymbol{p}} = \epsilon_{\boldsymbol{p}}$, the bulk viscosity vanishes. The nonvanishing bulk viscosity is predicted by the presence of the real part of the self-energy. However, because the self-energy of Eq. (4.1.43) has both real and imaginary parts in $O(z)$, we consider that such a kinetic equation is not fully grounded. Namely, if we consider the real part of the self-energy, we cannot ignore the imaginary part of the same order. The imaginary part of the self-energy invalidates the quasiparticle approximation, i.e., the fermion spectral function cannot be regarded as a delta function in $O(z)$ due to the imaginary part.

To further support our consideration, let us derive the equilibrium distribution function resulting from the kinetic equation of Eq. (4.2.44). As in the discussion in Chapter 2, the equilibrium distribution is defined from the condition that the collision term (4.2.45) vanishes. From this condition, the equilibrium distribution in the rest frame obeys the self-consistent equation of [109]

$$f_{\boldsymbol{k}}^{\mathrm{eq}} = \frac{1}{\exp[\beta(E_{\boldsymbol{k}}[f^{\mathrm{eq}}] - \mu)] + 1}. \tag{4.2.48}$$

By substituting the quasiparticle energy and expanding the right-hand side with respect to the fugacity, we obtain

$$f_{\boldsymbol{k}}^{\mathrm{eq}} = f_F(\epsilon_{\boldsymbol{k}} - \mu) + f_F'(\epsilon_{\boldsymbol{k}} - \mu)\,\mathrm{Re}[\Sigma_{\mathrm{LO}}(\epsilon_{\boldsymbol{k}} - \mu - i0^+, \boldsymbol{k})] + O(z^3), \tag{4.2.49}$$

with $f_F'(\varepsilon) \equiv \partial_\varepsilon f_F(\varepsilon)$. In contrast, the equilibrium distribution is obtained microscopically as

$$f_{\boldsymbol{k}}^{\mathrm{eq}} \equiv \mathcal{G}(\tau = -0^+, \boldsymbol{k}) = \lim_{\tau \to -0^+} \frac{1}{\beta} \sum_m e^{-i\omega_m^F \tau} \mathcal{G}(i\omega_m^F, \boldsymbol{k}). \tag{4.2.50}$$

Since $\mathcal{G}(\tau = -0^+, \boldsymbol{k})$ is given by Eqs. (4.1.41) and (4.1.43), we get

$$f_{\boldsymbol{k}}^{\mathrm{eq}} = f_F(\epsilon_{\boldsymbol{k}} - \mu) + \int_{-\infty}^{\infty} \frac{\mathrm{d}\varepsilon}{\pi} f_F(\varepsilon)\,\mathrm{Im}\left[\frac{\Sigma_{\mathrm{LO}}(\varepsilon - i0^+, \boldsymbol{k})}{[\varepsilon - \epsilon_{\boldsymbol{k}} + \mu - i0^+]^2}\right] + O(z^3), \tag{4.2.51}$$

with the use of Eq. (4.1.47). This equilibrium distribution can be expressed as

$$\begin{aligned} f_{\boldsymbol{k}}^{\mathrm{eq}} = {}& \mathcal{Z}_{\boldsymbol{k}} f_F(\epsilon_{\boldsymbol{k}} - \mu) + f_F'(\epsilon_{\boldsymbol{k}} - \mu)\,\mathrm{Re}[\Sigma_{\mathrm{LO}}(\epsilon_{\boldsymbol{k}} - \mu - i0^+, \boldsymbol{k})] \\ & + \mathrm{P}\int_{-\infty}^{\infty} \frac{\mathrm{d}\varepsilon}{\pi} \frac{1}{\varepsilon} \frac{\partial}{\partial \varepsilon}\Big[f_F(\varepsilon + \epsilon_{\boldsymbol{k}} - \mu)\,\mathrm{Im}[\Sigma_{\mathrm{LO}}(\varepsilon + \epsilon_{\boldsymbol{k}} - \mu - i0^+, \boldsymbol{k})]\Big] + O(z^3), \end{aligned} \tag{4.2.52}$$

where $\mathcal{Z}_{\boldsymbol{k}} \equiv 1 + \mathrm{Re}\,\Sigma_{\mathrm{LO}}'(\epsilon_{\boldsymbol{k}} - \mu - i0^+, \boldsymbol{k})$ is the quasiparticle residue, and the symbol P stands for the principal value of the integral. Thus, we can find two discrepancies between Eqs. (4.2.49) and (4.2.52). One is the quasiparticle residue, and the other is a term involving the imaginary part of the self-energy. Because all thermodynamic quantities in the kinetic theory are represented through the distribution function, they are also inconsistent with those derived from the microscopic computation. Therefore, the Landau kinetic equation employed in Refs. [74,75] is invalid at the order in which the self-energy contributes because its imaginary part is not negligible. We consider that this is the origin of the discrepancy between the bulk viscosity derived from the Kubo formula and that derived from the kinetic theory.

4.3   Summary

In this chapter, we introduced the quantum virial expansion as a non-perturbative computational method and discussed the bulk viscosity in the high-temperature limit. In Sec. 4.1, we reviewed the quantum virial expansion using the Matsubara formalism. We also reviewed the calculation of the thermodynamic quantities and obtained the first and second virial coefficients [Eqs. (4.1.50) and (4.1.51)] [107]. The virial expansion coefficients are important quantities characterizing the universality shown by the thermodynamics of the resonant Fermi gas. The higher-order coefficients were calculated [79, 82, 83, 85–87, 110–115] and agreed with the experimental results [116, 117]. In Sec. 4.2, we derived the Kubo formula for the bulk viscosity expressed by the contact-contact response function [Eq. (4.2.9)], and also derived the response of the physical quantities to the time-dependent scattering length from a microscopic perspective without relying on the hydrodynamic approach [Eqs. (4.2.18), (4.2.19), and (4.2.20)]. We then reviewed the calculation of the contact-contact response function in the quantum virial expansion and obtained the bulk viscosity [Eqs. (4.2.35) and (4.2.36)] [89–91]. Finally, we discussed the discrepancy between the bulk viscosity derived from the Kubo formula in the quantum virial expansion and the one derived from the kinetic theory. We pointed out that the kinetic theory is invalid due to the breakdown of the quasiparticle approximation at $O(z)$.

Chapter 5

Shear viscosity and thermal conductivity in the quantum virial expansion

In this chapter, we compute the shear viscosity and the thermal conductivity of the resonant Fermi gas in the quantum virial expansion. As the bulk viscosity reviewed in Chapter 4, they were also calculated in the quantum virial expansion via the Kubo formulas [39, 89, 91, 93]. However, the calculations of the shear viscosity and the thermal conductivity suffer from a divergence in the static limit due to a singularity called the pinch singularity [119, 120]. In Refs. [39, 89, 91, 93], an expansion of the spectral function was carried out, and then the expansion approximately resummed by the memory function method. The purpose of this chapter is to give an exact microscopic computation for the shear viscosity and the thermal conductivity in the high-temperature limit by taking into the account the singularity. The pinch singularity appears not only in the high-temperature limit but also in the weak coupling limit. The singularity was studied in the weak coupling limit [119, 120]. We derive a self-consistent equation incorporating terms with the singularity in the high-temperature limit by extending the methods in the weak coupling limit, mainly based on the Eliashberg method for the Fermi liquid [120] and its modern description [123].

In Sec. 5.1, we review the transport coefficients calculated in the quantum virial expansion using the memory function method. In Sec. 5.2, we introduce the pinch singularity and confirm its appearance in the Kubo formula. We also express the transport coefficient in the high-temperature limit by a vertex function. In Sec. 5.3, we then derive the self-consistent equation for the vertex function in the high-temperature limit and show that it is equal to the linearized Boltzmann equation. In Sec. 5.4, we solve the derived self-consistent equation and calculate specifically the shear viscosity and the thermal conductivity. We conclude this chapter in Sec. 5.5.

In this chapter, we consider the quantum virial expansion for the resonant Fermi gas, as in Chapter 4. The Hamiltonian of the system is given by Eq. (4.1.8), and the basic formulations of the quantum virial expansion are as described in Chapter 4.

5.1   Memory function method for shear viscosity

We first review the computation of the shear viscosity in the quantum virial expansion to see that a resummation is required for the expansion [39, 89, 91]. The shear viscosity η is computed from[1]

$$\eta = \lim_{\omega \to 0} \frac{\text{Im}[\mathcal{R}_{\Pi_{xy}\Pi_{xy}}(\omega + i0^+, \mathbf{0})]}{\omega}. \tag{5.1.1}$$

Here, $\hat{\Pi}_{xy}(t, \boldsymbol{x}) = e^{it\hat{H}}\hat{\Pi}_{xy}(\boldsymbol{x})e^{-it\hat{H}}$ is the xy-component of the stress tensor operator in the Heisenberg picture and $\hat{\Pi}_{xy}(\boldsymbol{x})$ is

$$\hat{\Pi}_{xy}(\boldsymbol{x}) = -\sum_{\sigma} \hat{\psi}_{\sigma}^{\dagger}(\boldsymbol{x}) \frac{\partial_x \partial_y}{m} \hat{\psi}_{\sigma}(\boldsymbol{x}). \tag{5.1.2}$$

The response function $\mathcal{R}_{\mathcal{AB}}(w, \boldsymbol{k})$ is defined by Eq. (2.2.7):

$$\mathcal{R}_{\mathcal{AB}}(w, \boldsymbol{k}) = i \int_0^{\infty} \mathrm{d}t \int \mathrm{d}\boldsymbol{x}\, e^{iwt - i\boldsymbol{k}\cdot\boldsymbol{x}} \langle [\hat{\mathcal{A}}(t, \boldsymbol{x}), \hat{\mathcal{B}}(0, \mathbf{0})] \rangle. \tag{5.1.3}$$

As the bulk viscosity in Chapter 4, the stress-stress response function of the resonant Fermi gas was calculated in the quantum virial expansion [89, 91], which results in the spectral function $\text{Im}[\mathcal{R}_{\Pi_{xy}\Pi_{xy}}(\omega + i0^+, \mathbf{0})]/\omega$ as

$$\frac{\text{Im}[\mathcal{R}_{\Pi_{xy}\Pi_{xy}}(\omega + i0^+, \mathbf{0})]}{\omega}$$
$$= \mathcal{P}\pi\delta(\omega) + \frac{z^2}{\lambda_T^d} \frac{(m/2\pi)^{d/2}}{\Gamma(2+d/2)} \frac{e^{\beta\omega}-1}{\omega} \int_0^{\infty} \mathrm{d}\varepsilon\, e^{-\beta\varepsilon} \varepsilon^{1+d/2} \text{Im}\left[\frac{\mathcal{T}_a(\varepsilon - \omega - i0^+)}{(\omega + i0^+)^2}\right]$$
$$+ \frac{z^2}{\lambda_T^d} \frac{(m/2\pi)^{d/2}}{\Gamma(2+d/2)} \frac{1 - e^{-\beta\omega}}{\omega} \int_0^{\infty} \mathrm{d}\varepsilon\, e^{-\beta\varepsilon} \varepsilon^{1+d/2} \text{Im}\left[\frac{\mathcal{T}_a(\varepsilon + \omega - i0^+)}{(\omega - i0^+)^2}\right] + O(z^3), \tag{5.1.4}$$

where $\mathcal{P}$ is the pressure given by Eqs. (4.1.36) and (4.1.51). From Eq. (5.1.1), the shear viscosity η is obtained by taking the static limit $\omega \to 0$ in Eq. (5.1.4). However, this limit cannot be taken in Eq. (5.1.4), and a resummation is required. For the spectral function $\text{Im}[\mathcal{R}_{\Pi_{xy}\Pi_{xy}}(\omega + i0^+, \mathbf{0})]/\omega$, there is a resummation method called the memory function method [118]. In the memory function method, the spectral function is supposed to have the Drude form of

$$\frac{\text{Im}[\mathcal{R}_{\Pi_{xy}\Pi_{xy}}(\omega + i0^+, \mathbf{0})]}{\omega} = \text{Im}\left[\frac{\eta_0}{\omega - i0^+ - M(\omega)}\right], \tag{5.1.5}$$

where $M(\omega)$ is called the memory function, and η_0 is a real constant. By comparing Eq. (5.1.4) with the Drude form of

$$\text{Im}\left[\frac{\eta_0}{\omega - i0^+ - M(\omega)}\right] = \eta_0 \text{Im}\left[\frac{1}{\omega - i0^+}\right] + \eta_0 \text{Im}\left[\frac{\mathcal{M}(\omega)}{(\omega - i0^+)^2}\right] + \cdots, \tag{5.1.6}$$

we can find $\eta_0 = \mathcal{P}$ and

$$M(\omega) = -\frac{z^2}{\mathcal{P}\lambda_T^d} \frac{(m/2\pi)^{d/2}}{\Gamma(2+d/2)} \frac{e^{\beta\omega}-1}{\omega} \int_0^{\infty} \mathrm{d}\varepsilon\, e^{-\beta\varepsilon} \varepsilon^{1+d/2} \mathcal{T}_a(\varepsilon - \omega + i0^+)$$
$$+ \frac{z^2}{\mathcal{P}\lambda_T^d} \frac{(m/2\pi)^{d/2}}{\Gamma(2+d/2)} \frac{1 - e^{-\beta\omega}}{\omega} \int_0^{\infty} \mathrm{d}\varepsilon\, e^{-\beta\varepsilon} \varepsilon^{1+d/2} \mathcal{T}_a(\varepsilon + \omega - i0^+) + O(z^2). \tag{5.1.7}$$

---

[1]See Appendix C for this Kubo formula.

Because of $\mathrm{Re}[M(0)] = 0$, the shear viscosity is obtained as [89, 91]

$$
\eta = \frac{\mathcal{P}}{\mathrm{Im}[M(0)]} = \begin{cases} \dfrac{2}{\pi\lambda_T^2} \left[\displaystyle\int_0^\infty \mathrm{d}x\, e^{-x} \frac{x^2}{[\ln(x\tilde{a}^2)]^2 + \pi^2} \right]^{-1} + O(z) & d = 2, \\[4mm] \dfrac{15\pi}{4\sqrt{2}\lambda_T^3} \left[\displaystyle\int_0^\infty \mathrm{d}x\, e^{-x} \frac{x^3}{x + \tilde{a}^{-2}} \right]^{-1} + O(z) & d = 3, \end{cases} \tag{5.1.8}
$$

where $\tilde{a} = \sqrt{2\pi}a/\lambda_T$ is the dimensionless scattering length. On the other hand, the shear viscosity in the high-temperature limit was calculated from the kinetic theory for $d = 3$ [69, 70] and for $d = 2$ [72, 73], as reviewed in Chapter 2. The result of Eq. (5.1.8) agrees with that calculated from the kinetic theory in the relaxation-time approximation.

The thermal conductivity κ was also computed in the quantum virial expansion via

$$
T\kappa = \lim_{\omega \to 0} \frac{\mathrm{Im}[\mathcal{R}_{\mathcal{J}_x^q \mathcal{J}_x^q}(\omega + i0^+, \mathbf{0})]}{\omega}, \tag{5.1.9}
$$

and the expansion was resummed by the memory function method [93]. Then, the thermal conductivity obtained using the memory function method agrees with that calculated from the kinetic theory in the relaxation-time approximation [71]. Here, $\hat{\mathcal{J}}_x^q(t, \mathbf{x}) = e^{it\hat{H}} \hat{\mathcal{J}}_x^q(\mathbf{x}) e^{-it\hat{H}}$ is the x-component of the heat current density operator in the Heisenberg picture [Eq. (2.2.55)] and $\hat{\mathcal{J}}_x^q(\mathbf{x})$ is

$$
\begin{aligned}
\hat{\mathcal{J}}_x^q(\mathbf{x}) &= \hat{\mathcal{Q}}_i(\mathbf{x}) - \frac{\mathcal{E} + \mathcal{P}}{mn} \hat{\mathcal{J}}_i(\mathbf{x}), \\
&= \sum_\sigma \frac{[\partial_i \hat{\psi}_\sigma^\dagger(\mathbf{x})][\partial_j \partial_j \hat{\psi}_\sigma(\mathbf{x})] - [\partial_j \partial_j \hat{\psi}_\sigma^\dagger(\mathbf{x})][\partial_i \hat{\psi}_\sigma(\mathbf{x})]}{4im^2} \\
&\quad + \frac{g}{im} \sum_{\sigma,\rho} \hat{\psi}_\sigma^\dagger(\mathbf{x})[\hat{\psi}_\rho^\dagger(\mathbf{x}) \overleftrightarrow{\partial_i} \hat{\psi}_\rho(\mathbf{x})]\hat{\psi}_\sigma(\mathbf{x}) - \frac{\mathcal{E} + \mathcal{P}}{n} \sum_\sigma \frac{\hat{\psi}_\sigma^\dagger(\mathbf{x}) \overleftrightarrow{\partial_i} \hat{\psi}_\sigma(\mathbf{x})}{im},
\end{aligned} \tag{5.1.10}
$$

where $\mathcal{E}$, $\mathcal{P}$, and n are the internal energy density, the pressure, and the particle number density, respectively.

5.2 Pinch singularity in Kubo formulas

5.2.1 Pinch singularity

We now turn to a singularity that causes a divergence in the quantum virial expansion. The need for the resummation comes from the so-called "pinch singularity," which breaks down the naive expansion [119, 120]. The pinch singularity arises from the product of the single-particle Green functions with the same frequency and momentum,

$$
\mathcal{G}^{\mathrm{R}}(\omega, \mathbf{k}) \mathcal{G}^{\mathrm{A}}(\omega, \mathbf{k}) = \frac{A(\omega, \mathbf{k})}{-2\,\mathrm{Im}\,\Sigma^{\mathrm{R}}(\omega, \mathbf{k})}, \tag{5.2.1}
$$

which appears in the static limit of the response function. Here, $\mathcal{G}^{\mathrm{R}}(\omega, \mathbf{k})$ and $\mathcal{G}^{\mathrm{A}}(\omega, \mathbf{k})$ are the retarded and advanced Green functions, respectively, and are given in the form of

$$
\mathcal{G}^{\mathrm{R}}(\omega, \mathbf{k}) = \frac{1}{\omega - \frac{\mathbf{k}^2}{2m} + \mu - \Sigma^{\mathrm{R}}(\omega, \mathbf{k})} = \mathcal{G}^{\mathrm{A}*}(\omega, \mathbf{k}), \tag{5.2.2}
$$

where $\Sigma^{\mathrm{R}}(\omega, \boldsymbol{k})$ is the retarded self-energy and $A(\omega, \boldsymbol{k})$ is the spectral function defined by $A(\omega, \boldsymbol{k}) \equiv -2\,\mathrm{Im}\,\mathcal{G}^{\mathrm{R}}(\omega, \boldsymbol{k})$. This product (5.2.1) diverges when the imaginary part of the self-energy vanishes. The vanishing of the imaginary part of the self-energy leads to the pinch singularity but also justifies the quasiparticle approximation, which underlies the kinetic theory. For this reason, it is necessary to discuss the pinch singularity to understand the relation between the microscopic and kinetic computations [121, 122].

The reatrded and advanced Green functions are obtained from the analytic continuation of the Matsubara Greem function $\mathcal{G}(i\omega_m^F, \boldsymbol{k})$ of Eq. (4.1.12),

$$\mathcal{G}^{\mathrm{R}}(\omega, \boldsymbol{k}) = \mathcal{G}^{\mathrm{A}*}(\omega, \boldsymbol{k}) = \mathcal{G}(\omega + i0^+, \boldsymbol{k}). \tag{5.2.3}$$

Thus, the retarded self-energy $\Sigma^{\mathrm{R}}(\omega, \boldsymbol{k})$ in the high-temperature limit is provided by Eq. (4.1.44):

$$\Sigma^{\mathrm{R}}(\omega, \boldsymbol{k}) = \Sigma_{\mathrm{LO}}(\omega + i0^+, \boldsymbol{k}) = \frac{z}{L^d} \sum_{\boldsymbol{p}} e^{-\beta \epsilon_{\boldsymbol{p}}} \mathcal{T}_a(\omega + \epsilon_{\boldsymbol{p}} - \epsilon_{\boldsymbol{k}+\boldsymbol{p}}/2 + \mu + i0^+), \tag{5.2.4}$$

where $O(z^2)$ terms are dropped. Then, the product of Eq. (5.2.1) is evaluated as

$$\mathcal{G}^{\mathrm{R}}(\omega, \boldsymbol{k})\mathcal{G}^{\mathrm{A}}(\omega, \boldsymbol{k}) = z^{-1}\frac{2\pi\delta(\omega - \epsilon_{\boldsymbol{k}} + \mu)}{-2\,\mathrm{Im}\,\Sigma_{\text{on-shell}}^{\mathrm{R}}(\boldsymbol{k})}, \tag{5.2.5}$$

where $\Sigma_{\text{on-shell}}^{\mathrm{R}}(\boldsymbol{k})$ is defined by

$$\Sigma_{\text{on-shell}}^{\mathrm{R}}(\boldsymbol{k}) = \frac{1}{L^d} \sum_{\boldsymbol{p}} e^{-\beta \epsilon_{\boldsymbol{p}}} \mathcal{T}_a(\epsilon_{\boldsymbol{k}-\boldsymbol{p}}/2 + i0^+). \tag{5.2.6}$$

Therefore, the product has the inverse power of the fugacity, which breaks down the naive expansion. Since this product reduces the order of the fugacity by one, the terms involving this product are enhanced in the high-temperature limit. We refer to the product of Eq. (5.2.5) as the singular product. Throughout this chapter, we consider the high-temperature limit. Namely, we only consider the lowest-order terms for the fugacity without overlooking the pinch singularity and drop higher-order corrections.

5.2.2   Kubo formula

We confirm that the pinch singularity appears in the Kubo formula of Eqs. (5.1.1) and (5.1.9). The response function is obtained from the analytic continuation of the imaginary-time correlator: $\mathcal{R}_{\mathcal{AB}}(\omega + i0^+, \boldsymbol{0}) = \chi_{\mathcal{AB}}(\omega + i0^+, \boldsymbol{0})$. To study the shear viscosity and the thermal conductivity in a unified manner, we consider an imaginary-time correlator

$$\chi_{\mathcal{OO}}(i\omega^B, \boldsymbol{0}) = \int_0^\beta \mathrm{d}\tau \int \mathrm{d}\boldsymbol{x}\, e^{i\omega^B \tau} \langle \mathcal{T}_\tau \hat{\mathcal{O}}(\tau, \boldsymbol{x}) \hat{\mathcal{O}}(0, \boldsymbol{0}) \rangle, \tag{5.2.7}$$

where $\hat{\mathcal{O}}(\tau, \boldsymbol{x}) = e^{\tau(\hat{H} - \mu\hat{N})} \hat{\mathcal{O}}(\boldsymbol{x}) e^{-\tau(\hat{H} - \mu\hat{N})}$ is an operator in the imaginary-time representation. Here, we suppose that the operator $\hat{\mathcal{O}}$ is a quadratic one

$$\hat{\mathcal{O}}(\boldsymbol{p} = \boldsymbol{0}) = \sum_\sigma \sum_{\boldsymbol{k}} \hat{\psi}_{\sigma; \boldsymbol{k}}^\dagger \mathcal{Q}(\boldsymbol{k}) \hat{\psi}_{\sigma; \boldsymbol{k}}, \tag{5.2.8}$$
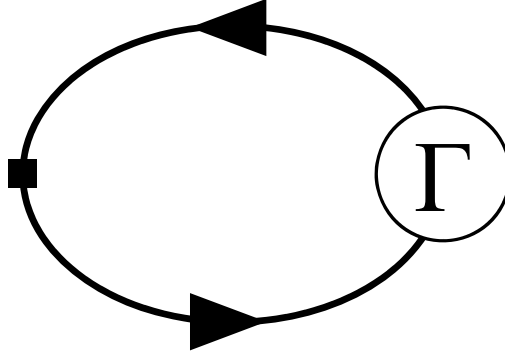
Figure 5.1: Diagrammatic representation of the imaginary-time correlator by using the vertex function Γ. The bold line represents the full propagator $\mathcal{G}$, as opposed to the thin line representing the free propagator G as in Fig. 4.1. The square denotes the bare vertex $\mathcal{Q}$.

where $\hat{\psi}_{\sigma;\boldsymbol{p}} \equiv L^{-d/2} \int \mathrm{d}\boldsymbol{x}\, e^{-i\boldsymbol{p}\cdot\boldsymbol{x}}\hat{\psi}_\sigma(\boldsymbol{x})$ is the Fourier component of the annihilation operator. From Eq. (5.1.2), the xy-component of the stress tensor operator is given by

$$\hat{\Pi}_{xy}(\boldsymbol{p}=\boldsymbol{0}) = \sum_\sigma \sum_{\boldsymbol{k}} \hat{\psi}^\dagger_{\sigma;\boldsymbol{k}} \pi_{xy}(\boldsymbol{k}) \hat{\psi}_{\sigma;\boldsymbol{k}}, \tag{5.2.9}$$

with $\pi_{xy}(\boldsymbol{k}) \equiv k_x k_y/m$, so that we can set $\mathcal{Q}(\boldsymbol{k}) = \pi_{xy}(\boldsymbol{k})$ for the shear viscosity. On the other hand, the heat current density operator is not a quadratic operator from Eq. (5.1.10) [93]:

$$\hat{\mathcal{J}}^q_x(\boldsymbol{p}=\boldsymbol{0}) = \sum_\sigma \sum_{\boldsymbol{k}} \hat{\psi}^\dagger_{\sigma;\boldsymbol{k}} j^q_x(\boldsymbol{k}) \hat{\psi}_{\sigma;\boldsymbol{k}} + \frac{g}{L^d} \sum_{\boldsymbol{Q},\boldsymbol{k},\boldsymbol{k}'} \frac{Q_x}{m} \hat{\psi}^\dagger_{\uparrow;\boldsymbol{Q}/2+\boldsymbol{k}} \hat{\psi}^\dagger_{\downarrow;\boldsymbol{Q}/2-\boldsymbol{k}} \hat{\psi}_{\downarrow;\boldsymbol{Q}/2-\boldsymbol{k}'} \hat{\psi}_{\uparrow;\boldsymbol{Q}/2+\boldsymbol{k}'},$$
$$\tag{5.2.10}$$

with

$$\boldsymbol{j}^q(\boldsymbol{k}) \equiv \left(\epsilon_{\boldsymbol{k}} - \frac{\mathcal{E}+\mathcal{P}}{n}\right) \frac{\boldsymbol{k}}{m}. \tag{5.2.11}$$

In the high-temperature limit, the first term of $\hat{\mathcal{J}}^q_x(\boldsymbol{p}=\boldsymbol{0})$ is dominant and the second term is negligible, so that we can set $\mathcal{Q}(\boldsymbol{k}) = j^q_i(\boldsymbol{k})$ for the thermal conductivity. This is because the relative momentum dependence of the second term inhibits the appearance of the singular product, which is the product of the single-particle Green functions with the same momentum. The contribution from the second term is not enhanced by the singularity in the high-temperature limit.

With the use of Eq. (5.2.8), the imaginary-time correlator (5.2.7) is written as

$$\chi_{\mathcal{O}\mathcal{O}}(i\omega^B,\boldsymbol{0}) = \frac{1}{L^d} \sum_{\sigma,\sigma'} \int_0^\beta \mathrm{d}\tau\, e^{i\omega^B\tau} \sum_{\boldsymbol{k},\boldsymbol{k}'} \mathcal{Q}(\boldsymbol{k}) \langle \mathcal{T}_\tau \bar{\psi}_{\sigma;\boldsymbol{k}}(\tau) \psi_{\sigma;\boldsymbol{k}}(\tau) \bar{\psi}_{\sigma';\boldsymbol{k}'}(0) \psi_{\sigma';\boldsymbol{k}'}(0) \rangle \mathcal{Q}(\boldsymbol{k}').$$
$$\tag{5.2.12}$$

We introduce the vertex function $\Gamma(i\omega^F_m + i\omega^B, i\omega^F_m; \boldsymbol{k})$ such that the correlator is denoted by

$$\chi_{\mathcal{O}\mathcal{O}}(i\omega^B,\boldsymbol{0}) = -\frac{2}{\beta L^d} \sum_m \sum_{\boldsymbol{k}} \mathcal{Q}(\boldsymbol{k}) \mathcal{G}(i\omega^F_m + i\omega^B, \boldsymbol{k}) \mathcal{G}(i\omega^F_m, \boldsymbol{k}) \Gamma(i\omega^F_m + i\omega^B, i\omega^F_m; \boldsymbol{k}), \tag{5.2.13}$$

which is represented diagrammatically in Fig. 5.1. Here, because the bare vertex $\mathcal{Q}(\boldsymbol{k})$ is diagonal with respect to the spin indices and independent of the spin indices, the vertex function is also diagonal and independent.
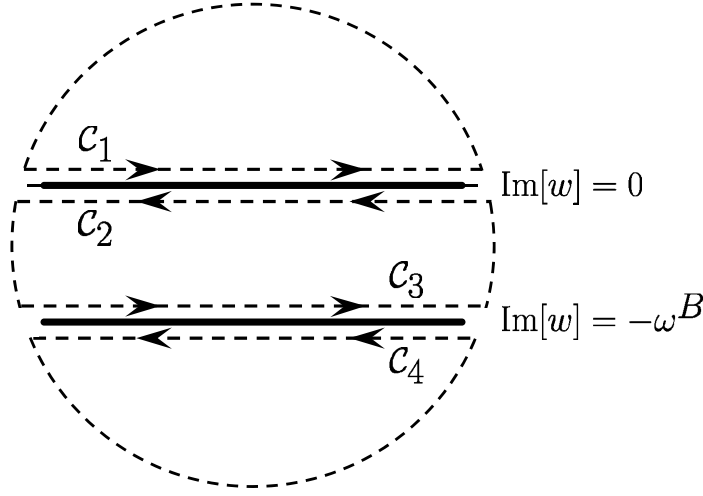
Figure 5.2:   Branch cut structure and contours of integration used to evaluate the imaginary-time correlator. The contour γ can be deformed to four lines: $\gamma \to \mathcal{C} = \mathcal{C}_1 + \mathcal{C}_2 + \mathcal{C}_3 + \mathcal{C}_4$. Here, the contribution from the circle with infinite radius is negligible. The complex variable w is parametrized as $w = \varepsilon + i0^+$ on $\mathcal{C}_1$, $w = \varepsilon - i0^+$ on $\mathcal{C}_2$, $w = \varepsilon - i\omega^B + i0^+$ on $\mathcal{C}_3$, and $w = \varepsilon - i\omega^B - i0^+$ on $\mathcal{C}_4$ with $\varepsilon \in \mathbb{R}$.

For the analytic continuation $i\omega^B \to \omega + i0^+$, it is necessary to express the correlator such that $\chi_{\mathcal{OO}}(w, \mathbf{0})$ is regular in the upper half-plane of $w \in \mathbb{C}$. To do this, we first rewrite the Matsubara frequency summation as the contour integral on γ:

$$\chi_{\mathcal{OO}}(i\omega^B, \mathbf{0}) = \frac{2}{L^d} \oint_\gamma \frac{\mathrm{d}w}{2\pi i} f_F(w) \sum_{\mathbf{k}} \mathcal{Q}(\mathbf{k}) \mathcal{G}(w + i\omega^B, \mathbf{k}) \mathcal{G}(w, \mathbf{k}) \Gamma(w + i\omega^B, w; \mathbf{k}), \quad (5.2.14)$$

where γ consists of counterclockwise closed contours around the singularities of $f_F(w)$. Here, the Green function $\mathcal{G}(w, \mathbf{k})$ has a branch on $\mathrm{Im}[w] = 0$ and the vertex function $\Gamma(w + i\omega^B, w; \mathbf{k})$ can have branches on $\mathrm{Im}[w] = 0$ and $\mathrm{Im}[w] = -\omega^B$, as shown in Appendix D. Thus, we can deform γ to $\mathcal{C}$, as depicted in Fig. 5.2. Then, the correlator is expressed as

$$
\begin{aligned}
\chi_{\mathcal{OO}}(i\omega^B, \mathbf{0}) = \frac{2}{L^d} \int_{-\infty}^{\infty} & \frac{\mathrm{d}\varepsilon}{2\pi i} \sum_{\mathbf{k}} f_F(\varepsilon) \mathcal{Q}(\mathbf{k}) \\
\times \Big\{ & \mathcal{G}(\varepsilon + i\omega^B, \mathbf{k}) \mathcal{G}(\varepsilon + i0^+, \mathbf{k}) \Gamma(\varepsilon + i\omega^B, \varepsilon + i0^+; \mathbf{k}) \\
& - \mathcal{G}(\varepsilon + i\omega^B, \mathbf{k}) \mathcal{G}(\varepsilon - i0^+, \mathbf{k}) \Gamma(\varepsilon + i\omega^B, \varepsilon - i0^+; \mathbf{k}) \\
& + \mathcal{G}(\varepsilon + i0^+, \mathbf{k}) \mathcal{G}(\varepsilon - i\omega^B, \mathbf{k}) \Gamma(\varepsilon + i0^+, \varepsilon - i\omega^B; \mathbf{k}) \\
& - \mathcal{G}(\varepsilon - i0^+, \mathbf{k}) \mathcal{G}(\varepsilon - i\omega^B, \mathbf{k}) \Gamma(\varepsilon - i0^+, \varepsilon - i\omega^B; \mathbf{k}) \Big\}.
\end{aligned}
\qquad (5.2.15)
$$

We can apply the analytic continuation $i\omega^B \to \omega + i0^+$ to this expression and obtain the

response function $\mathcal{R}_{\mathcal{O}\mathcal{O}}(\omega + i0^+, \mathbf{0})$ as

$$
\begin{aligned}
\mathcal{R}_{\mathcal{O}\mathcal{O}}(\omega + i0^+, \mathbf{0}) &= \chi_{\mathcal{O}\mathcal{O}}(\omega + i0^+, \mathbf{0}) \\
&= \frac{2}{L^d} \int_{-\infty}^{\infty} \frac{d\varepsilon}{2\pi i} \sum_{\mathbf{k}} \Big[f_F(\varepsilon + \omega) - f_F(\varepsilon) \Big] \mathcal{Q}(\mathbf{k}) \\
&\quad \times \mathcal{G}^{\mathrm{R}}(\varepsilon + \omega, \mathbf{k}) \mathcal{G}^{\mathrm{A}}(\varepsilon, \mathbf{k}) \Gamma(\varepsilon + \omega + i0^+, \varepsilon - i0^+; \mathbf{k}) \\
&\quad + \mathcal{R}_{\text{non-sing}}(\omega + i0^+, \mathbf{0}),
\end{aligned}
\tag{5.2.16}
$$

with the use of Eq. (5.2.3). One sees that Eq. (5.2.16) has a product of the retarded and advanced Green functions with the same frequency and momentum in the static limit. Here, $\mathcal{R}_{\text{non-sing}}(\omega + i0^+, \mathbf{0})$ is the contribution from the integrals on $\mathcal{C}_1$ and $\mathcal{C}_4$, and is given by

$$
\begin{aligned}
\mathcal{R}_{\text{non-sing}}(\omega + i0^+, \mathbf{0}) &= \frac{2}{L^d} \int_{-\infty}^{\infty} \frac{d\varepsilon}{2\pi i} \sum_{\mathbf{k}} f_F(\varepsilon) \mathcal{Q}(\mathbf{k}) \\
&\quad \times \Big\{ \mathcal{G}^{\mathrm{R}}(\varepsilon + \omega, \mathbf{k}) \mathcal{G}^{\mathrm{R}}(\varepsilon, \mathbf{k}) \Gamma(\varepsilon + \omega + i0'^+, \varepsilon + i0^+; \mathbf{k}) \\
&\quad - \mathcal{G}^{\mathrm{A}}(\varepsilon, \mathbf{k}) \mathcal{G}^{\mathrm{A}}(\varepsilon - \omega, \mathbf{k}) \Gamma(\varepsilon - i0^+, \varepsilon - \omega - i0'^+; \mathbf{k}) \Big\},
\end{aligned}
\tag{5.2.17}
$$

where the infinitesimal quantities obey $0'^+ > 0^+$ because of the sequence of the limits. This $\mathcal{R}_{\text{non-sing}}(\omega + i0^+, \mathbf{0})$ is not enhanced in the static limit because it does not involve the singular product.

We introduce a transport coefficient $\sigma_{\mathcal{O}}$ in the same form as the Kubo formulas,

$$
\sigma_{\mathcal{O}} \equiv \lim_{\omega \to 0} \frac{\mathrm{Im}[\mathcal{R}_{\mathcal{O}\mathcal{O}}(\omega + i0^+, \mathbf{0})]}{\omega}.
\tag{5.2.18}
$$

In the static limit, the term involving the singular product yields the leading-order contribution, and thus the transport coefficient $\sigma_{\mathcal{O}}$ is given by

$$
\sigma_{\mathcal{O}} = \frac{2\beta}{L^d} \sum_{\mathbf{k}} e^{-\beta \epsilon_{\mathbf{k}}} \mathcal{Q}(\mathbf{k}) \frac{\Gamma_{\mathrm{RA}}(\mathbf{k})}{-2 \,\mathrm{Im}\, \Sigma_{\text{on-shell}}^{\mathrm{R}}(\mathbf{k})},
\tag{5.2.19}
$$

where Eq. (5.2.5) is used. Here, $\Gamma_{\mathrm{RA}}(\mathbf{k})$ is the vertex function connecting to the singular product and is defined by

$$
\Gamma_{\mathrm{RA}}(\mathbf{k}) \equiv \Gamma(\epsilon_{\mathbf{k}} - \mu + i0^+, \epsilon_{\mathbf{k}} - \mu - i0^+; \mathbf{k}).
\tag{5.2.20}
$$

From Eq. (5.2.19), $\Gamma_{\mathrm{RA}}(\mathbf{k})$ is the only vertex function we need to calculate for the transport coefficient.

5.3 Self-consistent eqution for vertex function

In the previous section, we derived the formal expression for the transport coefficient $\sigma_{\mathcal{O}}$ by using the vertex function. In this section, we evaluate the leading-order vertex function in the quantum virial expansion. Since the singular product reduces the order of the fugacity by one, the leading-order vertex function is given by the sum of an infinite number of terms. To take
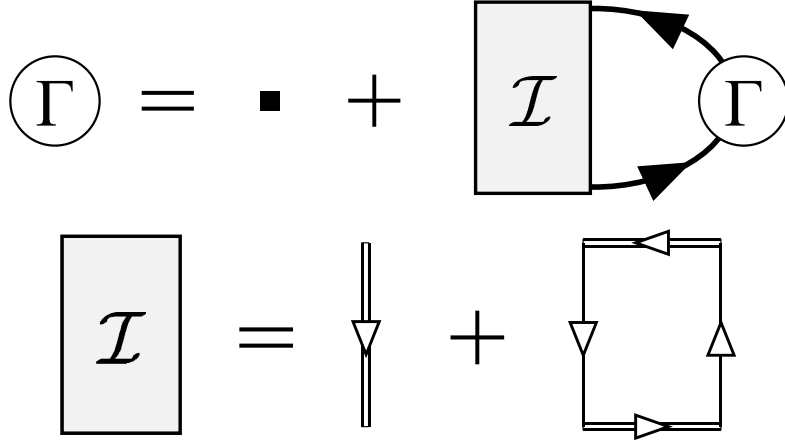
Figure 5.3:   The self-consistent equation for the vertex function (top) and the leading-order four-point functions (bottom). In the upper figure, the Green functions connected with the vertex function are the full propagator $\mathcal{G}$, denoted by the bold line. In the lower figure, the first term on the right-hand side represents the Maki-Thompson diagram and the second term represents the Aslamazov-Larkin diagram.

into account the contributions of the infinite number of terms, we consider the self-consistent equation for the vertex function, represented in Fig. 5.3 diagrammatically,

$$
\begin{aligned}
\Gamma(i\omega_m^F + i\omega^B, i\omega_m^F; \boldsymbol{k}) = \mathcal{Q}(\boldsymbol{k}) + \frac{1}{\beta}\sum_n \int_{\boldsymbol{p}} \mathcal{I}(i\omega_m^F + i\omega^B, i\omega_m^F; \boldsymbol{k}|i\omega_n^F + i\omega^B, i\omega_n^F; \boldsymbol{p}) \\
\times \mathcal{G}(i\omega_n^F + i\omega^B, \boldsymbol{p})\mathcal{G}(i\omega_n^F, \boldsymbol{p})\Gamma(i\omega_n^F + i\omega^B, i\omega_n^F; \boldsymbol{p}),
\end{aligned}
\tag{5.3.1}
$$

where $\mathcal{I}$ denotes the connected four-point function. Hereafter, we take the infinite-volume limit $L^{-d}\sum_{\boldsymbol{p}} \to \int_{\boldsymbol{p}}$. The pinch singularity can result from the product of the Matsubara Green functions of the same frequency and momentum in the limit $i\omega^B \to 0$ corresponding to the static limit. In the self-consistent equation, the singular product can arise from the product of the two Green functions connected with the vertex function.

Let us take the four-point function $\mathcal{I}$ specifically such that the second term of Eq. (5.3.1) has the zeroth-order contribution for the fugacity. Since the singular product reduces the order by one, we consider the four-point function $\mathcal{I}$ with a first-order contribution for the fugacity. As mentioned in Chapter 4, we can estimate the order of diagrams by using the techniques of the quantum virial expansion in the imaginary-time representation. The first-order contributions are given by diagrams of the Maki-Thompson and Aslamazov-Larkin types [39, 91], which are drawn in Fig. 5.3,

$$
\mathcal{I}_{\mathrm{MT}}(i\omega_m^F + i\omega^B, i\omega_m^F; \boldsymbol{k}|i\omega_n^F + i\omega^B, i\omega_n^F; \boldsymbol{p}) = \mathcal{T}_a(i\omega_m^F + i\omega_n^F + i\omega^B, \boldsymbol{k} + \boldsymbol{p}),
\tag{5.3.2}
$$

and

$$
\begin{aligned}
&\mathcal{I}_{\mathrm{AL}}(i\omega_m^F + i\omega^B, i\omega_m^F; \boldsymbol{k}|i\omega_n^F + i\omega^B, i\omega_n^F; \boldsymbol{p}) \\
&= -\frac{2}{\beta}\sum_l \int_{\boldsymbol{q}} \mathcal{T}_a(i\omega_l^B + i\omega^B, \boldsymbol{q})\mathcal{T}_a(i\omega_l^B, \boldsymbol{q})G(i\omega_l^B - i\omega_m^F, \boldsymbol{q} - \boldsymbol{k})G(i\omega_l^B - i\omega_n^F, \boldsymbol{q} - \boldsymbol{p}),
\end{aligned}
\tag{5.3.3}
$$

with $\mathcal{I} = \mathcal{I}_{\mathrm{MT}} + \mathcal{I}_{\mathrm{AL}}$ and $\mathcal{T}_a(i\omega_l^B, \boldsymbol{p}) \equiv \mathcal{T}_a(i\omega_l^B - \epsilon_{\boldsymbol{p}}/2 + 2\mu)$. It is sufficient for the leading-order vertex function to evaluate the four-point functions $\mathcal{I}_{\mathrm{MT}}$ and $\mathcal{I}_{\mathrm{AL}}$ with the full propagator $\mathcal{G}$ and the pair propagator D replaced by the free propagator G and the T-matrix $\mathcal{T}_a$.

The only vertex function required for the transport coefficient is $\Gamma_{\mathrm{RA}}(\boldsymbol{k})$, which is obtained by applying the following analytic continuations to the vertex function $\Gamma(i\omega_m^F + i\omega^B, i\omega_m^F; \boldsymbol{k})$:

$$\begin{aligned}
&1. \quad i\omega_m^F \;\to\; \epsilon_{\boldsymbol{k}} - \mu - i0^+, \\
&2. \quad i\omega^B \;\to\; 0 + i0'^+,
\end{aligned} \tag{5.3.4}$$

where the infinitesimal quantities obey $0'^+ > 0^+$ because of the sequence of the limits.[2] In the following, we apply these analytic continuations (5.3.4) to the self-consistent equation, particularly, to the contributions from the two diagrams, i.e., Maki-Thompson and Aslamazov-Larkin, and derive the leading-order self-consistent equation for $\Gamma_{\mathrm{RA}}(\boldsymbol{k})$.

5.3.1 Maki-Thompson contribution

We denote the contribution from the Maki-Thompson diagram in the form of a linear operator,

$$\begin{aligned}
\mathcal{L}_{\mathrm{MT}}[\Gamma](i\omega_m^F + i\omega^B, i\omega_m^F; \boldsymbol{k}) &\equiv \frac{1}{\beta} \sum_n \int_{\boldsymbol{p}} \mathcal{I}_{\mathrm{MT}}(i\omega_m^F + i\omega^B, i\omega_m^F; \boldsymbol{k} | i\omega_n^F + i\omega^B, i\omega_n^F; \boldsymbol{p}) \\
&\times \mathcal{G}(i\omega_n^F + i\omega^B, \boldsymbol{p})\mathcal{G}(i\omega_n^F, \boldsymbol{p})\Gamma(i\omega_n^F + i\omega^B, i\omega_n^F; \boldsymbol{p}).
\end{aligned} \tag{5.3.5}$$

In order to carry out the analytic continuations (5.3.4), it is necessary to express Eq. (5.3.5) so as to be regular in the lower half-plane of the complex variable for arguments containing $i\omega_m^F$, regular in the upper half-plane of the complex variable for arguments containing $i\omega^B$, and regular in the upper half-plane of the complex variable for arguments containing $i\omega_m^F + i\omega^B$. The Matsubara frequency summation in $\mathcal{L}_{\mathrm{MT}}[\Gamma]$ is expressed by the controur integral on $\mathcal{C}_{\mathrm{MT}}$ as

$$\begin{aligned}
\mathcal{L}_{\mathrm{MT}}[\Gamma](i\omega_m^F + i\omega^B, i\omega_m^F; \boldsymbol{k}) &= -\oint_{\mathcal{C}_{\mathrm{MT}}} \frac{\mathrm{d}w}{2\pi i} \int_{\boldsymbol{p}} f_F(w)\mathcal{T}_a(w + i\omega_m^F + i\omega^B, \boldsymbol{k} + \boldsymbol{p}) \\
&\times \mathcal{G}(w + i\omega^B, \boldsymbol{p})\mathcal{G}(w, \boldsymbol{p})\Gamma(w + i\omega^B, w; \boldsymbol{p}),
\end{aligned} \tag{5.3.6}$$

where the contour $\mathcal{C}_{\mathrm{MT}}$ runs around all the singularities of $f_F(w)$. We evaluate $\mathcal{L}_{\mathrm{MT}}[\Gamma]$ from the singularities of the integrand except for $f_F(w)$. Within the leading order, the singularity of the T-matrix $\mathcal{T}_a(w + i\omega_m^F + i\omega^B, \boldsymbol{k} + \boldsymbol{p})$ is negligible because the contribution from its singularity leads to $O(z^2)$. Therefore, $\mathcal{L}_{\mathrm{MT}}[\Gamma]$ in the high-temperature limit can be evaluated from the singularities of $\mathcal{G}(w + i\omega^B, \boldsymbol{p})$, $\mathcal{G}(w, \boldsymbol{p})$, and $\Gamma(w + i\omega^B, w; \boldsymbol{p})$. This means that we can take $\mathcal{C}_{\mathrm{MT}}$ to be $\mathcal{C}$ depicted in Fig. 5.2 in the high-temperature limit. Since the integral on $\mathcal{C}$ is rewritten as the integrals over ε as in Eq. (5.2.15), $\mathcal{L}_{\mathrm{MT}}[\Gamma]$ is given by

$$\begin{aligned}
&\mathcal{L}_{\mathrm{MT}}[\Gamma](i\omega_m^F + i\omega^B, i\omega_m^F; \boldsymbol{k}) \\
&= \int_{-\infty}^{\infty} \frac{\mathrm{d}\varepsilon}{2\pi i} \int_{\boldsymbol{p}} f_F(\varepsilon) \\
&\times \Big[\mathcal{T}_a(\varepsilon + i\omega_m^F + i\omega^B, \boldsymbol{k} + \boldsymbol{p})\mathcal{G}(\varepsilon + i\omega^B, \boldsymbol{p})\mathcal{G}(\varepsilon - i0^+, \boldsymbol{p})\Gamma(\varepsilon + i\omega^B, \varepsilon - i0^+; \boldsymbol{p}) \\
&\quad - \mathcal{T}_a(\varepsilon + i\omega_m^F, \boldsymbol{k} + \boldsymbol{p})\mathcal{G}(\varepsilon + i0^+, \boldsymbol{p})\mathcal{G}(\varepsilon - i\omega^B, \boldsymbol{p})\Gamma(\varepsilon + i0^+, \varepsilon - i\omega^B; \boldsymbol{p}) \Big] \\
&\quad + \mathcal{L}_{\mathrm{MT;non\text{-}sing}}[\Gamma].
\end{aligned} \tag{5.3.7}$$

---

[2]When there is no need to distinguish their magnitudes, we denote both as 0^+.

Here, $\mathcal{L}_{\mathrm{MT;non\text{-}sing}}[\Gamma]$ represents the integrals on $\mathcal{C}_1$ and $\mathcal{C}_4$, which do not involve the singular product after the analytic continuations. Then, we can apply the analytic continuations (5.3.4) to this expression and obtain

$$\mathcal{L}_{\mathrm{MT}}[\Gamma_{\mathrm{RA}}](\boldsymbol{k}) \equiv \mathcal{L}_{\mathrm{MT}}[\Gamma](\epsilon_{\boldsymbol{k}} - \mu + i0^+, \epsilon_{\boldsymbol{k}} - \mu - i0^+; \boldsymbol{k})$$
$$= \int_{\boldsymbol{p}} e^{-\beta\epsilon_{\boldsymbol{p}}} 2\,\mathrm{Im}\Big[\mathcal{T}_a(\epsilon_{\boldsymbol{k}-\boldsymbol{p}}/2 + i0^+)\Big] \frac{\Gamma_{\mathrm{RA}}(\boldsymbol{p})}{-2\,\mathrm{Im}\,\Sigma^{\mathrm{R}}_{\mathrm{on\text{-}shell}}(\boldsymbol{p})}. \tag{5.3.8}$$

5.3.2 Aslamazov-Larkin contribution

We also denote the contribution from the Aslamazov-Larkin diagram as

$$\mathcal{L}_{\mathrm{AL}}[\Gamma](i\omega_m^F + i\omega^B, i\omega_m^F; \boldsymbol{k}) \equiv \frac{1}{\beta}\sum_n \int_{\boldsymbol{p}} \mathcal{I}_{\mathrm{AL}}(i\omega_m^F + i\omega^B, i\omega_m^F; \boldsymbol{k}|i\omega_n^F + i\omega^B, i\omega_n^F; \boldsymbol{p})$$
$$\times \mathcal{G}(i\omega_n^F + i\omega^B, \boldsymbol{p})\mathcal{G}(i\omega_n^F, \boldsymbol{p})\Gamma(i\omega_n^F + i\omega^B, i\omega_n^F; \boldsymbol{p})$$
$$= -\oint_{\mathcal{C}_{\mathrm{AL}}} \frac{\mathrm{d}w}{2\pi i} \int_{\boldsymbol{p}} f_F(w)\mathcal{I}_{\mathrm{AL}}(i\omega_m^F + i\omega^B, i\omega_m^F; \boldsymbol{k}|w + i\omega^B, w; \boldsymbol{p})$$
$$\times \mathcal{G}(w + i\omega^B, \boldsymbol{p})\mathcal{G}(w, \boldsymbol{p})\Gamma(w + i\omega^B, w; \boldsymbol{p}), \tag{5.3.9}$$

where the contour $\mathcal{C}_{\mathrm{AL}}$ runs around all the singularities of $f_F(w)$. We investigate the analyticity of the four-point function $\mathcal{I}_{\mathrm{AL}}$ for the analytic continuations. By taking the summation over the Matsubara frequency, the four-point function $\mathcal{I}_{\mathrm{AL}}$ of Eq. (5.3.3) is calculated as

$$\mathcal{I}_{\mathrm{AL}}(i\omega_m^F + i\omega^B, i\omega_m^F; \boldsymbol{k}|i\omega_n^F + i\omega^B, i\omega_n^F; \boldsymbol{p})$$
$$= 2z \int_{\boldsymbol{q}} e^{-\beta\epsilon_{\boldsymbol{q}-\boldsymbol{k}}} \frac{\mathcal{T}_a(i\omega_m^F + i\omega^B + \epsilon_{\boldsymbol{q}-\boldsymbol{k}} - \mu, \boldsymbol{q})\mathcal{T}_a(i\omega_m^F + \epsilon_{\boldsymbol{q}-\boldsymbol{k}} - \mu, \boldsymbol{q})}{i\omega_n^F - i\omega_m^F - \epsilon_{\boldsymbol{q}-\boldsymbol{k}} + \epsilon_{\boldsymbol{q}-\boldsymbol{p}}} \tag{5.3.10}$$
$$+ ((\omega_n^F, \boldsymbol{k}) \leftrightarrow (\omega_m^F, \boldsymbol{p})) + O(z^2).$$

Thus, $\mathcal{I}_{\mathrm{AL}}(i\omega_m^F + i\omega^B, i\omega_m^F; \boldsymbol{k}|w + i\omega^B, w; \boldsymbol{p})$ has the singularities of the pole $w = i\omega_m^F + \epsilon_{\boldsymbol{q}-\boldsymbol{k}} - \epsilon_{\boldsymbol{q}-\boldsymbol{p}}$ and the branches on the axes $\mathrm{Im}[w] = 0$ and $\mathrm{Im}[w] = -\omega^B$ for $w \in \mathbb{C}$. To evaluate $\mathcal{L}_{\mathrm{AL}}[\Gamma]$, we can deform the contour $\mathcal{C}_{\mathrm{AL}}$ to $\mathcal{C} + \mathcal{C}_{\mathrm{pole}}$, where the contour $\mathcal{C}$ is shown in Fig. 5.2 and the contour $\mathcal{C}_{\mathrm{pole}}$ runs clockwise around the pole $w = i\omega_m^F + \epsilon_{\boldsymbol{q}-\boldsymbol{k}} - \epsilon_{\boldsymbol{q}-\boldsymbol{p}}$. The contour integral on $\mathcal{C}_{\mathrm{pole}}$ is calculated as

$$-\oint_{\mathcal{C}_{\mathrm{pole}}} \frac{\mathrm{d}w}{2\pi i} \int_{\boldsymbol{p}} f_F(w)\mathcal{I}^{\mathrm{AL}}(i\omega_m^F + i\omega^B, i\omega_m^F; \boldsymbol{k}|w + i\omega^B, w; \boldsymbol{p})$$
$$\times \mathcal{G}(w + i\omega^B, \boldsymbol{p})\mathcal{G}(w, \boldsymbol{p})\Gamma(w + i\omega^B, w; \boldsymbol{p})$$
$$= 2z \int_{\boldsymbol{p},\boldsymbol{q}} e^{-\beta\epsilon_{\boldsymbol{q}-\boldsymbol{k}}}\mathcal{T}_a(i\omega_m^F + i\omega^B + \epsilon_{\boldsymbol{q}-\boldsymbol{k}} - \mu, \boldsymbol{q})\mathcal{T}_a(i\omega_m^F + \epsilon_{\boldsymbol{q}-\boldsymbol{k}} - \mu, \boldsymbol{q}) \tag{5.3.11}$$
$$\times \mathcal{G}(i\omega_m^F + i\omega^B - \epsilon_{\boldsymbol{q}-\boldsymbol{p}} + \epsilon_{\boldsymbol{q}-\boldsymbol{k}}, \boldsymbol{p})\mathcal{G}(i\omega_m^F - \epsilon_{\boldsymbol{q}-\boldsymbol{p}} + \epsilon_{\boldsymbol{q}-\boldsymbol{k}}, \boldsymbol{p})$$
$$\times \Gamma(i\omega_m^F + i\omega^B - \epsilon_{\boldsymbol{q}-\boldsymbol{p}} + \epsilon_{\boldsymbol{q}-\boldsymbol{k}}, i\omega_m^F - \epsilon_{\boldsymbol{q}-\boldsymbol{p}} + \epsilon_{\boldsymbol{q}-\boldsymbol{k}}; \boldsymbol{p}).$$

The analytic continuations (5.3.4) can be applied to this expression. The contour integral on $\mathcal{C}$ can be computed in the same way as for the Maki-Thompson contribution, and we arrive at an expression to which the analytic connections can be applied. Therefore, we can apply

the analytic continuations to the Aslamazov-Larkin contribution and obtain

$$
\begin{aligned}
\mathcal{L}_{\mathrm{AL}}[\Gamma_{\mathrm{RA}}](\boldsymbol{k}) &\equiv \mathcal{L}_{\mathrm{AL}}[\Gamma](\epsilon_{\boldsymbol{k}} - \mu + i0^+, \epsilon_{\boldsymbol{k}} - \mu - i0^+; \boldsymbol{k}) \\
&= 2 \int_{\boldsymbol{k}_2, \boldsymbol{q}_1, \boldsymbol{q}_2} e^{-\beta \epsilon_{\boldsymbol{k}_2}} \mathcal{W}(\boldsymbol{k}, \boldsymbol{k}_2 | \boldsymbol{q}_1, \boldsymbol{q}_2) \frac{\Gamma_{\mathrm{RA}}(\boldsymbol{q}_1)}{-2 \operatorname{Im} \Sigma_{\mathrm{on\text{-}shell}}^{\mathrm{R}}(\boldsymbol{q}_1)},
\end{aligned}
\tag{5.3.12}
$$

where the transition rate $\mathcal{W}(\boldsymbol{k}_1, \boldsymbol{k}_2 | \boldsymbol{q}_1, \boldsymbol{q}_2)$ is introduced as

$$
\begin{aligned}
\mathcal{W}(\boldsymbol{k}_1, \boldsymbol{k}_2 | \boldsymbol{q}_1, \boldsymbol{q}_2) &\equiv |\mathcal{T}_a(\epsilon_{\boldsymbol{k}_1 - \boldsymbol{k}_2}/2 + i0^+)|^2 \\
&\times (2\pi)^{d+1} \delta(\epsilon_{\boldsymbol{k}_1} + \epsilon_{\boldsymbol{k}_2} - \epsilon_{\boldsymbol{q}_1} - \epsilon_{\boldsymbol{q}_2}) \delta^d(\boldsymbol{k}_1 + \boldsymbol{k}_2 - \boldsymbol{q}_1 - \boldsymbol{q}_2).
\end{aligned}
\tag{5.3.13}
$$

After the analytic continuations, only the contribution from the integral on $\mathcal{C}_{\mathrm{pole}}$ results in the leading order by the singular product. The contribution from the integral on $\mathcal{C}$ does not have the zeroth-order contribution because the four-point function $\mathcal{I}_{\mathrm{AL}}$ itself has the first-order for the fugacity, unlike the Maki-Thompson contribution.

5.3.3 Leading-order self-consistent equation and linearized Boltzmann equation

By combining the above results, the leading-order self-consistent equation for $\Gamma_{\mathrm{RA}}(\boldsymbol{k})$ is given by

$$
\Gamma_{\mathrm{RA}}(\boldsymbol{k}) = \mathcal{Q}(\boldsymbol{k}) + \mathcal{L}_{\mathrm{MT}}[\Gamma_{\mathrm{RA}}](\boldsymbol{k}) + \mathcal{L}_{\mathrm{AL}}[\Gamma_{\mathrm{RA}}](\boldsymbol{k}),
\tag{5.3.14}
$$

where $\mathcal{L}_{\mathrm{MT}}[\Gamma_{\mathrm{RA}}](\boldsymbol{k})$ and $\mathcal{L}_{\mathrm{AL}}[\Gamma_{\mathrm{RA}}](\boldsymbol{k})$ are defined in Eqs. (5.3.8) and (5.3.12). Therefore, the leading-order self-consistent equation is written as a closed equation for $\Gamma_{\mathrm{RA}}(\boldsymbol{k})$.

We can show that this self-consistent equation (5.3.14) is equivalent to the linearized Boltzmann equation. To do this, we introduce $\varphi(\boldsymbol{k})$ as

$$
\varphi(\boldsymbol{k}) \equiv \frac{\Gamma_{\mathrm{RA}}(\boldsymbol{k})}{-2 \operatorname{Im} \Sigma_{\mathrm{on\text{-}shell}}^{\mathrm{R}}(\boldsymbol{k})},
\tag{5.3.15}
$$

following [123], and write the self-consistent equation as

$$
\begin{aligned}
\mathcal{Q}(\boldsymbol{k}) &= -2 \operatorname{Im} \Sigma_{\mathrm{on\text{-}shell}}^{\mathrm{R}}(\boldsymbol{k}) \varphi(\boldsymbol{k}) - \int_{\boldsymbol{k}_2} e^{-\beta \epsilon_{\boldsymbol{k}_2}} 2 \operatorname{Im}\left[\mathcal{T}_a(\epsilon_{\boldsymbol{k} - \boldsymbol{k}_2}/2 + i0^+)\right] \varphi(\boldsymbol{k}_2) \\
&\quad - 2 \int_{\boldsymbol{k}_2, \boldsymbol{q}_1, \boldsymbol{q}_2} e^{-\beta \epsilon_{\boldsymbol{k}_2}} \mathcal{W}(\boldsymbol{k}, \boldsymbol{k}_2 | \boldsymbol{q}_1, \boldsymbol{q}_2) \varphi(\boldsymbol{q}_1) \\
&= - \int_{\boldsymbol{k}_2} e^{-\beta \epsilon_{\boldsymbol{k}_2}} 2 \operatorname{Im}\left[\mathcal{T}_a(\epsilon_{\boldsymbol{k} - \boldsymbol{k}_2}/2 + i0^+)\right] \Big(\varphi(\boldsymbol{k}) + \varphi(\boldsymbol{k}_2)\Big) \\
&\quad - 2 \int_{\boldsymbol{k}_2, \boldsymbol{q}_1, \boldsymbol{q}_2} e^{-\beta \epsilon_{\boldsymbol{k}_2}} \mathcal{W}(\boldsymbol{k}, \boldsymbol{k}_2 | \boldsymbol{q}_1, \boldsymbol{q}_2) \varphi(\boldsymbol{q}_1),
\end{aligned}
\tag{5.3.16}
$$

where Eq. (5.2.6) is used. Here, the optical theorem relates the imaginary part of the T-matrix to the transition rate,

$$
-2 \operatorname{Im}\left[\mathcal{T}_a(\epsilon_{\boldsymbol{k}_1 - \boldsymbol{k}_2}/2 + i0^+)\right] = \int_{\boldsymbol{q}_1, \boldsymbol{q}_2} \mathcal{W}(\boldsymbol{k}_1, \boldsymbol{k}_2 | \boldsymbol{q}_1, \boldsymbol{q}_2).
\tag{5.3.17}
$$

Therefore, the self-consistent equation for $\varphi(\boldsymbol{k})$ is obtained as

$$
\mathcal{Q}(\boldsymbol{k}) = \int_{\boldsymbol{k}_2, \boldsymbol{q}_1, \boldsymbol{q}_2} e^{-\beta \epsilon_{\boldsymbol{k}_2}} \mathcal{W}(\boldsymbol{k}, \boldsymbol{k}_2 | \boldsymbol{q}_1, \boldsymbol{q}_2) \Big[\varphi(\boldsymbol{k}) + \varphi(\boldsymbol{k}_2) - \varphi(\boldsymbol{q}_1) - \varphi(\boldsymbol{q}_2)\Big],
\tag{5.3.18}
$$

and also the leading-order transport coefficient $\sigma_{\mathcal{O}}$ is evaluated from Eq. (5.2.19) as

$$\sigma_{\mathcal{O}} = 2\beta \int_{\boldsymbol{k}} e^{-\beta\epsilon_{\boldsymbol{k}}} \mathcal{Q}(\boldsymbol{k})\varphi(\boldsymbol{k}). \tag{5.3.19}$$

Eq. (5.3.18) is nothing other than the linearized Boltzmann equation, as detailed in Chapter 2 [Eqs. (2.3.59) and (2.3.60)]. Eq. (5.3.19) also corresponds to Eqs. (2.3.64) and (2.3.65), which provide the shear viscosity and the thermal conductivity in the kinetic theory. Therefore, for the transport coefficient $\sigma_{\mathcal{O}}$ in the high-temperature limit, the microscopic calculation agrees with the kinetic one without approximation, such as the relaxation-time approximation or the approximation to the memory function.

5.4   Numerical results

5.4.1   Shear viscosity

For the shear viscosity, we set $\mathcal{Q}(\boldsymbol{k}) = \pi_{xy}(\boldsymbol{k})$. Then, the linearized Boltzmann equation can be solved by expanding $\varphi(\boldsymbol{k})$ with the generalized Laguerre polynomials:

$$\varphi(\boldsymbol{k}) = \beta\pi_{xy}(\boldsymbol{k}) \sum_{n=0}^{N} c_n^{(\eta)} L_n^{(d+2)/2}(\beta\epsilon_{\boldsymbol{k}}). \tag{5.4.1}$$

In the simplest case of truncation at $N = 0$, known as the relaxation-time approximation, we find $\varphi(\boldsymbol{k}) = z\tau_\eta \pi_{xy}(\boldsymbol{k})$ with the relaxation time for the shear viscosity,

$$(z\tau_\eta)^{-1} = \frac{\pi\beta^2}{\Gamma(d/2)\Gamma(2+d/2)} \left(\frac{m}{2\sqrt{2}\pi}\right)^d \int_0^\infty \mathrm{d}\varepsilon \, e^{-\beta\varepsilon} \varepsilon^d |\mathcal{T}_a(\varepsilon - i0^+)|^2. \tag{5.4.2}$$

We also find the shear viscosity in the relaxation-time approximation,

$$\lambda_T^d \eta = \frac{2}{\beta} z\tau_\eta = \begin{cases} \dfrac{2}{\pi} \left[\displaystyle\int_0^\infty \mathrm{d}x \, e^{-x} \dfrac{x^2}{[\ln(x\tilde{a}^2 s)]^2 + \pi^2} \right]^{-1} & d = 2, \\[3ex] \dfrac{15\pi}{4\sqrt{2}} \left[\displaystyle\int_0^\infty \mathrm{d}x \, e^{-x} \dfrac{x^3}{x + \tilde{a}^{-2}} \right]^{-1} & d = 3, \end{cases} \tag{5.4.3}$$

where $\tilde{a}$ is the dimensionless scattering length $\tilde{a} \equiv \sqrt{m/\beta}a$. These results agree with Eq. (5.1.8), which is obtained from the memory function method [89, 91]. Therefore, the memory function method, i.e., taking the Drude form of Eq. (5.1.5) and the memory function of Eq. (5.1.7), is equivalent to the relaxation-time approximation, or more microscopically, to approximating the vertex function as

$$\frac{\Gamma_{\mathrm{RA}}(\boldsymbol{k})}{-2z\,\mathrm{Im}[\Sigma_{\mathrm{on\text{-}shell}}^{\mathrm{R}}(\boldsymbol{k})]} = \tau_\eta \pi_{xy}(\boldsymbol{k}). \tag{5.4.4}$$

The results of the shear viscosity in the high-temperature limit are plotted in Fig. 5.4.
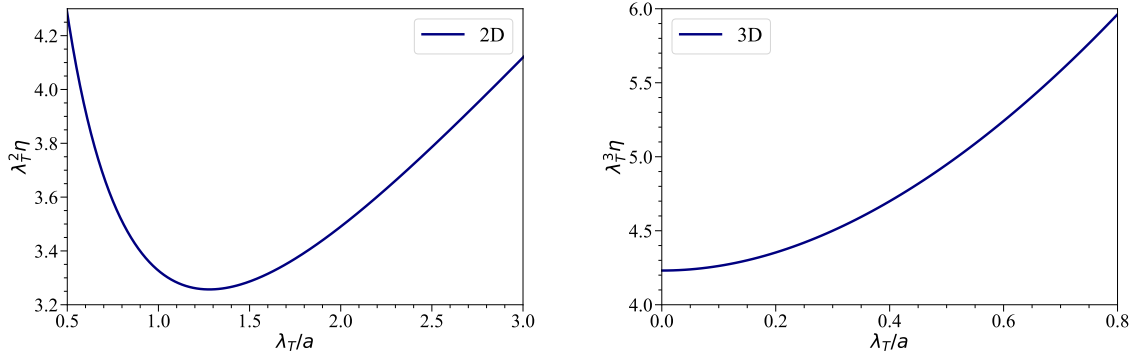
Figure 5.4: The shear viscosity in the high-temperature limit as a function of λ_T/a in the form of $\lambda_T^d \eta$ for $d = 2$ (left) and $d = 3$ (right). These results are computed from the solution using the expansion (5.4.1). In three dimensions, the shear viscosity is an even function of the scattering length. For example, when $\lambda_T/a = 0$ in three dimensions, the normalized shear viscosity in the high-temperature limit is $\lambda_T^3 \eta = 4.165$ in the relaxation time approximation and $\lambda_T^3 \eta = 4.231$ in the exact computation.

5.4.2 Thermal conductivity

For the thermal conductivity, we set $\mathcal{Q}(\boldsymbol{k}) = j_x^q(\boldsymbol{k})$. Then, the linearized Boltzmann equation can be solved by expanding $\varphi(\boldsymbol{k})$ with the generalized Laguerre polynomials again:[3]

$$\varphi(\boldsymbol{k}) = \frac{k_i}{m} \sum_{n=1}^{N} c_n^{(\kappa)} L_n^{d/2}(\beta \epsilon_{\boldsymbol{k}}). \tag{5.4.5}$$

In the simplest case of truncation at $N = 1$, known as the relaxation-time approximation, we find $\varphi(\boldsymbol{k}) = z \tau_\kappa j_i^q(\boldsymbol{k})$ with the relaxation time for the thermal conductivity,

$$(z\tau_\kappa)^{-1} = \frac{d-1}{d}(z\tau_\eta)^{-1}. \tag{5.4.6}$$

Thus, the thermal conductivity in the relaxation-time approximation is given by

$$\lambda_T^d m \kappa = \frac{d+2}{\beta} z \tau_\kappa = \begin{cases} \dfrac{8}{\pi} \left[\displaystyle\int_0^\infty ds \, \frac{e^{-s} s^2}{\ln(\tilde{a}^2 s) + \pi^2} \right]^{-1} & d = 2, \\[6mm] \dfrac{225\pi}{16\sqrt{2}} \left[\displaystyle\int_0^\infty ds \, \frac{e^{-s} s^3}{s + \tilde{a}^{-2}} \right]^{-1} & d = 3. \end{cases} \tag{5.4.7}$$

These results agree with the computations in the kinetic theory [71] and also agree with the results in the unitarity limit using the memory function method [93]. The results of the thermal conductivity in the high-temperature limit are plotted in Fig. 5.5

The ratio of the shear viscosity to the thermal conductivity is known as the Prandtl number,

$$\mathrm{Pr} \equiv \frac{\eta}{\kappa} \frac{c_\mathcal{P}}{mn}, \tag{5.4.8}$$

---

[3]The bare vertex $j_x^q(\boldsymbol{k})$ is represented by the generalized Laguerre polynomial as $\beta m j_x^q(\boldsymbol{k}) = -k_x L_1^{d/2}(\beta \epsilon_{\boldsymbol{k}})$ because of $\beta(\mathcal{E} + \mathcal{P})/n = (d+2)/2$ in the high-temperature limit. For this reason, the expansion starts at $n = 1$, not $n = 0$. This is consistent with the matching condition (2.3.35) for the equilibrium distribution in the kinetic computation.
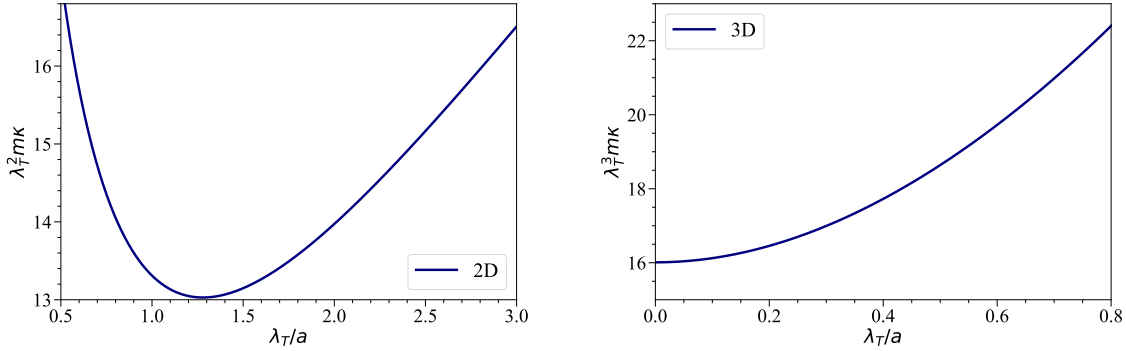
Figure 5.5: The thermal conductivity in the high-temperature limit as a function of λ_T/a in the form of $\lambda_T^d m\kappa$ for $d = 2$ (left) and $d = 3$ (right). These results are computed from the solution using the expansion Eq. (5.4.5). In three dimensions, the termal conductivity is an even function of the scattering length. For example, when $\lambda_T/a = 0$ in three dimensions, the normalized thermal conductivity in the high-temperature limit is $\lambda_T^3 m\kappa = 15.62$ in the relaxation time approximation and $\lambda_T^3 m\kappa = 16.01$ in the exact computation.

where $c_{\mathcal{P}}$ is the specific heat at constant pressure. The Prandtl number quantifies the relative importance of the shear viscosity to the thermal conductivity. This quantity appears in sound attenuation in a fluid [97], and was measured in ultracold atoms experiment [124]. In the the relaxation-time approximation, the Prandtl number Pr in the high-temperature limit is given by $\mathrm{Pr} = (d-1)/d$ because of $c_{\mathcal{P}} = (d+2)n/2$, and is independent of the scattering length. However, the Prandtl number computed with Eqs. (5.4.1) and (5.4.5) depends slightly on the scattering length, as plotted in Fig. 5.6.

5.5 Summary

In this chapter, we presented exact nonperturbative results for the shear viscosity and the thermal conductivity of the resonant Fermi gas in the high-temperature limit. We confirmed that the singular product (5.2.5) has the inverse power of the fugacity and derived the self-consistent equation of the vertex function in the high-temperature limit. Our results are Eqs. (5.3.15), (5.3.18), and (5.3.19). The only vertex function required for the transport coefficient in the high-temperature limit is $\Gamma_{\mathrm{RA}}(\boldsymbol{k})$. Then, the function $\varphi(\boldsymbol{k})$ is defined from $\Gamma_{\mathrm{RA}}(\boldsymbol{k})$ via Eq. (5.3.15) and obeys the linearized Boltzmann equation (5.3.18). The transport coefficient is provided by $\varphi(\boldsymbol{k})$ via Eq. (5.3.19). The kinetic theory entirely describes the shear viscosity and the thermal conductivity in the high-temperature limit. Our results provide a direct derivation of the kinetic theory in the quantum virial expansion. The linearized Boltzmann equation is understood as the leading-order equation obtained by applying the analytic continuations (5.3.4) to the self-consistent equation for the vertex function, which is represented diagrammatically in Fig. 5.3.

In Sec. 5.4, we computed the shear viscosity and the thermal conductivity in the high-temperature limit by solving the derived self-consistent equation, i.e., the linearized Boltzmann equation. Our results for the shear viscosity and the thermal conductivity are plotted
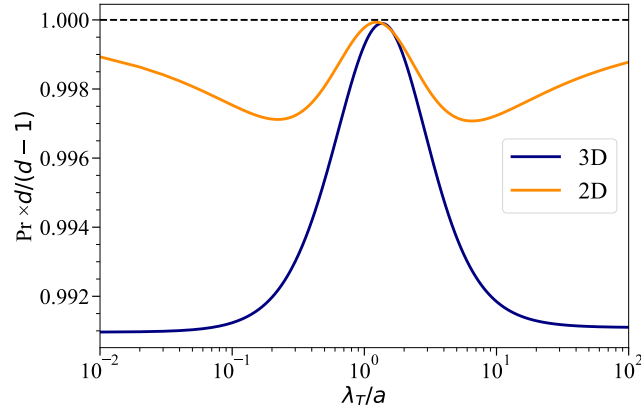
Figure 5.6: The rescaled Prandtl number $\mathrm{Pr} \times d/(d-1)$ as a function of λ_T/a computed from the results in Figs. 5.4 and 5.5.

in Figs. 5.4 and 5.5. The Prandtl number, which is the ratio of them, is plotted in Fig. 5.6. The thermal conductivity in two dimensions is a novel result of our work.

Chapter 6

Summary and prospects

Summary

In this thesis, we theoretically studied two-component Fermi gases near the two-body resonance in two and three dimensions, which are referred to as the resonant Fermi gases. The resonant Fermi gas is realized by taking advantage of the high tunability of ultracold atoms and exhibits universal behavior independent of the details of its interparticle interaction. To understand the universal nature of the transport properties, we investigated their transport coefficients, i.e., the bulk viscosity, the shear viscosity, and the thermal conductivity, for an arbitrary scattering length.

Chapter 2 was devoted to the review for studying the transport properties of the resonant Fermi gases. We first explained that the interparticle interaction is characterized only by the s-wave scattering length a at low energies. This property is the key of the universality of the resonant Fermi gas. Namely, the systems with different interaction potentials behave in the same way at low energies as long as the scattering lengths are the same. We then introduced the contact interaction model to describe the universal behavior of the resonant Fermi gas. Also, we derived the Kubo formula to calculate the transport coefficients and reviewed the kinetic theory, which is one of the approaches to calculate the transport coefficients in the high-temperature limit.

In Chapter 3, we focused on the bulk viscosity, which characterizes the dissipation caused by an expansion and contraction of the fluid volume. It was shown that the bulk viscosity vanishes in the unitarity limit because of no interaction scales [49]. The vanishing bulk viscosity at unitarity is intuitively understood because the entropy is not produced during an isotropic expansion due to no intrinsic scales in the interaction. In order to extend this understanding to the case where the scattering length is finite and investigate the bulk viscosity at finite scattering length, we constructed hydrodynamics with a spacetime-dependent scattering length. Because the scattering length can be tuned by applying an external magnetic field via the Feshbach resonance in ultracold atoms, one can realize the spacetime-dependent scattering length by modulating the applied magnetic field over spacetime. We showed that the spacetime-dependent scattering length not only appears explicitly as an external source of the momentum and energy continuity equations [Eqs. (3.2.3) and (3.2.4)], but also enters the constitutive relations through the modified bulk strain rate tensor [Eq. (3.2.25)] in both normal and superfluid phases. We also found the dependence of the bulk viscosity on the

scattering length near the free limit $|a| \to 0$ [Eqs. (3.2.28) and (3.3.31)] and near the unitarity limit $|a| \to \infty$ [Eqs. (3.2.29) and (3.3.32)]. The expression of the modified bulk strain rate tensor can be intuitively understood from the equivalence between the expansion (contraction) of the fluid volume and the contraction (expansion) of the scattering length because of no interaction scale other than the scattering length. This intuitive understanding of the modified bulk strain rate tensor provides an extension of the understanding of the vanishing bulk viscosity at unitarity to the case where the scattering length is finite. We can derive the modified bulk strain rate tensor from another method using the conformal symmetry, as discussed in Appendix B. This symmetry-based derivation supports the equivalence between the expansion (contraction) of the fluid volume and the contraction (expansion) of the scattering length.

The modified bulk strain rate tensor indicates that the dissipation proportional to the bulk viscosity can be induced through the modulated scattering length. As one of the applications of our hydrodynamics, we considered the time-dependent scattering length in a uniform system and showed that the dissipation proportional to the bulk viscosity appears in the contact density [Eq. (3.4.1)], the energy density [Eq. (3.4.2)], and the entropy density [Eq. (3.4.3)]. These results may be useful as a novel probe to measure the bulk viscosity. In particular, in the unitarity limit, the bulk viscosity ζ itself vanishes, but ζa^2 is supposed to be finite, and our results may also be useful for its measurement [Eq. (3.4.5)]. As discussed in Chapter 4, the bulk viscosity is expressed with the contact-contact response function [Eq. (4.2.9)]. The bulk viscosity is considered to capture the pair fluctuations and to have a strong signature at the superfluid phase transition driven by the pair fluctuations because the contact density $\hat{\mathcal{C}}(t, \boldsymbol{x})$ can be interpreted as the density of the fermion pair field $\hat{\Delta}(t, \boldsymbol{x})$: $\hat{\mathcal{C}}(t, \boldsymbol{x}) = \hat{\Delta}^\dagger(t, \boldsymbol{x})\hat{\Delta}(t, \boldsymbol{x})$ with $\hat{\Delta}(t, \boldsymbol{x}) = mg\hat{\psi}_\downarrow(t, \boldsymbol{x})\hat{\psi}_\uparrow(t, \boldsymbol{x})$ [90]. Therefore, the measurement of the bulk viscosity may provide valuable information about the pair fluctuations.

Chapters 4 and 5 were devoted to calculating the transport coefficients in the high-temperature regime, where $n\lambda_T^d \ll 1$ holds for the particle number density n and the thermal de Broglie wavelength $\lambda_T = \sqrt{2\pi/(mT)}$. In the high-temperature regime, the fugacity is small $z = e^{\mu/T} \ll 1$, so that the expansion in terms of the fugacity is valid. This expansion, referred to as the quantum virial expansion, is used as a non-perturbative method, which is applied to the strongly correlated regime, such as the unitarity limit [88]. In Chapter 4, we expressed the Kubo formula for the bulk viscosity with the contact-contact response function [Eq. (4.2.9)], and derived Eqs. (3.4.1)–(3.4.3) from the linear response theory [Eqs. (4.2.18)–(4.2.20)]. We then reviewed the calculation of the bulk viscosity via the Kubo formula in the quantum virial expansion [89–91]. The bulk viscosity calculated from the quantum virial expansion does not fully agree with that from the kinetic theory [74,75]. We pointed out that the reason for the discrepancy is the breakdown of the quasiparticle approximation, which is the basis of the kinetic theory.

On the other hand, for the shear viscosity and the thermal conductivity, the following two computational methods are known to provide the same results: the quantum virial expansion with resummation by the memory function method [39, 89, 91, 93] and the kinetic theory in the relaxation-time approximation [69–73]. To understand these coincidences, we directly derived the linearized Boltzmann equation in the quantum virial expansion in Chapter 5. Our derivation proves the agreement between the quantum virial expansion and the kinetic

theory in the high-temperature limit without any approximation. We confirmed the pinch singularity [Eq. (5.2.5)], which is the origin of the need for the resummation, and showed that the self-consistent equation of the vertex function is identical to the linearized Boltzmann equation in the high-temperature limit. Our method provides the exact transport coefficients in the high-temperature limit from the microscopic theory. We then computed the shear viscosity and the thermal conductivity in the high-temperature limit [Figs. 5.4 and 5.5]. We also computed the Prandtl number, which is defined from their ratio, and found that it slightly depends on the scattering length [Fig. 5.6].

Prospects

There are several interesting prospects for our studies. For example, it is interesting to investigate the flow induced by the spacetime-dependent scattering length using the hydrodynamics constructed in Chapter 3. In Chapter 3, we considered the application to a uniform system with a temporally modulated scattering length as a simple case, where the fluid velocity does not arise. An interesting flow may be found from the hydrodynamic approach by setting the scattering length to a specific configuration. From microscopic approaches, it was proposed that several intriguing phenomena can be realized by arranging the spacetime-dependent scattering length with specific configurations [125–135].

As another prospect, it is an important task to elaborate on the quantum virial expansion of the bulk viscosity multiplied by the square of the scattering length in the unitarity limit. The bulk viscosity obtained in the quantum virial expansion [Eq. (4.2.36)] is singular in the unitarity limit. It is necessary to resum higher-order corrections to obtain the expansion for the bulk viscosity in the unitarity limit. Although this resummation was achieved numerically [90], the origin of the divergence is not fully understood, and a systematic resummation method is not established. It is essential to identify the singularity that causes the divergence and to formulate a systematic expansion that incorporates the terms yielding the singularity.

As a further development of the quantum virial expansion, it is worthwhile to formulate the expansion in the real-time formalism [136] instead of the Matsubara formalism. In Chapter 5, we employed the Matsubara formalism to take advantage of the established quantum virial expansion, where the analytic continuations are unavoidable. In the real-time formalism, we can directly find the singular product that leads to the pinch singularity without the analytic continuations [123]. In addition, the derivation of the kinetic theory itself, rather than the linearized one, was achieved in the real-time formalism in the weak coupling limit [137]. It is also useful to formulate the quantum virial expansion in the real-time formalism for understanding more general non-equilibrium transport phenomena.

Thanks to their universality, the studies of the resonant Fermi gases can be applied to various systems which satisfies the following condition:

$$r_{\mathrm{R}} \quad \ll \quad n^{-1/d}, \quad \lambda_T, \quad |a|,$$

where r_{R} is the radius of the interparticle interaction potential. In ultracold atoms, the gases meet this condition by their high tunability, whereas there are systems in which this condition is naturally satisfied [8,9]. For example, in dilute nuclear matter, the neutron-neutron s-wave scattering length $a \simeq -18.5$ fm is larger than the radius $r_{\mathrm{R}} < 1$ fm [138]. Thus, the resonant Fermi gas can be regarded as an idealization of dilute nuclear matter and may be relevant

to the physics of neutron stars [139]. Understanding the inside of neutron stars is one of the important problems in nuclear physics, and the studies of the resonant Fermi gases may be useful for this problem. We hope that the studies of the resonant Fermi gases will provide valuable insights into strongly correlated Fermi systems and facilitate the understanding of systems linked by the universality.

Appendix A

Symmetries of resonant Fermi gases

In this appendix, we review symmetries of the resonant Fermi gas. We introduce the Galilean symmetry, the nonrelativistic conformal symmetry, and hidden symmetries that correspond to their extensions. In Sec. A.1, we review a symmetry group of the Schrödinger equation for a nonrelativistic spinless free particle, which is referred to as the Schrödinger group [140,141], including the Galilean boost and the conformal transformation. We also confirm that the system exhibits the conformal invariance in the unitarity limit [25–27]. In Sec. A.2, we review hidden symmetries of the resonant Fermi gas: the nonrelativistic general coordinate invariance and the conformal invariance [26]. These symmetries are the extensions of the Galilean and conformal symmetries. Sec. A.3 is devoted to the summary.

The discussion in this appendix is based mainly on Refs. [140,141] in Sec. A.1 and Ref. [26] in Sec. A.2.

A.1   Schrödinger group

We consider a non-relativistic system whose action is given by

$$
\begin{aligned}
S[\psi_\sigma, \psi_\sigma^\dagger] &= S_0[\psi_\sigma, \psi_\sigma^\dagger] + S_{\text{int}}[\psi_\sigma, \psi_\sigma^\dagger] \\
&= \int \mathrm{d}t \mathrm{d}\boldsymbol{x}\, \mathcal{L}_0(t, \boldsymbol{x}) + \int \mathrm{d}t \mathrm{d}\boldsymbol{x}\, \mathcal{L}_{\text{int}}(t, \boldsymbol{x}),
\end{aligned}
\tag{A.1.1}
$$

where $\mathcal{L}_0(t, \boldsymbol{x})$ and $\mathcal{L}_{\text{int}}(t, \boldsymbol{x})$ are the kinetic and interaction terms of the Lagrangian density, respectively:

$$
\mathcal{L}_0(t, \boldsymbol{x}) = \sum_{\sigma=\uparrow,\downarrow} \left[i\psi_\sigma^\dagger(t, \boldsymbol{x}) \overset{\leftrightarrow}{\partial_t} \psi_\sigma(t, \boldsymbol{x}) - \frac{[\partial_i \psi_\sigma(t, \boldsymbol{x})]^\dagger [\partial_i \psi_\sigma(t, \boldsymbol{x})]}{2m} \right],
\tag{A.1.2}
$$

$$
\mathcal{L}_{\text{int}}(t, \boldsymbol{x}) = -\frac{1}{2} \sum_{\sigma,\tau} \int \mathrm{d}\boldsymbol{y}\, \psi_\sigma^\dagger(t, \boldsymbol{x})\psi_\tau^\dagger(t, \boldsymbol{y})V(|\boldsymbol{x}-\boldsymbol{y}|)\psi_\tau(t, \boldsymbol{y})\psi_\sigma(t, \boldsymbol{x}).
\tag{A.1.3}
$$

Here, $\psi_\sigma(t, \boldsymbol{x})$ is a spin-1/2 fermion field with its mass m and $V(|\boldsymbol{x}-\boldsymbol{y}|)$ is an interparticle potential.[1] We employ the Lagrangian formalism rather than the Hamiltonian formalism for symmetry discussions and review the symmetries of this action. In particular, when the

---

[1]For the discussion of the symmetries, we take the interaction potential to be a general one, rather than a simplified contact interaction.

interaction potential $V(|\boldsymbol{x}-\boldsymbol{y}|)$ is scale invariant [see Eq. (A.1.24)], the action has a symmetry group referred to as the Schrödinger group [140, 141]. The conformal symmetry is one of the most important properties of the unitary Fermi gas.

A.1.1   U(1) phase and SU(2) spin rotation

Evidently, this action is invariant under the U(1) phase and SU(2) spin rotations,

$$\psi_\sigma(t, \boldsymbol{x}) \;\to\; \psi_\sigma'(t, \boldsymbol{x}) = e^{i\chi} \sum_\tau S_{\sigma\tau} \psi_\tau(t, \boldsymbol{x}), \tag{A.1.4}$$

with $e^{i\chi} \in \mathrm{U}(1)$ and $S_{\sigma\tau} \in \mathrm{SU}(2)$.

The infinitesimal transformation for the U(1) phase rotation is given by

$$\delta\psi_\sigma(t, \boldsymbol{x}) \equiv \psi_\sigma'(t, \boldsymbol{x}) - \psi_\sigma(t, \boldsymbol{x}) = i\chi\psi_\sigma(t, \boldsymbol{x}). \tag{A.1.5}$$

Its operator counterpart can be represented as

$$\delta\hat{\psi}_\sigma(t, \boldsymbol{x}) = -i\chi[\hat{M}/m, \, \hat{\psi}_\sigma(t, \boldsymbol{x})], \tag{A.1.6}$$

where the generator $\hat{M}$ is found to be the mass operator,

$$\hat{M} = \int \mathrm{d}\boldsymbol{x} \, \hat{\mathcal{M}}(t, \boldsymbol{x}), \qquad \hat{\mathcal{M}}(t, \boldsymbol{x}) \equiv m \sum_\sigma \hat{\psi}_\sigma^\dagger(t, \boldsymbol{x}) \hat{\psi}_\sigma(t, \boldsymbol{x}), \tag{A.1.7}$$

with the mass density operator $\hat{\mathcal{M}}(t, \boldsymbol{x})$. Here, the operator $\hat{\psi}_\sigma(t, \boldsymbol{x})$ obeys the canonical anti-commutation relations,

$$\begin{aligned} \{\hat{\psi}_\sigma(t, \boldsymbol{x}), \, \hat{\psi}_\tau^\dagger(t, \boldsymbol{y})\} &= \delta_{\sigma\tau}\delta^d(\boldsymbol{x} - \boldsymbol{y}), \\ \{\hat{\psi}_\sigma(t, \boldsymbol{x}), \, \hat{\psi}_\tau(t, \boldsymbol{y})\} &= \{\hat{\psi}_\sigma^\dagger(t, \boldsymbol{x}), \, \hat{\psi}_\tau^\dagger(t, \boldsymbol{y})\} = 0. \end{aligned} \tag{A.1.8}$$

A.1.2   Spacetime translation and spatial rotaion

As obvious spacetime symmetries, the action is invariant under the spacetime translation and the spatial rotation,

$$\psi_\sigma(t, \boldsymbol{x}) \;\to\; \psi_\sigma'(t, \boldsymbol{x}) = \psi_\sigma(t - \xi_0, \boldsymbol{x} - \boldsymbol{\xi}), \tag{A.1.9}$$

$$\psi_\sigma(t, \boldsymbol{x}) \;\to\; \partial_i\psi_\sigma'(t, \boldsymbol{x}) = \psi_\sigma(t, R^{-1}\boldsymbol{x}), \tag{A.1.10}$$

with $R \in \mathrm{SO}(d)$. As in the case of the U(1) rotation, the generators of the transformations can be found to be the Hamiltonian $\hat{H}$ for the time translation, the momentum $\hat{P}_i$ for the spatial translation, and the angular momentum $\hat{M}_{ij}$ for the spatial rotation:

$$\begin{aligned} \hat{H} = {}&\sum_\sigma \int \mathrm{d}\boldsymbol{x} \, \frac{[\partial_i\hat{\psi}_\sigma(t, \boldsymbol{x})]^\dagger[\partial_i\hat{\psi}_\sigma(t, \boldsymbol{x})]}{2m} \\ &+ \frac{1}{2}\sum_{\sigma,\tau} \int \mathrm{d}\boldsymbol{x}\mathrm{d}\boldsymbol{y} \, \hat{\psi}_\sigma^\dagger(t, \boldsymbol{x})\hat{\psi}_\tau^\dagger(t, \boldsymbol{y})V(|\boldsymbol{x} - \boldsymbol{y}|)\hat{\psi}_\tau(t, \boldsymbol{y})\hat{\psi}_\sigma(t, \boldsymbol{x}), \end{aligned} \tag{A.1.11}$$

$$\hat{P}_i = \int \mathrm{d}\boldsymbol{x} \, \hat{\mathcal{J}}_i(t, \boldsymbol{x}), \tag{A.1.12}$$

$$\hat{M}_{ij} = \int \mathrm{d}\boldsymbol{x} \left[x_i\hat{\mathcal{J}}_j(t, \boldsymbol{x}) - x_j\hat{\mathcal{J}}_i(t, \boldsymbol{x}) \right], \tag{A.1.13}$$

where $\hat{\mathcal{J}}_i(t, \boldsymbol{x})$ is the momentum density operator,

$$\hat{\mathcal{J}}_i(t, \boldsymbol{x}) \equiv -i \sum_\sigma \hat{\psi}_\sigma^\dagger(t, \boldsymbol{x}) \overleftrightarrow{\partial_i} \hat{\psi}_\sigma(t, \boldsymbol{x}). \tag{A.1.14}$$

In three dimensions, the dual operator $\hat{L}_i \equiv \frac{1}{2}\epsilon_{ijk}\hat{M}_{jk}$ corresponds to the well-known angular momentum operator, where ϵ_{ijk} is the antisymmetric tensor: $\epsilon_{123} = +1$.

A.1.3   Galilean transformation

Due to the form of the kinetic term $\mathcal{L}_0(t, \boldsymbol{x})$, the action is invariant under the following Galilean transformation:

$$\psi_\sigma(t, \boldsymbol{x}) \;\rightarrow\; \psi_\sigma'(t, \boldsymbol{x}) = e^{-i\frac{m}{2}\boldsymbol{V}^2 t + im\boldsymbol{V}\cdot\boldsymbol{x}} \psi_\sigma(t, \boldsymbol{x} - \boldsymbol{V}t), \tag{A.1.15}$$

which involves the phase factor $e^{-i\frac{m}{2}\boldsymbol{V}^2 t + im\boldsymbol{V}\cdot\boldsymbol{x}}$ in addition to the spatial translation $\boldsymbol{x} \to \boldsymbol{x} - \boldsymbol{V}t$. The Galilean invariance implies a relation between the U(1) symmetry and the spatial translation symmetry, which equates the mass flux with the momentum density.[2]

The infinitesimal transformation is given by

$$\delta\psi_\sigma(t, \boldsymbol{x}) = V_i \left[imx_i - t\partial_i\right] \psi_\sigma(t, \boldsymbol{x}), \tag{A.1.16}$$

and its operator counterpart is provided by

$$\delta\hat{\psi}_\sigma(t, \boldsymbol{x}) = -iV_i[\hat{K}_i(t) - t\hat{P}_i, \; \hat{\psi}_\sigma(t, \boldsymbol{x})], \tag{A.1.17}$$

where the operator $\hat{K}_i(t)$ is found to be

$$\hat{K}_i(t) = \int d\boldsymbol{x}\, x_i \hat{\mathcal{M}}(t, \boldsymbol{x}). \tag{A.1.18}$$

Although $\hat{K}_i(t)$ is not commutative with the Hamiltonian and is time-dependent,

$$[\hat{K}_i(t), \; \hat{H}] = i\hat{P}_i, \tag{A.1.19}$$

the generator itself does not depend on time,

$$i\frac{d}{dt}\left(\hat{K}_i(t) - t\hat{P}_i\right) = [\hat{K}_i(t) - t\hat{P}_i, \; \hat{H}] + i\frac{\partial}{\partial t}\left(\hat{K}_i(t) - t\hat{P}_i\right) = 0, \tag{A.1.20}$$

where the partial derivative acts on the time dependence of the operator $\hat{K}_i(t) - t\hat{P}_i$ in the Schrödinger picture. Here, $\hat{K}_i(t)$ physically stands for the center-of-mass coordinates, and the conservation of $\hat{K}_i(t) - t\hat{P}_i$ means Newton's first law of motion, i.e., the center-of-mass remains in motion with a constant momentum in nonrelativistic systems without external forces.

---

[2]Let J_μ be the Noether current of the mass conservation $\partial_\mu J_\mu = 0$ due to the U(1) symmetry and $T_{\mu i}$ be the Noether current of the momentum conservation $\partial_\mu T_{\mu i} = 0$ due to the spatial translation symmetry. Then, the Noether current derived from the Galilean symmetry is given as $J_\mu x_i - tT_{\mu i}$, and its conservation leads to $0 = \partial_\mu[J_\mu x_i - tT_{\mu i}] = J_i - T_{0i}$.

A.1.4 Scale transformation

Since the kinetic term $\mathcal{L}_0(t, \boldsymbol{x})$ has a first-order time derivative and a second-order spatial derivative, it is invariant under the following scale transformation:

$$
\begin{aligned}
t \;\to\; t' = e^{-2\lambda}t, \qquad \boldsymbol{x} \;\to\; \boldsymbol{x}' = e^{-\lambda}\boldsymbol{x}, \\
\psi_\sigma(t, \boldsymbol{x}) \;\to\; \psi'_\sigma(t', \boldsymbol{x}') = e^{\frac{d}{2}\lambda}\psi_\sigma(t, \boldsymbol{x}).
\end{aligned}
\tag{A.1.21}
$$

Under the scale transformation, the interaction term is transformed into

$$
\begin{aligned}
S_{\mathrm{int}}[\psi_\sigma, \psi_\sigma^\dagger] &\to S_{\mathrm{int}}[\psi'_\sigma, \psi'^\dagger_\sigma] \\
&= -\frac{1}{2}\sum_{\sigma,\tau}\int \mathrm{d}t\mathrm{d}\boldsymbol{x}\mathrm{d}\boldsymbol{y}\, e^{2d\lambda}\psi_\sigma^\dagger(e^{2\lambda}t, e^{\lambda}\boldsymbol{x})\psi_\tau^\dagger(e^{2\lambda}t, e^{\lambda}\boldsymbol{y}) \\
&\qquad \times V(|\boldsymbol{x}-\boldsymbol{y}|)\psi_\tau(e^{2\lambda}t, e^{\lambda}\boldsymbol{y})\psi_\sigma(e^{2\lambda}t, e^{\lambda}\boldsymbol{x}) \\
&= -\frac{1}{2}\sum_{\sigma,\tau}\int \mathrm{d}\tilde{t}\mathrm{d}\tilde{\boldsymbol{x}}\mathrm{d}\tilde{\boldsymbol{y}}\, e^{-2\lambda}\psi_\sigma^\dagger(\tilde{t}, \tilde{\boldsymbol{x}})\psi_\tau^\dagger(\tilde{t}, \tilde{\boldsymbol{y}})V(e^{-\lambda}|\tilde{\boldsymbol{x}}-\tilde{\boldsymbol{y}}|)\psi_\tau(\tilde{t}, \tilde{\boldsymbol{y}})\psi_\sigma(\tilde{t}, \tilde{\boldsymbol{x}}),
\end{aligned}
\tag{A.1.22}
$$

with

$$
\tilde{t} = e^{2\lambda}t, \qquad \tilde{\boldsymbol{x}} = e^{\lambda}\boldsymbol{x}, \qquad \tilde{\boldsymbol{y}} = e^{\lambda}\boldsymbol{y}.
\tag{A.1.23}
$$

Therefore, the interaction term is scale invariant if the interparticle interaction potential satisfies

$$
V(r) = e^{-2\lambda}V(e^{-\lambda}r).
\tag{A.1.24}
$$

This condition is trivially satisfied in a free particle system ($V = 0$), an inverse squared potential system ($V \propto r^{-2}$), and a two-dimensional contact interaction system ($V \propto \delta^2(r)$). Note that the two-dimensional contact interaction potential is classically scale invariant, but is not quantum-mechanically because of a scale anomaly. At unitarity, the interaction potential does not satisfy the condition (A.1.24) and is not invariant under the scale transformation. However, the scattering length is transformed as

$$
a \;\to\; a' = e^{\lambda}a
\tag{A.1.25}
$$

under the scale transformation because it is a length scale. From this transformation law, the infinite scattering length remains infinite under the scale transformation. In other words, the unitarity limit is maintained under the scale transformation. As long as the low-energy physics where only the scattering length is relevant is concerned, the system at unitarity can be considered to be scale invariant.[3]

The infinitesimal transformation of Eq. (A.1.21) is given by

$$
\delta\psi_\sigma(t, \boldsymbol{x}) = \lambda\left(\frac{d}{2} + x_i\partial_i + 2t\partial_t\right)\psi_\sigma(t, \boldsymbol{x}).
\tag{A.1.26}
$$

---

[3]The discussion here only guarantees that the two-body subsystem of the unitary Fermi gas is scale invariant, but does not guarantee that three- or more-body subsystems do not have a length scale. There may be three- or many-body bound states, for example, due to the quantum effect known as the Efimov effect [142]. In the unitary Fermi gas, the breaking of the scale invariance has not been found and is considered to be strictly scale invariant.

Its operator counterpart is provided by

$$\delta\hat{\psi}_\sigma(t, \boldsymbol{x}) = -i\lambda\left[\hat{D}(t) - 2t\hat{H},\ \hat{\psi}_\sigma(t, \boldsymbol{x})\right], \tag{A.1.27}$$

where the operator $\hat{D}(t)$ is found to be

$$\hat{D}(t) = \int \mathrm{d}\boldsymbol{x}\, x_i \hat{\mathcal{J}}_i(t, \boldsymbol{x}). \tag{A.1.28}$$

The generator $\hat{D}(t) - 2t\hat{H}$ is time-independent, but the operator $\hat{D}(t)$ is not commutative with the Hamiltonian:

$$[\hat{D}(t),\ \hat{H}] = 2i\hat{H}. \tag{A.1.29}$$

This commutation relation indicates the condition for the trace of the stress tensor:

$$2\hat{H} = -i[\hat{D}(t),\ \hat{H}] = \partial_t\hat{D}(t) = \int \mathrm{d}\boldsymbol{x}\, x_i\partial_t\hat{\mathcal{J}}_i(t, \boldsymbol{x}) = -\int \mathrm{d}\boldsymbol{x}\, x_i\partial_j\hat{\Pi}_{ij}(t, \boldsymbol{x}) = \int \mathrm{d}\boldsymbol{x}\, \hat{\Pi}_{ii}(t, \boldsymbol{x}), \tag{A.1.30}$$

where the stress tensor operator $\hat{\Pi}_{ij}(t, \boldsymbol{x})$ is introduced via the momentum conservation equation,

$$\partial_t\hat{\mathcal{J}}_i(t, \boldsymbol{x}) + \partial_j\hat{\Pi}_{ij}(t, \boldsymbol{x}) = 0. \tag{A.1.31}$$

A.1.5 Conformal transformation

Scale-invariant nonrelativistic systems are also invariant under the following conformal transformation [140, 141]:

$$t \ \rightarrow \ t' = \frac{t}{1 - ct}, \qquad \boldsymbol{x} \ \rightarrow \ \boldsymbol{x}' = \frac{\boldsymbol{x}}{1 - ct},$$
$$\psi_\sigma(t, \boldsymbol{x}) \ \rightarrow \ \psi'_\sigma(t', \boldsymbol{x}') = (1 - ct)^{d/2} \exp\left[i\frac{c}{1 - ct}\frac{m}{2}|\boldsymbol{x}|^2\right]\psi_\sigma(t, \boldsymbol{x}). \tag{A.1.32}$$

The infinitesimal transformation is given by

$$\delta\psi_\sigma(t, \boldsymbol{x}) = c\left[i\frac{m}{2}|\boldsymbol{x}|^2 - \frac{d}{2}t - tx_i\partial_i - t^2\partial_t\right]\psi_\sigma(t, \boldsymbol{x}), \tag{A.1.33}$$

and its operator counterpart is provided by

$$\delta\hat{\psi}_\sigma(t, \boldsymbol{x}) = -ic[\hat{C}(t) - t\hat{D}(t) + t^2\hat{H},\ \hat{\psi}_\sigma(t, \boldsymbol{x})], \tag{A.1.34}$$

where the operator $\hat{C}(t)$ is found to be

$$\hat{C}(t) = \int \mathrm{d}\boldsymbol{x}\, \frac{1}{2}|\boldsymbol{x}|^2\hat{\mathcal{M}}(t, \boldsymbol{x}). \tag{A.1.35}$$

The operator $\hat{C}(t)$ satisfies

$$[\hat{C}(t), \hat{H}] = i\hat{D}(t) \tag{A.1.36}$$

and the generator $\hat{C}(t) - t\hat{D}(t) + t^2\hat{H}$ is time-independent. This commutation relation is derived as

$$[\hat{C}(t), \hat{H}] = i\partial_t\hat{C}(t) = i\int \mathrm{d}\boldsymbol{x}\, \frac{|\boldsymbol{x}|^2}{2}\partial_t\hat{\mathcal{M}}(t, \boldsymbol{x}) = -i\int \mathrm{d}\boldsymbol{x}\, \frac{|\boldsymbol{x}|^2}{2}\partial_i\hat{\mathcal{J}}_i(t, \boldsymbol{x}) = i\hat{D}(t), \quad \tag{A.1.37}$$

with the mass conservation

$$\partial_t\hat{\mathcal{M}}(t, \boldsymbol{x}) + \partial_i\hat{\mathcal{J}}_i(t, \boldsymbol{x}) = 0. \tag{A.1.38}$$

Therefore, the time-independence of the generator, i.e., the conformal invariance of the system, follows solely from the scale invariance and the mass conservation.

A.1.6   Commutation relations

We summarize the commutation relations of the generators. The following operators form a closed algebra referred to as the Schrödinger algebra [140, 141]: Hamiltonian $\hat{H}$, mass $\hat{M}$, momentum $\hat{P}_i$, angular momentum $\hat{M}_{ij}$, Galilean boost $\hat{K}_i$, scale transformation $\hat{D}$, and conformal transformation $\hat{C}$:

$$[\hat{M}, \hat{H}] = [\hat{M}, \hat{P}_i] = [\hat{M}, \hat{M}_{ij}] = [\hat{M}, \hat{K}_i] = [\hat{M}, \hat{D}] = [\hat{M}, \hat{C}] = 0, \tag{A.1.39}$$

$$[\hat{M}_{ij}, \hat{H}] = [\hat{M}_{ij}, \hat{D}] = [\hat{M}_{ij}, \hat{C}] = 0, \tag{A.1.40}$$

$$[\hat{M}_{ij}, \hat{P}_k] = i(\delta_{ik}\hat{P}_j - \delta_{jk}\hat{P}_i), \tag{A.1.41}$$

$$[\hat{M}_{ij}, \hat{K}_k] = i(\delta_{ik}\hat{K}_j - \delta_{jk}\hat{K}_i), \tag{A.1.42}$$

$$[\hat{M}_{ij}, \hat{M}_{kl}] = i(\delta_{ik}\hat{M}_{jl} - \delta_{il}\hat{M}_{jk} - \delta_{jk}\hat{M}_{il} + \delta_{jl}\hat{M}_{ik}), \tag{A.1.43}$$

where all operators are in the Schrödinger picture.

A \ B	$\hat{H}$	$\hat{D}$	$\hat{C}$	$\hat{P}_j$	$\hat{K}_j$
$\hat{H}$	0	$-2i\hat{H}$	$-i\hat{D}$	0	$-i\hat{P}_j$
$\hat{D}$	$2i\hat{H}$	0	$-2i\hat{C}$	$i\hat{P}_j$	$-i\hat{K}_j$
$\hat{C}$	$i\hat{D}$	$2i\hat{C}$	0	$i\hat{K}_j$	0
$\hat{P}_i$	0	$-i\hat{P}_i$	$-i\hat{K}_i$	0	$-i\delta_{ij}\hat{M}$
$\hat{K}_i$	$i\hat{P}_i$	$i\hat{K}_i$	0	$i\delta_{ij}\hat{M}$	0

Table A.1: Commutation relations: $[A, B]$

In particular, $\hat{H}$, $\hat{D}$, and $\hat{C}$ form a subgroup:

$$[\hat{H}, \hat{D}] = -2i\hat{H}, \quad [\hat{H}, \hat{C}] = -i\hat{D}, \quad [\hat{C}, \hat{D}] = 2i\hat{C}. \tag{A.1.44}$$

With the use of

$$\hat{S}_1 = \frac{1}{2}(\hat{H} + \hat{C}), \quad \hat{S}_2 = \frac{1}{2}(\hat{H} - \hat{C}), \quad \hat{S}_3 = -\frac{1}{2}\hat{D}, \tag{A.1.45}$$

one can see that these operators obey the SO(2, 1) algebra,

$$[\hat{S}_1, \hat{S}_2] = -i\hat{S}_3, \quad [\hat{S}_2, \hat{S}_3] = i\hat{S}_1, \quad [\hat{S}_3, \hat{S}_1] = -i\hat{S}_2. \tag{A.1.46}$$

A.2   Nonrelativistic diffeomorphism

We discussed the symmetries of the action (A.1.1), especially, the Schrödinger group that emerges at unitarity. The action (A.1.1) has hidden symmetries that correspond to an extension of the Schrödinger group [26].

A.2.1 Resonant Fermi gases in curved space

To discuss the hidden symmetries, we promote the global symmetries to their local counterparts by coupling the action to an external U(1) gauge field $A_\mu(t, \boldsymbol{x})$ and a metric $g_{ij}(t, \boldsymbol{x})$ as external fields. The metric $g_{ij}(t, \boldsymbol{x})$ provides the infinitesimal line element in the curved space as

$$\mathrm{d}s^2 = g_{ij}(t, \boldsymbol{x})\mathrm{d}x^i \mathrm{d}x^j. \tag{A.2.1}$$

Hereafter, we distinguish the upper and lower indices, which are raised and lowered by the metric $g_{ij}(t, \boldsymbol{x})$ and its inverse $g^{ij}(t, \boldsymbol{x})$. We also introduce the covariant spatial derivative ∇_i with respect to the metric $g_{ij}(t, \boldsymbol{x})$ and the covariant temporal derivative ∇_t as

$$\nabla_t \mathcal{M}(t, \boldsymbol{x}) \equiv \frac{1}{\sqrt{g(t, \boldsymbol{x})}} \partial_t \left(\sqrt{g(t, \boldsymbol{x})} \mathcal{M}(t, \boldsymbol{x}) \right), \tag{A.2.2}$$

with the determinant of the metric $g(t, \boldsymbol{x}) \equiv \det[g_{ij}(t, \boldsymbol{x})]$. The covariant derivative ∇_i acts on a scalar quantity $\mathcal{M}(t, \boldsymbol{x})$, a covariant vector $\mathcal{J}_i(t, \boldsymbol{x})$, and a contravariant vector $\mathcal{J}^j(t, \boldsymbol{x})$ as

$$\begin{aligned}
\nabla_i \mathcal{M}(t, \boldsymbol{x}) &= \partial_i \mathcal{M}(t, \boldsymbol{x}), \\
\nabla_i \mathcal{J}_j(t, \boldsymbol{x}) &= \partial_i \mathcal{J}_j(t, \boldsymbol{x}) - \Gamma_{ij}^k(t, \boldsymbol{x}) \mathcal{J}_k(t, \boldsymbol{x}), \\
\nabla_i \mathcal{J}^j(t, \boldsymbol{x}) &= \partial_i \mathcal{J}^j(t, \boldsymbol{x}) + \Gamma_{ik}^j(t, \boldsymbol{x}) \mathcal{J}^k(t, \boldsymbol{x}),
\end{aligned} \tag{A.2.3}$$

where the Christoffel symbol $\Gamma_{ij}^k(t, \boldsymbol{x})$ is defined by

$$\Gamma_{ij}^k(t, \boldsymbol{x}) \equiv \frac{1}{2} g^{kl}(t, \boldsymbol{x}) \Big[\partial_j g_{il}(t, \boldsymbol{x}) + \partial_i g_{lj}(t, \boldsymbol{x}) - \partial_l g_{ij}(t, \boldsymbol{x}) \Big]. \tag{A.2.4}$$

The action with the external fields is given by

$$\begin{aligned}
S[\psi_\sigma, \psi_\sigma^\dagger; A_\mu, g_{ij}] &= S_0[\psi_\sigma, \psi_\sigma^\dagger; A_\mu, g_{ij}] + S_{\mathrm{int}} \\
&= \int \mathrm{d}t \mathrm{d}\boldsymbol{x} \, \sqrt{g(t, \boldsymbol{x})} \mathcal{L}_{0;\mathrm{curved}}(t, \boldsymbol{x}) + S_{\mathrm{int}},
\end{aligned} \tag{A.2.5}$$

where $\mathcal{L}_{0;\mathrm{curved}}(t, \boldsymbol{x})$ is the kinetic term of the Lagrangian density:

$$\mathcal{L}_{0;\mathrm{curved}}(t, \boldsymbol{x}) = \sum_{\sigma=\uparrow,\downarrow} \left[i\psi_\sigma^\dagger(t, \boldsymbol{x}) \overleftrightarrow{D_t} \psi_\sigma(t, \boldsymbol{x}) - \frac{g^{ij}(t, \boldsymbol{x})}{2m} [D_i \psi_\sigma(t, \boldsymbol{x})]^\dagger [D_j \psi_\sigma(t, \boldsymbol{x})] \right]. \tag{A.2.6}$$

Here, $D_t \equiv \partial_t - iA_t(t, \boldsymbol{x})$ and $D_i \equiv \nabla_i - iA_i(t, \boldsymbol{x})$ are the gauge covariant derivatives and the field $\psi_\sigma(t, \boldsymbol{x})$ is a scalar quantity. To give the interaction term in curved space as a local form, we use an auxiliary field $\pi(t, \boldsymbol{x})$:

$$\begin{aligned}
S_{\mathrm{int}} &= S_{\mathrm{int}}[\psi_\sigma, \psi_\sigma^\dagger, \pi; A_\mu, g_{ij}] \\
&= \int \mathrm{d}t \mathrm{d}\boldsymbol{x} \sqrt{g(t, \boldsymbol{x})} \left[q \sum_\sigma \psi_\sigma^\dagger(t, \boldsymbol{x}) \psi_\sigma(t, \boldsymbol{x}) \pi(t, \boldsymbol{x}) - \frac{\pi(t, \boldsymbol{x})^2}{2r_{\mathrm{R}}^2} - \frac{g^{ij}(t, \boldsymbol{x})}{2} \partial_i \pi(t, \boldsymbol{x}) \partial_j \pi(t, \boldsymbol{x}) \right].
\end{aligned} \tag{A.2.7}$$

In flat space $g_{ij}(t, \boldsymbol{x}) = \delta_{ij}$ in three dimensions, this interaction term leads to the following Yukawa interaction when the auxiliary field is integrated out with the use of its equation of motion:

$$V_{\mathrm{Yukawa}}(r; q, r_{\mathrm{R}}) = -\frac{q^2}{4\pi r} e^{-r/r_{\mathrm{R}}}. \tag{A.2.8}$$

In particular, the unitarity limit is achieved at $mq^2 r_{\mathrm{R}} = 21.1\ldots$ [26]. Although we take the interaction term that leads to the Yukawa potential in flat space, the detailed form of the interaction potential is irrelevant as far as the low-energy physics is concerned.

A.2.2 Nonrelativistic general coordinate transformation

The external fields naturally promote the U(1) symmetry and the spatial translation symmetry to their local counterparts. The action is invariant under the U(1) gauge transformation and the general coordinate transformation:

$$
\begin{aligned}
\psi_\sigma(t, \boldsymbol{x}) &\rightarrow \psi_\sigma'(t, \boldsymbol{x}) = e^{i\chi(t,\boldsymbol{x})}\psi_\sigma(t, \boldsymbol{x}), \\
A_\mu(t, \boldsymbol{x}) &\rightarrow A_\mu'(t, \boldsymbol{x}) = A_\mu(t, \boldsymbol{x}) + \partial_\mu \chi(t, \boldsymbol{x}),
\end{aligned}
\tag{A.2.9}
$$

and

$$
\begin{aligned}
x^i &\rightarrow x'^i = x'^i(\boldsymbol{x}), \\
\psi_\sigma(t, \boldsymbol{x}) \rightarrow \psi_\sigma'(t, \boldsymbol{x}') &= \psi_\sigma(t, \boldsymbol{x}), \qquad \pi(t, \boldsymbol{x}) \rightarrow \pi'(t, \boldsymbol{x}') = \pi(t, \boldsymbol{x}), \\
A_t(t, \boldsymbol{x}) \rightarrow A_t'(t, \boldsymbol{x}') = A_t(t, \boldsymbol{x}), &\qquad A_i(t, \boldsymbol{x}) \rightarrow A_i'(t, \boldsymbol{x}') = \frac{\partial x^j}{\partial x'^i} A_j(t, \boldsymbol{x}), \\
g_{ij}(t, \boldsymbol{x}) \rightarrow g_{ij}'(t, \boldsymbol{x}') &= \frac{\partial x^k}{\partial x'^i}\frac{\partial x^l}{\partial x'^j} g_{kl}(t, \boldsymbol{x}).
\end{aligned}
\tag{A.2.10}
$$

The infinitesimal versions are given by

$$
\delta\psi_\sigma(t, \boldsymbol{x}) = i\chi(t, \boldsymbol{x})\psi_\sigma(t, \boldsymbol{x}), \qquad \delta A_\mu(t, \boldsymbol{x}) = \partial_\mu \chi(t, \boldsymbol{x}),
\tag{A.2.11}
$$

and

$$
\begin{aligned}
x^i &\rightarrow x^i + \xi^i(\boldsymbol{x}), \\
\delta\psi_\sigma(t, \boldsymbol{x}) = -\xi^k(\boldsymbol{x})\partial_k\psi_\sigma(t, \boldsymbol{x}), &\qquad \delta\pi(t, \boldsymbol{x}) = -\xi^k(\boldsymbol{x})\partial_k\pi(t, \boldsymbol{x}), \\
\delta A_t(t, \boldsymbol{x}) = -\xi^k(\boldsymbol{x})\partial_k A_t(t, \boldsymbol{x}), & \\
\delta A_i(t, \boldsymbol{x}) = -\xi^k(\boldsymbol{x})\partial_k A_j(t, \boldsymbol{x}) &- A_k(t, \boldsymbol{x})\partial_i\xi^k(\boldsymbol{x}), \\
\delta g_{ij}(t, \boldsymbol{x}) = -\xi^k(\boldsymbol{x})\partial_k g_{kl}(t, \boldsymbol{x}) &- g_{ik}(t, \boldsymbol{x})\partial_j\xi^k(\boldsymbol{x}) - g_{kj}(t, \boldsymbol{x})\partial_i\xi^k(\boldsymbol{x}).
\end{aligned}
\tag{A.2.12}
$$

Because the action is coupled with the metric for space instead of spacetime, the gauge parameter $\xi^i(\boldsymbol{x})$ is time-independent. However, one can makes it spacetime-dependent with keeping the action invariant by modifying the transformation as

$$
\begin{aligned}
x^i &\rightarrow x^i + \xi^i(t, \boldsymbol{x}), \\
\delta\psi_\sigma(t, \boldsymbol{x}) = -\xi^k(t, \boldsymbol{x})\partial_k\psi_\sigma(t, \boldsymbol{x}), &\qquad \delta\pi(t, \boldsymbol{x}) = -\xi^k(t, \boldsymbol{x})\partial_k\pi(t, \boldsymbol{x}), \\
\delta A_t(t, \boldsymbol{x}) = -\xi^k(t, \boldsymbol{x})\partial_k A_t(t, \boldsymbol{x}) &- A_j(t, \boldsymbol{x})\dot{\xi}^j(t, \boldsymbol{x}), \\
\delta A_i(t, \boldsymbol{x}) = -\xi^k(t, \boldsymbol{x})\partial_k A_j(t, \boldsymbol{x}) &- A_k(t, \boldsymbol{x})\partial_i\xi^k(t, \boldsymbol{x}) - m g_{ij}(t, \boldsymbol{x})\dot{\xi}^j(t, \boldsymbol{x}), \\
\delta g_{ij}(t, \boldsymbol{x}) = -\xi^k(t, \boldsymbol{x})\partial_k g_{kl}(t, \boldsymbol{x}) &- g_{ik}(t, \boldsymbol{x})\partial_j\xi^k(t, \boldsymbol{x}) - g_{kj}(t, \boldsymbol{x})\partial_i\xi^k(t, \boldsymbol{x}).
\end{aligned}
\tag{A.2.13}
$$

This is called the nonrelativistic general coordinate transformation [26], which is a local version of the spatial translation including the Galilean boost. Indeed, if we set the gauge parameters as

$$
\chi(t, \boldsymbol{x}) = mx_i V^i, \qquad \xi^i(t, \boldsymbol{x}) = V^i t,
\tag{A.2.14}
$$

the infinitesimal transformation of the field $\psi_\sigma(t, \boldsymbol{x})$ results in Eq. (A.1.16). The nonrelativistic general coordinate invariance is a hidden symmetry that is exposed by putting the system in curved space and is a larger symmetry than the spatial translation and Galilean symmetries.

A.2.3 Scale and conformal transformations

The conformal symmetry can also be extended. The kinetic term is invariant under

$$t \to t' = t'(t),$$

$$\psi_\sigma(t, \boldsymbol{x}) \to \psi'_\sigma(t', \boldsymbol{x}) = \left(\frac{dt}{dt'}\right)^{d/4} \psi_\sigma(t, \boldsymbol{x}), \qquad \pi(t, \boldsymbol{x}) \to \pi'(t', \boldsymbol{x}) = \left(\frac{dt}{dt'}\right)^{d/4} \pi(t, \boldsymbol{x}),$$

$$A_t(t, \boldsymbol{x}) \to A'_t(t', \boldsymbol{x}) = \left(\frac{dt}{dt'}\right) A_t(t, \boldsymbol{x}), \qquad A_i(t, \boldsymbol{x}) \to A'_i(t', \boldsymbol{x}) = A_i(t, \boldsymbol{x}),$$

$$g_{ij}(t, \boldsymbol{x}) \to g'_{ij}(t', \boldsymbol{x}) = \left(\frac{dt}{dt'}\right)^{-1} g_{ij}(t, \boldsymbol{x}). \tag{A.2.15}$$

The infinitesimal version is given by

$$t \to t' = t + \alpha(t),$$

$$\delta\psi_\sigma(t, \boldsymbol{x}) = -\alpha(t)\dot{\psi}_\sigma(t, \boldsymbol{x}) - \frac{d}{4}\dot{\alpha}(t)\psi_\sigma(t, \boldsymbol{x}), \qquad \delta\pi(t, \boldsymbol{x}) = -\alpha(t)\pi(t, \boldsymbol{x}) - \frac{d}{4}\dot{\alpha}(t)\pi(t, \boldsymbol{x}),$$

$$\delta A_t(t, \boldsymbol{x}) = -\alpha(t)\dot{A}_t(t, \boldsymbol{x}) - \dot{\alpha}(t)A_t(t, \boldsymbol{x}), \qquad \delta A_i(t, \boldsymbol{x}) = -\alpha(t)\dot{A}_i(t, \boldsymbol{x}),$$

$$\delta g_{ij}(t, \boldsymbol{x}) = -\alpha(t)\dot{g}_{ij}(t, \boldsymbol{x}) + \dot{\alpha}(t)g_{ij}(t, \boldsymbol{x}). \tag{A.2.16}$$

This transformation is an extension of the scale and conformal transformations. In fact, one can reproduce the scale transformation (A.1.26) by taking the gauge parameters as

$$\alpha(t) = -2\lambda t, \qquad \xi^i(t, \boldsymbol{x}) = -\lambda x^i \tag{A.2.17}$$

and the conformal transformation (A.1.33) by taking them as

$$\alpha(t) = ct^2, \qquad \xi^i(t, \boldsymbol{x}) = ctx^i, \qquad \chi(t, \boldsymbol{x}) = \frac{m}{2}c|\boldsymbol{x}|^2. \tag{A.2.18}$$

The interaction term S_{int} is not invariant under the conformal transformation (A.2.16). However, as already mentioned, the system is considered to be conformal invariant at unitarity as long as the low-energy physics is concerned.

A.3 Summary

In this appendix, we reviewed the symmetries of the resonant Fermi gas: the U(1) symmetry, the spacetime translation symmetry, the spatial rotation symmetry, and the Galilean symmetry. We also reviewed the scale and conformal symmetries that emerge in the unitary Fermi gas. In Sec. A.1, we introduced the Schrödinger group, which consists of the U(1) phase rotation, the spacetime translation, the spatial rotation, the Galilean boost, the scale transformation, and the conformal transformation. In particular, we confirmed that

the trace of the stress tensor is related to the Hamiltonian in the conformal invariant system [Eq. (A.1.30)]. In the presence of a finite scattering length, Eq. (A.1.30) is modified by adding a term describing the conformal symmetry breaking due to the scattering length [see Eq. (3.1.15)]. We also confirmed that the system at unitarity can be considered to be conformal invariant as long as the low-energy physics is concerned. In Sec. A.2, we reviewed the nonrelativistic general coordinate and conformal invariances, which are exposed by putting the system in curved space [26]. Because the nonrelativistic general coordinate invariance can impose stronger constraints on systems than the Galilean invariance, it has been widely used not only for the resonant Fermi gases, but also for other nonrelativistic systems such as superfluids [143–147] and quantum Hall systems [148–153]. The conformal invariance in curved space was used to prove the vanishing bulk viscosity of the unitary Fermi gas [49]. Furthermore, as we will discuss in Appendix B, the conformal invariance provides a guiding principle in constructing the hydrodynamic equations with a spacetime-dependent scattering length, which are derived in Chapter 3.

Appendix B

Hydrodynamics with conformal invariance

In this chapter, we discuss hydrodynamics from the perspective of the conformal invariance and derive the hydrodynamic equations with a spacetime-dependent scattering length discussed in Chapter 3. In Sec. B.1, we consider a resonant Fermi gas with a finite and non-zero scattering length and give its Hamiltonian coupled with an external U(1) gauge field and a metric in order to take advantage of the nonrelativistic general coordinate and conformal invariances introduced in Appendix A. In the presence of the finite and non-zero scattering length, the conformal invariance of the system is explicitly broken. However, this invariance can be recovered formally by regarding the scattering length as a fictitious field properly transformed under the transformations. We derive the continuity equations and directly verify that they are covariant under the conformal transformation with a fictitious transformation for the scattering length. In Sec. B.2, we construct hydrodynamic equations for normal fluids with the scattering length as an external field. Our guiding principle in the construction is that the continuity equations maintain the covariance under the nonrelativistic general coordinate transformation and the recovered conformal transformation. We then show that the scattering length uniquely enters the constitutive relations, and arrive at the constitutive relations derived in Chapter 3. In Sec. B.3, we summarize this appendix. For the sake of simplicity, we discuss only the case of normal fluids.

B.1   Quantum field theory

B.1.1   Commutation relation and Hamiltonian

Let us consider nonrelativistic spin-$1/2$ fermions in d spatial dimension. The annihilation operator $\hat{\Psi}_\sigma(t, \boldsymbol{x})$ obeys the equal-time anti-commutation relations,

$$
\begin{aligned}
\{\hat{\Psi}_\sigma(t, \boldsymbol{x}), \hat{\Psi}_\tau^\dagger(t, \boldsymbol{y})\} &= \delta_{\sigma\tau}\delta^d(\boldsymbol{x} - \boldsymbol{y}), \\
\{\hat{\Psi}_\sigma(t, \boldsymbol{x}), \hat{\Psi}_\tau(t, \boldsymbol{y})\} &= \{\hat{\Psi}_\sigma^\dagger(t, \boldsymbol{x}), \hat{\Psi}_\tau^\dagger(t, \boldsymbol{y})\} = 0,
\end{aligned}
\tag{B.1.1}
$$

and its time evolution is governed by the Heisenberg equation of motion,

$$
i\partial_t \hat{\Psi}_\sigma(t, \boldsymbol{x}) = [\hat{\Psi}_\sigma(t, \boldsymbol{x}), \hat{H}(t)],
\tag{B.1.2}
$$

with the Hamiltonian $\hat{H}(t)$. As discussed in Appendix A, we can expose hidden symmetries by coupling the system to an external U(1) gauge field $A_\mu(t, \boldsymbol{x})$ and a metric $g_{ij}(t, \boldsymbol{x})$. The Hamiltonian with $A_\mu(t, \boldsymbol{x})$ and $g_{ij}(t, \boldsymbol{x})$ is provided by

$$\hat{H}(t) = \sum_{\sigma=\uparrow,\downarrow} \int \mathrm{d}\boldsymbol{x} \sqrt{g(t, \boldsymbol{x})} \left[\frac{g^{ij}(t, \boldsymbol{x})}{2m} [D_i \hat{\psi}_\sigma(t, \boldsymbol{x})]^\dagger [D_j \hat{\psi}_\sigma(t, \boldsymbol{x})] - A_t(t, \boldsymbol{x}) \hat{\psi}_\sigma^\dagger(t, \boldsymbol{x}) \hat{\psi}_\sigma(t, \boldsymbol{x}) \right]$$
$$+ \sum_{\sigma,\tau} \int \mathrm{d}\boldsymbol{x} \sqrt{g(t, \boldsymbol{x})} \frac{\lambda(t, \boldsymbol{x})}{2} \hat{\psi}_\sigma^\dagger(t, \boldsymbol{x}) \hat{\psi}_\tau^\dagger(t, \boldsymbol{x}) \hat{\psi}_\tau(t, \boldsymbol{x}) \hat{\psi}_\sigma(t, \boldsymbol{x}), \tag{B.1.3}$$

where $D_i \equiv \nabla_i - iA_i(t, \boldsymbol{x})$ is the gauge covariant derivative and $\lambda(t, \boldsymbol{x})$ is a spacetime-dependent bare coupling.[1] Here, we introduce the reduced annihilation operator $\hat{\psi}_\sigma(t, \boldsymbol{x})$ as

$$\hat{\psi}_\sigma(t, \boldsymbol{x}) \equiv g(t, \boldsymbol{x})^{-1/4} \hat{\Psi}_\sigma(t, \boldsymbol{x}). \tag{B.1.4}$$

It is convenient to represent physical observables such as the Hamiltonian in terms of $\hat{\psi}_\sigma(t, \boldsymbol{x})$ because $\hat{\psi}_\sigma(t, \boldsymbol{x})$ is transformed as a scalar under the general coordinate transformation,

$$\boldsymbol{x} \to \boldsymbol{x}' = \boldsymbol{x}'(\boldsymbol{x}), \qquad \hat{\psi}_\sigma(t, \boldsymbol{x}) \to \hat{\psi}'_\sigma(t, \boldsymbol{x}') = \hat{\psi}_\sigma(t, \boldsymbol{x}). \tag{B.1.5}$$

In contrast, $\hat{\Psi}_\sigma(t, \boldsymbol{x})$ is not transformed as a scalar in order to preserve the anti-commutation relation (B.1.1). The coupling $\lambda(t, \boldsymbol{x})$ is related to the scattering length $a(t, \boldsymbol{x})$ in the dimensional regularization as

$$\frac{1}{\lambda(t, \boldsymbol{x})} = \frac{ma(t, \boldsymbol{x})^{2-d}}{(d-2)\Omega_{d-1}}, \tag{B.1.6}$$

with $\Omega_{d-1} \equiv (4\pi)^{d/2}/[2\Gamma(2 - d/2)] = 2\pi, 4\pi$ for $d = 2, 3$. Here, the scattering length is assumed to have the spacetime dependence to be regarded as a fictitious field.

B.1.2 Symmetries

Owing to the presence of the U(1) gauge field and the metric, the Heisenberg equation (B.1.2) is covariant under the U(1) gauge transformation and the nonrelativistic general coordinate transformation.[2] Their infinitesimal transformations are provided by

$$\delta_\chi \hat{\psi}_\sigma(t, \boldsymbol{x}) = i\chi(t, \boldsymbol{x}) \hat{\psi}_\sigma(t, \boldsymbol{x}),$$
$$\delta_\chi A_\mu(t, \boldsymbol{x}) = \partial_\mu \chi(t, \boldsymbol{x}), \tag{B.1.7}$$

for the U(1) gauge transformation and

$$\delta_\xi \hat{\psi}_\sigma(t, \boldsymbol{x}) = -\xi^k(t, \boldsymbol{x}) \partial_k \hat{\psi}_\sigma(t, \boldsymbol{x}),$$
$$\delta_\xi A_t(t, \boldsymbol{x}) = -\xi^k(t, \boldsymbol{x}) \partial_k A_t(t, \boldsymbol{x}) - A_k(t, \boldsymbol{x}) \dot{\xi}^k(t, \boldsymbol{x}),$$
$$\delta_\xi A_i(t, \boldsymbol{x}) = -\xi^k(t, \boldsymbol{x}) \partial_k A_i(t, \boldsymbol{x}) - A_k(t, \boldsymbol{x}) \partial_i \xi^k(t, \boldsymbol{x}) - m g_{ik}(t, \boldsymbol{x}) \dot{\xi}^k(t, \boldsymbol{x}), \tag{B.1.8}$$
$$\delta_\xi g_{ij}(t, \boldsymbol{x}) = -\xi^k(t, \boldsymbol{x}) \partial_k g_{ij}(t, \boldsymbol{x}) - g_{ik}(t, \boldsymbol{x}) \partial_j \xi^k(t, \boldsymbol{x}) - g_{kj}(t, \boldsymbol{x}) \partial_i \xi^k(t, \boldsymbol{x}),$$
$$\delta_\xi a(t, \boldsymbol{x}) = -\xi^k(t, \boldsymbol{x}) \partial_k a(t, \boldsymbol{x}),$$

---

[1] In this appendix, we denote the coupling by $\lambda(t, \boldsymbol{x})$ to avoid confusing it with the metric determinant $g(t, \boldsymbol{x}) \equiv \det[g_{ij}(t, \boldsymbol{x})]$

[2] When we refer to an equation $A = B$ as being covariant under a transformation, we mean that $\delta A = \delta B$ under the transformation throughout this appendix.

for the nonrelativistic general coordinate transformation. Here, the scattering length is supposed to be transformed as a scalar.

The conformal invariance is explicitly broken by the presence of the scattering length. In fact, the Heisenberg equation (B.1.2) is not covariant under the conformal transformation of Eq. (A.2.16). However, it is possible to make the Heisenberg equation covariant by artificially imposing the following transformation law on the scattering length:

$$\delta_\alpha a(t, \boldsymbol{x}) = -\alpha(t)\dot{a}(t, \boldsymbol{x}) + \frac{1}{2}\dot{\alpha}(t)a(t, \boldsymbol{x}). \tag{B.1.9}$$

Accordingly, the Heisenberg equation becomes covariant under the following conformal transformation:

$$\begin{aligned}
\delta_\alpha \hat{\psi}_\sigma(t, \boldsymbol{x}) &= -\alpha(t)\dot{\hat{\psi}}_\sigma(t, \boldsymbol{x}) - \frac{d}{4}\dot{\alpha}(t)\hat{\psi}_\sigma(t, \boldsymbol{x}), \\
\delta_\alpha A_t(t, \boldsymbol{x}) &= -\alpha(t)\dot{A}_t(t, \boldsymbol{x}) - \dot{\alpha}(t)A_t(t, \boldsymbol{x}), \\
\delta_\alpha A_i(t, \boldsymbol{x}) &= -\alpha(t)\dot{A}_i(t, \boldsymbol{x}), \\
\delta_\alpha g_{ij}(t, \boldsymbol{x}) &= -\alpha(t)\dot{g}_{ij}(t, \boldsymbol{x}) + \frac{d}{4}\dot{\alpha}(t)g_{ij}(t, \boldsymbol{x}), \\
\delta_\alpha a(t, \boldsymbol{x}) &= -\alpha(t)\dot{a}(t, \boldsymbol{x}) + \frac{1}{2}\dot{\alpha}(t)a(t, \boldsymbol{x}).
\end{aligned} \tag{B.1.10}$$

B.1.3   Continuity equations

We can write the continuity equations for mass, momentum, and energy. The mass, momentum, and energy densities are defined by

$$\hat{\mathcal{M}}(t, \boldsymbol{x}) \equiv m \sum_\sigma \hat{\psi}_\sigma^\dagger(t, \boldsymbol{x})\hat{\psi}_\sigma(t, \boldsymbol{x}), \tag{B.1.11}$$

$$\hat{\mathcal{J}}_i(t, \boldsymbol{x}) \equiv -i \sum_\sigma \hat{\psi}_\sigma^\dagger(t, \boldsymbol{x})\overleftrightarrow{D}_i\hat{\psi}_\sigma(t, \boldsymbol{x}), \tag{B.1.12}$$

$$\hat{\mathcal{H}}(t, \boldsymbol{x}) \equiv \sum_\sigma \frac{g^{ij}(t, \boldsymbol{x})}{2m}[D_i\hat{\psi}_\sigma^\dagger(t, \boldsymbol{x})]^\dagger[D_j\hat{\psi}_\sigma(t, \boldsymbol{x})] \tag{B.1.13}$$

$$+ \sum_{\sigma,\tau} \frac{\lambda(t, \boldsymbol{x})}{2}\hat{\psi}_\sigma^\dagger(t, \boldsymbol{x})\hat{\psi}_\tau^\dagger(t, \boldsymbol{x})\hat{\psi}_\tau(t, \boldsymbol{x})\hat{\psi}_\sigma(t, \boldsymbol{x}), \tag{B.1.14}$$

where the energy density refers to that without the trapping potential term. The continuity equations can be straightforwardly derived from the Heisenberg equation and are provided by

$$\nabla_t\hat{\mathcal{M}}(t, \boldsymbol{x}) + \nabla_i\hat{\mathcal{J}}^i(t, \boldsymbol{x}) = 0, \tag{B.1.15}$$

$$\nabla_t\hat{\mathcal{J}}_i(t, \boldsymbol{x}) + \nabla_j\hat{\Pi}_i^j(t, \boldsymbol{x}) = F_{it}(t, \boldsymbol{x})\frac{\hat{\mathcal{M}}(t, \boldsymbol{x})}{m} + F_{ij}(t, \boldsymbol{x})\frac{\hat{\mathcal{J}}^j(t, \boldsymbol{x})}{m} - \frac{\partial_i a(t, \boldsymbol{x})}{\Omega_{d-1}a(t, \boldsymbol{x})^{d-1}}\frac{\hat{\mathcal{C}}(t, \boldsymbol{x})}{m}, \tag{B.1.16}$$

$$\nabla_t\hat{\mathcal{H}}(t, \boldsymbol{x}) + \nabla_i\hat{\mathcal{Q}}^i(t, \boldsymbol{x}) = F_{it}(t, \boldsymbol{x})\frac{\hat{\mathcal{J}}^i(t, \boldsymbol{x})}{m} - \frac{\dot{g}_{ij}(t, \boldsymbol{x})}{2}\hat{\Pi}^{ij}(t, \boldsymbol{x}) + \frac{\partial_t a(t, \boldsymbol{x})}{\Omega_{d-1}a(t, \boldsymbol{x})^{d-1}}\frac{\hat{\mathcal{C}}(t, \boldsymbol{x})}{m}, \tag{B.1.17}$$

where $\nabla_t \hat{\mathcal{O}}(t, \boldsymbol{x}) \equiv \partial_t[\sqrt{g(t, \boldsymbol{x})}\hat{\mathcal{O}}(t, \boldsymbol{x})]/\sqrt{g(t, \boldsymbol{x})}$ and the gauge field strength $F_{\mu\nu}(t, \boldsymbol{x}) \equiv \partial_\mu A_\nu(t, \boldsymbol{x}) - \partial_\nu A_\mu(t, \boldsymbol{x})$ are introduced. The right-hand sides of the momentum and energy continuity equations represent the external forces and the external powers supplied by the external fields. Here, the stress tensor $\hat{\Pi}_{ij}(t, \boldsymbol{x})$, the energy current density $\hat{Q}_i(t, \boldsymbol{x})$, and the contact density $\hat{\mathcal{C}}(t, \boldsymbol{x})$ are defined by

$$\hat{\Pi}_{ij}(t, \boldsymbol{x}) = \sum_\sigma \frac{D_i \hat{\psi}_\sigma^\dagger(t, \boldsymbol{x}) D_j \hat{\psi}_\sigma(t, \boldsymbol{x}) + D_j \hat{\psi}_\sigma^\dagger(t, \boldsymbol{x}) D_i \hat{\psi}_\sigma(t, \boldsymbol{x})}{2m}$$

$$+ g_{ij}(t, \boldsymbol{x}) \frac{\lambda(t, \boldsymbol{x})}{2} \sum_{\sigma,\rho} \hat{\psi}_\sigma^\dagger(t, \boldsymbol{x}) \hat{\psi}_\rho^\dagger(t, \boldsymbol{x}) \hat{\psi}_\rho(t, \boldsymbol{x}) \hat{\psi}_\sigma(t, \boldsymbol{x})$$

$$- g_{ij}(t, \boldsymbol{x}) \frac{g^{kl} \nabla_k \nabla_l}{4m} \left(\sum_\sigma \hat{\psi}_\sigma^\dagger(t, \boldsymbol{x}) \hat{\psi}_\sigma(t, \boldsymbol{x}) \right), \tag{B.1.18}$$

$$\hat{Q}_i(t, \boldsymbol{x}) = \sum_\sigma \frac{D_i \hat{\psi}_\sigma^\dagger(t, \boldsymbol{x})[g^{jk}(t, \boldsymbol{x}) D_j D_k \hat{\psi}_\sigma(t, \boldsymbol{x})] + [g^{jk}(t, \boldsymbol{x}) D_j D_k \hat{\psi}_\sigma^\dagger(t, \boldsymbol{x})] D_i \hat{\psi}_\sigma(t, \boldsymbol{x})}{4im^2}$$

$$+ \frac{\lambda(t, \boldsymbol{x})}{im} \sum_{\sigma,\rho} \hat{\psi}_\sigma^\dagger(t, \boldsymbol{x}) \left(\hat{\psi}_\rho^\dagger(t, \boldsymbol{x}) \overleftrightarrow{D_i} \hat{\psi}_\rho(t, \boldsymbol{x}) \right) \hat{\psi}_\sigma(t, \boldsymbol{x})$$

$$+ [\partial_t \ln \sqrt{g(t, \boldsymbol{x})}] \frac{\partial_i}{4m} \left(\sum_\sigma \hat{\psi}_\sigma^\dagger(t, \boldsymbol{x}) \hat{\psi}_\sigma(t, \boldsymbol{x}) \right), \tag{B.1.19}$$

$$\hat{\mathcal{C}}(t, \boldsymbol{x}) = \frac{m^2 \lambda(t, \boldsymbol{x})^2}{2} \sum_{\sigma,\rho} \hat{\psi}_\sigma^\dagger(t, \boldsymbol{x}) \hat{\psi}_\rho^\dagger(t, \boldsymbol{x}) \hat{\psi}_\rho(t, \boldsymbol{x}) \hat{\psi}_\sigma(t, \boldsymbol{x}). \tag{B.1.20}$$

The contact obtained by integrating the contact density $\hat{\mathcal{C}}(t, \boldsymbol{x})$ over the whole space is the important quantity in the universal relations of the resonant Fermi gas [29]. In addition to the continuity equations, the trace of the stress tensor satisfies

$$g_{ij}(t, \boldsymbol{x})\hat{\Pi}^{ij}(t, \boldsymbol{x}) = 2\hat{\mathcal{H}}(t, \boldsymbol{x}) + \frac{\hat{\mathcal{C}}(t, \boldsymbol{x})}{m\Omega_{d-1}a(t, \boldsymbol{x})^{d-2}} - \frac{d}{4m^2}g^{ij}(t, \boldsymbol{x})\nabla_i\nabla_j\hat{\mathcal{M}}(t, \boldsymbol{x}), \tag{B.1.21}$$

which follows from the definitions of Eqs. (B.1.11), (B.1.13), (B.1.18), and (B.1.20). This identity (B.1.21) corresponds to the traceless condition for the conformal invariance of Eq. (B.1.10).

The continuity equations are obviously U(1) gauge invariant, and also covariant under the general coordinate and conformal transformations because they inherit the covariance of the Heisenberg equation. We can verify these covariances directly with the help of the transformation laws of the local operators, which are derived from Eqs. (B.1.8) and (B.1.10) as

$$\delta_\xi \hat{\mathcal{M}}(t, \boldsymbol{x}) = -\xi^k(t, \boldsymbol{x})\partial_k \hat{\mathcal{M}}(t, \boldsymbol{x}), \tag{B.1.22a}$$

$$\delta_\xi \hat{\mathcal{J}}_i(t, \boldsymbol{x}) = -\xi^k(t, \boldsymbol{x})\partial_k \hat{\mathcal{J}}_i(t, \boldsymbol{x}) - \hat{\mathcal{J}}_k(t, \boldsymbol{x})\partial_i \xi^k(t, \boldsymbol{x}) + \hat{\mathcal{M}}(t, \boldsymbol{x})g_{ik}(t, \boldsymbol{x})\dot{\xi}^k(t, \boldsymbol{x}), \tag{B.1.22b}$$

$$\delta_\xi \hat{\mathcal{H}}(t, \boldsymbol{x}) = -\xi^k(t, \boldsymbol{x})\partial_k \hat{\mathcal{H}}(t, \boldsymbol{x}) + \hat{\mathcal{J}}_k(t, \boldsymbol{x})\dot{\xi}^k(t, \boldsymbol{x}), \tag{B.1.22c}$$

$$\delta_\xi \hat{\Pi}_{ij}(t, \boldsymbol{x}) = -\xi^k(t, \boldsymbol{x})\partial_k \hat{\Pi}_{ij}(t, \boldsymbol{x}) - \hat{\Pi}_{ik}(t, \boldsymbol{x})\partial_j \xi^k(t, \boldsymbol{x}) - \hat{\Pi}_{kj}(t, \boldsymbol{x})\partial_i \xi^k(t, \boldsymbol{x})$$
$$+ \hat{\mathcal{J}}_j(t, \boldsymbol{x})g_{ik}(t, \boldsymbol{x})\dot{\xi}^k(t, \boldsymbol{x}) + \hat{\mathcal{J}}_i(t, \boldsymbol{x})g_{jk}(t, \boldsymbol{x})\dot{\xi}^k(t, \boldsymbol{x}), \tag{B.1.22d}$$

$$\delta_\xi \hat{Q}_i(t, \boldsymbol{x}) = -\xi^k(t, \boldsymbol{x})\partial_k \hat{Q}_i(t, \boldsymbol{x}) - \hat{Q}_k(t, \boldsymbol{x})\partial_i \xi^k(t, \boldsymbol{x})$$
$$+ \hat{\mathcal{H}}(t, \boldsymbol{x})g_{ik}(t, \boldsymbol{x})\dot{\xi}^k(t, \boldsymbol{x}) + \hat{\Pi}_{ik}(t, \boldsymbol{x})\dot{\xi}^k(t, \boldsymbol{x}), \tag{B.1.22e}$$

$$\delta_\xi \hat{\mathcal{C}}(t, \boldsymbol{x}) = -\xi^k(t, \boldsymbol{x})\partial_k \hat{\mathcal{C}}(t, \boldsymbol{x}), \tag{B.1.22f}$$

and

$$\delta_\alpha \hat{\mathcal{M}}(t, \boldsymbol{x}) = -\alpha(t)\partial_t \hat{\mathcal{M}}(t, \boldsymbol{x}) - \frac{d}{2}\dot{\alpha}(t)\hat{\mathcal{M}}(t, \boldsymbol{x}), \tag{B.1.23a}$$

$$\delta_\alpha \hat{\mathcal{J}}_i(t, \boldsymbol{x}) = -\alpha(t)\partial_t \hat{\mathcal{J}}_i(t, \boldsymbol{x}) - \frac{d}{2}\dot{\alpha}(t)\hat{\mathcal{J}}_i(t, \boldsymbol{x}), \tag{B.1.23b}$$

$$\delta_\alpha \hat{\mathcal{H}}(t, \boldsymbol{x}) = -\alpha(t)\partial_t \hat{\mathcal{H}}(t, \boldsymbol{x}) - \frac{d+2}{2}\dot{\alpha}(t)\hat{\mathcal{H}}(t, \boldsymbol{x}), \tag{B.1.23c}$$

$$\delta_\alpha \hat{\Pi}_{ij}(t, \boldsymbol{x}) = -\alpha(t)\partial_t \hat{\Pi}_{ij}(t, \boldsymbol{x}) - \frac{d}{2}\dot{\alpha}(t)\hat{\Pi}_{ij}(t, \boldsymbol{x}), \tag{B.1.23d}$$

$$\delta_\alpha \hat{\mathcal{Q}}_i(t, \boldsymbol{x}) = -\alpha(t)\partial_t \hat{\mathcal{Q}}_i(t, \boldsymbol{x}) - \frac{d+2}{2}\dot{\alpha}(t)\hat{\mathcal{Q}}_i(t, \boldsymbol{x}) + \frac{d}{2}\ddot{\alpha}(t)\frac{\partial_i \hat{\mathcal{M}}(t, \boldsymbol{x})}{4m^2}, \tag{B.1.23e}$$

$$\delta_\alpha \hat{\mathcal{C}}(t, \boldsymbol{x}) = -\alpha(t)\partial_t \hat{\mathcal{C}}(t, \boldsymbol{x}) - 2\dot{\alpha}(t)\hat{\mathcal{C}}(t, \boldsymbol{x}). \tag{B.1.23f}$$

When one verifies the covariance of the energy conservation under the conformal transformation, the operator identity (B.1.21) is needed.

B.2   Hydrodynamics for normal fluids

To move on to hydrodynamics, we denote the expectation values for the operators as

$$\mathcal{O}(t, \boldsymbol{x}) \equiv \mathrm{Tr}\left[\hat{\rho}\hat{\mathcal{O}}(t, \boldsymbol{x})\right], \tag{B.2.1}$$

where the density matrix operator $\hat{\rho}$ is arbitrary but independent of time because we work in the Heisenberg picture. From Eqs. (B.1.15), (B.1.16), and (B.1.17), we have the continuity equations of the expectation values as

$$\nabla_t \mathcal{M}(t, \boldsymbol{x}) + \nabla_i \mathcal{J}^i(t, \boldsymbol{x}) = 0, \tag{B.2.2}$$

$$\nabla_t \mathcal{J}_i(t, \boldsymbol{x}) + \nabla_j \hat{\Pi}_i^j(t, \boldsymbol{x}) = F_{it}(t, \boldsymbol{x})\frac{\mathcal{M}(t, \boldsymbol{x})}{m} + F_{ij}(t, \boldsymbol{x})\frac{\mathcal{J}^j(t, \boldsymbol{x})}{m} - \frac{\partial_i a(t, \boldsymbol{x})}{\Omega_{d-1}a(t, \boldsymbol{x})^{d-1}}\frac{\mathcal{C}(t, \boldsymbol{x})}{m}, \tag{B.2.3}$$

$$\nabla_t \mathcal{H}(t, \boldsymbol{x}) + \nabla_i \mathcal{Q}^i(t, \boldsymbol{x}) = F_{it}(t, \boldsymbol{x})\frac{\mathcal{J}^i(t, \boldsymbol{x})}{m} - \frac{\dot{g}_{ij}(t, \boldsymbol{x})}{2}\Pi^{ij}(t, \boldsymbol{x}) + \frac{\partial_t a(t, \boldsymbol{x})}{\Omega_{d-1}a(t, \boldsymbol{x})^{d-1}}\frac{\mathcal{C}(t, \boldsymbol{x})}{m}. \tag{B.2.4}$$

These are the continuity equations in the hydrodynamics. Also, the operator identity (B.1.21) leads to

$$g_{ij}(t, \boldsymbol{x})\Pi^{ij}(t, \boldsymbol{x}) = 2\mathcal{H}(t, \boldsymbol{x}) + \frac{\mathcal{C}(t, \boldsymbol{x})}{m\Omega_{d-1}a(t, \boldsymbol{x})^{d-2}} + O(\partial^2). \tag{B.2.5}$$

Hydrodynamics requires constitutive relations that express the physical quantities in terms of fluid variables in order for the continuity equations to form a set of closed equations. Here, the fluid variables are the local thermodynamic quantities and the fluid velocity $v_i(t, \boldsymbol{x})$. We construct the constitutive relations so that each expectation value obeys the same transformation laws as in Eqs. (B.1.22) and (B.1.23). If a quantity $\mathcal{O}(t, \boldsymbol{x})$ is transformed as

$$\delta_\xi \mathcal{O}(t, \boldsymbol{x}) = -\xi^k(t, \boldsymbol{x})\partial_k \mathcal{O}(t, \boldsymbol{x}), \tag{B.2.6}$$

$$\delta_\alpha \mathcal{O}(t, \boldsymbol{x}) = -\alpha(t)\partial_t \mathcal{O}(t, \boldsymbol{x}) - \Delta_\mathcal{O}\dot{\alpha}(t)\mathcal{O}(t, \boldsymbol{x}) \tag{B.2.7}$$

under the general coordinate and conformal transformations, we refer to the quantity $\mathcal{O}(t, \boldsymbol{x})$ as a scalar field with conformal dimension $\Delta_\mathcal{O}$, for later convenience.

B.2.1 Conserved charge densities

The mass density $\mathcal{M}(t, \boldsymbol{x})$ itself is a local thermodynamic quantity and obeys the same transformation laws as in Eqs (B.1.22a) and (B.1.23a). In other words, the mass density is a scalar field with conformal dimension $d/2$.

We define the fluid velocity $v_i(t, \boldsymbol{x})$ via the momentum density as

$$\mathcal{J}_i(t, \boldsymbol{x}) = \mathcal{M}(t, \boldsymbol{x}) v_i(t, \boldsymbol{x}), \tag{B.2.8}$$

which is the constitutive equation for the momentum density. From the transformation laws of $\mathcal{J}_i(t, \boldsymbol{x})$, the velocity $v_i(t, \boldsymbol{x})$ is transformed as

$$\delta_\xi v_i(t, \boldsymbol{x}) = -\xi^k(t, \boldsymbol{x}) \partial_k v_i(t, \boldsymbol{x}) - v_k(t, \boldsymbol{x}) \partial_i \xi^k(t, \boldsymbol{x}) + g_{ik}(t, \boldsymbol{x}) \dot{\xi}^k(t, \boldsymbol{x}), \tag{B.2.9}$$

$$\delta_\alpha v_i(t, \boldsymbol{x}) = -\alpha(t) \partial_t v_i(t, \boldsymbol{x}). \tag{B.2.10}$$

The transformation law of Eq. (B.2.9) consists of terms coming from the vector nature of $v_i(t, \boldsymbol{x})$ and a term that leads to a translation $\boldsymbol{v} \to \boldsymbol{v} + \boldsymbol{V}$ under the Galilean boost $\xi^k(t, \boldsymbol{x}) = V^k t$.

In order for the energy density $\mathcal{H}(t, \boldsymbol{x})$ to be consistent with the transformation laws of Eqs. (B.1.22c) and (B.1.23c), it is expressed as

$$\mathcal{H}(t, \boldsymbol{x}) = \mathcal{E}(t, \boldsymbol{x}) + \frac{\mathcal{M}(t, \boldsymbol{x})}{2} g^{ij}(t, \boldsymbol{x}) v_i(t, \boldsymbol{x}) v_j(t, \boldsymbol{x}), \tag{B.2.11}$$

where $\mathcal{E}(t, \boldsymbol{x})$ is a scalar field with conformal dimension $1 + d/2$ and is identified as the internal energy density.

B.2.2 Stress tensor

The stress tensor is expressed as

$$\Pi_{ij}(t, \boldsymbol{x}) = \mathcal{P}(t, \boldsymbol{x}) g_{ij}(t, \boldsymbol{x}) + \mathcal{M}(t, \boldsymbol{x}) v_i(t, \boldsymbol{x}) v_j(t, \boldsymbol{x}) - \sigma_{ij}^{(a)}(t, \boldsymbol{x}), \tag{B.2.12}$$

where $\mathcal{P}(t, \boldsymbol{x})$ is the pressure and is a scalar field with conformal dimension $1 + d/2$. In order to satisfy the same transformation laws as in Eqs. (B.1.22d) and (B.1.23d), the viscous term $\sigma_{ij}^{(a)}(t, \boldsymbol{x})$ must be transformed as

$$\delta_\xi \sigma_{ij}^{(a)}(t, \boldsymbol{x}) = -\xi^k(t, \boldsymbol{x}) \partial_k \sigma_{ij}^{(a)}(t, \boldsymbol{x}) - \sigma_{ik}^{(a)}(t, \boldsymbol{x}) \partial_j \xi^k(t, \boldsymbol{x}) - \sigma_{kj}^{(a)}(t, \boldsymbol{x}) \partial_i \xi^k(t, \boldsymbol{x}), \tag{B.2.13}$$

$$\delta_\alpha \sigma_{ij}^{(a)}(t, \boldsymbol{x}) = -\alpha(t) \partial_t \sigma_{ij}^{(a)}(t, \boldsymbol{x}) - \frac{d}{2} \dot{\alpha}(t) \sigma_{ij}^{(a)}(t, \boldsymbol{x}). \tag{B.2.14}$$

In the unitarity limit, the viscous term satisfying Eq. (B.2.13) was constructed in Ref. [49], which reads

$$\sigma_{ij}^{(a)}(t, \boldsymbol{x}) = \eta(t, \boldsymbol{x}) V_{ij}(t, \boldsymbol{x}) + \zeta(t, \boldsymbol{x}) g_{ij}(t, \boldsymbol{x}) V(t, \boldsymbol{x}) + O(\partial^2), \tag{B.2.15}$$

with the shear and bulk strain rate tensors in curved space given by

$$V_{ij}(t, \boldsymbol{x}) \equiv \nabla_i v_j(t, \boldsymbol{x}) + \nabla_j v_i(t, \boldsymbol{x}) + \partial_t g_{ij}(t, \boldsymbol{x}) - \frac{2}{d} g_{ij}(t, \boldsymbol{x}) V(t, \boldsymbol{x}), \tag{B.2.16}$$

$$V(t, \boldsymbol{x}) \equiv \nabla_i v^i(t, \boldsymbol{x}) + \partial_t \ln \sqrt{g(t, \boldsymbol{x})}. \tag{B.2.17}$$

Under the conformal transformation, each strain rate tensor is transformed as

$$\delta_\alpha V_{ij}(t, \boldsymbol{x}) = -\alpha(t)\partial_t V_{ij}(t, \boldsymbol{x}), \tag{B.2.18}$$

$$\delta_\alpha V(t, \boldsymbol{x}) = -\alpha(t)\partial_t V(t, \boldsymbol{x}) - \dot{\alpha}(t)V(t, \boldsymbol{x}) + \frac{d}{2}\ddot{\alpha}(t). \tag{B.2.19}$$

In order for Eq. (B.2.14) to be satisfied, the shear viscosity $\eta(t, \boldsymbol{x})$ must be a scalar field with conformal dimension $d/2$ and the bulk viscosity $\zeta(t, \boldsymbol{x})$ must vanish. Therefore, the bulk viscosity $\zeta(t, \boldsymbol{x})$ vanishes in the unitarity limit.

When there is a finite and non-zero scattering length, it can enter the hydrodynamic equations as an external field, and it is possible to circumvent the vanishing bulk viscosity. We consider the modified bulk strain rate tensor as

$$V^{(a)}(t, \boldsymbol{x}) = V(t, \boldsymbol{x}) - \tilde{V}(t, \boldsymbol{x}), \tag{B.2.20}$$

where the modification term $\tilde{V}(t, \boldsymbol{x})$ is constructed by the scattering length. When the scattering length is set to be a constant, $\tilde{V}(t, \boldsymbol{x})$ must vanish to recover the usual hydrodynamics. This means that the scattering length in $\tilde{V}(t, \boldsymbol{x})$ must be accompanied by at least one derivative. In order for Eqs. (B.2.13) and (B.2.14) to be satisfied and for the bulk viscosity to exist as a scalar field with conformal dimension $d/2$, the modified bulk strain rate tensor must obey the transformation laws as

$$\delta_\xi V^{(a)}(t, \boldsymbol{x}) = -\xi^k(t, \boldsymbol{x})\partial_k V^{(a)}(t, \boldsymbol{x}), \tag{B.2.21}$$

$$\delta_\alpha V^{(a)}(t, \boldsymbol{x}) = -\alpha(t)\partial_t V^{(a)}(t, \boldsymbol{x}) - \dot{\alpha}(t)V^{(a)}(t, \boldsymbol{x}). \tag{B.2.22}$$

Eq. (B.2.19) has a term proportional to $\ddot{\alpha}(t)$, and differs from Eq. (B.2.22) because of this term. In order to eliminate this difference, the vanishing bulk viscosity is derived in the unitarity limit. By comparing the transformation laws of $V(t, \boldsymbol{x})$ with Eqs. (B.2.21) and (B.2.22), we can find the transformation laws that the modification term $\tilde{V}(t, \boldsymbol{x})$ must satisfy as

$$\delta_\xi \tilde{V}(t, \boldsymbol{x}) = -\xi^k(t, \boldsymbol{x})\partial_k \tilde{V}(t, \boldsymbol{x}), \tag{B.2.23}$$

$$\delta_\alpha \tilde{V}(t, \boldsymbol{x}) = -\alpha(t)\partial_t \tilde{V}(t, \boldsymbol{x}) - \dot{\alpha}(t)\tilde{V}(t, \boldsymbol{x}) + \frac{d}{2}\ddot{\alpha}(t). \tag{B.2.24}$$

From these transformation laws, we can construct $\tilde{V}(t, \boldsymbol{x})$ obeying these transformation laws as

$$\tilde{V}(t, \boldsymbol{x}) = d[\partial_t \ln a(t, \boldsymbol{x}) + v^k(t, \boldsymbol{x})\partial_k \ln a(t, \boldsymbol{x})], \tag{B.2.25}$$

and thus we obtain the modified bulk strain tensor as

$$V^{(a)}(t, \boldsymbol{x}) = V(t, \boldsymbol{x}) - d[\partial_t \ln a(t, \boldsymbol{x}) + v^k(t, \boldsymbol{x})\partial_k \ln a(t, \boldsymbol{x})], \tag{B.2.26}$$

The modification term $\tilde{V}(t, \boldsymbol{x})$ is the only term consisting of the scattering length up to first order in derivatives that obeys Eqs. (B.2.23) and (B.2.24). This modified bulk strain rate tensor $V^{(a)}(t, \boldsymbol{x})$ is a scalar field with conformal dimension 1. Therefore, when the bulk viscosity is a scalar field with conformal dimension $d/2$, the bulk viscous term with $\tilde{V}^a(t, \boldsymbol{x})$ satisfies Eq. (B.2.14). In flat space $g_{ij}(t, \boldsymbol{x}) \rightarrow \delta_{ij}$, the modified bulk strain rate tensor $V^{(a)}(t, \boldsymbol{x})$ is reduced to Eq. (3.2.25).

B.2.3 Contact density

By substituting the constitutive relations for the energy density and the stress tensor into Eq. (B.2.5), we obtain

$$\frac{\mathcal{C}(t,\boldsymbol{x})}{m\Omega_{d-1}a(t,\boldsymbol{x})^{d-2}} = d\mathcal{P}(t,\boldsymbol{x}) - 2\mathcal{E}(t,\boldsymbol{x}) - d\zeta(t,\boldsymbol{x})V^{(a)}(t,\boldsymbol{x}) + O(\partial^2). \tag{B.2.27}$$

Here, we introduce the contact density in local thermal equilibrium as

$$\frac{\mathcal{C}_{\text{eq}}(t,\boldsymbol{x})}{m\Omega_{d-1}a(t,\boldsymbol{x})^{d-2}} \equiv d\mathcal{P}(t,\boldsymbol{x}) - 2\mathcal{E}(t,\boldsymbol{x}), \tag{B.2.28}$$

which is understood as the local extension of one of the universal relations known as the pressure relation [28, 29]. With the use of $\mathcal{C}_{\text{eq}}(t,\boldsymbol{x})$, the constitutive relation for the contact density is written as

$$\mathcal{C}(t,\boldsymbol{x}) = \mathcal{C}_{\text{eq}}(t,\boldsymbol{x}) - dm\Omega_{d-1}a(t,\boldsymbol{x})^{d-2}\zeta(t,\boldsymbol{x})V^{(a)}(t,\boldsymbol{x}) + O(\partial^2). \tag{B.2.29}$$

B.2.4 Energy current density

The energy current density is expressed as

$$\mathcal{Q}_i(t,\boldsymbol{x}) = \Big[\mathcal{H}(t,\boldsymbol{x}) + \mathcal{P}(t,\boldsymbol{x})\Big]v_i(t,\boldsymbol{x}) - \sigma_{ij}^{(a)}(t,\boldsymbol{x})v^j(t,\boldsymbol{x}) + q_i^{(a)}(t,\boldsymbol{x}) + V(t,\boldsymbol{x})\frac{\partial_i\mathcal{M}(t,\boldsymbol{x})}{4m^2}, \tag{B.2.30}$$

with

$$\sigma_{ij}^{(a)}(t,\boldsymbol{x}) = \eta(t,\boldsymbol{x})V_{ij}(t,\boldsymbol{x}) + \zeta(t,\boldsymbol{x})g_{ij}(t,\boldsymbol{x})V^{(a)}(t,\boldsymbol{x}) + O(\partial^2), \tag{B.2.31}$$

$$q_i^{(a)}(t,\boldsymbol{x}) = -\kappa(t,\boldsymbol{x})\partial_i T(t,\boldsymbol{x}) + O(\partial^2). \tag{B.2.32}$$

Here, the temperature $T(t,\boldsymbol{x})$ and the thermal conductivity $\kappa(t,\boldsymbol{x})$ are both scalar fields with conformal dimensions 1 and $d/2$, respectively. Although a term proportional to $\partial_i a(t,\boldsymbol{x})$ can be added to $\mathcal{Q}_i(t,\boldsymbol{x})$ so as to keep the transformation laws in Eqs. (B.1.22e) and (B.1.23e) intact, that term is forbidden by the second law of thermodynamics, which we discuss below [Eq. (B.2.36)]. The last term in Eq. (B.2.30) is necessary to generate the last term of the transformation law in Eq. (B.1.23e), but we neglect it below because it is the second order in derivatives.

B.2.5 Entropy production equation

The entropy density is introduced as

$$\mathcal{E}(t,\boldsymbol{x}) + \mathcal{P}(t,\boldsymbol{x}) = T(t,\boldsymbol{x})\mathcal{S}(t,\boldsymbol{x}) + \mu(t,\boldsymbol{x})\mathcal{M}(t,\boldsymbol{x}), \tag{B.2.33}$$

where $\mu(t,\boldsymbol{x})$ is the local mass chemical potential. In the same way as the derivation of Eq. (3.2.17), the total differential of $\mathcal{S}(t,\boldsymbol{x})$ is given by

$$T(t,\boldsymbol{x})\text{d}\mathcal{S}(t,\boldsymbol{x}) = \text{d}\mathcal{E}(t,\boldsymbol{x}) - \mu(t,\boldsymbol{x})\text{d}\mathcal{M}(t,\boldsymbol{x}) - \frac{\mathcal{C}_{\text{eq}}(t,\boldsymbol{x})}{m\Omega_{d-1}a(t,\boldsymbol{x})^{d-1}}\text{d}a(t,\boldsymbol{x}). \tag{B.2.34}$$

Then, the thermodynamic relations combined with the continuity equations and the constitutive relations lead to the entropy production equation,

$$\nabla_t \mathcal{S}(t, \boldsymbol{x}) + \nabla_i \left[\mathcal{S}(t, \boldsymbol{x}) v^i(t, \boldsymbol{x}) + \frac{q^{(a)i}(t, \boldsymbol{x})}{T(t, \boldsymbol{x})} \right] = \frac{\Phi(t, \boldsymbol{x})}{T(t, \boldsymbol{x})}, \qquad (\text{B.2.35})$$

with the dissipation function provided by

$$\Phi(t, \boldsymbol{x}) = \kappa(t, \boldsymbol{x}) \frac{\partial_i T(t, \boldsymbol{x}) \partial^i T(t, \boldsymbol{x})}{T(t, \boldsymbol{x})} + \frac{\eta(t, \boldsymbol{x})}{2} V_{ij}(t, \boldsymbol{x}) V^{ij}(t, \boldsymbol{x}) + \zeta(t, \boldsymbol{x}) [V^{(a)}(t, \boldsymbol{x})]^2 + O(\partial^3).$$
$$(\text{B.2.36})$$

Here the production rate of the entropy density is found to be non-negative when $\kappa(t, \boldsymbol{x}) \geq 0$, $\eta(t, \boldsymbol{x}) \geq 0$, and $\zeta(t, \boldsymbol{x}) \geq 0$, so that the second law of thermodynamics is satisfied.

B.3   Summary

In this appendix, we constructed the covariant hydrodynamics with the spacetime-dependent scattering length under the nonrelativistic general coordinate and conformal transformations. The constitutive relations [Eqs. (B.2.8), (B.2.11), (B.2.12), (B.2.30), and (B.2.29)] are consistent with the transformation laws of their operator counterparts under the general coordinate and conformal transformations. Up to first order in derivatives, the scattering length uniquely enters only the stress tensor and the contact density through the modified bulk strain rate tensor $V^{(a)}(t, \boldsymbol{x})$ [Eq. (B.2.26)]. In flat space $g_{ij}(t, \boldsymbol{x}) = \delta_{ij}$, these constitutive relations are reduced to those derived in Chapter 3.

What was important in the derivation of $V^{(a)}(t, \boldsymbol{x})$ in this appendix is that $V(t, \boldsymbol{x})$ of Eq. (B.2.17) and $\tilde{V}(t, \boldsymbol{x})$ of Eq. (B.2.25) have the same transformation laws under the nonrelativistic general coordinate and conformal transformations. This understanding for $V^{(a)}(t, \boldsymbol{x})$ based on the conformal symmetry supports the intuitive understanding discussed in Chapter 3.

Appendix C

Derivation of Kubo formulas for shear viscosity and thermal conductivity

In Chapter 5, we employed Eq. (5.1.1) as the Kubo formula for the shear viscosity:

$$\eta = \lim_{\omega \to 0} \frac{\mathrm{Im}[\mathcal{R}_{\Pi_{xy}\Pi_{xy}}(\omega + i0^+, \mathbf{0})]}{\omega}. \tag{C.1}$$

On the other hand, the Kubo formula for the shear viscosity η is given by Eq. (2.2.52):

$$\eta = \lim_{\omega \to 0} \mathrm{Re}[\eta(\omega + i0^+)], \tag{C.2}$$

where $\eta(w)$ is the complex shear viscosity defined by Eq. (2.2.50):

$$\eta(w) = \frac{\mathcal{R}_{\Pi_{xy}\Pi_{xy}}(w, \mathbf{0}) - \int_0^\beta \mathrm{d}\tau \int \mathrm{d}\boldsymbol{x} \, \langle \delta\hat{\Pi}_{xy}(-i\tau, \mathbf{0})\delta\hat{\Pi}_{xy}(0, \mathbf{0}) \rangle}{iw}. \tag{C.3}$$

In this appendix, we discuss the relation between Eqs. (C.1) and (C.2). Here, $\hat{\Pi}_{xy}(t, \boldsymbol{x}) = e^{it\hat{H}}\hat{\Pi}_{xy}(\boldsymbol{x})e^{-it\hat{H}}$ is the xy-component of the stress tensor operator in the Heisenberg picture. The response function $\mathcal{R}_{\mathcal{AB}}(w, \boldsymbol{k})$ is defined by Eq. (2.2.7):

$$\mathcal{R}_{\mathcal{AB}}(w, \boldsymbol{k}) = i \int_0^\infty \mathrm{d}t \int \mathrm{d}\boldsymbol{x} \, e^{iwt - i\boldsymbol{k}\cdot\boldsymbol{x}} \langle [\hat{\mathcal{A}}(t, \boldsymbol{x}), \hat{\mathcal{B}}(0, \mathbf{0})] \rangle. \tag{C.4}$$

The real part of the complex shear viscosity for $w \to \omega + i0^+$ is expressed as

$$\begin{aligned}
\mathrm{Re}[\eta(\omega + i0^+)] = {} & \frac{\mathrm{Im}[\mathcal{R}_{\Pi_{xy}\Pi_{xy}}(\omega + i0^+, \mathbf{0})]}{\omega} \\
& - \pi\delta(\omega) \left[\mathrm{Re}[\mathcal{R}_{\Pi_{xy}\Pi_{xy}}(i0^+, \mathbf{0})] - \int_0^\beta \mathrm{d}\tau \int \mathrm{d}\boldsymbol{x} \, \langle \delta\hat{\Pi}_{xy}(-i\tau, \mathbf{0})\delta\hat{\Pi}_{xy}(0, \mathbf{0}) \rangle \right].
\end{aligned} \tag{C.5}$$

Thus, Eqs. (C.1) and (C.2) are equal if the second term on the right-hand side cancels. Here,

the response function $\mathcal{R}_{\Pi_{xy}\Pi_{xy}}(i0^+, \mathbf{0})$ is written as

$$
\begin{aligned}
\mathcal{R}_{\Pi_{xy}\Pi_{xy}}(i0^+, \mathbf{0}) &= i \int_0^\infty \mathrm{d}t \int \mathrm{d}\boldsymbol{x}\, e^{-0^+ t} \langle [\hat{\Pi}_{xy}(t, \boldsymbol{x}),\, \hat{\Pi}_{xy}(0, \mathbf{0})] \rangle \\
&= \lim_{\epsilon \searrow 0} i \int_0^\infty \mathrm{d}t \int \mathrm{d}\boldsymbol{x}\, e^{-\epsilon t} \langle [\delta\hat{\Pi}_{xy}(t, \boldsymbol{x}),\, \delta\hat{\Pi}_{xy}(0, \mathbf{0})] \rangle \\
&= -\lim_{\epsilon \searrow 0} \int_0^\infty \mathrm{d}t \int \mathrm{d}\boldsymbol{x} \int_0^\beta \mathrm{d}\tau\, e^{-\epsilon t} \langle \partial_t \delta\hat{\Pi}_{xy}(t - i\tau, \boldsymbol{x}) \delta\hat{\Pi}_{xy}(0, \mathbf{0}) \rangle, \qquad \text{(C.6)}
\end{aligned}
$$

where $\delta\hat{\Pi}_{xy}(t, \boldsymbol{x}) = \hat{\Pi}_{xy}(t, \boldsymbol{x}) - \langle \hat{\Pi}_{xy}(t, \boldsymbol{x}) \rangle$ and Eq. (2.2.48) are used. The temporal integration by parts leads to

$$
\begin{aligned}
\mathcal{R}_{\Pi_{xy}\Pi_{xy}}(i0^+, \mathbf{0}) &= \int_0^\beta \mathrm{d}\tau \int \mathrm{d}\boldsymbol{x}\, \langle \delta\hat{\Pi}_{xy}(-i\tau, \boldsymbol{x}) \delta\hat{\Pi}_{xy}(0, \mathbf{0}) \rangle \\
&\quad - \lim_{\epsilon \searrow 0} \epsilon \int_0^\infty \mathrm{d}t \int \mathrm{d}\boldsymbol{x} \int_0^\beta \mathrm{d}\tau\, e^{-\epsilon t} \langle \delta\hat{\Pi}_{xy}(t - i\tau, \boldsymbol{x}) \delta\hat{\Pi}_{xy}(0, \mathbf{0}) \rangle. \qquad \text{(C.7)}
\end{aligned}
$$

When the second term on the right-hand side vanishes, the second term of Eq. (C.5) is cancelled out. Because of the limit $\epsilon \searrow 0$, the second term of Eq. (C.7) vanishes if the following integral is finite:

$$
I = \int_0^\infty \mathrm{d}t \int \mathrm{d}\boldsymbol{x} \int_0^\beta \mathrm{d}\tau\, \langle \delta\hat{\Pi}_{xy}(t - i\tau, \boldsymbol{x}) \delta\hat{\Pi}_{xy}(0, \mathbf{0}) \rangle. \qquad \text{(C.8)}
$$

Therefore, if the correlation $\langle \delta\hat{\Pi}_{xy}(t - i\tau, \boldsymbol{x}) \delta\hat{\Pi}_{xy}(0, \mathbf{0}) \rangle$ approaches zero faster than t^{-1} in the limit $t \to \infty$, this integral I is finite and Eqs. (C.1) and (C.2) are equal.

This correlation $\langle \delta\hat{\Pi}_{xy}(t - i\tau, \boldsymbol{x}) \delta\hat{\Pi}_{xy}(0, \mathbf{0}) \rangle$ is supposed to become zero in $t \to \infty$, unless there is zero-energy mode, for example, by free particles or sound waves. We assumed that this correlation goes to zero of $t \to \infty$, and employed Eq. (C.1) as the Kubo formula for the shear viscosity in Chapter 5. In addition, for the thermal conductivity, when we assume that the correlation between the heat current density operators $\langle \delta\hat{\mathcal{J}}_x^q(t - i\tau, \boldsymbol{x}) \delta\hat{\mathcal{J}}_x^q(0, \mathbf{0}) \rangle$ goes to zero of $t \to \infty$, we can show that Eq. (2.2.57) is equal to Eq. (5.1.9) in the same way.

Appendix D

Spectral representation of three-point function

In this appendix, we derive the spectral representation of the following three-point function to understand the analyticity of the vertex function:

$$\mathcal{K}(\tau_1, \tau_2, \tau_3) = \langle \mathcal{T}_\tau \psi^\dagger(\tau_1)\psi(\tau_2)\mathcal{O}(\tau_3)\rangle, \tag{D.1}$$

where the spin degrees of freedom and the spatial coordinates are omitted, for simplicity. Here, let $\mathcal{O}(\tau_3)$ be a quadratic operator. By comparing the definition of the vertex function (5.2.12) and (5.2.13) with Eq. (D.1), one can map the vertex function to the three-point function $\mathcal{K}(\tau_1, \tau_2, \tau_3)$. Our derivation reviewed in this appendix partly follows that in [120] (see appendix therein).

We compute the Fourier transformation of $\mathcal{K}(\tau_1, \tau_2, \tau_3)$, which is defined by

$$\mathcal{K}(i\omega_m^F, i\omega_n^F, i\omega^B) = \frac{1}{\beta^{3/2}} \int_0^\beta \mathrm{d}\tau_1 \int_0^\beta \mathrm{d}\tau_2 \int_0^\beta \mathrm{d}\tau_3 \, e^{i\omega_m^F\tau_1 - i\omega_n^F\tau_2 - i\omega^B\tau_3} \mathcal{K}(\tau_1, \tau_2, \tau_3). \tag{D.2}$$

The three-point function is separated into six cases according to the order of the imaginary time. For the imaginary-time periodicity, it is convenient to treat the three cases mapped to each other by cyclic permutations as one set. Accordingly, we separate the three-point function into the following two parts:

$$\mathcal{K}(\tau_1, \tau_2, \tau_3) = \mathcal{K}_{1\text{-}2\text{-}3}(\tau_1, \tau_2, \tau_3) + \mathcal{K}_{2\text{-}1\text{-}3}(\tau_1, \tau_2, \tau_3), \tag{D.3}$$

with

$$\mathcal{K}_{1\text{-}2\text{-}3}(\tau_1, \tau_2, \tau_3) \equiv \mathcal{K}(\tau_1, \tau_2, \tau_3)\Big[\Theta(\tau_1, \tau_2, \tau_3) + \Theta(\tau_2, \tau_3, \tau_1) + \Theta(\tau_3, \tau_1, \tau_2)\Big], \tag{D.4}$$

$$\mathcal{K}_{2\text{-}1\text{-}3}(\tau_1, \tau_2, \tau_3) \equiv \mathcal{K}(\tau_1, \tau_2, \tau_3)\Big[\Theta(\tau_2, \tau_1, \tau_3) + \Theta(\tau_1, \tau_3, \tau_2) + \Theta(\tau_3, \tau_2, \tau_1)\Big], \tag{D.5}$$

where the step function of three variables is introduced as $\Theta(\tau_1, \tau_2, \tau_3) \equiv \Theta(\tau_1 - \tau_2)\Theta(\tau_2 - \tau_3)$.

Let us find the spectral representation of $\mathcal{K}_{1\text{-}2\text{-}3}(\tau_1, \tau_2, \tau_3)$. By using the complete basis $|a\rangle$, $\mathcal{K}_{1\text{-}2\text{-}3}(\tau_1, \tau_2, \tau_3)$ is expressed as

$$\mathcal{K}_{1\text{-}2\text{-}3}(\tau_1, \tau_2, \tau_3) = \sum_{a,b,c} \frac{\mathcal{K}'_{a,b,c}}{Z} e^{-(\tau_3 - \tau_1)E'_a - (\tau_1 - \tau_2)E'_b - (\tau_2 - \tau_3)E'_c}$$

$$\times \Big[e^{-\beta E'_a}\Theta(\tau_1, \tau_2, \tau_3) - e^{-\beta E'_b}\Theta(\tau_2, \tau_3, \tau_1) + e^{-\beta E'_c}\Theta(\tau_3, \tau_1, \tau_2)\Big], \tag{D.6}$$

with $\mathcal{K}'_{a,b,c} \equiv \langle a|\psi^\dagger|b\rangle\langle b|\psi|c\rangle\langle c|\mathcal{O}|a\rangle$. Here, the energy E'_a is defined by $(\hat{H} - \mu\hat{N})\,|a\rangle = E'_a\,|a\rangle$. Then, the Fourier components are calculated as

$$
\mathcal{K}_{1\text{-}2\text{-}3}(i\omega^F_m, i\omega^F_n, i\omega^B) = \sum_{a,b,c} \frac{\mathcal{K}'_{a,b,c}}{\beta^{1/2}Z}\delta_{\omega^F_m,\,\omega^F_n + \omega^B}
$$

$$
\times \Bigg[\frac{e^{-\beta E'_a}}{(E'_c - E'_a - i\omega^B)(E'_b - E'_a - i\omega^F_n - i\omega^B)}
$$

$$
- \frac{e^{-\beta E'_b}}{(E'_a - E'_b + i\omega^F_m)(E'_c - E'_b - i\omega^B + i\omega^F_m)}
$$

$$
+ \frac{e^{-\beta E'_c}}{(E'_b - E'_c - i\omega^F_n)(E'_a - E'_c + i\omega^F_m - i\omega^F_n)} \Bigg]. \tag{D.7}
$$

Because of the Kronecker delta $\delta_{\omega^F_m,\,\omega^F_n + \omega^B}$, the three-point function can be denoted as a two-variable function of $i\omega^F_n + i\omega^B$ and $i\omega^F_n$:

$$
\tilde{\mathcal{K}}_{1\text{-}2\text{-}3}(i\omega^F_n + i\omega^B, i\omega^F_n) \equiv \mathcal{K}_{1\text{-}2\text{-}3}(i\omega^F_n + i\omega^B, i\omega^F_n, i\omega^B) \tag{D.8}
$$

$$
= \sum_{a,b,c} \frac{\mathcal{K}'_{a,b,c}}{\beta^{1/2}Z}\Bigg[\frac{e^{-\beta E'_a}}{(E'_c - E'_a - i\omega^B)(E'_b - E'_a - i\omega^F_n - i\omega^B)}
$$

$$
- \frac{e^{-\beta E'_b}}{(E'_a - E'_b + i\omega^F_n + i\omega^B)(E'_c - E'_b + i\omega^F_n)} + \frac{e^{-\beta E'_c}}{(E'_b - E'_c - i\omega^F_n)(E'_a - E'_c + i\omega^B)} \Bigg]. \tag{D.9}
$$

Thus, $\tilde{\mathcal{K}}_{1\text{-}2\text{-}3}(w + i\omega^B, w)$ for $w \in \mathbb{C}$ has the singularities on $\text{Im}[w] = 0$ and $\text{Im}[w] = -\omega^B$. The spectral representation of $\mathcal{K}_{2\text{-}1\text{-}3}(\tau_1, \tau_2, \tau_3)$ can be obtained in the same way as

$$
\tilde{\mathcal{K}}_{2\text{-}1\text{-}3}(i\omega^F_n + i\omega^B, i\omega^F_n) \equiv \mathcal{K}_{2\text{-}1\text{-}3}(i\omega^F_n + i\omega^B, i\omega^F_n, i\omega^B) \tag{D.10}
$$

$$
= \sum_{a,b,c} \frac{\mathcal{K}'_{a,b,c}}{\beta^{1/2}Z}\Bigg[\frac{e^{-\beta E'_a}}{(E'_c - E'_a - i\omega^F_n)(E'_b - E'_a - i\omega^F_n - i\omega^B)}
$$

$$
- \frac{e^{-\beta E'_b}}{(E'_a - E'_b + i\omega^F_n + i\omega^B)(E'_c - E'_b + i\omega^B)} + \frac{e^{-\beta E'_c}}{(E'_b - E'_c - i\omega^B)(E'_a - E'_c + i\omega^F_n)} \Bigg]. \tag{D.11}
$$

Thus, $\tilde{\mathcal{K}}_{2\text{-}1\text{-}3}(w + i\omega^B, w)$ for $w \in \mathbb{C}$ has the singularities on $\text{Im}[w] = 0$ and $\text{Im}[w] = -\omega^B$.

We define the Fourier component of $\mathcal{K}(\tau_1, \tau_2, \tau_3)$ reduced to a two-variable function as

$$
\tilde{\mathcal{K}}(i\omega^F_n + i\omega^B, i\omega^F_n) \equiv \mathcal{K}(i\omega^F_n + i\omega^B, i\omega^F_n, i\omega^B)
$$

$$
= \tilde{\mathcal{K}}_{1\text{-}2\text{-}3}(i\omega^F_n + i\omega^B, i\omega^F_n) + \tilde{\mathcal{K}}_{2\text{-}1\text{-}3}(i\omega^F_n + i\omega^B, i\omega^F_n). \tag{D.12}
$$

Then, $\tilde{\mathcal{K}}(w + i\omega^B, w)$ for $w \in \mathbb{C}$ has the singularities on $\text{Im}[w] = 0$ and $\text{Im}[w] = -\omega^B$. The three-point function $\tilde{\mathcal{K}}(i\omega^F_n + i\omega^B, i\omega^F_n)$ corresponds to $\mathcal{G}(i\omega^F_n + i\omega^B)\mathcal{G}(i\omega^F_n)\Gamma(i\omega^F_n + i\omega^B, i\omega^F_n)$ in Chapter 5. Therefore, the singularities of the vertex function $\Gamma(w + i\omega^B, w)$ does not exist other than on $\text{Im}[w] = 0$ and $\text{Im}[w] = -\omega^B$.

Acknowledgements

Bibliography

[1] W. D. Phillips, "Laser cooling and trapping of neutral atoms," Rev. Mod. Phys. **70**, 721 (1998).

[2] W. Ketterle, D. S. Durfee, and D. M. Stamper-Kurn, "Making, probing and understanding Bose-Einstein condensates," Proceedings of the International School of Physics "Enrico Fermi", Course CXL, edited by M. Inguscio, S. Stringari, and C. Wieman (IOS Press, Amsterdam) pp. 67-176 (1999).

[3] W. Ketterle, M. W. Zwierlein, "Making, probing and understanding ultracold Fermi gases," Proceedings of the International School of Physics "Enrico Fermi", Course CLXIV, edited by M. Inguscio, W. Ketterle, and C. Salomon (IOS Press, Amsterdam) pp. 95-287 (2008).

[4] H. Feshbach, "Unified theory of nuclear reactions," Ann. Phys. **5**, 357 (1958).

[5] A. J. Moerdijk, B. J. Verhaar, and A. Axelsson, "Resonances in ultracold collisions of ^{6}Li, ^{7}Li, and ^{23}Na," Phys. Rev. A **51**, 4852 (1995).

[6] S. Inouye, M. R. Andrews, J. Stenger, H.-J. Miesner, D. M. Stamper-Kurn, and W. Ketterle, "Observation of Feshbach resonances in a Bose-Einstein condensate," Nature (London) **392**, 151 (1998).

[7] C. Chin, R. Grimm, P. Julienne, and E. Tiesinga, "Feshbach resonances in ultracold gases," Rev. Mod. Phys. **82**, 1225 (2010).

[8] I. Bloch, J. Dalibard, and W. Zwerger, "Many-body physics with ultracold gases," Rev. Mod. Phys. **80**, 885 (2008).

[9] S. Giorgini, L. P. Pitaevskii, and S. Stringari, "Theory of ultracold atomic Fermi gases," Rev. Mod. Phys. **80**, 1215 (2008).

[10] C. A. Regal, M. Greiner, and D. S. Jin, "Observation of Resonance Condensation of Fermionic Atom Pairs," Phys. Rev. Lett. **92**, 040403 (2004).

[11] M. W. Zwierlein, C. A. Stan, C. H. Schunck, S. M. F. Raupach, A. J. Kerman, and W. Ketterle, "Condensation of Pairs of Fermionic Atoms near a Feshbach Resonance," Phys. Rev. Lett. **92**, 120403 (2004).

[12] C. Chin, M. Bartenstein, A. Altmeyer, S. Riedl, S. Jochim, J. H. Denschlag, and R. Grimm, "Observation of the Pairing Gap in a Strongly Interacting Fermi Gas," Science **305**, 1128 (2004).

[13] T. Bourdel, L. Khaykovich, J. Cubizolles, J. Zhang, F. Chevy, M. Teichmann, L. Tarruell, S. Kokkelmans, and C. Salomon, "Experimental Study of the BEC-BCS Crossover Region in Lithium 6," Phys. Rev. Lett. **93**, 050401 (2004).

[14] J. Kinast, S. L. Hemmer, M. E. Gehm, A. Turlapov, and J. E. Thomas, "Evidence for superfluidity in a resonantly interacting Fermi gas," Phys. Rev. Lett. **92**, 150402 (2004).

[15] M. W. Zwierlein, J. R. Abo-Shaeer, A. Schirotzek, C. H. Schunck, and W. Ketterle, "Vortices and superfluidity in a strongly interacting Fermi gas," Nature **435**, 1047 (2005).

[16] G. F. Bertsch, *Many-Body X Challenge*, in: Proceedings of the Tenth International Conference on Recent Progress in Many-Body Theories, edited by R. F. Bishop *et al.* (World Scientific, Singapore 2000)

[17] G. A. Baker, "The MBX Challenge Competition: a neutron matter model," Int. J. Mod. Phys. **15**, 1314 (2001).

[18] Q. Chen, J. Stajic, S. Tan, and K. Levin, "BCS-BEC Crossover: From High Temperature Superconductors to Ultracold Superfluids," Phys. Rep. **412**, 1 (2005).

[19] G. A. Baker, "Neutron matter model," Phys. Rev. C **60**, 054311 (1999).

[20] H. Heiselberg, "Fermi systems with long scattering lengths," Phys. Rev. A **63**, 043606 (2001).

[21] T.-L. Ho, "Universal Thermodynamics of Degenerate Quantum Gases in the Unitarity Limit," Phys. Rev. Lett. **92**, 090402 (2004).

[22] S. Nascimbéne, N. Navon, K. J. Jiang, F. Chevy, and C. Salomon, "Exploring the thermodynamics of a universal Fermi gas," Nature **463**, 1057(2010).

[23] M. Horikoshi, S. Nakajima, M. Ueda, and T. Mukaiyama, "Measurement of Universal Thermodynamic Functions for a Unitary Fermi Gas," Sciemce **327**, 442 (20010).

[24] M. J. Ku, A. T. Sommer, L. W. Cheuk and M. W. Zwierlein, "Revealing the superfluid lambda transition in the universal thermodynamics of a unitary fermi gas," Science **335**, 563 (2012).

[25] T. Mehen, I. W. Stewart, and M. B. Wise, "Conformal invariance for non-relativistic field theory," Phys. Lett. B **474**, 145 (2000).

[26] D. T. Son and M. Wingate, "General coordinate invariance and conformal invariance in nonrelativistic physics: Unitary Fermi gas," Ann. Phys. **321**, 197 (2006).

[27] Y. Nishida and D. T. Son, "Nonrelativistic conformal field theories," Phys. Rev. D **76**, 086004 (2007).

[28] S. Tan, "Energetics of a Strongly Correlated Fermi Gas," Ann. Phys. **323**, 2952 (2008). "Large Momentum Part of a Strongly Correlated Fermi Gas," Ann. Phys. **323**, 2971 (2008); "Generalized Virial Theorem and Pressure Relation for a Strongly Correlated Fermi Gas," Ann. Phys. **323**, 2987 (2008).

[29] E. Braaten and L. Platter, "Exact Relations for a Strongly Interacting Fermi Gas from the Operator Product Expansion," Phys. Rev. Lett. **100**, 205301 (2008).

[30] F. Werner, L. Tarruell, and Y. Castin, "Number of Closed-Channel Molecules in the BEC-BCS Crossover," Eur. Phys. J. B **68**, 401 (2009).

[31] S. Zhang and A. J. Leggett, "Universal Properties of the Ultracold Fermi Gas," Phys. Rev. A **79**, 023601 (2009).

[32] R. Combescot, F. Alzetto, and X. Leyronas, "Particle Distribution Tail and Related Energy Formula," Phys. Rev. A **79**, 053640 (2009).

[33] F. Werner and Y. Castin, "General Relations for Quantum Gases in Two and Three Dimensions: Two-Component Fermions," Phys. Rev. A 86, 013626 (2012).

[34] E. Braaten, "Universal Relations for Fermions with Large Scattering Length," in Chap. 6, *The BCS-BEC Crossover and the Unitary Fermi Gas*, edited by W. Zwerger, Lecture Notes in Physics No. 836, Springer-Verlag (Berlin), Heidelberg, 2012.

[35] D. T. Son and E. G. Thompson, "Short-distance and short-time structure of a unitary Fermi gas," Phys. Rev. A **81**, 063634 (2010).

[36] E. Taylor and M. Randeria, "Viscosity of strongly interacting quantum fluids: Spectral functions and sum rules," Phys. Rev. A **81**, 053610 (2010).

[37] J. Hofmann, "Current Response, Structure Factor and Hydrodynamic Quantities of a Two- and Three-Dimensional Fermi Gas from the Operator-Product Expansion," Phys. Rev. A **84**, 043603 (2011).

[38] W. D. Goldberger and I. Z. Rothstein, "Structure-Function Sum Rules for Systems with Large Scattering Lengths," Phys. Rev. A **85**, 013613 (2012).

[39] T. Enss, R. Haussmann, and W. Zwerger, "Viscosity and scale invariance in the unitary Fermi gas," Ann. Phys. **326**, 770-796 (2011).

[40] K. M. O'Hara, S. L. Hemmer, M. E. Gehm, S. R. Granade, J. E. Thomas, "Observation of a Strongly Interacting Degenerate Fermi Gas of Atoms," Science **298**, 2179 (2002).

[41] T. Bourdel, J. Cubizolles, L. Khaykovich, K. M. F. Magalhães, S. J. J. M. F. Kokkelmans, G. V. Shlyapnikov, and C. Salomon, "Measurement of the Interaction Energy near a Feshbach Resonance in a Fermi Gas," Phys. Rev. Lett. **91**, 020402 (2003).

[42] T. Schäfer and C. Chafin, "Scaling Flows and Dissipation in the Dilute Fermi Gas at Unitarity," in Chap. 10, *The BCS-BEC Crossover and the Unitary Fermi Gas*, edited by W. Zwerger Lecture Notes in Physics No. 836, Springer-Verlag (Berlin), Heidelberg, 2012.

[43] T. Schäfer, "Fluid Dynamics and Viscosity in Strongly Correlated Fluids," Ann. Rev. Nucl. Part. Sci. **64**, 125 (2014).

[44] C. Cao, E. Elliott, J. Joseph, H. Wu, J. Petricka, T. Schäfer and J. E. Thomas, "Universal Quantum Viscosity in a Unitary Fermi Gas," Science **331**, 58 (2011).

[45] C. Cao, E. Elliott, H. Wu, and J. E. Thomas, "Searching for perfect fluids: Quantum viscosity in a universal Fermi gas," New J. Phys. **13**, 075007 (2011).

[46] E. Elliott, J. A. Joseph, and J. E. Thomas, "Observation of Conformal Symmetry Breaking and Scale Invariance in Expanding Fermi Gases," Phys. Rev. Lett. **112**, 040405 (2014).

[47] E. Elliott, J. A. Joseph, and J. E. Thomas, "Anomalous Minimum in the Shear Viscosity of a Fermi Gas," Phys. Rev. Lett. **113**, 020406 (2014).

[48] J. A. Joseph, E. Elliott, and J. E. Thomas, "Shear Viscosity of a Unitary Fermi Gas Near the Superfluid Phase Transition," Phys. Rev. Lett. **115**, 020401 (2015).

[49] D. T. Son, "Vanishing bulk viscosities and conformal invariance of the unitary Fermi gas," Phys. Rev. Lett. **98**, 020604 (2007).

[50] L. P. Pitaevskii and A. Rosch, "Breathing modes and hidden symmetry of trapped atoms in two dimensions," Phys. Rev. A **55**, R853 (1997)

[51] F. Werner, Y. Castin, "Unitary gas in an isotropic harmonic trap: Symmetry properties and applications," Phys. Rev. A 74, 053604 (2006).

[52] E. Vogt, M. Feld, B. Fröhlich, D. Pertot, M. Koschorreck, and M. Köhl, "Scale Invariance and Viscosity of a Two-Dimensional Fermi Gas," Phys. Rev. Lett. **108**, 070404 (2012).

[53] M. Holten, L. Bayha, A. C. Klein, P. A. Murthy, P. M. Preiss, and S. Jochim, "Anomalous breaking of scale invariance in a two-dimensional Fermi gas," Phys. Rev. Lett. **121**, 120401 (2018).

[54] T. Peppler, P. Dyke, M. Zamorano, I. Herrera, S. Hoinka, and C. J. Vale, "Quantum anomaly and 2D-3D crossover in strongly interacting Fermi gases," Phys. Rev. Lett. **121**, 120402 (2018).

[55] P. A. Murthy, N. Defenu, L. Bayha, M. Holten, P. M. Preiss, T. Enss, and S. Jochim, "Quantum scale anomaly and spatial coherence in a 2D Fermi superfluid," Science **365**, 268 (2019).

[56] P. K. Kovtun, D. T. Son, and A. O. Starinets, "Viscosity in Strongly Interacting Quantum Field Theories from Black Hole Physics," Phys. Rev. Lett. **94**, 111601 (2005).

[57] G. Policastro, D. T. Son, and A. O. Starinets, "Shear Viscosity of Strongly Coupled $N = 4$ Supersymmetric Yang-Mills Plasma," Phys. Rev. Lett. **87**, 081601 (2001).

[58] T. Schäfer and D. Teaney, "Nearly perfect fluidity: from cold atomic gases to hot quark gluon plasmas," Rept. Prog. Phys. **72**. 126001 (2009).

[59] A. Adams, L. D. Carr, T. Schäfer, P. Steinberg, and J. E. Thomas, "Strongly correlated quantum fluids: ultracold quantum gases, quantum chromodynamic plasmas and holographic duality," New J. Phys. **14**, 115009 (2012).

[60] M. Brigante, H. Liu, R. C. Myers, S. Shenker, and S. Yaida, "Viscosity bound and causality violation," Phys. Rev. Lett. **100**, 191601 (2008).

[61] M. Brigante, H. Liu, R. C. Myers, S. Shenker, and S. Yaida, "Viscosity bound violation in higher derivative gravity," Phys. Rev. D **77**, 126006 (2008).

[62] A. Buchel, R. C. Myers, and A. Sinha, "Beyond $\eta/s = 1/4\pi$," JHEP **03**, 084 (2009).

[63] Y. Kats and P. Petrov, "Effect of curvature squared corrections in AdS on the viscosity of the dual gauge theory," JHEP **01**, 044 (2009).

[64] A. Rebhan and D. Steineder, "Violation of the Holographic Viscosity Bound in a Strongly Coupled Anisotropic Plasma," Phys. Rev. Lett. **108**, 021601 (2012).

[65] R. Kubo, "Statistical-mechanical theory of irreversible processes. I. General theory and simple applications to magnetic and conduction problems," J. Phys. Soc. Jpn. **12**, 570-586 (1957).

[66] H. Mori, "Collective motion of particles at finite temperatures," Prog. Theor. Phys. **28**, 763-783 (1962).

[67] L. P. Kadanoff and P. C. Martin, "Hydrodynamic Equations and Correlation Functions," Ann. Phys. **24**, 419 (1963)

[68] J. M. Luttinger, "Theory of thermal transport coefficients," Phys. Rev. **135**, A1505-A1514 (1964).

[69] P. Massignan, G. M. Bruun, and H. Smith, "Viscous relaxation and collective oscillations in a trapped Fermi gas near the unitarity limit," Phys. Rev. A **71**, 033607 (2005).

[70] G. M. Bruun and H. Smith, "Viscosity and thermal relaxation for a resonantly interacting Fermi gas," Phys. Rev. A **72**, 043605 (2005).

[71] M. Braby, J. Chao, and T. Schäfer, "Thermal conductivity and sound attenuation in dilute atomic Fermi gases," Phys. Rev. A **82**, 033619 (2010).

[72] G. M. Bruun, "Shear viscosity and spin-diffusion coefficient of a two-dimensional Fermi gas," Phys. Rev. A **85**, 013636 (2012).

[73] T. Schäfer, "Shear viscosity and damping of collective modes in a two-dimensional Fermi gas," Phys. Rev. A **85**, 033623 (2012).

[74] K. Dusling and T. Schäfer, "Bulk viscosity and conformal symmetry breaking in the dilute Fermi gas near unitarity," Phys. Rev. Lett. **111**, 120603 (2013).

[75] C. Chafin and T. Schäfer, "Scale breaking and fluid dynamics in a dilute two-dimensional Fermi gas," Phys. Rev. A **88**, 043636 (2013).

[76] S. E. Pollack, D. Dries, R. G. Hulet, K. M. F. Magalhães, E. A. L. Henn, E. R. F. Ramos, M. A. Caracanhas, and V. S. Bagnato, "Collective excitation of a Bose-Einstein condensate by modulation of the atomic scattering length," Phys. Rev. A **81**, 053627 (2010).

[77] L. W. Clark, A. Gaj, L. Feng, and C. Chin, "Collective emission of matter-wave jets from driven Bose-Einstein condensates," Nature (London) **551**, 356-359 (2017).

[78] N. Arunkumar, A. Jagannathan, and J. E. Thomas, "Designer spatial control of interactions in ultracold gases," Phys. Rev. Lett. **122**, 040405 (2019).

[79] P. F. Bedaque and G. Rupak, "Dilute resonating gases and the third virial coefficient" Phys. Rev. B **67**, 174513 (2003).

[80] T.-L. Ho and E. J. Mueller, "High Temperature Expansion Applied to Fermions near Feshbach Resonance," Phys. Rev. Lett. **92**, 160404 (2004).

[81] C. J. Horowitz and A. Schwenk, "The Virial Equation of State of Low-Density Neutron Matter," Phys. Lett. B **638**, 153 (2006).

[82] G. Rupak, "Universality in a 2-component Fermi System at Finite Temperature," Phys. Rev. Lett. **98**, 090403 (2007).

[83] X.-J. Liu, H. Hu, and P. D. Drummond, "Virial Expansion for a Strongly Correlated Fermi Gas," Phys. Rev. Lett. **102**, 160401 (2009).

[84] X.-J. Liu, H. Hu, P. D. Drummond, "Three attractively interacting fermions in a harmonic trap: Exact solution, ferromagnetism, and high-temperature thermodynamics," Phys. Rev. A **82** 023619 (2010).

[85] H. Hu, X.-J. Liu, P. D. Drummond, "Universal contact of strongly interacting fermions at finite temperatures," New J. Phys. **13**, 035007 (2011).

[86] D. B. Kaplan and S. Sun, "New Field-Theoretic Method for the Virial Expansion," Phys. Rev. Lett. **107**, 030601 (2011).

[87] X. Leyronas, "Virial expansion with Feynman diagrams," Phys. Rev. A **84**, 053633 (2011).

[88] X.-J. Liu, "Virial expansion for a strongly correlated Fermi system and its application to ultracold atomic Fermi gases," Phys. Rept. **524**, 37-83 (2013).

[89] Y. Nishida, "Viscosity spectral functions of resonating fermions in the quantum virial expansion," Ann. Phys. **410**, 167949 (2019).

[90] T. Enss, "Bulk viscosity and contact correlations in attractive Fermi gases," Phys. Rev. Lett. **123**, 205301 (2019).

[91] J. Hofmann, "High-temperature expansion of the viscosity in interacting quantum gases," Phys. Rev. A **101**, 013620 (2020).

[92] K. Fujii and Y. Nishida, "Bulk viscosity of resonating fermions revisited: Kubo formula, sum rule, and the dimer and high-temperature limits," Phys. Rev. A **102**, 023310 (2020).

[93] B. Frank, W. Zwerger, and T. Enss, "Quantum critical thermal transport in the unitary Fermi gas," Phys. Rev. Research **2**, 023301 (2020).

[94] L. D. Landau and E. M. Lifshitz, in *Quantum mechanics: non-relativistic theory*, Course of Theoretical Physics Vol. 3 (Pergamon, New York, 1977).

[95] C. J. Pethick and H. Smith, in *Bose-Einstein condensation in dilute gases*, (Cambridge university press, 2002).

[96] S. K. Adhikari, "Quantum scattering in two dimensions," Am. J. Phys. **54**, 362 (1986).

[97] L. D. Landau and E. M. Lifshitz, in *Fluid Mechanics*, 2nd ed. (Butterworth-Heinemann, Oxford, UK, 1987).

[98] D. Forster, *Hydrodynamic Fluctuations, Broken Symmetry, and Correlation Functions*, (Benjamin/Cummings, New York, 1975)

[99] L. D. Landau, "Theory of the Suyerfluidity of Helium II," Phys. Rev. **60**, 356 (1941).

[100] L. D. Landau and E. M. Lifshitz, in *Physical Kinetics*, Course of Theoretical Physics Vol. X (Pergamon, New York, 1981).

[101] S. Chapman and T. G. Cowling, in *The mathematical theory of nonuniform gases: an account of the kinetic theory of viscosity, thermal conduction and diffusion in gases*, (Cambridge university press, 1970).

[102] M. A. Escobedo, M. Mannarelli, and C. Manuel, "Bulk viscosities for cold Fermi superfluids close to the unitary limit," Phys. Rev. A **79**, 063623 (2009).

[103] Y.-H. Hou, L. P. Pitaevskii, and S. Stringari, "Scaling solutions of the two-fluid hydrodynamic equations in a harmonically trapped gas at unitarity," Phys. Rev. A **87**, 033620 (2013).

[104] B. Mukherjee, Z. Yan, P. B. Patel, Z. Hadzibabic, T. Yefsah, J. Struck, and M. W. Zwierlein, "Homogeneous Atomic Fermi Gases," Phys. Rev. Lett. **118**, 123401 (2017).

[105] L. D. Landau and E. M. Lifshitz, *Statistical Physics Part 1*, Vol. 5 (Butterworth Heinemann, Oxford, U.K., 1981).

[106] C. A. R. Sá de Melo, M. Randeria, and J. R. Engelbrecht, "Crossover from BCS to Bose superconductivity: Transition temperature and time-dependent Ginzburg-Landau theory," Phys. Rev. Lett. **71**, 3202 (1993).

[107] E. Beth and G. E. Uhlenbeck, "The quantum theory of the non-ideal gas. II. Behaviour at low temperatures," Physica **4**, 915 (1937).

[108] E. Taylor and M. Randeria, "Apparent Low-Energy Scale Invariance in Two-Dimensional Fermi Gases," Phys. Rev. Lett. **109**, 135301 (2012).

[109] G. Baym and C. Pethick, *Landau Fermi-Liquid Theory: Concepts and Applications* (Wiley, New York, 1991).

[110] D. Rakshit, K. M. Daily, D. Blume, "Natural and unnatural parity states of small trapped equal-mass two-component Fermi gases at unitarity and fourth-order virial coefficient," Phys. Rev. A **85**, 033634 (2012).

[111] V. Ngampruetikorn, M. M. Parish and J. Levinsen, "High-temperature limit of the resonant fermi gas," Phys. Rev. A **91**, 013606 (2015).

[112] S. Endo and Y. Castin, "Absence of a four-body Efimov effect in the $2 + 2$ fermionic problem," Phys. Rev. A **92**, 053624 (2015).

[113] Y. Yan and D. Blume, "Path-integral monte carlo determination of the fourth-order virial coefficient for a unitary two-component fermi gas with zero-range interactions," Phys. Rev. Lett. **116**, 230401 (2016).

[114] S. Endo and Y. Castin, "The interaction-sensitive states of a trapped two-component ideal fermi gas and application to the virial expansion of the unitary fermi gas," J. Phys. A **49**, 265301 (2016).

[115] Y. Hou and J. E. Drut, "Fourth- and Fifth-Order Virial Coefficients from Weak Coupling to Unitarity," Phys. Rev. Lett. **125**, 050403 (2020).

[116] C. Carcy, S. Hoinka, M. G. Lingham, P. Dyke, C. C. N. Kuhn, H. Hu, and C. J. Vale, "Contact and Sum Rules in a Near-Uniform Fermi Gas at Unitarity," Phys. Rev. Lett. **122**, 203401 (2019).

[117] B. Mukherjee, P. B. Patel, Z. Yan, R. J. Fletcher, J. Struck, and M. W. Zwierlein, "Spectral Response and Contact of the Unitary Fermi Gas," Phys. Rev. Lett. 122, 203402 (2019).

[118] W. Götze and P. Wölfle "Homogeneous Dynamical Conductivity of Simple Metals," Phys. Rev. B **6**, 1226 (1972).

[119] J. S. Langer, "Some Considerations of Analyticity in the Many-Fession Problem," Phys. Rev. **124**, 997 (1961).

[120] G. M. Eliashberg, "Transport equation for a degenerate system of Fermi particles," Sov. Phys. JETP **14**, 886 (1962).

[121] S. Jeon, "Hydrodynamic Transport Coefficients in Relativistic Scalar Field Theory," Phys. Rev. D **52**, 3591 (1995).

[122] S. Jeon and L. G. Yaffe, "From Quantum Field Theory to Hydrodynamics: Transport Coefficients and Effective Kinetic Theory," Phys. Rev. D **53**, 5799 (1996).

[123] Y. Hidaka and T. Kunihiro, "Renormalized linear kinetic theory as derived from quantum field theory: A novel diagrammatic method for computing transport coefficients," Phys. Rev. D **83**, 076004 (2011).

[124] P. B. Patel, Z. Yan, B. Mukherjee, R. J. Fletcher, J. Struck, M. W. Zwierlein, "Universal Sound Diffusion in a Strongly Interacting Fermi Gas," Science **370**, 1222 (2020).

[125] M. I. Rodas-Verde, H. Michinel, and V. M. Pérez-García, "Controllable soliton emission from a Bose-Einstein condensate," Phys. Rev. Lett. **95**, 153903 (2005).

[126] R. Balbinot, A. Fabbri, S. Fagnocchi, A. Recati, and I. Carusotto, "Nonlocal density correlations as a signature of Hawking radiation from acoustic black holes," Phys. Rev. A **78**, 021603(R) (2008).

[127] M. Salerno, V. V. Konotop, and Yu. V. Bludov, "Long-living Bloch oscillations of matter waves in periodic potentials," Phys. Rev. Lett. **101**, 030405 (2008).

[128] A. Bulgac and S. Yoon, "Large amplitude dynamics of the pairing correlations in a unitary Fermi gas," Phys. Rev. Lett. **102**, 085302 (2009).

[129] J. Gong, L. Morales-Molina, and P. Hänggi, "Many-body coherent destruction of tunneling," Phys. Rev. Lett. **103**, 133002 (2009).

[130] Y. Nishida and D. Lee, "Weakly bound molecules trapped with discrete scaling symmetries," Phys. Rev. A **86**, 032706 (2012).

[131] Á. Rapp, X. Deng, and L. Santos, "Ultracold lattice gases with periodically modulated interactions," Phys. Rev. Lett. **109**, 203005 (2012).

[132] M. Di Liberto, C. E. Creffield, G. I. Japaridze, and C. Morais Smith, "Quantum simulation of correlated-hopping models with fermions in optical lattices," Phys. Rev. A **89**, 013624 (2014).

[133] S. Greschner, G. Sun, D. Poletti, and L. Santos, "Density-dependent synthetic gauge fields using periodically modulated interactions," Phys. Rev. Lett. **113**, 215303 (2014).

[134] C. Langmack, D. H. Smith, and E. Braaten, "Association of atoms into universal dimers using an oscillating magnetic field," Phys. Rev. Lett. **114**, 103002 (2015).

[135] D. H. Smith, "Inducing resonant interactions in ultracold atoms with a modulated magnetic field," Phys. Rev. Lett. **115**, 193002 (2015).

[136] M. Le Bellac, *Thermal Field Theory* (Cambridge University Press, Cambridge, 2000).

[137] T. Kita, "Introduction to nonequilibrium statistical mechanics with quantum field theory," Prog. Theor. Phys. **123**, 581-658 (2010).

[138] I. Šlaus, Y. Akaishi, and H. Tanaka, "Neutron-neutron effective range parameters," Phys. Rep. **173**, 257 (1989).

[139] M. Horikoshi and M. K.-Gonokami, "Cold atom quantum simulator for dilute neutron matter," Int. J Mod. Phys. E **28**, 1930001 (2019).

[140] U. Niederer, "The maximal kinematical invariance group of the free Schrodinger equation," Helv. Phys. Acta **45**, 802 (1972).

[141] C. R. Hagen, "Scale and Conformal Transformations in Galilean-Covariant Field Theory," Phys. Rev. D **5**, 377 (1972).

[142] V. Efimov, "Energy levels arising from resonant twobody forces in a three-body system," Phys. Lett. B **33**, 563 (1970); "Weakly-bound states of three resonantlyinteracting particles," Yad. Fiz. **12**, 1080 (1970) [Sov. J. Nuc. Phys. **12**, 589 (1971)]; "Energy Levels of Three Resonantly Interacting Particles," Nucl. Phys. A **210**, 157 (1973).

[143] C. Hoyos, S. Moroz, and D. T. Son, "Effective theory of chiral two-dimensional superfluids," Phys. Rev. B **89**, 174507 (2014).

[144] S. Moroz and C. Hoyos, "Effective theory of two-dimensional chiral superfluids: gauge duality and Newton-Cartan formulation," Phys. Rev. B **91**, 064508 (2015).

[145] M. Geracie, "Transport in superfluid mixtures," Phys. Rev. B **95**, 134510 (2017).

[146] K. Fujii and Y. Nishida, "Low-energy effective field theory of superfluid ^{3}He-B and its gyromagnetic and Hall responses," Ann. Phys. **395**, 170 (2018).

[147] T. Furusawa, K, Fujii, Y. Nishida "Hall viscosity in the A-phase of superfluid ^{3}He," [arXiv:2008.08276].

[148] C. Hoyos and D. T. Son, "Hall Viscosity and Electromagnetic Response," Phys. Rev. Lett. **108**, 066805 (2012).

[149] D. T. Son, "Newton-Cartan Geometry and the Quantum Hall Effect," [arXiv:1306.0638].

[150] O. Andreev, M. Haack, and S. Hofmann, "On nonrelativistic diffeomorphism invariance," Phys. Rev. D **89**, 064012 (2014).

[151] O. Andreev, "More on nonrelativistic diffeomorphism invariance," Phys. Rev. D **91**, 024035 (2015).

[152] M. Geracie, D. T. Son, C. Wu, and S.-F. Wu, "Spacetime Symmetries of the Quantum Hall Effect," Phys. Rev. D **91**, 045030 (2015).

[153] C. Wu and S.-F. Wu, "Hořava-Lifshitz gravity and effective theory of the fractional quantum Hall effect," JHEP. **01**, 120 (2015).